ARS JOURNAL

A PUBLICATION OF THE AMERICAN ROCKET SOCIETY

FORMERLY JET PROPULSION

Applied Science Dept.

PUBLIC LIBRARY
DEC 28
ST. LOUIS

Guidance Issue

Editorial Introduction . . . . . Charles J. Mundo and Martin Summerfield 899

Authors in This Special Issue 900

INVITED ARTICLES

IGY Results on the Shape of the Earth . . . . . John A. O'Keefe 902

Lunar Trajectories . . . . . Aubrey B. Mickelwait 905

First Flight of a Ballistic Missile . . . . . Albert D. Wheelon 915

Stabilization and Attitude Control of Satellite Vehicles . . . . . William E. Frye and Edward V. B. Stearns 927

Guidance Techniques for Interplanetary Travel . . . . . Charles D. Reed and Charles J. Mundo 931

Radio Guidance . . . . . E. King Stodola 940

Recent Progress in Inertial Guidance . . . . . John Hovorka, John W. Hursh, E. J. Frey, William G. Denhard, Lester R. Grohe, P. J. Gillinson Jr. and W. E. Vander Velde 946

Doppler Radars for Guidance—Design Techniques and Performance . . . . . Walter R. Fried 967

Principles of Doppler-Inertial Guidance . . . . L. H. Dworetsky and A. Edwards 987

Infrared Tracking . . . . . R. W. Powell 973

Celestial Guidance . . . . . R. B. Horsfall 981

DEPARTMENTS

Technical Literature Digest 990

1959 INDEX OF PAPERS PUBLISHED IN ARS JOURNAL 998

December 1959 Volume 29 Number 12

The

Avco Everett Research Laboratory

announces

it is expanding its activities
to explore and bring to engineering
fruition electric propulsion for space
vehicles, generation of electricity
for both ground station and space
application through MHD, and satellite
and space vehicle design.

IF THIS OPPORTUNITY
INTERESTS YOU. WRITE:

DR. ARTHUR KANTROWITZ. DIRECTOR
AVCO EVERETT RESEARCH LABORATORY
2385 REVERE BEACH PARKWAY
EVERETT. MASSACHUSETTS

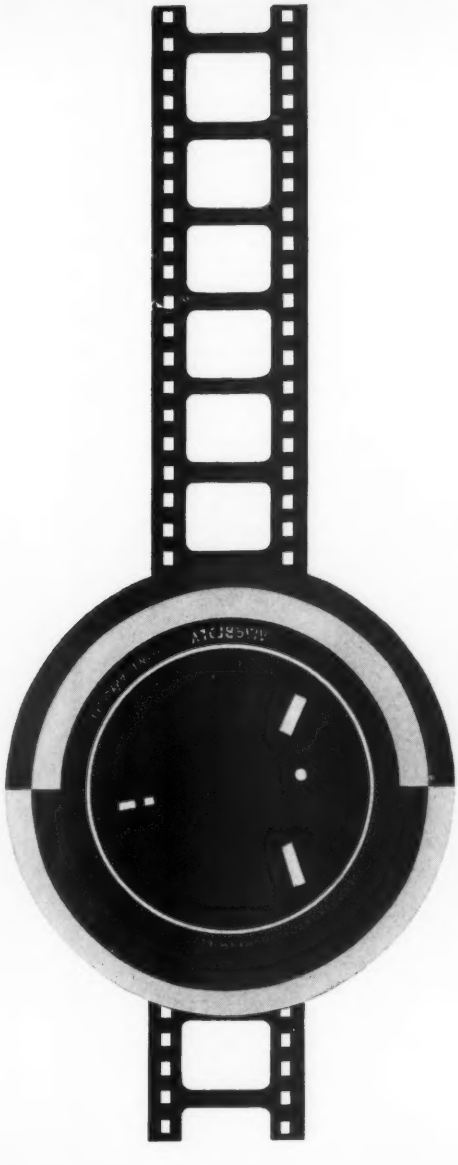

New focus on photographic reconnaissance systems... by Bulova

Bulova advances high acuity

In both opto-mechanics and electronics, Bulova is enhancing the state of the art. Bulova designs are improving acuity. Bulova electronics are simplifying readout devices. Bulova advanced precision production and assembly techniques are assuring more accurate instruments capable of withstanding higher adverse environmental conditions.

This proven capability—from conception to manufacture—stands ready to support your efforts.

Experience in precision design and manufacture is the Bulova tradition—the Bulova capability—it has been for over 80 years. For more information write—

Industrial & Defense Sales, 62-10 Woodside Avenue, Woodside 77, N.Y.

BULOVA

ARS JOURNAL

A PUBLICATION OF THE AMERICAN ROCKET SOCIETY

FORMERLY JET PROPULSION

EDITOR — Martin Summerfield

ASSOCIATE TECHNICAL EDITOR — Irvin Glassman

MANAGING EDITOR — Barbara Nowak

ASSISTANT EDITOR — Julie Hight

ART EDITOR — John Culin

ASSOCIATE EDITORS

J. George Adashko, *Russian Supplement;* **Ali Bulent Cambel,** *Northwestern University, Book Reviews;* **Charles J. Mundo Jr.,** *American Bosch Arma Corporation, Electronics;* **M. H. Smith,** *Princeton University, Technical Literature Digest*

CONTRIBUTOR

George F. McLaughlin

ADVERTISING AND PROMOTION MANAGER

William Chenoweth

ADVERTISING PRODUCTION MANAGER

Walter Brunke

ADVERTISING REPRESENTATIVES

New York
D. C. Emery and Associates
400 Madison Ave., New York, N. Y.
Telephone: Plaza 9-7460

Los Angeles
James C. Galloway and Co.
6535 Wilshire Blvd., Los Angeles, Calif.
Telephone: Olive 3-3223

Chicago
Jim Summers and Associates
35 E. Wacker Dr., Chicago, Ill.
Telephone: Andover 3-1154

Detroit
R. F. Pickrell and Associates
318 Stephenson Bldg., Detroit, Mich.
Telephone: Trinity 1-0790

Boston
Robert G. Melendy
17 Maugus Ave., Wellesley Hills, Mass.
Telephone: Cedar 5-6503

Pittsburgh
John W. Foster
239 4th Ave., Pittsburgh, Pa.
Telephone: Atlantic 1-2977

American Rocket Society

500 Fifth Avenue, New York 36, N. Y.

Founded 1930

OFFICERS

President	John P. Stapp
Vice-President	Howard S. Seifert
Executive Secretary	James J. Harford
Treasurer	Robert M. Lawrence
Secretary and Asst. Treasurer	A. C. Slade
General Counsel	Andrew G. Haley
Director of Publications	Irwin Hersey

BOARD OF DIRECTORS

Terms expiring on dates indicated

James R. Dempsey	1961	Simon Ramo	1960
Alfred J. Eggers Jr.	1959	H. W. Ritchey	1959
Krafft Ehricke	1959	William L. Rogers	1959
Samuel K. Hoffman	1960	David G. Simons	1961
J. Preston Layton	1960	John L. Sloop	1961
A. K. Oppenheim	1961	Martin Summerfield	1959
William H. Pickering	1961	Wernher von Braun	1960
		Maurice J. Zucrow	1960

TECHNICAL COMMITTEE CHAIRMEN

Lawrence S. Brown, Guidance and Navigation
Milton U. Clauser, Magnetohydrodynamics
Herbert L. Karsch, Logistics and Operations
William H. Dorrance, Hypersonics
Herbert Friedman, Instrumentation
George Gerard, Structures and Materials
Milton Greenberg, Physics of the Atmosphere and Space
Stanley V. Gunn, Nuclear Propulsion
Andrew G. Haley, Space Law and Sociology
Samuel Herrick, Astrodynamics
Maxwell W. Hunter, Missiles and Space Vehicles
David B. Langmuir, Ion and Plasma Propulsion
Y. C. Lee, Liquid Rockets
Max Lowy, Communications
Richard A. Schmidt, Test Facilities and Support Equipment
Paul E. Sandorff, Education
William B. Shippen, Ramjets
John L. Sloop, Propellants and Combustion
Ivan E. Tuhy, Solid Rockets
Stanley C. White, Human Factors and Bio-Astronautics
George F. Wislicenus, Underwater Propulsion
Abe M. Zarem, Power Systems

Scope of ARS JOURNAL

This Journal is devoted to the advancement of astronautics through the dissemination of original papers disclosing new scientific knowledge and basic applications of such knowledge. The sciences of astronautics are understood here to embrace selected aspects of jet and rocket propulsion, space flight mechanics, high-speed aerodynamics, flight guidance, space communications, atmospheric and outer space physics, materials and structures, human engineering, overall system analysis, and possibly certain other scientific areas. The selection of papers to be printed will be governed by the pertinence of the topic to the field of astronautics, by the current or probable future significance of the research, and by the importance of distributing the information to the members of the Society and to the profession at large.

Information for Authors

Manuscripts must be as brief as the proper presentation of the ideas will allow. Exclusion of dispensable material and conciseness of expression will influence the Editors' acceptance of a manuscript. In terms of standard-size double-spaced typed pages, a typical maximum length is 22 pages of text (including equations), 1 page of references, 1 page of abstract and 12 illustrations. Fewer illustrations permit more text, and vice versa. Greater length will be acceptable only in exceptional cases.

Short manuscripts, not more than one-quarter of the maximum length stated for full articles, may qualify for publication as Technical Notes or Technical Comments. They may be devoted to new developments requiring prompt disclosure or to comments on previously published papers. Such manuscripts are usually published within a few months of the date of receipt.

Sponsored manuscripts are published occasionally as an ARS service to the industry. A manuscript that does not qualify for publication, according to the above-stated requirements as to subject, scope or length, but which nevertheless deserves widespread distribution among jet propulsion engineers, may be printed as an extra part of the Journal or as a special supplement, if the author or his sponsor will reimburse the Society for actual publication costs. Estimates are available on request. Acknowledgment of such financial sponsorship appears as a footnote on the first page of the article. Publication is prompt since such papers are not in the ordinary backlog.

Manuscripts must be double spaced on one side of paper only with wide margins to allow for instructions to printer. Include a 100 to 200 word abstract. State the authors' positions and affiliations in a footnote on the first page. Equations and symbols may be handwritten or typewritten; clarity for the printer is essential. Greek letters and unusual symbols should be identified in the margin. If handwritten, distinguish between capital and lower case letters, and indicate subscripts and superscripts. References are to be grouped at the end of the manuscript and are to be given as follows: For journal articles: authors first, then title, journal, volume, year, page numbers; for books: authors first, then title, publisher, city, edition and page or chapter numbers. Line drawings must be clear and sharp to make clear engravings. Use black ink on white paper or tracing cloth. Lettering should be large enough to be legible after reduction. Photographs should be glossy prints, not matte or semi-matte. Each illustration must have a legend; legends should be listed in order on a separate sheet.

Manuscripts must be accompanied by written assurance as to security clearance in the event the subject matter lies in a classified area or if the paper originates under government sponsorship. Full responsibility rests with the author.

Submit manuscripts in duplicate (original plus first carbon, with two sets of illustrations) to the Editor, Martin Summerfield, Professor of Aeronautical Engineering, Princeton University, Princeton, N. J. Preprints of papers presented at ARS national meetings are automatically considered for publication.

ARS JOURNAL is published monthly by the American Rocket Society, Inc. and the American Interplanetary Society at 20th & Northampton Sts., Easton, Pa., U. S. A. Editorial offices: 500 Fifth Ave., New York 36, N. Y. Price: $12.50 per year, $2.00 per single copy. Second-class mail privileges authorized at Easton, Pa. This publication is authorized to be mailed at the special rates of postage prescribed by Section 132.122. Notice of change of address should be sent to the Secretary, ARS, at least 30 days prior to publication. Opinions expressed herein are the authors and do not necessarily reflect the views of the Editors or of the Society.

© Copyright 1959 by the American Rocket Society, Inc.

ED ALERT . . . key to preparedness . . . job of Martin-Activation. The opportunity for REAL engineers and technicians to
ugh problems and apply their specialties to an organized program in missile base operation. The rewards: ground floor oppor-
for unlimited professional advancement. Direct all resumes of qualifications to: Dean Pearson, Director of Engineering Staffing,
Martin-Activation, P. O. Box 2371, Denver, Colorado.
TEST OPERATIONS
WEAPONS SYSTEMS MAINTENANCE
PLANS AND PROGRAMS
DESIGN INSTALLATIONS
MARTIN
ACTIVATION

Why Lockheed's all-purpose AGENA is

America's most versatile satellite

Discoverer Program "Firsts" by AGENA Satellites

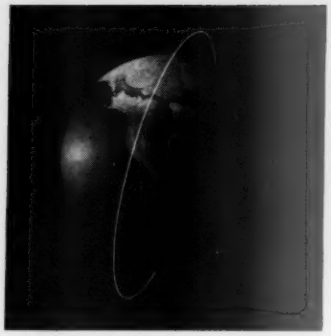

First to be put on a polar orbit. Only the Agena, with its horizon-scanner and its response to signals from earth, can be placed on a precise, predicted orbit over the pole.

First to be controlled on orbit. The Agena is also unique in its ability to be turned 180° to a tail-first position and tilted to a 60° downward angle for capsule ejection.

First to carry new systems into spa The Agena has proved out ma devices – control, communicati telemetry, life-sustaining – to be u in other advanced space progra

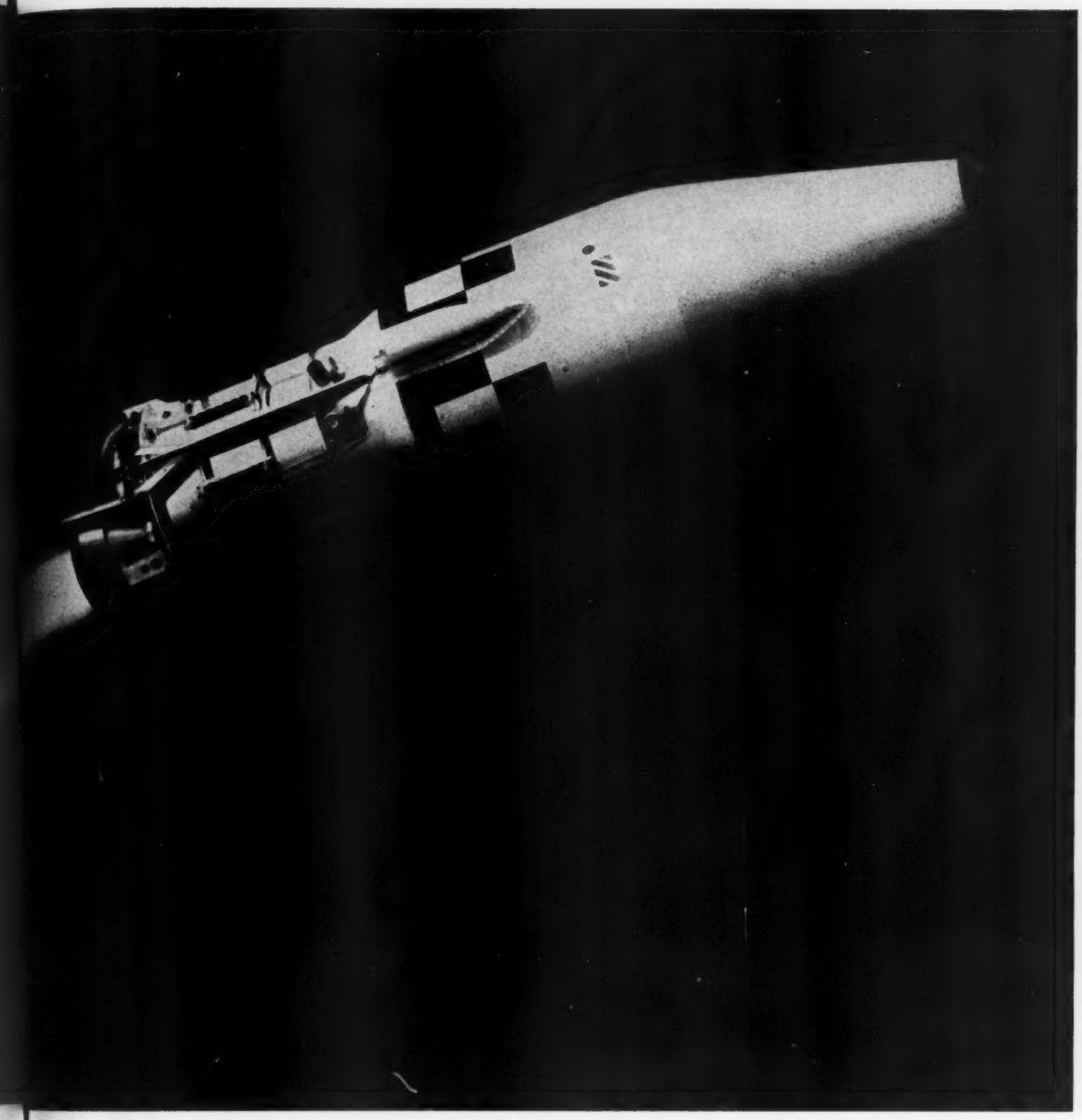

Agena is the largest and heaviest true satellite the U.S. has ever put on orbit. It is the only satel-
at can be put on a precise, predicted orbit...that can be controlled while on orbit...that can
a recovery capsule. It can carry a wide variety of very heavy and specialized payloads. The
satellite is now used exclusively in the Discoverer Program, directed by the Advanced
arch Projects Agency and managed by the Ballistic Missile Division of the U.S. Air Force.

LOCKHEED

MISSILES AND SPACE DIVISION

MISSILE RESEARCH & DEVELOPMENT • BALLISTIC MISSILE SYSTEMS MANAGEMENT
ROCKETRY • ULTRASONIC AERODYNAMICS • SPACE INVESTIGATIONS • NUCLEAR PHYSICS
ADVANCED ELECTRONICS • HIGH-SPEED AUTOMATIC DATA REDUCTION
SATELLITES • RAMJET PROPULSION TESTING

A. L. Feldman

Al Feldman is thirty-one. A Cornell BSME, he joined Aerojet as a development engineer in 1954. His present job: Head, Propulsion Systems Department, Liquid Rocket Plant, Sacramento. The assignment: design and development of rocket engines for the TITAN missile.

His talent for careful analysis and willingness to meet the toughest problems have brought Al Feldman recognition and responsibility. But his progress at Aerojet is not unique. We'd welcome the chance to discuss similar opportunities with *you*. Send your resume to: Director of Scientific and Engineering Personnel, Box 296D—Azusa, California, or, Box 1947D—Sacramento, California.

Aerojet-General® CORPORATION

AZUSA AND NEAR SACRAMENTO, CALIFORNIA • A SUBSIDIARY OF THE GENERAL TIRE & RUBBER COMPANY

Editorial Introduction to the Guidance Issue

THE PURPOSE of this special issue is to survey some of the important new concepts in guidance that have developed recently and to indicate their effects on the design of guidance systems. Each paper was specially invited by the Editors from a recognized authority in his particular area. The issue as a whole attempts to provide an understanding of the fundamental theory underlying the development of a modern guidance system, the principles of the mechanisms used to implement the guidance system, and finally, an indication of the literature where additional details may be found.

The nature of the guidance problem is defined in the first three papers by O'Keefe, Wheelon and Mickelwait: O'Keefe in the introductory paper "IGY Results on the Shape of the Earth" discusses the startling new concepts concerning the pear-shaped figure of the Earth which have come into being from an analysis of the IGY satellite tracking data. No precision guidance system for either long range missiles or spacecraft can function accurately without taking into account the undulations that exist in the shape of the spheroid.

Wheelon in "Free Flight of a Ballistic Missile" describes the trajectory problems that arise in connection with missile travel in the near vicinity of the Earth. He develops a simple model of the trajectory in terms of a spherical nonrotating Earth to calculate the burnout miss coefficients. He then extends this model to treat the effects of rotation, oblateness, gravitational anomalies, geophysical constants and the gravity of the moon.

Mickelwait in a paper titled "Lunar Trajectories" extends the trajectory considerations into space. He points out the new complexities that arise in the lunar shots and emphasizes the interrelationships that exist between guidance, propulsion and the trajectory.

The problems of ballistic guidance defined in the papers are then turned to the consideration of the kinds of guidance equipment which will execute these trajectories in spaceflight. Stodola's paper on "Radio Guidance" explores a particular phase of the space guidance problem in detail: The question of radio communication with the spacecraft. The whole problem of radio guidance centers around obtaining a sufficiently high signal-to-noise ratio and an adequate frequency bandwidth to permit the description of the motion of the vehicle with the needed accuracy. A series of nomographs is given which enable the reader to quickly visualize the tradeoff between the design parameters involved.

Frye and Stearns survey what has been accomplished in "Stabilization and Attitude Control of Satellite Vehicles." This is one of the problems that must be solved before man is put into an orbit about the Earth or any precision guidance vehicle is launched into deep space. To date, Discover II and Lunik III have been the only successful attempts at attitude stabilization that have been publicized.

Bock and Mundo survey the kinds of guidance techniques that appear to be suitable for probes to the near planets. From an examination of the trajectory problem they evolve the characteristics that are desirable for the measurement parameters. They show how the three measurable parameters, position, velocity and acceleration, fulfill these characteristics. Techniques of measuring these parameters are then surveyed in the light of these requirements.

The direction of the papers then turns to the consideration of the terrestrial guidance of cruise missiles, although many of the techniques discussed here carry over into the guidance of ballistic missiles.

Powell points out in "Infrared Tracking" that, different from other forms of guidance, the higher speeds and altitudes of modern military aircraft are simplifying the problems of infrared guidance equipment. The problem of infrared guidance is similar to that of radio: A bandwidth vs. signal-to-noise ratio question. Improvement in cell characteristics, optical materials and filter design techniques have all contributed to making infrared a feasible guidance medium.

Horsfall shows how one of man's oldest guidance techniques, celestial guidance, has been automated for modern cruise missiles. He treats the error equations of guidance and the problems of tracking.

Hovorka in a paper titled "Recent Progress in Inertial Guidance" provides a compilation of the thinking of the staff specialists at MIT's Instrumentation Laboratory on inertial navigation, a field in which this laboratory pioneered and which, after 10 years of research and development, is upon the threshold of becoming the principal guidance method used for ICBM's as well as shorter range missiles.

Fried surveys "Doppler Radars for Guidance —Design Techniques and Performance." He develops an understanding of the problems that underlie airborne Doppler radar and shows the advantages and limitations of different methods of instrumenting such systems. Dworetzky and Edwards give the first comprehensive treatment of the subject of Doppler-inertial systems in the unclassified literature. This class of system makes its measurements by selecting on a frequency basis the most accurate source of information. In general, the best low frequency information is derived from Doppler radar because it, to some degree, avoids the problems of gyro drift, while the inertial navigation provides the high frequency information lost in the smoothing time of the Doppler radar. They point out that this type of system has the capacity to accomplish functions, such as gyro compassing, which neither of the elements could do alone in an airborne system.

The Editors are proud to offer this special issue to our readers and are grateful to the authors for their fine contributions.

CHARLES J. MUNDO, Editor, Guidance Issue
MARTIN SUMMERFIELD, Editor, ARS Journal

Authors in this Special Issue

Bock

Dworetzky

Edwards

Fried

Frye

Horsfall

Hovorka

Mickelwait

Charles D. Bock is Head of the Technical Staff of the Chief Engineer, Arma Division, American Bosch Arma Corp. He was previously Technical Director for the Missile Guidance Department where he led the development of the essential components for the ICBM guidance program as well as making many contributions in the system planning. He is responsible for many patents in the areas of electronics, computer instrumentation and fire control systems. He has directed development of numerous fire control and gun direction systems, and initiated basic component and system developments embodied in essentially all Arma instruments and systems. Dr. Bock has received the Special Naval Ordnance Award and is listed in American Men of Science. He received the B.A. degree in 1929 from Kalamazoo College and the Ph.D. degree in 1933 from Yale University.

Lawrence H. Dworetzky is Associate Head, Special Products Engineering Department at General Precision Laboratories, where he participated in the early development of Doppler navigators and later managed a group devoted to the development of Doppler-inertial navigators. Prior to that Mr. Dworetzky served as Instructor and later as Assistant Professor at Cooper Union, where he taught theoretical and applied mechanics, electricity, magnetism and other courses in physics. He received the B.M.E. in 1943 and the M.M.E. in 1948, both from New York University.

Andrew Edwards is Section Head for Advanced Development, Special Products Department, at General Precision Laboratories, where he has been concerned with the design and flight testing of Doppler-inertial systems. He has worked for the Sperry Gyroscope Co. as a project engineer on the design and analysis of guidance systems for missiles. From 1954 to 1956 he was on active duty with the U. S. Army Signal Corps as an operations officer and later commanding officer of an electronic countermeasures unit. Mr. Edwards received the B.S. degree in electrical engineering in 1947 from Newark College of Engineering and the M.S., also in electrical engineering, in 1949 from Northwestern University.

Walter R. Fried is widely known for his contributions in antenna and Doppler radar design. He began his engineering education at Loughborough College, England, and received the B.S. degree from the University of Cincinnati in 1948, and the M.S. degree from Ohio State University in 1953, both in electrical engineering. At Communication and Navigation Laboratory of WADC he has worked on antenna design and long distance communication systems. He conducted early experiments in pulse propagation techniques via the ionosphere, which led to new modulation methods for long distance communication equipment. In 1956 he was appointed Section Chief in the Weapons Guidance Laboratory at WADC. He was a member of the U. S. delegation to the Sixth Communication Conference of the ICAO and the author of the U. S. position on self-contained navigation. Mr. Fried is presently Senior Scientist on the Research and Development Planning Staff, General Precision Laboratory.

William E. Frye is Consulting Scientist for Advanced Systems Research, and Manager, Subsystem D Guidance and Control Development, Lockheed Missiles and Space Division. He received his B.A. and M.S. degrees in physics in 1937 and 1938 from the University of Illinois, then his Ph.D. in 1941 from the University of Chicago for work on the determination of the atomic field of bromine from electron scattering. From 1948 to 1956 he was Leader, Guidance and Navigation Group, Electronics Division, Rand Corp., where he was responsible for accuracy and feasibility analysis of self-contained guidance and navigation systems, and at the same time was a lecturer at UCLA. From 1946 to 1948 he worked for North American Aviation, Inc.

Robert Bruce Horsfall is an authority on automatic guidance and astro tracking systems. He has written extensively in this field and holds numerous patents in it. He is currently Staff Specialist, Advanced Engineering Department at Autonetics. He received his B.A. degree from Reed College in 1930 and his M.A. and Ph.D.

degrees from the University of Illinois. He spent 10 years with the Bausch & Lomb Optical Co. joining North American Aviation's Aerophysics Laboratory in 1947 as a research engineer.

John Hovorka is Staff Physicist with the MIT Instrumentation Laboratory where he has been concerned with inertial navigation and fire control studies, and Lecturer with the MIT Department of Aeronautics and Astronautics. After receiving his B.S. degree from Queens College in 1942 and his M.S. degree from the University of Illinois in 1943 he then served at the Radiation Laboratory at MIT, working on the application of electronics to servo techniques in fire control. In 1946 he joined Gulf Research where he was engaged in applications of infrared spectroscopy.

Aubrey B. Mickelwait is Member of the Technical Staff, Guidance Research Laboratory, Space Technology Laboratories. He is a graduate of Carnegie Institute of Technology where he obtained his B.S., M.S. and Ph.D. degrees in physics. Dr. Mickelwait has published papers in the areas of quantum field theory, theoretical physics and meson theory. Since joining STL in 1955 he has been engaged in research and systems analysis work on the Atlas, Titan, Thor and Minuteman guidance systems, and also design work on trajectories, payloads and guidance systems for space vehicles such as the Pioneer and Explorer.

Charles J. Mundo is Staff Consultant, Arma Division, American Bosch Arma Corp. He is a specialist on guidance, specifically self-contained inertial and aided inertial systems and ground-based aided inertial systems. From 1942 to 1946, he was a Technical Specialist with the Air Force, doing development work on guided bombs, missiles and radar at MIT Radiation Laboratory. Subsequently, until 1951, he was engaged in instructing and research on nuclear isomers at the Carnegie Institute. Dr. Mundo is Consulting Editor on guidance for ARS JOURNAL and for ASTRONAUTICS, a member of the American Rocket Society's Technical Panel on Guidance and also a director of the New York and Long Island Sections of ARS. He received his B.S. and Sc.D. degrees from the Carnegie Institute.

John A. O'Keefe, long one of the nation's top geodesists, has won new fame by "changing" the shape of the Earth. Now with NASA, he had been with the Army Corps of Engineers for 15 years and had been Chief of the Research and Analysis Branch, Geodetic Division, Army Map Service. Actively engaged in the study of measurement of long distances by means of Earth satellites, Dr. O'Keefe has worked on measurement of long distances, including the distance to the moon, by means of occultations, measurement of intercontinental distances by eclipses and theories of map projection. He received a B.A. degree from Harvard College and a Ph.D. from the University of Chicago.

Richard W. Powell has written numerous technical papers and is considered a leading authority on infrared devices and their applications. He received his B.S. and M.S. degrees in electrical engineering in 1940 and 1947 from the California Institute of Technology. From 1940 to 1948 he was affiliated with Lockheed and then G. M. Giannini and Co., Inc. as Chief Development Engineer. Since 1950 he has been employed by the Aerojet-General Corp. where he is now Manager, Avionics Division. Prior to this he was Chief Engineer, exercising supervision of research, development and pilot production of infrared systems and sub-assemblies.

Edward V. B. Stearns is Research and Development Scientist, Advanced Systems Research, and Manager, Requirements Evaluation, XA Weapon System at Lockheed Missiles and Space Division. As Manager of the Inertial Guidance Department in 1957–1958, he directed efforts on analysis, design and development of inertial guidance systems. Prior to that he was with J. B. Rea Co. as project engineer, Radioplane Co. and the Rand Corp., where he conducted detailed analytical studies of navigation and reconnaissance systems with particular emphasis on long range inertial navigation systems, and also with Douglas Aircraft Co., Inc. Mr. Stearns was affiliated with the University of California Radiation Laboratory where he built and tested model magnets for a projected uranium separation plant. He received his B.A. in physics from the University of California in 1943 and did graduate work in physics, mathematics and engineering from 1947–1952.

E. King Stodola is Special Engineering Consultant to the President of Reeves Instrument Corp., and director of the Engineering Liaison Department. Before joining Reeves in 1947, Mr. Stodola was with the Signal Corps Engineering Labs at Belmar, N. J. as Chief of the Special Development Section, working on pulsed Doppler and other radar projects, and was associated with the first moon radar shots. He has been granted numerous patents in the fields of radar, communication and control systems. Mr. Stodola received the B.S. degree in electrical engineering in 1936 and the E.E. degree in 1947 from Cooper Union.

Albert Wheelon is Senior Member of the Technical Staff, Space Technology Laboratories, and Manager, Applied Physics Department. He received the B.S. degree in engineering science from Stanford University and the Ph.D. for work on meson theory of nuclear forces from MIT where he was a teaching fellow. Dr. Wheelon is currently working on ballistic missiles, space vehicles and radiowave propagation. His research has been directed to elasticity, tropospheric and ionospheric scatter propagation and the associated problems of turbulence theory, line-of-sight phase and amplitude instabilities, applied mathematics, and orbital analysis for Earth satellites, ballistic missiles and space vehicles. He is a consultant to the Director of the National Bureau of Standards, Boulder Laboratories and a lecturer in the Engineering Department at UCLA.

Mundo

O'Keefe

Powell

Stearns

Stodola

Wheelon

IGY Results on the Shape of the Earth

JOHN A. O'KEEFE

Goddard Space Flight Center, NASA
Silver Spring, Md.

Before guidance has any meaning one must know where the vehicle has to go. In terrestrial navigation, this is defined by the cartographer, in space by the astronomer. The "where" is defined by geodetic charts. The accuracy of these charts control the accuracy of guidance, unless some terminal contact procedure is used.

At the beginning of the space age there were large uncertainties in the mapping of the relative positions between the American and Eurasian continents. It was necessary, in a cartographical sense, to connect these continents if precision guidance were to have any meaning. Tracking data from the IGY satellites have afforded us that opportunity. A second and perhaps unexpected result of the satellite tracking effort was Dr. O'Keefe's discovery that the Earth was not an oblate sphere, but was instead slightly pear-shaped, with a bulge in the southern hemisphere. This newly discovered undulation in the shape of the Earth not only affects terrestrial guidance, but also will affect the precision space trajectories that must be followed when flights are undertaken to other planets.

Because of the impact of these results, it is appropriate to start this special issue on guidance with a review of information on the shape of the Earth.

—C. J. MUNDO

THE INTERNATIONAL Geophysical Year has brought the answer to a fundamental question about the nature of the Earth's gravitational field. This question relates to the broad scale undulations of the field, that is, to the size of the waves in the field whose wave length is comparable with the Earth's circumference.

There appeared in 1958 two important books on the Earth's field which presented diametrically opposite points of view on this fundamental question (1, 2).[1] One of these books was the fifth edition of "The Earth" by Jeffreys. In it the height of the low harmonics—the above-mentioned very long waves—was estimated to be about 100 m in terms of the rise and fall of the sea level surface of the Earth above a mathematical ellipsoid. Jeffreys reached this estimate by a harmonic analysis of the existing gravity information but without reference to the theory of isostasy. (See (1), p. 178.)

On the other hand, Heiskanen and Vening Meinesz (2) asserted that the Earth's field was much smoother. They did not analyze the gravity in spherical harmonics; their results, therefore, were not immediately comparable with those of Jeffreys. They did, however, elaborate what they referred to as the basic hypothesis of geodesy, which furnishes the basis for comparison. (See (2), pp. 72–73.) The basic hypothesis of geodesy asserts that the Earth approaches rather closely to a spheroid of fluid equilibrium. Deviations from the spheroid of fluid equilibrium should be measured, they suggested, in terms of the product P of the number of milligals of anomaly Δg by the area of the anomaly A in square megameters, i.e.

$$P = A\Delta g$$

For any individual patch of gravity anomalies, they suggested that there should be an upper limit to P, and that this upper limit is, in fact, approximately 30 milligal (megameters)^2. They further suggested that the Earth's surface does not contain more than 10 such areas.

Heiskanen and Vening Meinesz employed their basic hypothesis to justify the calculation of the height of the sea level surface (above an assumed mathematical ellipsoid) at a fixed point from gravity measurements within 3000 km of the point. Evidently, this approach is only possible if there is no important contribution from remote areas to the potential at the fixed point. In fact, the authors calculated that the expected contribution from the 10 or so patches of large anomaly will be of the order of 2.6 m. Heiskanen and Vening Meinesz do not confirm the broad harmonics of Jeffreys, and in effect they assert that these harmonics yield overall disturbances nearer 3 m than 100.

As a result of the measurements of positions of satellites during the IGY, especially the measurements of 1957 Beta 2 made by King-Hele and his collaborators in England (3) on the one hand and the radio interferometer measurements made in the western hemisphere by NRL on 1958 Beta 2 and 1958 Epsilon, it has been possible to determine empirically several of the broad scale undulations of the surface of the Earth.

The methods which have been employed to find even harmonics depend on the fact that these harmonics cause secular (i.e., progressive, as opposed to periodic) motions of the perigee and node of satellite orbits. The node of a satellite orbit is the line along which the orbital plane intersects the plane of the Earth's equator. The right ascension of the node Ω is measured from the vernal equinox. It regresses (moves clockwise as seen from the north) at the rate

$$\dot{\Omega} = \frac{3}{2}\frac{n\cos i}{p^2 GM_\oplus} A_{2,0}$$

where

n = mean motion of the satellite in the orbit
i = inclination
p = semiparameter of the orbit
G = universal constant of gravitation
$M_\oplus$ = Earth's mass
$A_{2,0}$ = coefficient of the zonal harmonic of the second degree in the expansion of the Earth's gravitational field

At the same time, the argument of perigee ω increases. The argument of perigee is the geocentric angle in the plane of the orbit from the line of nodes to the perigee. The rate of

Received Nov. 12, 1959.

[1] Numbers in parentheses indicate References at end of paper.

increase of the perigee is given, to the first order, by

$$\dot{\omega} = \frac{3n}{p^2 GM_\oplus}\left(1 - \frac{5}{4}\sin^2 i\right)A_{2,0}$$

From these two expressions, it is possible to deduce the flattening of the Earth; this was done by Hertz and Marchant (4) and later by numerous others. All found that the international value of $A_{2,0}$ of approximately 17.37 in megameter-kilosecond units was wrong; the value is certainly very close to 17.56.

There are higher order corrections to the two simple formulas given, which take into account the effects of the fourth zonal harmonic. On this point there has been some controversy; very recently a solution has been arrived at, and all investigators agree in assigning a small positive value to the fourth harmonic.

Of the odd harmonics, those of the first degree can be ignored. These correspond to a displacement of the origin of coordinates from the center of gravity. No real evidence has as yet been deduced for such a shift. In fact, in setting up the Vanguard coordinate system, a determined attempt was made (5) to place the origin at the Earth's center.

The harmonics of degrees three and five produce perturbations in the inclination of the orbit, its eccentricity, the right ascension of the node and the argument of perigee. The calculation of these rates of change is made by the method of variation of constants (6) which are closely related to the Hamiltonian equations

$$\frac{dq}{dt} = \frac{\partial H}{\partial p} \qquad \frac{dp}{dt} = -\frac{\partial H}{\partial q}$$

Here the quantities q, p are coordinates and their conjugate momenta, H is the Hamiltonian function (essentially the total energy, kinetic plus potential), and t is the time. By using elements which are very nearly constant, the Hamiltonian can be split into a constant part, which can be left out, and a small perturbation function R. The ordinary elements are not really canonical variables, and so the equations are not as neat as those given above. But we still find that the time derivative of each element can be expressed in terms of the derivative of the variable function R with respect to other elements. Once the perturbation function has been obtained, the calculations of the variations of the elements is easy.

Both Kozai (7) and the NASA group (8) have found that the observed perturbations are accounted for by the third harmonic, with relatively little remaining to be accounted for by higher odd harmonics.

In Table 1 are given the amplitudes of the corresponding zonal harmonics as determined by Jacchia (9) and Kozai (7) at Harvard, by King-Hele in England (3), and by the group at NASA (8).

In order to understand the significance of these figures, it is necessary to begin by noting the form which a fluid Earth, having the same angular momentum as the actual Earth, would assume. This has been dealt with by Henriksen (14) at the Army Map Service (1959) who finds that it should have a flattening of 1/300. From his theory can be found the second and fourth harmonics shown under the column "Theoretical Values" in Table 1. The number 1/300 will undoubtedly appear paradoxical as an estimate of the flattening of the fluid Earth, since the figure of 1/297.3 has been accepted for many years. The present situation is not that there has been an error in the past calculations of the flattening of the fluid Earth, rather that the previous calculations, such as those of Tisserand (10), were on a different basis, involving at one point the assumption that the actual flattening of the Earth agreed with that calculated by hydrostatic theory. Since we now know that this is not the case, it is obviously incorrect at the present time to calculate the hydrostatic flattening of the Earth on this basis. One can, however, substitute the measured value of the physical flattening of the Earth for this assumption.

Analytically, one may say that the precession determines the ratio $(C - A)/C$, C being the Earth's moment of inertia about the axis of rotation and A the moment of inertia about an axis in the equatorial plane; whereas the satellite measurements of the physical flattening determine for us the quantity $C-A$. The ratio of these two quantities is the quantity C, which is the Earth's moment of inertia around a polar axis. From C the hydrostatic value of the Earth's flattening can be determined by a mathematical argument, developed by Clairaut and refined by Airy (11) (covering some 76 equations in Tisserand), which although rather long, has been gone over so many times in the last century and a half that it is reasonably sure to be correct. It is in this way that Henriksen (14) determined the value of the hydrostatic flattening as 1/300. Corresponding to this are the values of the second and fourth zonal harmonics shown in the column marked "Theoretical."

If one refers the undulations, therefore, to this assumed figure for a fluid Earth, the amplitudes, which are shown in Table 1, are found for the geoid heights corresponding to the zonal harmonics of orders two, three and four. It will be seen at once that these values confirm the hypothesis of Jeffreys and are in direct contradiction to the ideas of Vening Meinesz and Heiskanen. The undulations of the geoid are indeed of the order of 100 m in height.

In this discussion, only the zonal harmonics of orders two, three and four have been evaluated; the more numerous tesseral harmonics which correspond to them have not been determined. It is very much more difficult to do this from studies of the satellites because the rotation of the Earth tends to average the effects of the tesseral harmonics, since these latter depend only on longitude. If there existed a satellite whose period was not far from a day, such as the proposed

Table 1 Summary of recent results on the Earth's gravitational field

Coefficients of the harmonics in the potential in units of megameters and kiloseconds

	Jacchia	King-Hele	Kozai	NASA	Theoretical	NASA-Theoretical $N_{n,0}$
$A_{2,0}$	-17.557 ± 0.010	-17.564 ± 0.003	-17.549*	-17.555 ± 0.001	-17.372	-72.1
$A_{3,0}$	...	...	0.228 ± 0.008	0.25 ± 0.03	0	$+15.4$
$A_{4,0}$	$+1.6 \pm 0.3$	$+0.9 \pm 0.15$	$+1.4$*	$+1.12 \pm 0.04$	$+1.95$	-8.0

* These values have been calculated, not from the quantities given in Smithsonian Rep. no. 22, but from privately communicated corrections to these values kindly supplied by Dr. Kozai.

24,000-mile satellite, it would be possible to fix the values of the tesseral harmonics fairly accurately. At the present time, the most probable hypothesis is that the values of the tesseral harmonics of a given order are comparable with the value of the zonal harmonics of the same order, since both are related to the strength of the Earth's interior at a certain critical depth. The critical depth depends upon the degree of the harmonic. Thus, as Jeffreys pointed out (1) harmonics of degree three require strength at the outer boundary of the core, and in general, harmonics of degree n require strength at a depth comparable with a/n, where n is the degree of the harmonic. In a way, therefore, the new discoveries indicate strength in the Earth's interior at various depths. This strength makes possible the existence of zonal and tesseral harmonics alike of a given degree. Hence, it is reasonable to suppose that there exist large tesseral harmonics of orders two, three and four. On the other hand, the rather small values for five and six may possibly indicate that all harmonics of these orders will be found to be small. This statement cannot be made with any great assurance; further evidence covering the magnitudes of the higher harmonics would be of great value.

From the point of view of theory of satellites and ballistic rockets at a distance not far above the Earth's surface, it is the low harmonics which produce the maximum perturbations. It is clear that in attempting to guess the midcourse errors in position of such bodies resulting from gravity, we must use the large estimates for the undulations of the geoid, such as those of Kaula (12) rather than the smaller ones.

Up to the present time, the observations of satellites have not given us any way of determining the zero-degree harmonic of the Earth's gravitational field. This is numerically equal to the product of the absolute constant of gravity by the total mass of the Earth. It has been possible, however, to determine this from measurements of the distance of the moon, especially those by Yaplee et al. (13). The results are still somewhat preliminary, but they hold great promise for the future. They suggest a value for GM of 398.618 which is close to the value expected from the best arc measurements at the surface of the Earth in combination with modern gravimetric measurements.

A remarkable feature of these results is the extent to which the Vanguard test sphere has figured. It would be difficult to imagine a simpler experiment than this: A spherical body is fired at an altitude such that altitude drag is small; it is equipped with a transmitting radio and nothing more; and it is observed regularly. Despite its simplicity, this experiment has been of great value for the unraveling of the figure of the Earth as well as the study of solar effects. The key to its usefulness lies, of course, in the length of time over which it has been observed and the persistence with which accurate measurements have been made.

References

1 Jeffreys, H., "The Earth," Cambridge University Press, 1958, p. 187.

2 Heiskanen, V. A. and Vening Meinesz, F. M., "The Earth and its Gravity Field," McGraw-Hill, 1958, pp. 72, 73.

3 King-Hele, D. G. and Merson, R. H., "A New Value for the Earth's Flattening Derived from Measurements of Satellite Orbits," *Nature*, vol. 183, 1959, pp. 881–882.

4 Hertz, H. G. and Marchant, M., Harvard Announcement Card no. 1408, June 24, 1958.

5 Fischer, I., *J. Geophys. Res.*, vol. 64, 1959, p. 73.

6 Moulton, F. R., "Celestial Mechanics," MacMillan, 1914, p. 399.

7 Kozai, Y., "The Earth's Gravitational Potential Derived from the Motion of Satellite 1958 β_2," Smithsonian Astrophys. Obs., Special Rep. 22, 1959, pp. 1–6.

8 O'Keefe, J. A., Eckels, A. and Squires, R. K., "The Gravitational Field of the Earth," *Astronomical J.*, vol. 64, 1959, p. 245.

9 Jacchia, L., "The Earth's Gravitational Potential as Derived from Satellites 1957 β_1 and 1958 β_2," Smithsonian Astrophys. Obs., Special Rep. 19, 1959, pp. 1–5.

10 Tisserand, F., "Traité de Mécanique Céleste," Gauthier-Villars, Paris, 1891.

11 Airy, Sir George B., Phil. Trans. Royal Soc., London, Series A, part III, 1826, p. 548.

12 Kaula, W., Army Map Service Technical Rep. no. 24, 1959.

13 Yaplee, B. S., Bruton, R. H., Roman, N. G., Craig, K. J. and Scanlan, T. F., "Radar Echoes from the Moon at a Wavelength of 10 Centimeters," Proc. IRE, vol. 46, no. 1, Jan. 1958.

14 Henriksen, S. W., "The Hydrostatic Flattening of the Earth," *Annals of IGY*, vol. 11, 1959.

ARS SOLID PROPELLANTS CONFERENCE

January 28–29, 1960

Princeton University, Princeton, N. J.

Unstable Burning—Theoretical
Unstable Burning—Experimental
Grain Design
Combustion, Gas Kinetics and Ignition
Interrelations of Nozzle Geometry and Nozzle Performance

Lunar Trajectories

AUBREY B. MICKELWAIT

Space Technology Laboratories, Inc.
Los Angeles, Calif.

The status of three-dimensional lunar trajectories and techniques for treating them analytically are reviewed. The problem of a lunar satellite is treated in detail. This study is framed in the light of equipment limitation and interaction. Curves showing the interrelationship of flight parameters and also miss coefficients are presented.

AT THE present time it is fair to say that the rudiments of lunar trajectories are well-understood both in analytical approaches and through extensive computer calculations. A bibliography of much of the published work has been included here, although, unfortunately, much important work is still buried in classified documents.

One might well ask, after the many years of extensive effort in celestial mechanics on the general study of motion in n-body gravitational fields (27),[1] why the field of lunar trajectories needs to be reopened at all. Unfortunately, most of the effort in classical mechanics has been of little value in understanding the type of orbits we deal with here, namely, highly eccentric elliptical or hyperbolic collision trajectories. Furthermore, the astronomical approach has not emphasized the study of orbits in terms of a set of variable initial conditions, the most useful approach for actual flight trajectories. On the other hand, it is true, as will be discussed later, that celestial mechanics has contributed much in the way of techniques for rapid and precise computation of what may be called navigational trajectories suitable for exact flight tables (2, 5, 30).

An important point in the treatment of lunar flight mechanics is that the equipment limitations and interactions be introduced into the analysis at as early a stage as possible; otherwise, the analysis tends to evolve in a needlessly complex way, one which is difficult to apply in realistic situations and is often overoptimistic. For this reason, the paper is concerned with the relationships between specific trajectories and the overall system; that is, it will include a discussion of practical trajectory problems, although the theoretical trajectory aspects will also be reviewed.

A space mission is a complex of relationships among the purpose of the mission, the general characteristics of the vehicle's propulsion system, the overall probability of successfully completing the mission, and an extensive set of systems considerations which include vehicle configuration, propulsion, payload, minimum and maximum permissible burnout velocity, powered flight guidance, ground tracking systems, position of launch site, range safety, free-flight guidance and control, target approach velocity, distance of closest approach to the target, the terminal injection propulsion system, etc. A superficial picture of system considerations for a space mission might run as follows.

If our mission is to satellite the moon, we must first have the propulsion necessary simply to place some payload weight at a minimum velocity. The payload required may be precisely defined by the purpose of the mission (i.e., 100 lb of experiments and structure may be specified). In addition, certain of the experiments may place constraints upon later portions of the trajectory and in turn on the vehicle itself. In general, to make the most measurements for the greatest length of time and in the most detail, the approach velocity to the moon should be as low as possible. Of course, since we are to satellite the moon, the velocity of the vehicle with respect to the moon must be reduced, and this in turn requires a propulsion unit in the payload which can produce the required change. The amount of propulsion required is, of course, not only a function of the thrust of the engine and specific impulse of propellants, but it is also a function of how close it is planned to come to the moon initially, the approach velocity and the properties of the subsequent satellite orbit. The attitude of the vehicle or, more precisely, the orientation of the terminal propulsion system must also be determined. If the attitude is fixed in inertial space by, say, spin stabilization, then the problems of orientation during powered flight must be weighed against the increased effectiveness of the retarding thrust near the moon. Furthermore, the trajectory must be designed so that an appropriate ground station can "see" the vehicle at the right time despite the rotation of the Earth, since a simple timer adjusted before launch is probably not a satisfactory solution.

Of course, all of these terminal problems reflect back to the booster stages and their flight characteristics. The accuracy of burnout guidance is crucial. If the final stage is essentially unguided, as is the case when a simple solid propellant third stage is used, the "miss" at the moon with such a stage, were there no subsequent corrections, would be so great that the probability of success of the mission would be too low to justify the attempt. Thus, in addition to booster guidance, vernier corrections to the payload at some later time in the trajectory are also required. So, just as terminal requirements for payload weight affect the vehicle configuration, the contributions of midcourse and terminal guidance affect the booster guidance necessary to achieve a final specified accuracy. But then the propellant and structure required for vernier corrections also must be included in the payload, and so on.

Because of the rotation of the Earth, only a small part of each day is possible for launching a vehicle to the moon. Moreover, because the plane of the moon is inclined with respect to the equator, the vehicle's trajectory plane is inclined to both, and, as a consequence, feasible launch periods during a given day during the lunar month have differing accuracy and propulsion requirements.

The point of this brief and loose summary of interrelationships in a spaceflight is to emphasize the extreme dependence of each aspect upon the other and, in particular, to emphasize the central role played by orbital analysis (29).

General Orbital Kinematics and Guidance Analysis

Planar Dynamics in the Earth's Field

It is impossible to solve completely the equations of motion

Received July 17, 1959.

[1] Numbers in parentheses indicate References at end of paper.

of a vehicle in the combined Earth-moon gravity field. Instead, the analysis usually proceeds in an approximate fashion along the following lines (5,10,26,33). The transit of vehicle from Earth to moon is treated as a succession of two-body problems; that is, the vehicle is controlled solely by the Earth's field in the initial phase and then passes into a terminal region where only the moon controls its motion. To further simply the problem, it is assumed that the moon moves in a circular orbit about an inertial Earth; the influence of both the sun's and the moon's mass on the Earth's motion is ignored. First, the properties of the orbit will be analyzed by restricting our attention to the planar dynamics.

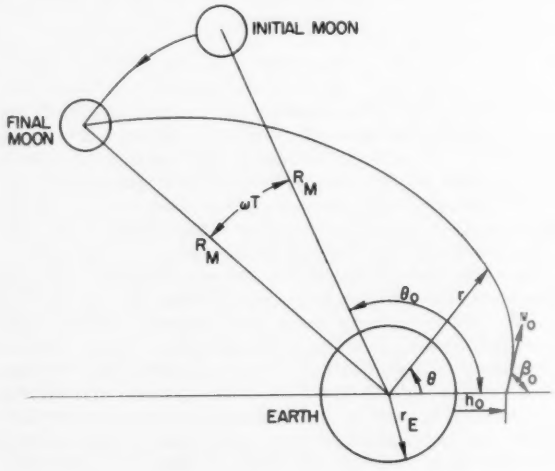

- ω – ANGULAR VELOCITY OF MOON
- T – TOTAL TIME OF FLIGHT
- r, θ – NONROTATING POLAR COORDINATES OF VEHICLE
- v_0 – BURNOUT VELOCITY
- β_0 – BURNOUT FLIGHT PATH ANGLE
- r_E – RADIUS OF EARTH
- h_0 – BURNOUT ALTITUDE
- ωT – ANGLE MOON ROTATES DURING TIME OF FLIGHT
- R_M – DISTANCE FROM THE CENTER OF THE EARTH TO THE CENTER OF THE MOON
- θ_0 – INITIAL POSITION OF MOON

Fig. 1 Planar geometry

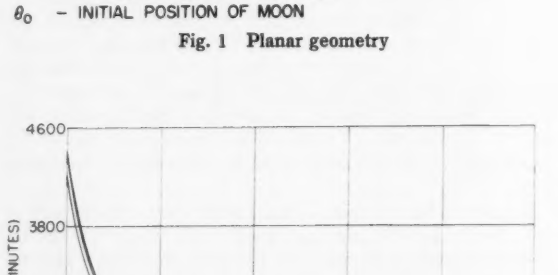

Fig. 2 Time of flight t vs. burnout velocity v_0 for various flight path angles at burnout (h_0=200 nautical miles)

Although strictly speaking, the vehicle does not move in a plane passing through the center of the Earth, for our purposes we can assume it does. Using a polar coordinate system with origin at the Earth's center of mass (assumed spherical in shape) with r = the radial distance to the vehicle, θ the in-plane angle measured from the burnout radius (see Fig. 1), the vehicle's equations of motion may be written as

$$\ddot{r} - r\dot{\theta}^2 = -\mu_E/r^2 \quad [1]$$

$$r\ddot{\theta} + 2\dot{r}\dot{\theta} = 0 \quad [2]$$

where $\mu_E = GM_E = 1.4077 \times 10^{16}$ ft^3/sec^2 is the universal gravitational constant times the Earth's mass. Equations [1 and 2] yield two first integrals which state that energy per unit mass E and angular momentum per unit mass J are conserved

$$E = \frac{1}{2}[\dot{r}^2 + (r\dot{\theta})^2] - \frac{\mu_E}{r} = \text{constant} \quad [3]$$

$$J = r^2\dot{\theta} = \text{constant} \quad [4]$$

Since we ignore the moon's mass in the initial phase, an interesting class of orbits is also ignored (33). These orbits are true minimum energy trajectories, because the mass of the moon is used to pull the vehicle during multiple revolutions of the Earth to the moon. "Minimum energy," as usually used in design analysis, means the minimum energy to reach the moon's vicinity while moving on an ellipse and without considering the moon's field. The difference between the two definitions implies a change of burnout velocity of approximately 200 fps. The class of orbits ignored poses difficult guidance problems and is interesting only as a mathematical oddity.

Equations [3 and 4] yield immediately the two planar properties of interest

$$t = \int_{r_0}^{r_1} \frac{dr}{\sqrt{2E + \frac{2\mu_E}{r} - \frac{J^2}{r^2}}} \quad [5]$$

$$\theta = \int_{r_0}^{r_1} \frac{J\,dr}{r^2\sqrt{2E + \frac{2\mu_E}{r} - \frac{J^2}{r^2}}} \quad [6]$$

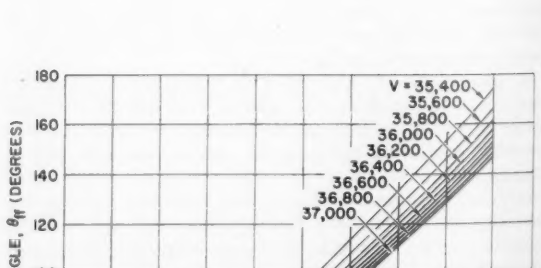

Fig. 3 Free-flight in-plane angle θ_{ff} vs. burnout flight path angle β_0 for various velocities at burnout (h_0=200 nautical miles)

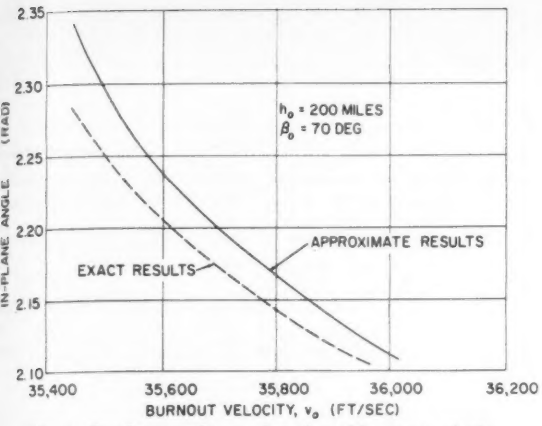

Fig. 4 In-plane angle as a function of burnout velocity

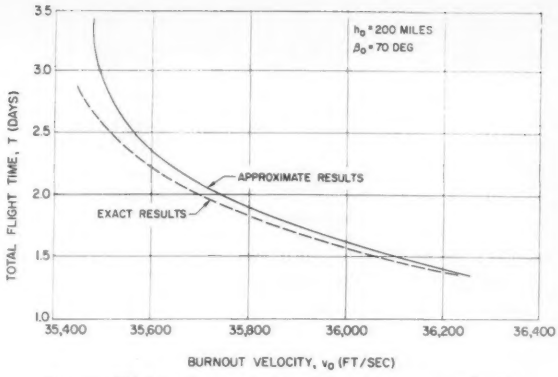

Fig. 5 Flight time as a function of burnout velocity

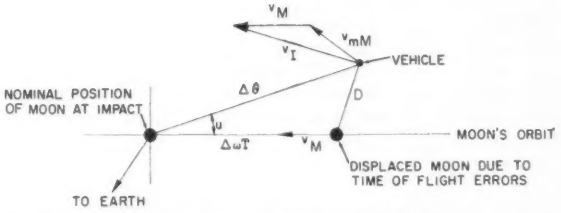

Fig. 6 Details of geometry in the vicinity of the moon

where

t = time of flight
θ = angle turned from an initial radius r_0 to a final radius r_1

It should be noted in these equations that both t and θ depend, through E and J, on all initial conditions, say, v_0, r_0 and β_0; where v_0 is the burnout velocity, r_0 the burnout radius, and β_0 the burnout flight path angle (see Fig. 1). However, Equation [5] shows that the time of flight should be insensitive to β_0 for orbits with large changes in r, since β_0 enters the integral only through J^2/r^2, which will contribute little to t as soon as r has increased appreciably. The same argument applies to θ; that is, θ will depend strongly on β_0 through the J term in the numerator of Equation [6]; however, both θ and T will depend only on E in the denominator rather than r_0 and v_0 separately. Lunar orbits can then be categorized to a good approximation by burnout energy and flight path angle alone.

Setting r_0 equal to the burnout radius and r_1 equal to the radius of a mean circular orbit, 1.261×10^9 ft, we have the flight time and in-plane angle as functions of β_0 and v_0 as in Figs. 2 and 3. Unless specifically varied, h_0 and β_0 are assumed to be 200 nautical miles and 70 deg, respectively, which are realistic values for the kinds of vehicles under consideration.

Because the effect of the moon has been ignored, the flight times and in-plane angles calculated from Equations [5 and 6] should be only approximately valid. The approximation should become increasingly poor as minimum energy is approached and the vehicle spends more time in the combined field of Earth and moon before arrival. This is borne out by the curves labeled "exact results" in Figs. 4 and 5, which represent exact numerical integration of the complete three-body problem. It is evident from Figs. 4 and 5 that there are errors of 4 deg in θ and 5×10^5 sec in T at low velocities, so that the analytic results are adequate for navigational calculations only when burnout velocities are several hundred feet per second above minimum. As far as some design criteria involving total time of flight and the in-plane angle θ, such as visibility from ground tracking stations, the results in Figs. 4 and 5 are adequate.

To integrate the entire system properly, however, two additional steps must be taken. First, the effects of lunar gravity must be included in some approximate fashion; second, the effect of the relative orientation of the lunar, equatorial and vehicle's planes on the launch conditions must be considered (i.e., the three-dimensional problems).

Planar Dynamics in the Moon's Field

The effect of the moon's gravity on the vehicle's orbit can be treated with varying degrees of sophistication. However, the simplest approximation is accurate enough for design criteria. Thus, instead of stopping the trajectory at some radius short of R_m the mean circular lunar radius, turning off Earth's gravity, and then injecting into the moon's gravity, we take the conditions from the previous analysis at $r = R_m$ and regard them as occurring at an infinite distance from the moon. This is possible, of course, only because the moon's gravity has a significant effect over a distance that is small compared to the entire trajectory.

It is useful in discussing guidance accuracies and approach conditions to convert the injection conditions relative to the Earth into the three frequently used parameters: V_{mM} the velocity relative to the moon at injection into the lunar gravity field; $\bar{b}$ the vector impact parameter, that is, the vector distance that would occur between the moon and the vehicle's trajectory if the moon had no gravity; and u the inclination of the vehicle's plane relative to the lunar orbital plane, again ignoring the lunar gravity field (see Fig. 6).

In the particular case that $u = 0$ (see Fig. 7), i.e., the vehicle flies in the lunar orbit plane, it is a simple matter to relate b and V_{mM} to other properties of the approach trajectory near the moon. Assuming the approach trajectory can be calculated from one-body relations in a coordinate system centered at the moon, and that this is consistent with the other approximations in this analysis, we find that the approach trajectory is always hyperbolic, since the vehicle's energy is always positive relative to the moon. The trajectory can be described in polar coordinates centered at the moon by

$$r = J^2/\mu_m(1 + e \cos \theta) \qquad [7]$$

where

θ is measured from distance of closest approach
J = angular momentum relative to the moon
$\mu_m \cong (1/81.45)\mu_E = GM_m$

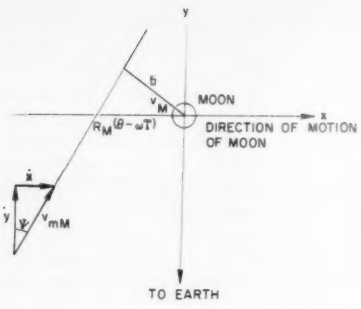

b - IMPACT PARAMETER (PERPENDICULAR DISTANCE BETWEEN THE MOON'S CENTER AND ASYMPTOTE OF THE INCOMING HYPERBOLA
v_M - VELOCITY OF THE MOON
v_{mM} - VEHICLE VELOCITY RELATIVE TO THE MOON
R_M - DISTANCE FROM VEHICLE TO MOON AT TIME VEHICLE CROSSES $(\theta-\omega T)$ MOON'S ORBIT
ψ - ANGLE BETWEEN THE V_{mM} AND THE y-AXIS
x,y - RECTANGLAR COORDINATES CENTERED AT MOON (x IN MOON'S ORBIT, y ALONG RADIUS TO EARTH)

Fig. 7 Geometry in the vicinity of the moon

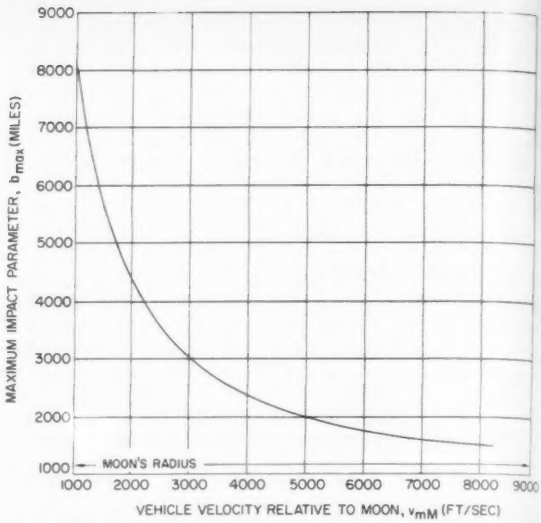

Fig. 8 Maximum impact parameter as function of vehicle velocity relative to the moon

e is the eccentricity of the approach hyperbola and can itself be determined from

$$e = (1 + 2EJ^2/\mu_m^2)^{1/2} \quad [8]$$

so that when E and J are specified in terms of velocity of the vehicle with respect to the moon at large distances from the moon V_{mM} and b, the orbit around the moon is determined. Now

$$J = bV_{mM} \quad [9]$$

and

$$E = (1/2)(V_{mM})^2 \quad [10]$$

Using Equations [7 to 10], and letting D be the distance of closest approach, the following relation between b, V_{mM} and D can easily be derived

$$b = D\sqrt{1 + 2\mu_M/DV_{mM}^2} \quad [11]$$

With D the moon's radius, Equation [11] gives the maximum value allowed for b for an impact to result (see Fig. 8). For the lowest possible V_{mM} (~4000 fps) corresponding to minimum energy at takeoff, the second term in Equation [11] is the order of unity. In other words, at low velocities the geometrical cross section is effectively doubled by the lunar gravity. Since dV_{mM}/dv_0 is about equal to 8, the focusing effect is practically gone at takeoff velocities much above 36,000 fps.

It is relatively simple to relate $\dot{r}$ and $r\dot{\theta}$ the two polar components of velocity relative to the Earth to V_{mM} in the case that $u = 0$, as follows

$$V_{mM} = \sqrt{\dot{r}^2 + (r\dot{\theta} - V_m)^2} \quad [12]$$

where V_m is the moon's orbital velocity ~3340 fps.

Again, in the case that $u = 0$, we see from Fig. 7 that $R_m \times (\theta - \omega T)$ is the distance from the moon at time of crossing the lunar orbit. This, of course, is not the distance of closest approach, since the vehicle will be closer either before or after crossing the lunar orbit unless V_{mM} is parallel to a radial line from the Earth; the relation between b and $R_M(\theta - \omega T)$, however, is obtained from

$$b = \cos\psi\, R_m(\theta - \omega T) \quad [13]$$

where

$$\psi = \tan^{-1}(V_m - r\dot{\theta})/\dot{r} \quad [14]$$

The quantity $(\theta - \omega T)$ is useful in guidance analysis, since it can be related to dispersions in initial conditions directly through Equations [5 and 6]. That is

$$\Delta(\theta - \omega T) = (\theta - \omega T - \theta_0) - (\theta - \omega T - \theta_0)_0 = \left[\frac{\partial(\theta - \omega T)}{\partial q_i}\right]\Delta q_i + \ldots \quad [15]$$

where q_i is any of the initial velocity and position variables, such as v_0, β_0 and r_0. For a successful impact $(\theta - \omega T - \theta_0)_0$ is nominally set equal to zero, of course, and the coefficients $\partial(\theta - \omega T)/\partial q_i$ give the first-order effects of initial dispersions Δq_i.

Three-Dimensional Considerations

In the case that u is not equal to zero, the terminal geometry connecting velocities and positions relative to the Earth to injection conditions in the approach hyperbola is much more involved (14,26). However, the picture can be simplified by noting that for velocities only several hundred feet above minimum the vehicle is traveling essentially radially from the Earth when it approaches the moon, so that the distance of closest approach (or miss distance in the case of impact missions) is given to a good approximation by

$$D = R_m[(\Delta\theta - \omega\Delta T)^2 + 4\Delta\theta\omega\Delta T \sin^2(u/2)]^{1/2} \quad [16]$$

In the event that initial conditions can be chosen such that $(\Delta\theta - \omega\Delta T)$ vanishes, then D is directly governed by the inclination between the planes u. In the low velocity case, where this sort of picture is not valid, it turns out that the inclination has relatively small influence anyway, and answers obtained with $u = 0$ continue to give realistic results.

Before discussing the interaction of ballistic error coefficients with burnout conditions, the geometrical relationship of inclination u with burnout conditions will be established. It is convenient to specify launch variables and lunar position in an inertial coordinate system such as in Fig. 9. We are ignoring, of course, the Earth's motion around the Earth-moon barycenter and the barycenter's motion around

he sun. Following astronomical convention (15), the line of intersection of the equatorial plane and the moon plane, the "nodal line," is taken as one axis. In Fig. 9, Earth longitudes λ_b are measured in the equator with respect to the unar descending node, the moon's longitude λ_m with respect o the same node in the moon plane. We can imagine the various great circles, equator, vehicle trajectory and moon's orbit on a sphere surrounding the Earth, and from the resulting geometrical relationships it is easy to show that

$$\sin u = \frac{\sin \lambda_b \sin [\phi_0 + \sin^{-1} (\sin \gamma \sin i)]}{\sin \gamma \sin \theta(\lambda_b, \lambda_M)} \qquad [17]$$

nd in-plane angle from burnout to impact

$$\theta = \cos^{-1} \{\cos (\lambda_M - \gamma) \cos [\phi_0 + \sin^{-1} (\sin \gamma \sin i)] + \sin (\lambda_M - \gamma) \sin [\phi_0 + \sin^{-1}(\sin \gamma \sin i)] \times \sqrt{1 - (\sin^2 \lambda_b \sin^2 \gamma)}\} \ldots \qquad [18]$$

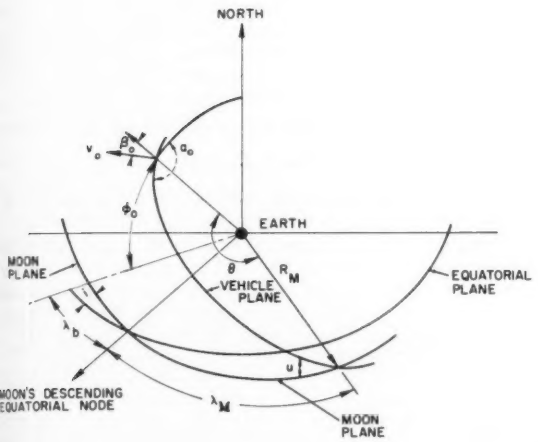

α_0 BURNOUT AZIMUTH
v_0 BURNOUT VELOCITY
β_0 BURNOUT FLIGHT PATH ANGLE
ϕ_0 LATITUDE OF BURNOUT POINT
θ IN-PLANE ANGLE
R_M RADIUS OF MOON
i INCLINATION OF MOON PLANE TO EQUATORIAL PLANE
λ_M LONGITUDE OF MOON FROM ITS DESCENDING EQUATORIAL NODE
u ANGLE BETWEEN MOON PLANE AND VEHICLE PLANE
λ_b LONGITUDE OF BURNOUT POINT FROM MOON'S DESCENDING EQUATORIAL NODE

Fig. 9 Geometry of Earth to moon trajectory

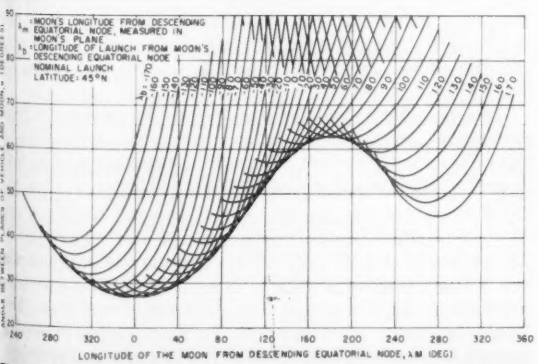

Fig. 10 Angle between vehicle plane and moon's plane u vs. position of moon at impact λ_m^I for various launch longitudes

Burnout flight path azimuth

$$\alpha_0 = \sin^{-1} [\sin \lambda_b \sin \gamma \sin (\lambda_M - \gamma)/\sin \theta] \qquad [19]$$

where

γ = $\tan^{-1}(\tan \lambda_b/\cos i)$
ϕ_0 = burnout latitude
i = inclination of the lunar plane with respect to the equator (~18.5 deg in 1959)
λ_m = longitude of the moon at impact

It is important to note from Equations [17, 18, and 19] that u, θ and α_0 are fixed once λ_b (essentially the time of day) and λ_m (day of the month) are specified. Furthermore, as shown above, θ is determined also by the burnout variables v_0, γ_0 and β_0; therefore, the time of day and day of month directly interact with the trajectory conditions at the beginning of free flight through the in-plane angle θ.

Figs. 10, 11 and 12 show the dependence of u, θ and α_0 on λ_b and λ_m. As is apparent from Fig. 10 and as can be deduced from Equation [17], the minimum inclination for any burnout energy occurs when launch conditions are adjusted so that $\lambda_b = -90$ deg.

On the other hand, for any burnout velocity, the orbit with the maximum allowable azimuth occurs when the moon at impact is farthest south, that is, when $\lambda_M = 90$ deg. Since

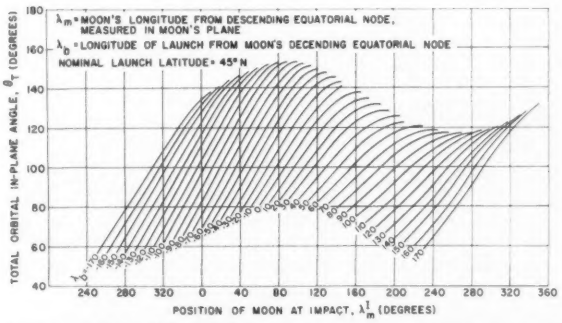
λm = MOON'S LONGITUDE FROM DESCENDING EQUATORIAL NODE, MEASURED IN MOON'S PLANE
λb = LONGITUDE OF LAUNCH FROM MOON'S DECENDING EQUATORIAL NODE
NOMINAL LAUNCH LATITUDE = 45° N
TOTAL ORBITAL IN-PLANE ANGLE, θT (DEGREES)
POSITION OF MOON AT IMPACT, λmI (DEGREES)

Fig. 11 Total orbital in-plane angle θ vs. position of moon at impact λ_m^I for various launch longitudes

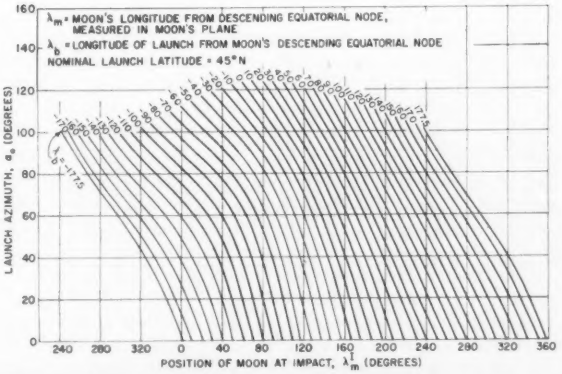
λm = MOON'S LONGITUDE FROM DESCENDING EQUATORIAL NODE, MEASURED IN MOON'S PLANE
λb = LONGITUDE OF LAUNCH FROM MOON'S DESCENDING EQUATORIAL NODE
NOMINAL LAUNCH LATITUDE = 45° N
LAUNCH AZIMUTH, α0 (DEGREES)
POSITION OF MOON AT IMPACT, λmI (DEGREES)

Fig. 12 Launch azimuth α_0 vs. position of moon at impact λ_m^I for various launch longitudes

orbits with burnout azimuths near 90 deg take maximum advantage of the Earth's rotation, the class of orbits with burnout velocities less than 36,100 fps (see Fig. 12) which impact when the moon is halfway between descending and ascending nodes makes most efficient use of the booster capabilities. The dependence of θ on λ_b and λ_m can also place a real restriction on burnout conditions. Equation [18] shows that the maximum allowable θ decreases from 180 deg (at latitudes between ± 18 deg) to $\theta \leqq 108$ deg at the North Pole (see Fig. 13) as the burnout latitude is moved northward. Since θ increases with decreasing velocity (see Fig. 4) there is evidently a minimum allowable velocity depending upon the burnout latitude which is above the theoretical two-dimensional value

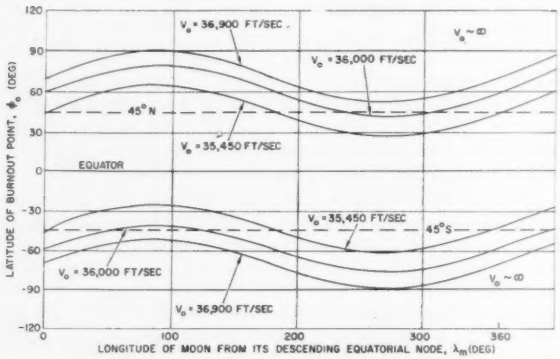

Fig. 13 Maximum allowable latitudes of burnout for various times of the lunar month

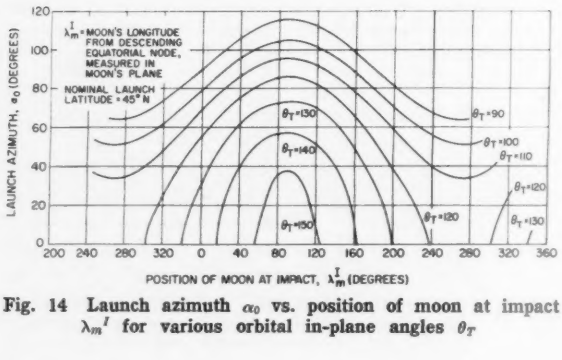

Fig. 14 Launch azimuth α_0 vs. position of moon at impact $\lambda_m{}^I$ for various orbital in-plane angles θ_T

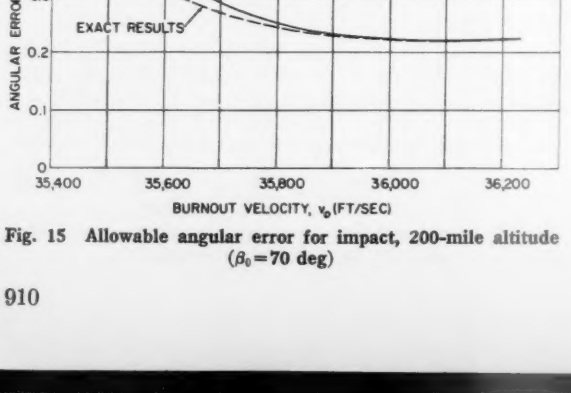

Fig. 15 Allowable angular error for impact, 200-mile altitude ($\beta_0 = 70$ deg)

("Hohmann" transfer ellipse). Restricting burnout azimuths to easterly directions for various practical reasons will raise even further the minimum burnout velocity as is evident from Fig. 14, obtained by eliminating λ_b between $\alpha_0(\lambda_b, \lambda_m)$ and $\theta(\lambda_b, \lambda_m)$ to give $\alpha_0(\theta, \lambda_m)$. In practical analysis the burnout point can be related to the launch point by assuming a planar orbit during powered flight having an in-plane angle θ_{p_f}. Since θ_{p_f} can be of the order of 15 to 20 deg, this will further restrict takeoff conditions significantly. In short, the geometry of the Earth-moon-vehicle planes imposes definite constraints on allowable burnout conditions and defines preferential launch times and dates throughout the lunar month.

Free-Flight Dispersions (6,11,26,33)

The variation of u with time and burnout variables, together with the dependence of closest approach on u (see Eq. [16]) implies a daily variation of sensitivity on impact to errors in burnout conditions. We do not consider dispersions in position here because guidance systems can control these much better than they can control the burnout velocity vector. The sensitivity of lunar trajectories to azimuth and flight path angle variations can be calculated from purely geometrical considerations. An azimuth variation $\Delta\alpha_0$ is equivalent to rotating the orbit plane around the burnout radius r_0 so that

$$\partial b/\partial\alpha_0 = R_m \sin\theta \qquad [20]$$

Since θ is a slowly varying function of v_0 (see Fig. 4), azimuth sensitivity is relatively independent of v_0 over the range of velocities of practical interest. Flight path angle dispersions are not related as directly to impact parameter dispersions, since β_0 enters the dynamic variable J. As noted in the discussions following Equations [5 and 6], the time of flight is largely independent of β_0, thus the "on orbit miss" $R_m \times \Delta(\theta - \omega T)$ for a flight path angle variation is given by

$$R_m\Delta(\theta - \omega T) = R_m(\partial\theta/\partial\beta_0)\Delta\beta_0 \qquad [21]$$

Furthermore, it can be deduced from Equation [5] that $\partial\theta/\partial\beta_0$ is essentially independent of velocity and equal to 2 for $\beta_0 \sim 70$ deg. The on orbit miss is therefore given by $2R_m\Delta\beta_0$. However, as we have already observed (see Eq. [13]), the dispersed impact parameter Δb assuming the nominal value equal to zero, can be directly related to $R_m\Delta(\theta - \omega T)$. The conclusion is then that $\partial b/\partial\beta_0$ is essentially independent of burnout velocity, but as we have already noted in Equation [11], the maximum allowable dispersion in b is itself a function of burnout velocity. This dependence can be put into convenient form (see Fig. 15) by calculating the maximum allowable dispersion in β_0 to just impact the moon, realizing, of course, that the variation of the lunar gravity focusing effect with takeoff velocity is making the major change in allowable $\Delta\beta_0$. Referring to Fig. 3, we see that $\partial T/\partial\beta_0 \approx 0$; therefore, the impact dispersion due to $\Delta\beta_0$ should be independent of inclination u, at least for velocities above 36,000 fps where V_M is parallel to R_m. By referring again to Fig. 15, which shows the behavior of maximum allowable $\Delta\beta_0$ with changes in v_0, we see that this is indeed the case.

The sensitivity to v_0 dispersions does not follow directly from geometrical properties of the trajectory, since the time of flight depends on burnout energy. Equations [5 and 6] may be used to compute $\partial\theta/\partial v_0$ and $\partial t/\partial v_0$ and then

$$\Delta b = R_m[\partial(\theta - \omega T)/\partial v_0]\Delta v_0 \qquad [22]$$

Δb can be related to distance of closest approach in the normal way. The maximum allowable velocity error for a successful impact to occur is shown in Fig. 16 as a function of v_0. Evidently the sensitivity to velocity dispersions differs in two important respects from the sensitivities to angular dispersions. First, there is a characteristic takeoff energy and flight path angle such that to first order $\partial\theta/\partial v_0 = \omega\partial T/\partial v_0$ (for instance

$v_0 = 36{,}000$ fps, $r_0 = 2.2 \times 10^7$ ft, $\beta_0 = 70$ deg), and, therefore, the two-dimensional miss (i.e., $u = 0$) is largely due to second-order terms; second, when u is appreciably different from zero, the velocity sensitivity is strongly affected by the behavior of u (see Eq. [16]), and, therefore, Δv_{max} is subject to day-to-day variations. Fig. 16 shows results calculated under the assumption that the minimum u is obtained (i.e., when $\lambda_b = -90$ deg); Fig. 17, on the other hand, shows the day-to-day variation for various launch velocities. At low velocities the maximum allowable Δv_0 is weakly dependent on u and therefore is weakly dependent on launch day; whereas near the two-dimensional minima $\Delta v_{0\ max}$ depends critically on u and therefore depends critically on launch day. In summary, the azimuth sensitivity is independent of burnout velocity; the flight path angle sensitivity is a monotonically increasing function of burnout velocity, and the velocity sensitivity itself is strongly dependent on velocity and inclination of the trajectory plane to the lunar orbit plane. It should be noted that the approximate methods outlined here are within 10 per cent of exact computer calculations at minimum energy and approach exact agreement by the time $v_0 = 36{,}000$ fps. This is merely a statement of the fact that the less time spent in the lunar field the better the approximation implied by the model outlined here becomes.

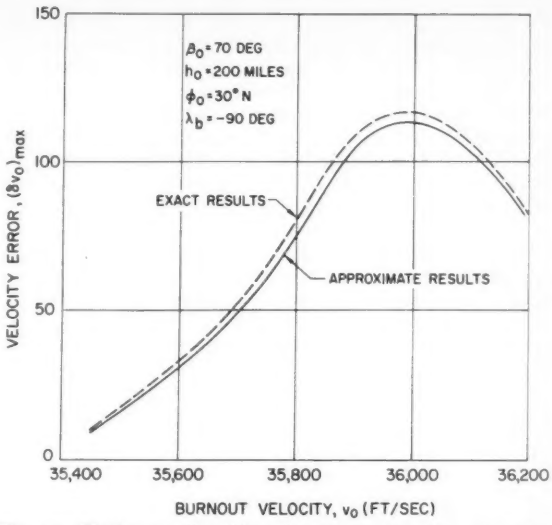

Fig. 16 Maximum allowable velocity error for impact on the moon (burnout time chosen to minimize angle between vehicle plane and moon plane)

Interaction of Trajectories and Missions

To illustrate the central role of trajectory analysis in system design, we will examine some of the problems peculiar to a lunar satellite mission, the probable second step in lunar missions.

Lunar Satellite (34)

The goal of a lunar satellite mission is to place some minimum weight of experimental equipment and associated power supply, telemetry, etc., into an orbit indefinitely bound to the moon. Barring catastrophic events, i.e., gross malfunctions, the vehicle should have a given a priori probability of success. An additional purpose may be to guarantee a range of final orbital elements relative to the moon with the same given probability.

We have already seen that the behavior of the powered flight guidance system can be summarized in terms of the probability of limiting the dispersion of burnout quantities v_0, β_0 and α_0 within specified limits, and that the choice of trajectory can alter the effect near the moon of a given set of burnout dispersions. Evidently, there is no reason from the viewpoint of accuracy to operate with a burnout velocity above 36,000 fps when $\beta_0 = 70$ deg, $r_0 = 2.2 \times 10^7$ ft, since there the velocity sensitivity is minimized, the flight path angular sensitivity is minimum at minimum energy, and azimuth sensitivity is relatively independent of v_0. The optimum velocity from the booster guidance standpoint depends on the 1 σ values of $\Delta\beta_0$, Δv_0 and $\Delta\alpha_0$ and lies somewhere between minimum energy (35,350 fps) and 36,000 fps. On the other hand, the available booster configuration and minimum payload requirements may limit maximum v_0 well below 36,000 fps. In addition, the probability of a booster configuration achieving a given burnout velocity is increased if the margin between v_0 and the velocity physically realizable by the system is increased.

If the definition of mission success is minimal, i.e., if any lunar capture or impact is regarded as a success, then, from the standpoint of free flight and terminal conditions, there is a wide choice of burnout conditions. The differential equations of the combined Earth-moon gravity field have one first integral, the Jacobi integral, which can be written as follows (5, 27)

$$J = v^2 - \omega^2(x^2 + y^2) - 2\left[\frac{GM_e}{r_e} + \frac{GM_m}{r_m}\right] = \text{constant} \quad [23]$$

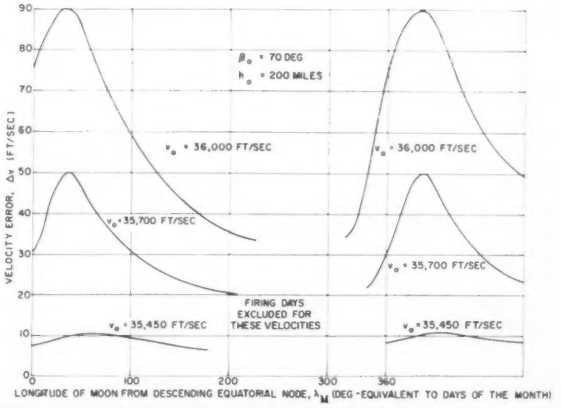

Fig. 17 Total allowable velocity error for impact on the moon (burnout latitude, 45 deg N)

where the x, y, z axes centered at the Earth-moon barycenter are rotating with the Earth and moon, the z axis is along the direction of rotation, the x axis directed toward the moon, and r_e and r_m are vehicle distances from the Earth and moon, respectively. For a given value of J, the vehicle is restricted to a region of space defined by Equation [23] and the conditions that $|v| \geqq 0$. The particular Jacobi surface of interest here is the largest one which is still closed about the moon, since this provides a sufficient condition for a stable satellite around the moon. Set $J = J_0$ for this surface; then if the vehicle is inside this surface and has a value of $J \leqq J_0$, it will remain inside the surface indefinitely. We are ignoring, of course, the small effect of the sun on the vehicle's motion.

A single value of retarding velocity can be chosen such that if a trajectory enters this region, this retarding velocity will insure that the final $J \leqq J_0$. Of course, the smaller the vehicle's velocity before retardation (i.e., the smaller the initial J value), the smaller the payload weight that must be expended as propellant. Fig. 18 shows a projection of this critical surface J_0 on the Earth-moon plane together with

segments of trajectories entering this region. The different segments correspond to 25 fps changes in takeoff velocity. The point of interest here is that the locus of points corresponding to a given time after burnout lies roughly along a straight line and the points are almost linearly distributed along this locus according to the variation in burnout velocity. Evidently, if retardation is to take place at some fixed time it is desirable, at least from the velocity dispersion standpoint, to have as large a segment of this locus contained inside J_0 as possible. The standard trajectory should then have an initial velocity such that it is midway on this locus. With this criterion for the standard trajectory, the velocity and angular tolerances at burnout can easily be obtained from the work in the previous section. For the particular set of burnout conditions in Fig. 18, we find that the maximum allowable flight path angle dispersion is about ± 1.2 deg, the maximum allowable burnout velocity dispersion is about ± 125 fps, and the maximum allowable azimuth dispersion is about 2.5 deg. If

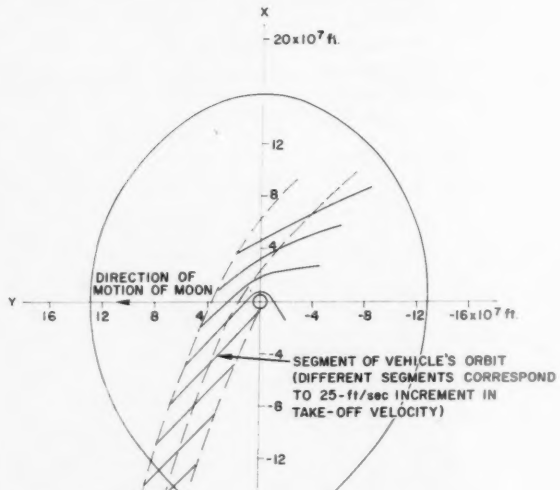

Fig. 18 Variation of orbits inside the critical Jacobi region as a result of burnout velocity increments

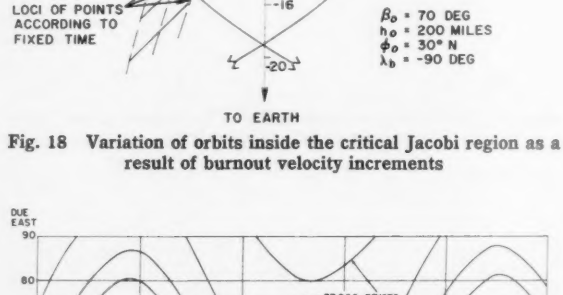

Fig. 19 Necessary variation of azimuth at burnout for various burnout velocities and time of month (less than 0 deg azimuth, no launch possible)

the burnout velocity is increased above the low velocity used in Fig. 18, the allowable velocity tolerance will increase somewhat. On the other hand, the allowable angular tolerance will decrease rapidly. Referring to Figs. 15 and 16, the reader can see that this choice of initial condition for a satellite orbit gives the maximum velocity tolerance allowed for hard impact ($v_0 = 36{,}000$ fps) and about twice the maximum allowable angular dispersion for impact ($v_0 = 35{,}350$ fps), and these large allowable dispersions have been obtained with a takeoff energy which is close to minimum.

By examining payload constraints, free-flight sensitivity and terminal conditions we have arrived at a suitable trajectory for this mission. However, there are additional constraints on the trajectory so far not considered, which will also influence the final choice. For example, range safety requirements will establish an allowable sector for burnout azimuths. As is shown in Fig. 19, the burnout azimuth is strongly dependent upon both the day of the month and the launch velocity (in general, the lower the launch velocity, the farther north the burnout azimuth must be). On the other hand, we must allow a suitable interval of days for launching the vehicle, since it is difficult to guarantee the launch on a single given day. This may mean that the takeoff velocity must be increased to maintain burnout azimuth within the allowable sector and to insure a large enough interval of allowable firing days.

In addition to insuring an adequate number of launch days, a reasonable launch period during each day must be allowed for. Referring to Fig. 9, we see that allowable α_0, β_0 and v_0 change as launch time changes. Evidently, a combination of azimuth, flight path angle and velocity changes can be engineered into the guidance system to compensate for hold periods. However, any combination will, in general, conflict with the other constraints we are discussing.

Another restriction on takeoff velocity will come from the need for visibility of the vehicle at the time of injection into the terminal phase. Taking into consideration the in-plane angle θ turned by the vehicle during its free flight and taking into consideration the total angle turned by the Earth during the time of flight t, regions of allowable takeoff velocities can be established which satisfy the visibility constraint. Fortunately, since the time of flight changes rapidly at low velocity (see Fig. 5), these allowable groups of velocities lie close to one another in the low velocity region, so that this trajectory constraint is not severe.

So far, we have not discussed in detail the constraints imposed by the powered flight itself. For example, the energy which a given booster configuration can achieve is strongly dependent upon the burnout flight path angle, in general increasing with increasing values of β_0. However, a definite maximum β_0 exists due to heating and structural limitations; that is, if the vehicle flies too rapidly while still in the atmosphere, overheating and control problems may arise. In addition, we stated previously that the booster guidance system could be summarized by a given set of dispersions and burnout quantities; however, the ability of the booster guidance system to control the burnout variables can be a function of powered flight quantities, such as downrange distance, altitude, relative orientation of velocity vector, line-of-sight to the launch point, etc. Powered flight constraints such as these may require changes in burnout conditions over and above those described earlier to meet the original requirements for the mission.

If we make the definition of the mission more stringent by requiring a tighter satellite orbit around the moon or by requiring solar heating effects to be limited more carefully, then the terminal conditions play an even stronger role in determining the suitable trajectory. Suppose it is desired to establish a satellite orbit with a minimum and maximum height about the surface so that the vehicle's payload is eclipsed from the sun for less than some maximum length of time on each revolution and no more than a given number of days or

a total number of revolutions. It is useful, when considering these more stringent terminal requirements, to start by considering the sensitivity of the impact parameter b to dispersions near the beginning of free flight. We have already noted previously how these can be calculated and how they are effected by different initial conditions. To obtain the required probability of success, the nominal impact parameter must be biased outward from that impact parameter which leads to the minimum allowable approach distance on the satellite orbit. The attitude of the vehicle at the time of application of retarding thrust now plays a more important role. The maximum use of the retarding thrust, of course, is made when it is applied co-linear with the velocity of the vehicle at the distance of closest approach hyperbola, whatever the angle of the velocity vector at the distance of closest approach. This orientation of the thrust velocity at distance of closest approach may require a large reorientation of the vehicle during powered flight near the Earth, which may be impossible. If this is the case, the optimum time of firing on the incoming hyperbola will not be at the distance of closest approach, and the nominal impact parameter b must be biased even further to allow for this degradation in effectiveness. It should also be noted that, in general, the tighter the satellite orbit desired, the higher the retarding thrust, and thus, the larger the amount of propellants needed to do the job, hence a smaller useful payload.

Since a satellite is usually designed to deliver experimental information over long periods of time, and since batteries have finite lifetimes, this sort of mission will undoubtedly require a continuous source of power. If the source used is solar power, it is obvious, of course, that a vehicle in a satellite orbit will be shielded from the sun during certain periods of the orbit. However, rather large changes can be made both in the inclination of the satellite plane relative to the plane of the ecliptic and the line of nodes of the satellite orbit in the ecliptic by relatively minor relocations of the injection point. In general, if solar eclipsing is to be avoided, the satellite orbit should have an inclination greater than 45 deg relative to the ecliptic, and, if possible, the nodal line should have just been passed by the lunar shadow as the lunar shadow moves in its annual rotation of 1 deg per day. If these two things are done, the maximum length of each individual eclipse will be minimized and the time of injection to the first eclipse will be maximized. It is obvious that manipulating the position of perigee and the size of the major axis by changing injection conditions can influence the eclipse situation as well.

Midcourse Guidance (18)

These more stringent terminal requirements will probably be too difficult for the powered flight guidance to satisfy, and additional corrective maneuvers during the midcourse portion of the trajectory will be necessary. Many guidance and control systems can be postulated to do the job; however, it is important that the weight and power requirements of such a system be as small as possible. We can show that by using some simple trajectory analysis a rather rudimentary approach is sufficient. As discussed in the previous section, the impact parameter changes as a result of changes in initial conditions. The impact parameter change is a vector quantity, and, in general, the three important impact parameter changes caused by changes in v_0, β_0 and α_0 are not co-linear vectors; that is, they do not lie along a single line. Recalling the theoretical analysis of these impact parameter changes, we would expect the change due to azimuth to be roughly perpendicular to the trajectory plane, the change due to flight path angle to lie in the orbital plane, and the change due to velocity to lie somewhere between these two directions. This indicates that velocity corrections made immediately after booster burnout, which would give impact parameter changes in the same direction as the velocity error at burnout, would be unable to correct both β and α errors. In general, a

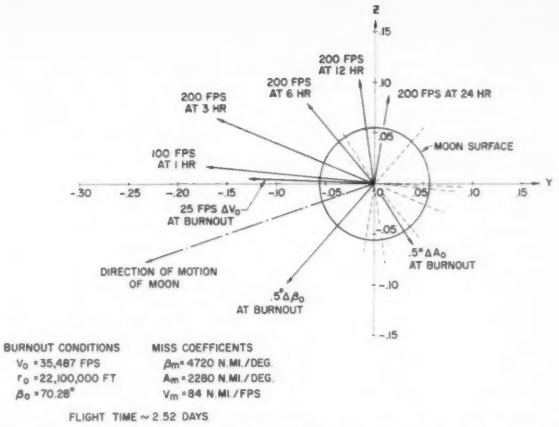

Fig. 20 Vector impact parameter change from burnout errors and midcourse correction

capability of making impact parameter changes in two perpendicular directions is required. Looking at Fig. 20 where the effect of vernier corrections as a function of time after burnout is shown, we see that the resultant impact parameter changes rotate through an angle greater than 90 deg from the direction obtained immediately after burnout, so that by choosing the time correctly, any combination of angular errors can be eliminated with two vernier corrections made in a fixed direction in inertial space. Of course, the relative effectiveness of the vernier correction decreases as the vehicle approaches the moon, so that, again, there will be a strong interaction between time of firing of the vernier correction and the total useful payload that can be carried. As implied by the previous discussion, this system needs additional information about the trajectory subsequent to burnout to improve the accuracy of knowledge of burnout conditions. This additional information should be obtained through radio tracking, since it is vital in the early lunar missions to attempt to keep as many of the guidance functions as possible on the ground, i.e., by radio techniques, so as to minimize the weight and power requirements on the vehicle payload.

These more stringent terminal requirements will also place more emphasis on accurate trajectory computations. In the analysis that has been presented so far, the terminal phase has been analyzed by making the approximation of a single force center (the moon) situated in a nonrotating coordinate system. Since this approximate analysis is not adequate for tight orbits, particularly if long term safety against collision is desired, accurate computer runs or additional analysis which will include the perturbations due to the Earth's gravity field and the rotation around the Earth must be carried out. This is particularly true near the boundaries of safe regions as delineated by the simple approximation. Fortunately, astronomers have already devised numerous ways of making rapid, precise computer calculations, so that trajectories with 10-mile accuracy in the vicinity of the moon are easily computed (2,16).

A study of the relationships between an entire space mission and the trajectory analysis shows that a small change in any of the indicated areas will result in a partially or wholly new trajectory. This extreme sensitivity of the trajectory to minor changes in the system means that each system change should be closely coordinated with trajectory considerations; perhaps more important, the implications of each change in the trajectory on the success of the mission must also be carefully considered.

Conclusions

It has been the purpose of this paper to summarize the available theoretical methods for analyzing lunar trajectories and to suggest some of the practical problems involved in arriving at an actual lunar trajectory. Although only the lunar satellite mission has been dealt with in any detail, the principles and practical problems outlined apply to other lunar missions. However, there are also important differences. The extremely narrow terminal requirements which will be set when a soft lunar landing is contemplated will require consideration of many additional factors. Thus, for instance, the final impact velocity will have to be controlled within several hundred feet per second. Since this velocity control is required at a particular distance from the center of the moon, it will be necessary to include terminal guidance in addition to midcourse and booster guidance required for satellite missions. The sensors for this terminal guidance probably will require information about the lunar surface which will not be determined until actual experiments have been carried out. However, with suitable trajectory analysis, the requirements placed upon the terminal guidance system can be minimized, thereby increasing the effective payload for experiments and the overall probability of success. For example, although it is relatively simple to eliminate the radial component of approach velocity, it is not easy to reduce the tangential component. However, by designing a nominal trajectory to land vertically without terminal corrections, and by finding a nominal trajectory that minimizes the angular dispersions of the approach velocity from the local vertical, the corrections required of the terminal equipment may be minimized.

In brief, with the help of astronomers and with the system design activity generated in the last several years, the basic problems of lunar flight mechanics are well understood. The emphasis in analysis has shifted from abstract isolated studies to particular problems facing specific missions.

Acknowledgment

The author wishes to express his thanks to R. C. Booton, Jr., E. H. Tompkins, Lem Wong and R. A. Park for their contributions to the background and preparation of this article.

References

1 Alexandrov, I., "The Lunar Potential," Aeronutronic Systems Inc., Interim Tech Note no. 1, Dec. 12, 1958.

2 Baker, R. M. L., Jr., "Practical Limitations on Orbit Determination," presented at the Inst. Aero. Sci. Semi-Annual Meeting, Los Angeles, July 1958.

3 Benedikt, E. T., "Collision Trajectories in the Three-Body Problem," Proc. Amer. Astronaut. Soc., Western Region Meeting, Palo Alto, Aug. 1958.

4 Buchheim, R. W., "Artificial Satellites of the Moon," Proc. VII IAF Congress (Rome, 1956), Associazione Italiana Razzi, Rome, 1956, pp. 587–643.

5 Buchheim, R. W., "Motion of a Small Body in Earth-Moon Space," Rand Rep. RM-1726, June 4, 1956.

6 Buchheim, R. W., "Lunar Instrument Carrier—Attitude Stabilization," Rand Rep. RM-1730, June 4, 1956.

7 Buchheim, R. W., Herrick, S., Vestine, E. H., and Wilson, A. G., "Some Aspects of Astronautics," IRE Trans. on Mil. Eelctronics, MIL-2 no. 1, Dec. 1958, pp. 8–19.

8 Col:, D. M., "Times Required for Continuous Thrust Earth-Moon Trips," Jet Propulsion, vol. 27, 1957, pp. 416–417.

9 Drenick, R., "The Perturbation Calculus in Missile Ballistics," *J. Franklin Inst.*, vol. 251, 1951, pp. 423–436.

10 Egorov, V. A., "Certain Problems of Moon Flight Dynamics," *Uspekhi Fiz. Nauk*, vol. 63, 1957, English Translation in Russian Literature of Satellites Part I, International Physical Index, N. Y., 1958, pp. 107–174. (See also "Yegerov.")

11 Ehricke, K. A., "Cislunar Operations," ARS preprint 467–57, June 1957.

12 Gates, C. R., "Terminal Guidance of a Lunar Probe," Calif. Inst. Tech., Jet Propulsion Lab., External Publication 506, May 14, 1958.

13 Gold, L., "Earth-Moon Rocket Trajectories I," ARS preprint 646-58, June 1958.

14 Goldbaum, G. C. and Gunkel, R. J., "Comparison of Two- and Three-Dimensional Analyses of Earth-Moon Flight," Proc. Amer. Astronaut. Soc., Western Regional Meeting, Palo Alto, Aug. 1958.

15 Herrick, S., "Formulae, Constants, Definitions, Notations for Geocentric and Heliocentric Orbits," Systems Laboratories Corp., Rep. 8NI, 2nd ed., May 28, 1957.

16 Herrick, S., Baker, R. M. L., Jr. and Hilton, C. G., "Gravitational and Related Constants for Accurate Space Navigation," Proc. VIII IAF Congress (Barcelona, 1957), Springer-Verlag, Wien, 1958, pp. 197–235.

17 Hilton, C. G. and Herrick, S., "Coordinate Systems for Lunar Vehicle Orbits," Aeronutronic Systems Publication U-245, Aug. 8, 1958.

18 Hunter, M. W., Klemperer, W. B. and Gunkel, R. J., "Impulsive Midcourse Correction of a Lunar Shot," presented at the IX IAF Congress, Amsterdam, Sept. 1958.

19 Koskela, P., "Selenocentric Coordinates for the Air Force Lunar Trajectory Program," Aeronutronic Systems Inc., Interim Tech. Note. no. 2, Dec. 12, 1958.

20 Koskela, P., "Selenographic Coordinates for the Air Force Lunar Trajectory Program," Aeronutronic Systems Inc., Publication U-325, Jan. 6, 1959.

21 Kramer, S. B., "Trajectory Governs Moon Shot's Value," *Aviation Week*, Jan. 19, 1959, pp. 48–57.

22 Lawden, D. F., "The Determination of Minimal Orbits," *J. Brit. Interplanet. Soc.*, vol. 11, 1952, pp. 216–224.

23 Lawden, D. F., "Orbital Transfer Via Tangential Ellipses," *J. Brit. Interplanet. Soc.*, vol. 11, 1952, pp. 278–289.

24 Lieske, H. A., "Lunar Orbit Studies," in WADC Technical Rep. 58-270, March 1958. (Report secret, article unclassified.)

25 Lieske, H. A., "Circumlunar Trajectory Studies," Rand Paper P-1441, June 25, 1958.

26 Mickelwait, A. B. and Booton, R. C., Jr., "Analytical and Numerical Studies of Three-Dimensional Trajectories to the Moon," Space Technology Laboratories, Inc., dated 10 November 1958, presented at the IAS National Summer Meeting, June 16–19, 1959.

27 Moulton, F. R., "An Introduction to Celestial Mechanics," Macmillan, New York, 2nd ed., 1941.

28 Nautical Almanac Office, U. S. Naval Observatory, *American Ephemeris and Nautical Almanac*, published yearly by the U.S. Government Printing Office, Wash., D. C.

29 Walters, L. G., "Lunar Trajectory Mechanics," *Navigation*, vol. 6, 1958, pp. 51–58.

30 Wolaver, L. E. and Young, F. O., "Precision Earth-Moon Trajectories as a Two-Point Boundary Problem," WCLJY Internal Memo 58-55, WADC, Aug. 1958.

31 Xenakis, G., "Some Flight Control Problems of a Circumnavigating Lunar Vehicle," WADC Technical Rep. 58-270, March 1958. (Report secret, paper unclassified.)

32 Xenakis, G., "Some Flight Control Problems of a Circumnavigating Lunar Vehicle," Flight Control Lab., WADC, Wright-Patterson Air Force Base, Ohio, (WADC TN-58-82) dated March 1958, presented at the WADC Symposium on Guidance Control of Space Vehicles, March 1958.

33 Yegerov, V. A., "Some Problems Relating to the Dynamics of Flight to the Moon," Proc. VIII IAF Congress (Barcelona, 1957), Springer-Verlag, Wien, 1958, pp. 480–482.

34 "1958 NASA/USAF Space Probes (ABLE-1) Final Report," Vols. I, II, III, Space Technology Laboratories, Inc., Feb. 1959.

35 "Proceedings of Lunar and Planetary Exploration Colloquium," vol. I, no. 2, dated 15 July 1958, North American Aviation, Downey, Calif.

Free Flight of a Ballistic Missile

ALBERT D. WHEELON

Space Technology Laboratories, Inc.
Los Angeles, Calif.

The free flight portion of a ballistic missile trajectory is described in analytic form. A simplified analysis using a spherical, nonrotating Earth model is discussed first, and the corresponding error coefficients determined for the missile burnout variables. Necessary corrections for the Earth's rotation and oblateness are then introduced. Finally, consideration is given to the effect of gravitation anomalies and uncertainties in the fundamental geophysical constants which are found to be very small.

THE TRAJECTORY of a ballistic missile consists of three phases: Powered flight, free flight and aerodynamic re-entry. The free flight phase represents more than 80 per cent of the flight time and distance covered by long range ballistic missiles and is the basis for the entire flight. Powered flight and re-entry are extensive subjects in themselves, and will not be discussed in this paper. However, the basic requirements for these flight regimes are determined by the free flight trajectory.

The only influence exerted on the missile during this period is the force of gravity, which must be anticipated precisely. Since no control is exercised during free flight, the burden of establishing a proper ballistic trajectory rests with the guidance and control of the powered flight phase. Conversely, the actual trajectory which is flown usually depends on propulsion, re-entry and accuracy considerations, which in turn dictate which powered flight is used. The re-entry trajectory is completely determined by the weight-to-drag ratio and the free flight trajectory, so that restrictions on re-entry heating must be reflected back through the trajectory sequence. In addition, the accuracy of ballistic missiles depends significantly on the free flight trajectory which is flown. The point of the matter here is that the free flight trajectory is the largest dynamic factor in the trajectory, yet has the least control. This means that the powered and re-entry phases must be properly adjusted to establish a desirable free flight trajectory, and to guarantee that this is accomplished with high accuracy.

Long range ballistic missiles became a practical reality in 1940 with the German V-2, and have developed rapidly in succeeding years. The analysis of ballistic trajectories had been partially developed in previous centuries by astronomers and artillery men. Artillery trajectories were analyzed with a flat Earth gravitational model, and the omnipresent aerodynamic drag forces meant that such trajectories had no genuine free flight phase. On the other hand, celestial mechanics was devoted to predicting periodic orbits in the solar system and was not, of course, concerned with *controlling* such orbits. This substantial gap between celestial and artillery trajectories was not closed until the incentive for planning actual ballistic missile flights was presented.

It was generally recognized, of course, that long range surface-to-surface rockets would follow elliptical trajectories around an ideal spherical Earth. However, the practical problem of planning and accurately guiding long range[1] ballistic missiles requires realistic free flight trajectories including rotational and oblateness corrections. The evaluation of significant perturbations and geophysical uncertainties was also required. Having established a set of actual trajectories, it is possible to determine an optimum trajectory with respect to specific guidance, propulsion and re-entry limitations.

This paper presents an analytical treatment of free flight trajectories which is intended to provide the basis for further analysis of long range rockets. The same problems have presumably been studied in many countries, and a bibliography of visible evidence of some of this effort is included here.

We study first the simplest case of ballistic trajectories from point to point on a stationary Earth. These trajectories are the planar Kepler elliptical paths, which are amenable to complete analysis. The burnout requirements for initiation of free flight to a specified range are established from the general description of the motion of a body in a central force field. The required burnout speed for various ranges and lofting conditions are computed, and the optimum burnout angle calculated for each range. The time of flight is computed for various free flight trajectories to a number of ranges.

All of the numerical results presented are based on zero burnout height. Strictly speaking, this corresponds to impulsive burning at the launch site and an immediate realization of burnout speed. Actually, a ballistic missile acquires its burnout energy only after several minutes of rocket thrusting which ends at substantial altitudes. One can replace part of the ballistic trajectory with the powered flight phase by proper continuous joining, and it is our intention that the results presented here be used in this way. The reason for this normalization is to avoid—in a consistent way—detailed powered flight considerations which depend on vehicle staging, specific impulse, stage weight ratios, burning time, etc., which are seldom identical for two missiles.

The next step is to use these results to study the propagation of burnout errors along the perturbed trajectory and the impact errors produced thereby.

Significant corrections to this simplified analysis are required by the effects of the Earth's rotation. Trajectories on a rotating Earth are described analytically by working in an inertial reference frame. The Earth's rotation then appears as:

1 Circumferential motion of the target during the flight time.

2 An initial tangential velocity component as the missile leaves the rotating launch site.

Three-dimensional guidance equations are established analytically by adjusting of the inertial trajectory with respect to these factors. The unwieldly equations are best suited to numerical reduction, and the analytic derivation of rotating Earth error coefficients is not discussed.

The oblateness corrections which must be amended to spherical Earth free flight trajectories are evaluated with a

Received July 10, 1959.

[1] Those trajectories which require a Newtonian $1/r^2$ gravitational force description, as opposed to short range trajectories which can be based on a flat Earth constant gravitational model.

perturbation method which relies on the smallness of the Earth's eccentricity (i.e., 1/300). General expressions for range and cross range corrections are established in this way for all launch and target locations, with various (lofted) trajectory options. The miscellaneous errors produced by uncertainties in the fundamental geophysical constants and unrecognized gravitational anomalies are estimated last. These effects are minor compared with the rotational and oblateness (bias) corrections, and are considered as "impact noise" for ballistic missiles.

Trajectories on a Spherical Earth

The purpose of this section is to develop analytic descriptions of free flight trajectories about a stationary spherical Earth. We first study the classical equations of motion in the nominal trajectory plane and from these derive the "hit equation." The latter establishes the necessary requirements on the components of the burnout velocity vector in order that impact occur at a predetermined range. The burnout speed required for each range and burnout angle is then computed, and the optimum burnout angle for each range determined. Lastly, the time of flight is computed as a function of range and burnout angle. The results of this section form the basic description of a ballistic missile trajectory, to which rotational and oblateness corrections will be added in subsequent sections.

The simplest description of the free flight trajectory of a ballistic missile on a spherical Earth disregards the atmosphere, oblateness and rotation of the Earth. The total mass of the Earth (M) may then be considered to be concentrated at the Earth's center, and the missile moves under a Newtonian inverse-square force directed toward this point—so long as it does not intersect the Earth's surface. Because the force field is a central field, the resulting trajectory lies in a plane containing the launch (burnout) point and the Earth's center.

If the initial velocity vector is properly aligned in azimuth, however, the trajectory plane will also intersect the target point (T). The planar geometry shown in Fig. 1 may then be used to describe the elliptical free flight path in this trajectory plane. The in-plane range angle ϕ specifies the angular separation between launch point and target, and may be converted to great circle linear range R by multiplying with the mean equatorial radius of the Earth

$$\begin{aligned} a &= 2.0926\ 10^7 \text{ ft} \\ &= 6378 \text{ km} \\ &= 3963 \text{ statute miles} \\ &= 3442 \text{ naut miles} \end{aligned} \qquad [1]$$

A number of representative range angles ϕ and the equivalent linear range R values are given in Table 1, and will be used to illustrate many of the results which follow.

Table 1 Conversion table for range angle ϕ and great circle linear range R

Range angle ϕ, deg	Linear range R nautical miles	km
8° 20′	500	927
15	900	1,668
30	1,800	3,335
60	3,600	6,671
75	4,500	8,339
90	5,400	10,006
120	7,200	13,342
140	8,400	15,565
180	10,800	20,012

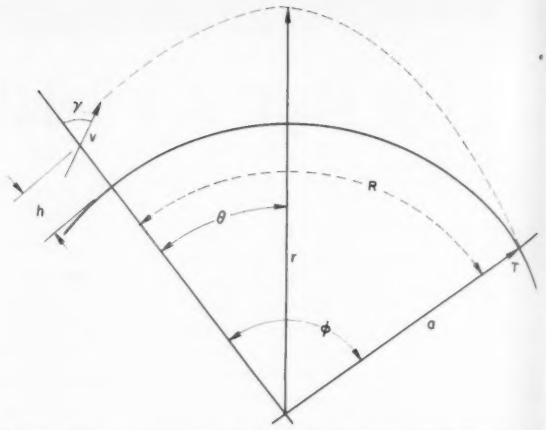

Fig. 1 Polar coordinates for analysis of planar ballistic missile trajectory

Equations of Motion

The guidance problem for ballistic missiles is to insure that the elliptical free flight trajectory established by the burnout conditions intersects the Earth's surface ($r = a$) at the desired range ϕ. To establish the corresponding constraints imposed on the burnout conditions, one must be able to describe the entire free flight trajectory. This description is derived from the differential equations of motion for the missile which, in turn, follow from the Lagrangian function (1).[2] The latter is naturally written with the in-plane polar coordinates (r, θ) of Fig. 1

$$\mathcal{L} = \frac{m}{2}(\dot{r}^2 + r^2\dot{\theta}^2) + \frac{GMm}{r} \qquad [2]$$

where overdots denote time derivatives and GM is the gravitational product of the Earth.

$$GM = 1.4077\ 10^{16} \text{ ft}^3/\text{sec}^2 = 3.9861\ 10^{20} \text{ cm}^3/\text{sec}^2 \qquad [3]$$

The Euler-Lagrange equations of motion (1) follow directly from Equation [2] and are independent of the missile mass m.

$$\ddot{r} - r\dot{\theta}^2 + GM/r^2 = 0 \qquad [4]$$

$$\frac{d}{dt}(r^2\dot{\theta}) = 0 \qquad [5]$$

The second equation expresses the conservation of angular momentum in a central field, and may be integrated in terms of the burnout speed V and the burnout angle γ identified in Fig. 1

$$r^2\dot{\theta} = p = r_0 V \sin\gamma \qquad [6]$$

where

$$r_0 = a + h \qquad [7]$$

and h is the burnout height of the missile.

The angular momentum integral Equation [6] can be used to express time derivatives in terms of θ derivatives since

$$\frac{d}{dt} \equiv \frac{d\theta}{dt}\frac{d}{d\theta} = \frac{p}{r^2}\frac{d}{d\theta} \qquad [8]$$

This relation allows one to write a simple differential equation

[2] Numbers in parentheses indicate References at end of paper.

whose solution describes the geometrical relation between r and θ. It is convenient to define

$$u(\theta) = 1/r(\theta)$$

and

$$\lambda = r_0 V^2/GM$$

The parameter λ is the dimensionless ratio of twice the kinetic to potential energy at burnout, and plays a central role in determining the nature of the trajectory. Combining these definitions with Equations [4 and 6] one finds

$$\frac{d^2u}{d\theta^2} + u = \frac{GM}{p^2} = \frac{1}{\lambda r_0 \sin^2 \gamma} \qquad [9]$$

It is convenient to identify the polar axis with the burnout position, as shown in Fig. 1, so that $t = 0$ corresponds to $\theta = 0$. The solution of Equation [9] which satisfies the appropriate initial conditions

$$u(0) = 1/r_0$$

and

$$\left.\frac{du}{d\theta}\right|_0 = -\frac{1}{r_0} \cot \gamma \qquad [10]$$

is found to be

$$r_0 u(\theta) = \frac{r_0}{r(\theta)} = \frac{1 - \cos \theta}{\lambda \sin^2 \gamma} + \frac{\sin (\gamma - \theta)}{\sin \gamma} \qquad [11]$$

For $\lambda < 1$, it is relatively easy to show that Equation [11] is the polar equation of an ellipse about the Earth's center. Written in terms of the burnout variables, the result is slightly more complicated than the corresponding astronomical expression involving orbital eccentricity e and mean anomaly M. However, it is important to use the burnout parameters to describe the subsequent motion, since they are the quantities which are actually controlled by a guidance system.

Hit Equation

The next step is to determine which of the many possible ballistic trajectories will actually impact at a predetermined range. The family of successful trajectories is characterized by particular combinations of burnout angle and speed. The condition that the missile impact on the target is expressed analytically by requiring that the missile intersect the Earth's surface at the point where the in-plane angle equals the desired range angle (i.e., $r = a$ when $\theta = \phi$). Inserting this condition into Equation [11] establishes the all-important "hit equation"

$$\frac{r_0}{a} = \frac{1 - \cos \phi}{\lambda \sin^2 \gamma} + \frac{\sin (\gamma - \phi)}{\sin (\gamma)} \qquad [12]$$

This equation expresses the necessary relation between the burnout parameters (V, γ and $h = r_0 - a$) which insure that the missile impacts at a range ϕ.

The burnout speed V required to impact at a range ϕ, for a fixed burnout angle γ and height h can be computed by solving the hit Equation [12] for λ and recalling the previous definition

$$V^2 = \frac{GM}{r_0} \frac{1 - \cos \phi}{[(r_0/a) \sin^2 \gamma + \sin (\phi - \gamma) \sin \gamma]} \qquad [13]$$

Since $r_0 = a(1 + h/a)$, the fundamental geophysical constant for ballistic missiles is GM/a and has the absolute values

$$GM/a = 6.7268\ 10^8\ \text{ft}^2/\text{sec}^2 = 6.2494\ 10^{11}\ \text{cm}^2/\text{sec}^2 \qquad [14]$$

The burnout speed required is plotted in Fig. 2 vs. burnout angle γ for the range angles listed in Table 1. The curves in

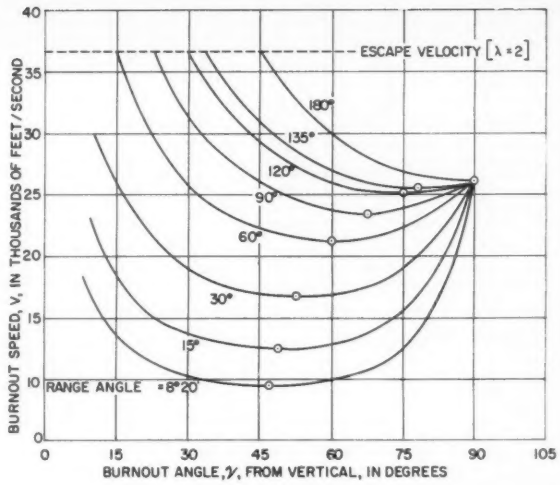

Fig. 2 Variation of required burnout speed with burnout angle γ and range angle ϕ for nonrotating spherical Earth ($h = 0$). Circles mark minimum speed points

Fig. 2 are normalized in each case by choosing burnout to occur at the Earth's surface ($h = 0$). This choice avoids powered flight considerations, which are necessarily dependent on range, vehicle staging, performance, etc. It is noteworthy that burnout speeds between 10,000 and 25,000 fps (several miles per sec) are required to reach the long ranges considered in Table 1. For very short ranges, one can expand Equation [13] in powers of the range angle ϕ and obtain the usual "flat Earth" result

$$V^2 \cong \frac{GM}{2a} \frac{\phi}{\sin \gamma \cos \gamma} = \frac{gR}{\sin 2\gamma} \qquad [15]$$

The burnout velocity requirement curves plotted in Fig. 2 indicate that there is an infinite set of suitable burnout pairs (V, γ) which all lead to the same impact range. Several alternative trajectory profiles to a range of $\phi = 90$ deg ($R =$ 5400 nautical miles) for zero burnout height ($r_0 = a$) are plotted in Fig. 3 to suggest the multiplicity of trajectories.

Optimum Burnout Angle

It is of considerable practical importance to ask if an *optimum* burnout angle and speed combination exists which would lead to maximum range payload capability for a fixed missile (2, 3). Inspection of Fig. 2 indicates that there is an optimum burnout angle γ^* for each range which requires the least speed to reach that range. Equivalently, for a fixed burnout speed capability, the optimum burnout angle γ^* leads to a maximum range.[3] However, one is cautioned that a minimum speed trajectory may not be desirable from a guidance standpoint. The optimum γ for each range is indicated by a circle in Fig. 2.

The minimum speed inclination evidently depends on range, and decreases steadily from $\gamma^* = 90$ to 45 deg, as the range angle changes from $\phi = 180$ to 0 deg. The short range limit is familiar in ordinary artillery applications, where $\gamma =$ 45 deg corresponds to maximum projectile range for a fixed charge (see Eq. [15]). One can compute the optimum burnout angle γ^* for an arbitrary range by differentiating Equa-

[3] Note, however, that this is not necessarily equivalent to minimum *energy*, which is determined by both V and h.

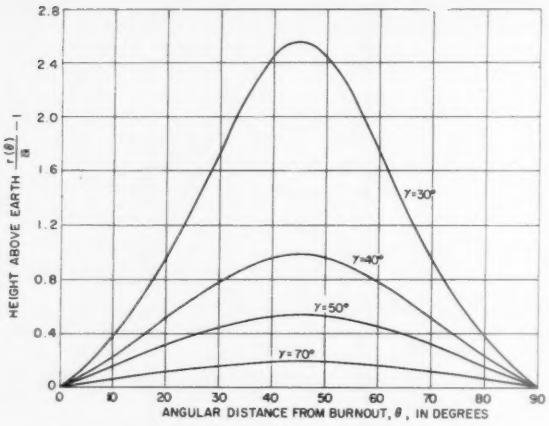

Fig. 3 Trajectory profiles for $\phi = \pi/2$ and $h = 0$

tion [13] with respect to γ and equating the resulting expression to zero

$$\tan 2\gamma^* = \frac{\sin \phi}{\cos \phi - (1 + h/a)} \qquad [16]$$

The optimum burnout angle γ^* is plotted in Fig. 4 vs. range angle for several values of burnout height. When the burnout height is negligible compared with the Earth's radius (as it often is), Equation [16] gives

$$\gamma^* = (\phi + \pi)/4 \qquad [17]$$

The latter formula is usually a good approximation, except at very short ranges, where Fig. 4 indicates that special elevation settings are required to hit a target from an *elevated* launch point.

Time of Flight

At this point in the development we are able to compute the time of flight for a ballistic missile as a function of the range-constrained burnout variables. The total flight time has practical significance in its own right. These results are also an essential ingredient of the analysis of trajectories on a rotating Earth discussed in the next section. If one wishes to determine where the missile is on the elliptical trajectory at a particular time after launch, one must return to the differential equations of motion [4 and 5] to determine $r(t)$ and $\theta(t)$ as functions of time. The first step is to integrate the angular momentum integral [6] with respect to time, substituting the derived geometrical relationship [11] between r and θ

$$\int_0^t dt\, r_0 V \sin \gamma = \int_0^{\theta(t)} dx\, r^2(x)$$

or

$$t = \frac{r_0}{V \sin \gamma} \int_0^{\theta(t)} dx \left[\frac{1 - \cos x}{\lambda \sin^2 \gamma} + \frac{\sin (\gamma - x)}{\sin \gamma}\right]^{-2} \qquad [18]$$

This indefinite integral can be performed analytically to give t as a function[4] of θ

$$t = \frac{r_0}{V \sin \gamma} \left\{ \frac{\cot \gamma\,(1 - \cos \theta) + (1 - \lambda) \sin \theta}{(2 - \lambda)\left[\dfrac{1 - \cos \theta}{\lambda \sin^2 \gamma} + \dfrac{\sin (\gamma - \theta)}{\sin \gamma}\right]} + \frac{2 \sin \gamma}{\lambda \left(\dfrac{2}{\lambda} - 1\right)^{3/2}} \tan^{-1}\left[\frac{\sqrt{(2/\lambda) - 1}}{\sin \gamma \cot \dfrac{\theta}{2} - \cos \gamma}\right] \right\} \qquad [19]$$

The time from launch to impact, or total flight time T is computed by setting $\theta = \phi$ in Equation [19]. This simplifies the denominator of the first term in Equation [19], and one finds

$$T = \frac{r_0}{V \sin \gamma} \left\{ \frac{(1 - \cos \phi) \cot \gamma + (1 - \lambda) \sin \phi}{(2 - \lambda)\,(r_0/a)} + \frac{2 \sin \gamma}{\lambda[(2/\lambda) - 1]^{3/2}} \tan^{-1}\left[\frac{\sqrt{(2/\lambda) - 1}}{\sin \gamma \cot \phi/2 - \cos \gamma}\right] \right\} \qquad [20]$$

where the hit Equation [12] should be used to express λ in terms of ϕ and γ. The total flight time for several range angles is plotted in Fig. 5 as a function of burnout angle γ. These plots show that the flight time decreases steadily as the velocity vector is lowered toward the local horizontal.

Error Coefficients

The hit Equation [12] determines those combinations of V, γ and h which are consistent with impact at the range ϕ. In practice, one selects a particular combination of burnout variables (V, γ, h) as a design point, and then tries to measure and control the missile's flight so as to achieve that condition at burnout. This is the basic guidance problem, of course, and is characterized by both measurement errors and missile control errors. These errors, although partially corrected by the guidance system during powered flight, result in burnout errors δV, $\delta\gamma$, δh, etc., which are characteristic of the particular system employed.

Our task is to determine how such burnout errors are translated into impact errors as the missile travels over the perturbed free flight trajectory. This propagation of burnout errors is best described with "error coefficients," which describe, for instance, how many miles of range error are produced for each foot per second of error in the burnout speed. These error coefficients depend upon the actual trajectory which is flown (i.e., γ and ϕ), and it is sometimes possible to minimize the impact error with respect to the actual guidance system employed by lofting the trajectory. To compute the in-plane error coefficients, we differentiate the hit Equation [12] implicitly with respect to ϕ and each of the burnout variables

$$2\frac{\delta V}{V}\left(\frac{1 - \cos \phi}{\lambda \sin^2 \gamma}\right) + \frac{\delta h}{a}\left(1 + \frac{1 - \cos \phi}{\lambda \sin^2 \gamma}\right) = \delta\gamma\left[\frac{\cos(\gamma - \phi)}{\sin \gamma} - \frac{\cos \gamma}{\sin^3 \gamma} \sin (\gamma - \phi) - 2 \cot \gamma \frac{1 - \cos \phi}{\lambda \sin^2 \gamma}\right] + \delta\phi\left[\frac{\sin \phi}{\lambda \sin^2 \gamma} - \frac{\cos (\gamma - \phi)}{\sin \gamma}\right] \qquad [21]$$

According to Fig. 1, the range error is given by

$$\delta R = a\delta\phi \qquad [22]$$

and is thus related individually to each of the burnout errors through Equation [21]. The ratio $r_0/a = 1 + (h/a)$ is sufficiently near unity that one may replace it by this value in the first-order expressions which follow.

We shall analyze the effect of burnout errors by considering independent variations of each of the burnout variables in se-

[4] Actually, one would prefer to have θ as a function of t, but this seems to be impossible analytically.

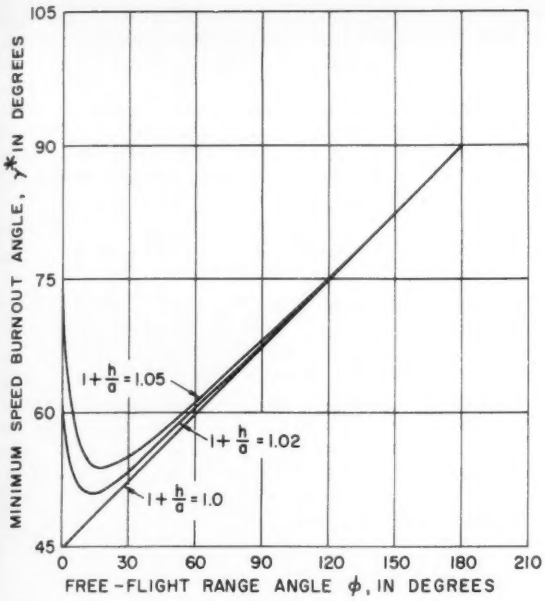

Fig. 4 Burnout angle requiring minimum burnout speed to achieve specified free-flight range

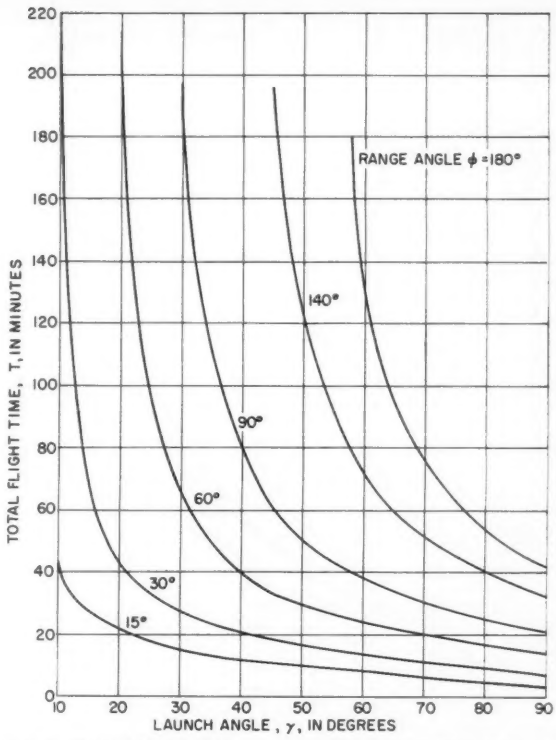

Fig. 5 Total ballistic flight time to various ranges plotted vs. burnout angle γ, assuming burnout at Earth's surface

quence. In practice, however, burnout errors are produced jointly by limitations of the guidance system and so are really interdependent. The statistical combination of these burnout position and velocity errors which, in turn, produce a composite impact error for a particular guidance system, is a subject in itself and will not be discussed further here.

Burnout Speed Errors

To find the effect of errors in the burnout speed, one assumes that all of the other burnout errors are perfectly controlled. Variations in the burnout speed δV give rise to range errors, since more or less energy is imparted to the trajectory at burnout, and this modifies the trajectory profile and impact point. The appropriate error coefficients are computed from Equations [21 and 22] as

$$\frac{\delta R}{\delta V} = 2\,\frac{a}{V}\,\frac{1-\cos\phi}{\sin\phi - \lambda\sin\gamma\cos(\gamma-\phi)} \qquad [23]$$

$$\frac{\delta R}{\delta \gamma} = a\left[\frac{\cot\gamma\sin(\gamma-\phi) - \cos(\gamma-\phi) + \cos\gamma(1-\cos\phi)/\lambda\sin^2\gamma}{(\sin\phi/\lambda\sin\gamma) - \cos(\gamma-\phi)}\right]$$

The energy variable λ may be eliminated by means of the hit Equation [12] (with $r_0 = a$) to give

$$\frac{\delta R}{\delta V} = 2\,\frac{a}{V}\,[\sin\phi + \tan\gamma(1-\cos\phi)] \qquad [24]$$

This expression is plotted in Fig. 6 as a function of burnout angle for several range angles ϕ. The optimum burnout angle is indicated on each curve by a circle. If the optimum burnout angle is used, these curves indicate that a variation in burnout speed of 1 fps causes a range miss of 1 nautical mile at ICBM ranges, and approximately $\frac{1}{4}$ mile at IRBM ranges. The speed error becomes more sensitive as the velocity vector is lowered to the local horizontal, reflecting the extreme care which must be exercised in controlling the energy content of a nearly-satellite orbit to insure that it "drops" on a target far around the Earth. Lofted trajectories (smaller γ) evidently are less sensitive to speed errors, but imply performance penalties because of the greater absolute burnout speeds required to fly such steep trajectories (see Fig. 2).

Burnout Angle Error

The range miss due to errors in controlling and/or measuring the elevation of the burnout velocity vector in the trajectory plane can be computed by taking the ratio of appropriate factors in Equation [21]

or

$$\frac{\delta R}{\delta \gamma} = 2a\left[1 + \frac{\sin(\phi - 2\gamma)}{\sin 2\gamma}\right] \qquad [25]$$

This angular error coefficient is plotted vs. burnout angle in Fig. 7 for the range angles listed in Table 1. An important feature of these curves is that $\delta R/\delta\gamma$ becomes zero at the minimum speed burnout angle γ^* for each range. This behavior is an extension of the accuracy insensitivity of cannon fire as the elevation angle increases past the maximum range setting ($\gamma = 45$ deg), where the impact points first advance and then retreat, forming a dense pattern. This behavior is a property of all ballistic trajectories and has important practical applications. Evidently, the burnout angle need not be

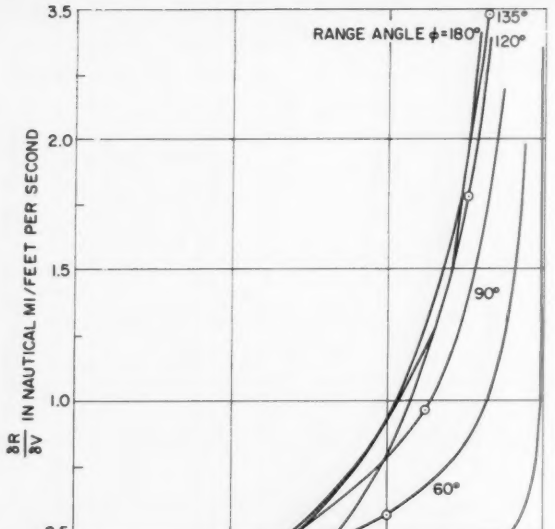

Fig. 6 Velocity miss coefficient vs. burnout angle for various range angles

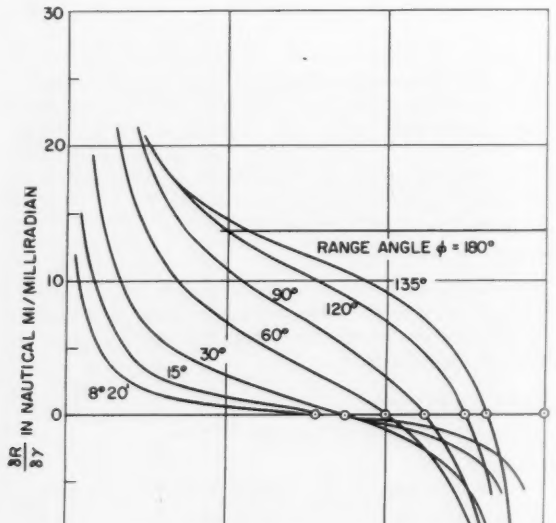

Fig. 7 Burnout angle miss coefficient vs. burnout angle for various range angles

accurately controlled by the guidance system if the minimum speed trajectory is chosen,[5] which is usually quite acceptable to the propulsion designer.

Height Errors

The variation of impact range with errors in burnout height about the nominal design point can also be inferred from Equation [21]

$$\frac{\delta R}{\delta h} = 2 \tan \gamma - \frac{\sin (\gamma - \phi)}{\sin \gamma} \qquad [26]$$

This expression is plotted vs. burnout angle γ in Fig. 8 for the range angles listed in Table 1. These dimensionless error coefficients indicate that several miles of range error are produced by each mile of height error, the exact value depending on the range and burnout angle. These curves have the same general behavior as those in Fig. 6, which is logical, since the primary effect of burnout height errors is to change the (potential) energy content of the ellipse. The same accuracy advantages of lofting the trajectory noted in connection with speed errors apply here also.

Downrange Position Errors

Variations in the downrange burnout position (δD) of the missile from the programmed value translate directly into range errors

$$\delta R/\delta D = 1 \qquad [27]$$

since their effect is simply to rotate the trajectory ellipse in Fig. 1 clockwise about the center of the Earth.

Lateral Position Errors

If the burnout point is displaced laterally out of the nominal trajectory plane by an amount δn, one can use spherical trigonometry to show that this produces a transverse error δL at impact given by

$$\delta L/\delta n = \cos \phi \qquad [28]$$

This lateral error cancels one-quarter way around the Earth, and is just reversed on the opposite side of the globe.

Lateral Velocity Errors

The nominal trajectory plane is defined by three points: The target, the burnout point and the center of the Earth. Ideally, the guidance system arranges to have the burnout velocity vector lie in this plane. However, if there is a small lateral velocity component δV_n, it will produce a transverse impact error δL given by

$$\frac{\delta L}{\delta V_n} = \frac{a}{V} \frac{\sin \phi}{\sin \gamma} \qquad [29]$$

This error is quite important in practice, and is maximum for ICBM ranges (ϕ = 90 deg). Interestingly enough, it vanishes for flights half way around the Earth, since all great circle planes between the antipodes are equivalent. This error is most severe for steep flights, since the out-of-plane velocity component then produces a greater azimuthal angular error with the velocity vector projected on the local tangent plane (i.e., $V \sin \gamma$).

Trajectories on a Rotating Earth

The foregoing analysis assumed that the missile travels around a stationary, spherical Earth. The study must now

[5] However, there are nonvanishing quadratic errors $\delta R \propto (\delta\gamma)^2$ which may be significant in such cases.

be enlarged by recognizing the rotation of the Earth about its polar axis. If this rotation is neglected at ICBM ranges, impact errors of several hundred miles will result. It is therefore necessary to program such corrections accurately in the guidance system. The rotational motion makes two distinct changes in the stationary, round-Earth trajectory analysis.

1 *Target Motion:*
During the missile flight time T, the target moves a distance

$$\omega a T \cos \beta \qquad [30]$$

in longitude, where $\omega = 7.29\ 10^{-5}$ radians/sec is the angular speed of rotation and β the target latitude. Normal ICBM flight times are approximately a half hour, according to Fig. 5, which would cause an *uncompensated* impact error of almost 400 miles at 45-deg latitude.

2 *Launch Site Motion:*
Because of the Earth's rotation, the missile has a linear velocity $\omega a \cos \alpha$ as it stands on the launch pad, even *before* it is launched. The eastward tangential velocity of rotation depends on the launch latitude α and must be added vectorially to the velocity developed during powered flight by the rocket motors, to give the total burnout velocity vector in an inertial reference frame. At the Earth's equator, this speed is approximately 1500 fps and is therefore comparable with the required burnout speeds indicated in Fig. 2. The guidance system attempts to establish the burnout velocity vector in the plane defined by the burnout and target points. If one recognizes only the propulsion produced velocity vector in adjusting the trajectory plane, however, a lateral velocity component out of this plane is created by the rotational velocity. According to the analysis to be developed below and the azimuthal error coefficient Equation [29], this lateral velocity component produces a transverse impact error given by

$$\delta L = a \sin \phi \frac{\omega a \cos \alpha}{V \sin \gamma} (\sin \alpha \cos \beta \cos \psi - \cos \alpha \sin \beta) \qquad [31]$$

where the coordinate angles are identified in Fig. 9. This effect leads to transverse errors of several hundred miles at ICBM ranges. The corresponding change of burnout speed produces range errors which are also significant.

The difficult problem in analyzing rotating Earth trajectories is to combine the target motion and launch site motion effects in a dynamically consistent manner. The following section shows how the exact guidance relations for ballistic trajectories between points on a rotating sphere can be established in analytic form. However, these relations are most efficiently reduced to numerical form with the aid of high speed digital computing machines, and this discussion does not include extensive numerical results.

Kinematics

One can use either an Earth-fixed or inertial reference frame to describe ballistic trajectories on a rotating Earth. Seen from the Earth's surface, the rotation produces apparent forces on the missile

$$\vec{F}' = \vec{F}_G - 2m\,\vec{\omega} \times \vec{V} - m\vec{\omega} \times (\vec{\omega} \times \vec{r}) \qquad [32]$$

in addition to that of gravity $\vec{F}_G$. $\vec{\omega}$ is the Earth's angular rotation velocity (spin) vector, $\vec{V}$ the missile velocity, and $\vec{r}$ the instantaneous position vector of the missile. The second term in Equation [32] represents the Coriolis force, which acts always to deflect the missile to its own right in the northern hemisphere. Since this effect is proportional to both ω and V, the high burnout speeds of ballistic missiles suggest that rotational effects are quite important. The third term describes the centrifugal force which is directed normal to the

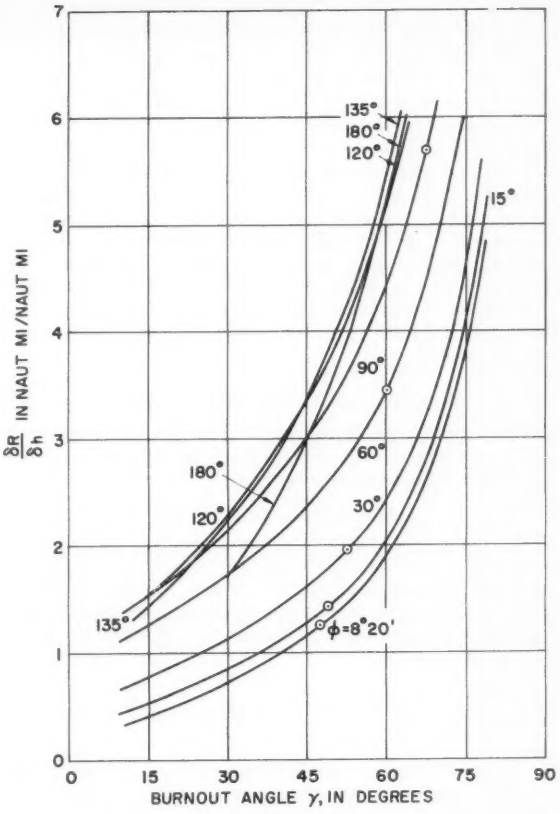

Fig. 8 Height range miss coefficient vs. burnout angle for various range angles

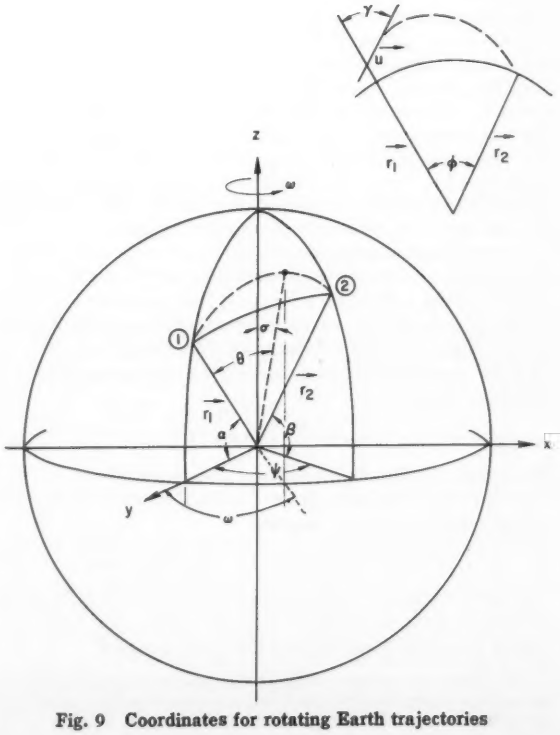

Fig. 9 Coordinates for rotating Earth trajectories

spin axis of the Earth. These two forces are fictitious, of course, and result from using a rotating Earth-fixed system to describe the (inertially plane) free flight trajectory.

In this development, we shall use an inertial frame of reference, in which only the gravitational force must be counted as such. The rotational effects then occur as variations of the initial and final conditions of the motion. We employ the system of rectangular coordinates shown in Fig. 9, using the north pole as the z-axis, with the (y, z)-plane so chosen that the burnout point lies therein at the zero time reference ($t = 0$). Consider a ballistic missile at the burnout point (1) with latitude α and zero relative longitude. The target point (2) is at latitude β and longitude ψ_0 with respect to the burnout point when the missile enters free flight. However, the important target position is that at impact, when the longitude is

$$\psi = \psi_0 + \omega T \qquad [33]$$

if T is the adjusted flight time. The burnout and impact points are conveniently described by the spherical angles of Fig. 9 and rectangular unit vectors

$$\vec{r}_1 = r_0[\vec{j}\cos\alpha + \vec{k}\sin\alpha] \qquad [34]$$

$$\vec{r}_2 = a[\vec{i}\cos\beta\sin\psi + \vec{j}\cos\beta\cos\psi + \vec{k}\sin\beta] \qquad [35]$$

where $r_0 = h + a$, as before.

The time-varying range angle ϕ for rotating Earth trajectories is determined from the position vectors and the definition of included angle

$$\cos\phi = \frac{\vec{r}_1\cdot\vec{r}_2}{r_0 a} = \cos\alpha\cos\beta\cos\psi + \sin\alpha\sin\beta \qquad [36]$$

This relation may be employed to compute the rotationally modified range once the adjusted flight time T is computed, so as to estimate ψ through Equation [33].

Guidance Equations

The guidance relations for ballistic trajectories on a rotating globe are essentially three-dimensional, time-varying generalizations of the planar "hit Equation" [12]. These guidance equations are transcendental relations among the magnitude and direction cosines of the velocity vectors required to hit the moving target. The objective of this analysis is to determine the velocity's direction cosines as functions of the cutoff speed V. The condition that the target point coincide with the trajectory plane after T seconds of flight detemines the right-left heading commands. The requirement that the missile hit the point (2) as it passes through this plane determines the climb angle as a function of speed. The normalization for direction cosines forms the third equation.

From an inertial point of view, the missile is given two initial velocity components: a tangential velocity due to the Earth's rotation in the x-direction $\vec{i}\omega r_0\cos\alpha$; and a velocity $\vec{V}$ relative to the launching site, which is imparted by the thrust program. The two components must be added vectorially to give the resultant burnout velocity $\vec{U}$ in the star-fixed inertial reference frame

$$\vec{U} = \vec{V} + \vec{i}\,\omega r_0\cos\alpha \qquad [37]$$

We denote the direction cosines of the cutoff velocity $\vec{V}$ with respect to the same rectangular axis by l, m and n, so that the initial velocity vector $\vec{U}$ becomes

$$\vec{U} = \vec{i}(lV + \omega r_0\cos\alpha) + \vec{j}(mV) + \vec{k}(nV) \qquad [38]$$

The motion is planar in the inertial reference system,[6] and the trajectory plane is determined by the initial (total) velocity vector $\vec{U}$ of Equation [38] and the Earth's center.

[6] An observer on the rotating globe observes apparent deviations from planar motion and attributes them to the Coriolis and centrifugal forces of Equation [30].

The first guidance condition requires that the burnout velocity vector $\vec{U}$ lie in the plane defined by $\vec{r}_1$ and $\vec{r}_2$. This may be expressed analytically by noting that $(\vec{r}_1 \times \vec{r}_2)$ is a vector normal to their common plane. In order that U have no component pointing out of this plane, we must have

$$\vec{U}\cdot(\vec{r}_1 \times \vec{r}_2) = 0$$

which yields our first "guidance relation"

$$\left(\frac{\omega r_0\cos\alpha}{V} + l\right)\cdot(\sin\alpha\cos\beta\cos\psi - \cos\alpha\sin\beta) + n\cos\beta\cos\alpha\sin\psi = m\cos\beta\sin\alpha\sin\psi \qquad [39]$$

The second guidance relation follows from the planar hit Equation [12] derived earlier

$$\frac{r_0}{a} = \frac{GM}{r_0|\vec{U}|^2}\frac{1-\cos\phi}{\sin^2\gamma} + \frac{\sin(\gamma-\phi)}{\sin\gamma} \qquad [40]$$

The in-plane angle range ϕ is measured in the adjusted plane of motion and is defined by Equation [36]. The angle γ between the local vertical at the launching point and the resultant velocity U is computed from

$$\cos\gamma = \frac{\vec{U}\cdot\vec{r}_1}{|\vec{U}|r_0} = \frac{m\cos\alpha + n\sin\alpha}{[(l + \omega r_0\cos\alpha/V)^2 + m^2 + n^2]^{1/2}} \qquad [41]$$

The burnout speed of the composite velocity $|\vec{U}|$ is computed from Equation [38]

$$|\vec{U}| = V\left[\left(l + \frac{\omega r_0\cos\alpha}{V}\right)^2 + m^2 + n^2\right]^{1/2} \qquad [42]$$

The third guidance relation follows from the usual normalization of the direction cosines

$$l^2 + m^2 + n^2 = 1 \qquad [43]$$

In principle, one may now solve the three guidance relations [39, 40 and 43] for l, m and n as functions of V. Unfortunately, the flight time T is concealed in these equations by its explicit appearance in ψ (see Eq. [33]), and hence in ϕ. To obtain consistency, we equate the flight time to the T-dependent integral expression [20] with V replaced by the composite speed $|\vec{U}|$

$$T = \frac{r_0}{|\vec{U}|\sin\gamma}\int_0^{\phi(T)} dx\left[\frac{GM}{r_0|U|^2}\frac{1-\cos x}{\sin^2\gamma} + \frac{\sin(\gamma - x)}{\sin\gamma}\right]^{-2} \qquad [44]$$

which may be reduced to a form similar to that of Equation [20]. This relation determines T as a function of l, m, n and V, and thus permits one to eliminate it in solving the guidance equations. In practice, one must employ an iteration procedure based on guessing T; solving for l, m and n; computing a new T, and so on. This process converges remarkably well in virtue of the apparent stability of expression Equation [44] to *small* variations in the burnout conditions (see Fig. 5).

The three guidance equations or "rotating hit equations" [39, 40 and 43] form the basis for computing other properties of trajectories which are adjusted to hit a moving target. For instance, one can plot the speed required to reach a given target as a function of any one of the direction cosines for a stationary globe in Fig. 2. The new burnout speed curves reach minimum values for burnout angles γ^{**} which are generally different than the corresponding γ^* for a stationary globe. This effect is quite significant for long range trajectories when one fires with the Earth's rotation (i.e., to the east). However, it is very difficult to extract such conditions from the "rotating hit equations" analytically, and numerical methods are employed to solve such problems in practice.

Error Coefficients for a Rotating Earth

In principle, it is possible to calculate error coefficients for rotating Earth by implicitly differentiating the three guidnce Equations [39, 40 and 43], in the same manner that was sed in the previous section. However, it is very difficult to ork analytically with this *system* of guidance equations, nd the results are most efficiently extracted with a large igital computing machine. In practice, one finds that the rror coefficients for rotating and stationary Earth trajecories are quite similar. This can be explained in terms of the lative insensitivity of the error coefficients plotted in Figs. 7 and 8 to the burnout variables, since the rotational corections can be considered as small modifications (±10 per nt) of the nominal burnout conditions.

Oblateness Correction

We have assumed so far that the gravitational force acting n a ballistic missile is a simple $1/r^2$ central field directed ward the Earth's center. An important correction to this escription is required by the oblateness of the Earth. The arth is flattened at the poles and bulges at the equator. his latitude variation of mass creates a noncentral force field hich exerts important torques on, and additional forces in, e nominal trajectory plane. The Earth is well-represented an oblate spheroid with eccentricity $e = 1/297$. A latitudeependent potential has been developed in spherical harmonics to describe this effect and the constants therein adsted by means of geophysical measurements (4). Denoting e co-latitude by σ

$$(r, \sigma) = -\frac{GMm}{a}\left[\frac{a}{r} + J\frac{a^3}{r^3}\left(\frac{1}{3} - \cos^2\sigma\right) + \frac{8}{35}D\frac{a^5}{r^5}P_4(\sigma)\ldots\right] \quad [45]$$

ith

$$P_4(\sigma) = \frac{1}{8}\left(35\cos^4\sigma - 30\cos^2\sigma + 3\right) \quad [46]$$

here the coefficients of these harmonic terms are measured (4)

$$J = 0.0016370 \pm 0.0000041 \quad [47]$$

nd

$$D = 0.0000107 \quad [48]$$

nce the oblate potential Equation [45] depends on both dial distance and latitude of the missile, the range and crossnge corrections will depend on both burnout and impact ordinates, as well as the free flight trajectory which is own. One can make a crude estimate of the oblateness fect (which ignores these factors) by multiplying the missile nge with the coupling constant J. The order of magnitude this correction at ICBM ranges is

$$\delta R \simeq Ja\phi \simeq 10 \text{ miles} \quad [49]$$

vidently, it behooves one to include oblateness corrections the original guidance relations. On the other hand, the D rm in Equation [45] produces impact errors which are approximately one hundred times less than the J effect and will disregarded.

We shall calculate oblateness corrections using a straightrward perturbation expansion (5) in the small coupling nstant J. The calculation is most efficiently performed out the nominal trajectory plane. A one-to-one relationip between the co-latitude σ and in-plane position angle θ n be established with spherical trigonometry

$$\cos\sigma = \cos\theta\sin\alpha + \sin\theta\cos\alpha \times (1 - \cos^2\beta\sin^2\psi/\sin^2\phi)^{1/2} \quad [50]$$

Here α, β and ψ are the latitude and longitude position angles identified in Fig. 9, and ϕ is the nominal range angle which is related to them by Equation [36]. Since r is the same in both the spherical and trajectory plane coordinate systems, the oblate potential can be rewritten

$$V = -\frac{GMm}{a}\left[\frac{a}{r} + J\frac{a^3}{r^3}f(\theta)\right] \quad [51]$$

where

$$f(\theta) = 1/3 - (A\cos\theta + B\sin\theta)^2 \quad [52]$$

and the constants are given in terms of the coordinate angles by

$$A = \sin\alpha \quad [53]$$

$$B = \cos\alpha(1 - \cos^2\beta\sin^2\psi/\sin^2\phi)^{1/2} \quad [54]$$

The oblateness corrections are conveniently computed by decomposing the impact error into downrange and crossrange components.

Range Corrections

The range correction can be computed by studying the new equations of motion in the nominal trajectory plane—as modified by the oblateness. One can combine the oblate potential Equation [51] and the kinetic energy expressed in the (in-plane) polar coordinates of Fig. 1 to construct a new Lagrangian

$$\mathfrak{L} = \frac{m}{2}(\dot{r}^2 + r^2\dot{\theta}^2) + \frac{GMm}{a}\left[\frac{a}{r} + J\frac{a^3}{r^3}f(\theta)\right] \quad [55]$$

The oblateness-modified equations of motion become

$$\ddot{r} - r\dot{\theta}^2 + \frac{GM}{a}\left[\frac{a}{r^2} + 3J\frac{a^3}{r^4}f(\theta)\right] = 0 \quad [56]$$

$$\frac{d}{dt}(r^2\dot{\theta}) = J\frac{GMa^2}{r^3}\frac{df}{d\theta} \quad [57]$$

The second equation may be integrated

$$r^2\dot{\theta} = p(1 + \epsilon) \quad [58]$$

in terms of the unperturbed angular momentum p of Equation [6] and the as yet unknown function

$$\epsilon = J\frac{GMa^2}{p}\int_0^t dt'\,\frac{1}{r^3}\frac{df}{d\theta} \quad [59]$$

Equation [58] allows time derivatives to be converted to θ derivatives, as before

$$\frac{d}{dt} \equiv \frac{p(1+\epsilon)}{r^2}\frac{d}{d\theta}$$

If one again sets $U = 1/r$ and follows a consistent plan to keep only first-order terms in J, the perturbed geometrical equation for motion in the nominal trajectory plane becomes

$$\frac{d^2U}{d\theta^2} + U = \frac{GM}{p^2} + J\frac{GMa^2}{p^2}\cdot\left[3U^2f(\theta) - U\frac{dU}{d\theta}\frac{df}{d\theta} - \frac{2GM}{p^2}\int_0^\theta d\theta' U(\theta')\frac{df}{d\theta'}\right] \quad [60]$$

A straightforward perturbation procedure is to substitute the expression [11] for $U(\theta)$ about a spherical Earth into the right-hand side of Equation [60], and to solve the (harmonic) differential equation with the added driving term in brackets representing the oblateness induced distortion of the elliptical trajectory. This can be done, and the indefinite integrals evaluated in closed form (5). However, it is substantially easier to approximate $U(\theta)$ on the right-hand side by the burn-

out value $1/r_0$. Since the oblateness potential term itself falls off rapidly with r, and since economical ballistic trajectories seldom rise far above the Earth (compared with a), this approximation is probably good to 10 per cent, or less than 1 mile according to Equation [49]. The above equation is thus simplified to

$$\frac{d^2U}{d\theta^2} + U = \frac{GM}{p^2} + J\frac{GM}{p^2}\left[\left(3 - 2\frac{GMa}{p^2}\right)f(\theta) + 2\frac{GMa}{p^2}f(0)\right]$$

since $r_0 = a$ to our accuracy. This equation may be solved and the initial conditions of Equation [10] invoked to yield a perturbed $U(\theta)$. Recalling that $\lambda \sin^2\gamma = p^2/GMa$

$$aU(\theta) = \frac{1 - \cos\theta}{\lambda\sin^2\gamma} + \frac{\sin(\gamma - \theta)}{\sin\gamma} + \frac{J}{\lambda^2\sin^4\gamma}\int_0^\theta dx \times \sin(\theta - x)\,[(3\lambda\sin^2\gamma - 2)f(x) - 2f(0)] \quad [61]$$

Impact occurs when $U = 1/a$, and this will now happen at $\theta = \phi + \delta\phi$, where $\delta\phi$ is the range (angle) correction. Using the results of our discussion of error coefficients the range error at impact $\delta R = a\delta\phi$ becomes

$$\delta R = -\frac{Ja}{\lambda^2\sin^3\gamma\cos\gamma}\int_0^\phi dx \sin(\phi - x)\,[(3\lambda\sin^2\gamma - 2)f(x) - 2f(0)] \quad [62]$$

Finally, substituting for $f(\theta)$ from Equation [59] and performing the integration

$$\delta R = \frac{-Ja}{\lambda^2\sin^3\gamma\cos\gamma}\left\{2\left(\frac{1}{3} - A^2\right)(1 - \cos\phi) + \left(\lambda\sin^2\gamma - \frac{2}{3}\right)[(1 - \cos\phi) + A^2(\cos^2\phi + \cos\phi - 2) - B^2(1 - \cos\phi)^2 - 2AB\sin\phi\,(1 - \cos\phi)]\right\} \quad [63]$$

To illustrate this result, we assume $\alpha = \beta = 45$ deg, and a minimum energy orbit to $\phi = 90$ deg

$$\delta R = -10.8 \text{ nautical miles (undershoot)} \quad [64]$$

which agrees with the approximate estimate [49] remarkably well.

Crossrange Error

The oblate potential also produces forces acting normal to the unperturbed plane of motion, and these give rise to lateral errors at impact. Using Newton's second law of motion, and denoting the normal to the unperturbed plane by $\vec{n}_0$, the equation for lateral displacement L becomes

$$\frac{d^2L}{dt^2} = \frac{F_n}{m} = -\frac{1}{m}\vec{n}_0\cdot\vec{\nabla}V \quad [65]$$

One can write out the gradient in spherical coordinates (r, σ, ω) of Fig. 9 as

$$\vec{\nabla}V = \vec{e}_r\frac{\partial V}{\partial r} + \vec{e}_\sigma\frac{1}{r}\frac{\partial V}{\partial\sigma} + \vec{e}_\omega\frac{1}{r\sin\sigma}\frac{\partial V}{\partial\omega} \quad [66]$$

The oblate potential Equation [45] is independent of longitude (ω). Since e_r lies in the unperturbed plane of motion, $\vec{n}_0\cdot\vec{e}_r = 0$, and Equation [65] becomes

$$\frac{d^2L}{dt^2} = -2J\frac{GMa^2}{r^3}\sin\sigma\cos\sigma\,(\vec{n}_0\cdot\vec{e}_\sigma) \quad [67]$$

Applying spherical trigonometry to Fig. 9, one can show that

$$\vec{n}_0\cdot\vec{e}_\sigma = -\frac{\sin\psi\cos\alpha\cos\beta}{\sin\phi\sin\sigma}$$

and since $\cos\sigma = A\cos\theta + B\sin\theta$ by Equation [50], the lateral equation of motion becomes

$$\frac{d^2L}{dt^2} = -2J\frac{GMa^2}{r^3(t)}\frac{\sin\psi\cos\alpha\cos\beta}{\sin\phi}[A\cos\theta(t) + B\sin\theta(t)] \quad [68]$$

This differential equation really describes the accumulation of crossrange error, since any motion out of the nominal plane must be counted as oblateness correction, $\delta L = L(T) = L(\phi)$. Equation [68] may be integrated to give the total lateral error δL at the impact point, if the unperturbed solutions for $\cos\theta$ and $\sin\theta$ are substituted into the right-hand side. We find it convenient to convert t integrations to θ integrations by means of the unperturbed angular momentum change [8], so that

$$\delta L = -\frac{2JGMa^2}{p^2}\frac{\sin\psi\cos\alpha\cos\beta}{\sin\phi}\int_0^\phi d\theta' r^2(\theta') \times \int_0^{\theta'} d\theta'' \frac{A\cos\theta'' + B\sin\theta''}{r(\theta'')} \quad [69]$$

To the same approximation used previously, one may hold r constant in these integrations and calculate

$$\delta L = -\frac{2Ja}{\lambda\sin^2\gamma}\frac{\sin\psi\cos\alpha\cos\beta}{\sin\phi}[A(1 - \cos\phi) + B(\phi - \sin\phi)] \quad [70]$$

Explicit corrections may now be computed from a knowledge of the burnout and impact coordinates (α, β, ψ, ϕ) and the ballistic energy variables (λ, γ).

Geophysical Problems

We have now discussed all the major influences exerted on the free flight trajectory of a ballistic missile. It is valuable, however, to consider briefly the miscellaneous perturbations which also affect such a motion. Of especial interest are inherent uncertainties in the fundamental geophysical constants and the influence of gravitational anomalies. Ballistic guidance depends upon one's ability to anticipate the absolute gravitational attraction exerted on the missile by the Earth over the entire free flight trajectory. The fundamental geophysical constant GM/a and the mean equatorial radius a enter explicitly into the guidance equation, so that present uncertainties in the knowledge of these constants is necessarily reflected in range bias errors which are *uncertain a priori*. Furthermore, in order to compute accurately the rotational and oblateness corrections discussed in the sections "Trajectories on a Rotating Earth" and "Oblateness Correction," respectively, one must know both the spin rate ω and coupling constant J. On the other hand, variations about the mean gravitational field, such as gravitational anomalies and solar-lunar effects, can cause minor errors if they are not included in the guidance program.

Uncertainties in the Physical Constants

Both the mean radius and the ratio GM/R enter the planar hit Equation [12], and we must inquire as to the accuracies with which these are presently known. It is convenient to re-

write the hit equation explicitly in terms of GM/a and

$$1 + \frac{h}{a} = \frac{GM}{a} \frac{1}{(1 + h/a)V^2} \frac{1 - \cos \phi}{\sin^2 \gamma} + \frac{\sin (\gamma - \phi)}{\sin \gamma} \quad [71]$$

Percentile uncertainties in the fundamental geophysical constant GM/a are evidently equivalent to percentile uncertainties in V^2, and the burnout speed error coefficient Equation [24] may be used to estimate the *range* error incurred by using an incorrect value of GM/a in programming the guidance system

$$\delta R = \frac{\delta(GM/a)}{(GM/a)} \cdot a[\sin \phi + \tan \gamma(1 - \cos \phi)] \quad [72]$$

The individual uncertainties in G and M are quite large, and it seems that the ratio is best determined from measurements of the acceleration of gravity at the Earth's surface

$$GM/a = ag \quad [73]$$

The corresponding percentile variation is

$$\frac{\delta(GM/a)}{(GM/a)} = \frac{\delta a}{a} + \frac{\delta g}{g}$$

The probable uncertainty in the equatorial radius δa is now ess than 100 m (6). The estimated error (7) in the Potsdan absolute gravity standard is about 4 milligal.[7] Combining these estimates, we find

$$\frac{\delta(GM/a)}{(GM/a)} \simeq 2\ 10^{-5} \quad [74]$$

and the corresponding range error can be inferred from Fig. 6. For example, at ICBM range with a minimum speed trajectory, one finds

$$\delta R \simeq 0.2 \text{ miles} \quad [75]$$

is the irreducible range accuracy.

The mean equatorial radius a also enters into Equation [71] through the ratio h/a. The range error produced by an uncertainty in a alone can be inferred from the burnout height error coefficient in Equation [26]

$$\delta R = \delta a \frac{h}{a} \left[2 \tan \gamma - \frac{\sin (\gamma - \phi)}{\sin \gamma} \right] \quad [76]$$

The bracketed quantity is less than 6 for all ballistic trajectories of interest, whereas h/a itself is always less than one-tenth because of powered flight gravity loss considerations. Hence

$$\delta r < \delta a < 100 \text{ meters} \quad [77]$$

which is quite modest. The point of the matter is that one is using only an r-differential course relative to the *uncertain* sphere, so that the absolute radius is less important in this connection.

The angular spin rate of the Earth ω introduced previously is now known to better than one part in 10^7, corresponding to the accuracy of astronomical time standards and slight perturbations in the Earth's spin rate. The rotational corrections discussed in the section on guidance equations are several hundred miles, so that the uncertainty in making these corrections is only a few inches!

The uncertainty in the oblateness coupling constant J given by Equation [47] is about one part in 400. However, the oblateness corrections themselves are only of the order 10 miles for long-range trajectories, so that the impact point would be uncertain by less than 40 m.

[7] 1 gal = 1 cm/sec²; 1 g = 980 gal.

Gravitational Anomalies

World-wide measurements of the acceleration of gravity show departures from the international ellipsoid represented by Equation [45]. These anomalies are probably due to local concentrations or shortages of material in the Earth's crust. The corresponding modification of the acceleration of gravity is about 30 milligal, if one compensates isostatically[8] for the conspicuous land masses and ocean troughs. Tanni (8) has studied the distribution of these "free-air anomalies" and finds some reason to believe that latitude-dependent term should be added to the potential Equation [45] to represent a tri-axial ellipsoid, or "potato shape" of the Earth

$$\delta V = E \frac{GMm}{a} \left[\frac{a^3}{r^3} \sin^2 \sigma \cos (2\omega - k) \right] \quad [78]$$

If all of the residual anomalies are lumped into this harmonic, the value inferred from Tanni's data (8) is

$$E \simeq 2\ 10^{-5} \quad [79]$$

Others argue that the "potato" shape is fictitious, and the matter is still in doubt. However, we do notice that this harmonic changes by its total amount E in a longitude change of 90 deg, and so might well produce a "resonance effect" with a 5400-nautical-mile ICBM trajectory. The perturbation scheme discussed in the previous section is well suited to evaluating such effects and was used to compute the impact errors for typical trajectories corresponding to the potential term Equation [78]. These errors can be as large as a quarter and half mile at long range, indicating that the resonance effect does indeed conspire to *increase* the simple estimate that one might make: $ER \simeq 0.1$ mile.

One need not use the harmonic series representation of the Earth's gravitational potential field, especially if it is not clear into which harmonic term the anomalies should be lumped. In fact, potential theory (9) tells one how to compute the Earth's potential at any exterior point in terms of all the surface gravity values exactly. If one considers only variations δg about the value g_0 corresponding to the Newtonian r^{-2} potential, one can write the modification of the potential at any exterior point r, σ, ω (see Fig. 9) in terms of the surface values of δg over the variable points (a, ξ, η)

$$\delta V(r, \sigma, \omega) = \frac{1}{4\pi} \int_0^{\pi} d\xi \sin \xi \int_0^{2\pi} d\eta\ F\left(\frac{r}{a},\ \cos \Theta\right) \delta g(\xi, \eta) \quad [80]$$

where

$$\cos \Theta = \cos \sigma \cos \xi + \sin \sigma \sin \xi \cos (\omega - \eta) \quad [81]$$

and the kernel is given by

$$K(\rho, \cos x) = \frac{2}{(1 - 2\rho \cos x + \rho^2)^{1/2}} - \frac{1}{\rho} - \sin h^{-1} (\cos x) + \sin h^{-1} \left(\cot x - \frac{\csc x}{\rho} \right) \quad [82]$$

Here δg is the magnitude of the acceleration of gravity measured in the *radial* direction at the Earth's surface. The gradient of expression [80] can be used to predict the force field perturbations exerted on the missile at altitude in terms of the measured surface values of δg. The range and cross-range errors which would result from ignoring the effect of Equation [80] in planning ballistic trajectories are most conveniently computed using the perturbation procedure developed in the previous section. This is a lengthy process,

[8] This involves placing an equal and opposite mass at a depth of approximately 113 km, so that the net mass shift in a given solid angle measured from the Earth's center is zero. Such combinations should behave as mass doublets and so loose their effect at large distances (i.e., missile altitudes) quite rapidly.

however, and one is encouraged to seek simpler methods for computing the approximate effect of specific anomalies.

To estimate the effect of a single anomaly, one may assume a pulse potential anomaly of magnitude Λ and angular width ϵ, at a central angle position θ_0

$$\delta V = \frac{GM}{a} \cdot \left\{ \begin{matrix} \Lambda, \theta_0 < \theta < \theta_0 + \epsilon \\ 0, \text{ otherwise} \end{matrix} \right\} \quad [83]$$

The perturbation theory outlined in the previous section can be used to calculate the corresponding in-plane range error

$$\delta R \simeq -\Lambda \epsilon a \cos \theta_0 \left(\frac{3\lambda \sin^2 \gamma - 2}{\lambda^2 \cos \gamma \sin^3 \gamma} \right) \quad [84]$$

This result shows that the impact error is directly proportional to: (a) the magnitude Λ of the pulse, (b) the linear distance ϵa over which the pulse extends, and (c) the distance of the pulse from burnout. Evidently, the pulse is most disasterous if it occurs near burnout ($\theta_0 = 0$), for then the trajectory modifications so produced have the entire free flight trajectory over which to develop errors. A 200-milligal anomaly extended over 200 miles is an extreme gravitational variation, although its single effect for ICBM flights is only about 20 m. It is apparent that even combinations of severe anomalies can only cause small impact errors for ballistic missiles.

Miscellaneous Effects

Herrick (10) has shown that the gravitational attractions of the sun and moon, if neglected, cause impact errors which are measured in feet, and are thus negligible. The point here is not that these fields are weak (for they cause the tides), but rather that their balance with the offsetting centrifugal forces[9] exerted on the Earth—and hence on the missile—changes very little during the short flight time of a ballistic missile.

General relativistic effects produce a central force modification of the basic Newtonian potential which is similar to the oblateness potential of Equation [45]. If C is the speed of light

$$V_{rel} = \frac{GMm}{a} \left[\frac{a}{r} + \left(\frac{V \sin \gamma}{C} \right)^2 \frac{a^3}{r^3} \right] \quad [85]$$

Comparison of the equivalent coupling in this expression with J in Equation [45]

$$\left[\frac{V_0 \sin \gamma}{C} \right]^2 < 4 \ 10^{-10} \ll J \simeq 10^{-3}$$

shows that the error due to neglecting general relativistic effects is six orders of magnitude smaller than the oblateness correction indication by Equation [49].

[9] Produced by motion round the sun and the Earth-moon center of mass, respectively.

Acknowledgment

The author thanks S. Ramo, D. E. Wooldridge, G. F. Floyd, J. C. Fletcher, S. Herrick, R. A. Park and especially L. Blitzer for valuable discussions of these problems.

References

1 Whitaker, E. T., "A Treatise on the Analytical Dynamics of Particles and Rigid Bodies," Cambridge University Press, 1944.

2 Baker, C. D., and Hart, J. J., "Maximum Range of a Projectile in a Vacuum," *Amer. J. Phys.*, vol. 23, 1955, pp. 253–255.

3 Blitzer, L. and Wheelon, A. D., "Maximum Range of a Projectile in Vacuum on a Spherical Earth," *Amer. J. Phys.*, vol. 25, 1957, pp. 21–24.

4 Jeffreys, H., "The Earth," Cambridge University Press, 1952, p. 129.

5 Blitzer, L., Weisfeld, M. and Wheelon, A. D., "Perturbations of a Satellite's Orbit Due to the Earth's Oblateness," *J. Appl. Phys.*, vol. 27, 1956, p. 1141.

6 Private communication from Dr. John A. O'Keefe, 1955.

7 Private communication from Prof. Weiko Heiskanen, 1954.

8 Tanni, L., "On the Continental Undulations of the Geoid as Determined from the Present Gravity Material," *Pub. of the Isostatic Institute of Int. Assoc. of Geodesists*, no. 18, 1948, Helsinki.

9 Kellogg, O. D., "Foundations of Potential Theory," Dover Press, New York, 1953.

10 Private communication from Prof. Samuel Herrick, 1954.

Bibliography

Baker, C. D. and Hart, J. J., "Maximum Range of a Projectile in a Vacuum," *Amer. J. Phys.*, vol. 23, 1955, pp. 253–255.

Blitzer, L. and Wheelon, A. D., "Maximum Range of a Projectile in Vacuum on a Spherical Earth," *Amer. J. Phys.*, vol. 25, 1957, pp. 21–24.

Ehricke, K. A., "Error Analysis of Keplerian Flights Involving a Single Central Force Field and Transfer Between Two Central Force Fields," *Navigation*, vol. 6, 1958, pp. 5–23; *see also* Convair Astronautics Rep. AM-7-551, Jan. 17, 1958.

Fried, B. D. and Richardson, J. M., "Optimum Rocket Trajectories," *J. Appl. Phys.*, vol. 27, 1956, pp. 955–961.

Frye, W. E., "On the Accuracy of the Long Range Ballistic Rocket," *J. Appl. Phys.*, vol. 22, 1951, p. 585.

Kalensher, B. E., "Equations of Motion of a Missile and a Satellite for an Oblate-Spheroidal Rotating Earth," Calif. Inst. Tech., Jet Propulsion Lab., Memo 20-142, 1957.

Kelly, A. J., "Effect of Thrust Termination Process Upon Range Dispersion of a Ballistic Missile," ARS JOURNAL, vol. 29, no. 6, June 1959, pp. 432–440.

Lawden, D. F., "Minimal Rocket Trajectories," JOURNAL OF THE AMERICAN ROCKET SOCIETY, vol. 23, 1953, pp. 360–367.

Reece, J. W., Joseph, R. D. and Shaffer, D., "Ballistic Missile Performance," JET PROPULSION, vol. 26, April 1956, pp. 251–255.

Schütte, K, "Die Bahnbestimmung aus dem Vektor der Bahngeschwindigkeit und der Einfluss einer Aenderung desselben auf die Bahnelemente," Proc. IV IAF Congress (Zurich, 1953), pp. 89–101.

Singer, S. F. and Wentworth, R. C., "A Method for Calculating Impact Points of Ballistic Rockets," JET PROPULSION, vol. 27, 1957, pp. 407–409.

Stabilization and Attitude Control of Satellite Vehicles

WILLIAM E. FRYE and
EDWARD V. B. STEARNS

Lockheed Aircraft Corp.
Sunnyvale, Calif.

The status of concepts and techniques in the field of satellite attitude control and stabilization as reflected in the open literature of the last five years is reviewed. Stabilization by means of the gravity gradient, aerodynamic torques and radiation pressure is examined. Various attitude sensors and control torque generators are discussed. The sources of disturbing torques are briefly summarized.

THIS paper will attempt to review the "state-of-the-art" in the field of attitude control and stabilization of satellites by examination of the unclassified literature and publications of the past five years. Although artificial satellites have been the subject of intensive study and design effort for more than 12 years, and have been successfully launched for almost two years, only one satellite has been reported to have been attitude controlled on orbit at the time of this writing (July 1, 1959).[1] An indication of the increasing importance of attitude stabilization is contained in the reports of plans for such sophisticated future satellite applications as the communications, astronomical observatory, reconnaissance and Project Mercury (man-in-space) satellites.

For purposes of clarification of terms, the following distinction between attitude stabilization, control and indication will be assumed in this paper:

Stabilization implies giving the vehicle a configuration having a naturally stable orientation to which the body will tend to return if perturbed slightly in attitude or from which it resists being disturbed as in spin stabilization. Examples that will be discussed are gravity gradient, radiation pressure and aerodynamic pressure stabilization. Although these effects may be stabilizing influences in some applications they can become sources of undesired disturbing torques in others, so that one can truthfully say, "the concept of the vehicle as gently floating through space in a completely undisturbed manner is ... naive. The vehicle must continually be contending with its environment in one way or another" (1).[2]

Attitude control is defined as the attempt to constrain the attitude of the body to a particular desired orientation. This implies the ability to generate or initiate restoring torques whenever the attitude deviates from the desired orientation. Control systems thus employ active means of generating torques and forces to regulate the attitude. Examples of such control means are gas reaction jets or rockets and inertia reaction wheels.

Along with the "muscles" that control orientation goes some means of sensing attitude and providing signals to the input of the control system. Such attitude indication is usually accomplished by employing devices and instruments, such as gyros, horizon scanners, star, sun or planet sensors, accelerometers, pendulums and many others as part of the feedback loop through the control system and vehicle attitude. In addition to their role of providing the "intelligence" to the control system, attitude indicators are valuable in their own right as transducers of attitude information to a telemetry system for transmission to the ground for evaluation.

Although the title of this paper indicates the application to satellite vehicles, some of the sensing and control methods discussed here are equally applicable to space missions other than satellites, such as lunar, planetary and sun probes, some of which may involve satellite phases of operation.

Although not explicitly discussed here, guidance during ascent to orbit can influence attitude control and stabilization indirectly, for example through the initial conditions in attitude at injection, the air drag and aerodynamic forces especially at perigee, and the orbit eccentricity (6). The ascent guidance requirements can vary widely depending on the particular mission, ranging from the relatively simple task of placing the vehicle in any orbit to the stringent requirements for precise orbit matching and rendezvous of satellites which might rival the ICBM requirements for accuracy and timing.

Because of security restrictions, it is not possible to give adequate credit to certain individuals and organizations whose pioneering work in the field of satellite stabilization and control has not been reported in the open literature.

Gravity Gradient Stabilization

The existence of a natural satellite of the Earth—the moon—which always maintains the same face toward the Earth, has inspired investigations leading to an understanding of the role that the gravitational force plays in stabilizing a satellite. Astronomers and mathematicians for many years have studied the librations of the moon, that is, the apparent oscillations about its center of gravity relative to the line of sight to the Earth. Routh (2) has derived the equations of motion about the axis normal to the orbit plane and deduced that the motion is stable if the principal axis of least moment of inertia lying on the moon's equator would point toward the Earth and if the moments of inertia about the two principal axes assumed to lie in the equatorial plane were sufficiently unequal. This result is attributed to Laplace. The method of stabilization derives its torque from the gradient of the gravity field; its analysis may be simplified if applied to a configuration in which two similar masses are concentrated at the ends of a rigid weightless rod—hence the term of "dumbbell effect" is applied.

The torques on a satellite due to the gravitational field have been discussed in a number of recent papers (3–15).

Received Aug. 4, 1959.

[1] Discoverer II, launched on April 13, 1959, was reported as successfully attitude stabilized on orbit. Vanguard and Explorer satellites have been spin stabilized at injection into orbit as a consequence of ascent guidance requirements. Published information regarding Sputniks indicates that no attempt was made to stabilize their attitude but rather that their tumbling motions were employed as a means to measure upper atmosphere properties. See Sedov, L. I., "Dynamic Effects on the Motion of Earth Sputniks," Proc. IXth IAF Congress, Aug. 1958, Amsterdam.

[2] Numbers in parentheses indicate References at end of paper.

The equations of motion for the satellite attitude have been derived and solved with varying degrees of rigor and completeness by Klemperer and Baker (3), Roberson (4–6), Davis (11), Stocker and Vachino (12) and Schindler (13). The importance of the choice of a coordinate reference system has been pointed out by Roberson (6). Following his notation, one can derive the attitude equations for small angles from the well-known Euler equations as

$$I_x\ddot{\theta}_1 + 4\omega_0^2(I_y - I_z)\theta_1 + \omega_0(I_x + I_z - I_y)\dot{\theta}_3 = \sum \text{external and control torques } D_x(t) + \text{parametric excitation function } P_x(\theta, \dot{\theta}, t) \quad [1]$$

$$I_y\ddot{\theta}_2 + 3\omega_0^2(I_x - I_z)\theta_2 = D_y(t) + P_y(\theta, \dot{\theta}, t) \quad [2]$$

$$I_z\ddot{\theta}_3 + \omega_0^2(I_y - I_x)\theta_3 - \omega_0(I_x + I_z - I_y)\dot{\theta}_1 = D_z(t) + P_z(\theta, \dot{\theta}, t) \quad [3]$$

where

I_x, I_y, I_z = moments of inertia about the principal axes
$\theta_1, \theta_2, \theta_3$ = attitude deviation angles in roll, pitch and yaw, respectively, relative to the forward sense of the vehicle motion in the instantaneous orbital plane and the vertical
ω_0 = mean angular velocity of orbital motion

The parametric excitation torques $P(\theta, \dot{\theta}, t)$ depend on the choice of axes and are usually quite small.

Davis (11) has shown that the second term on the left of each of the Equations [1, 2 and 3] may be interpreted as arising from a combination of the effect of torques due to the gradient of the gravitational field and the centrifugal force of orbital motion. In the case of pitch (Eq. [2]) only the gravity gradient exerts a torque on the vehicle of magnitude $3\omega_0^2(I_x - I_z)\theta_2$; for yaw (Eq. [3]) the centrifugal force (due to the use of a rotating frame of reference) exerts a torque of magnitude $\omega_0^2(I_y - I_x)\theta_3$. For roll (Eq. [1]) the gravity gradient gives a term $3\omega_0^2(I_y - I_z)\theta_1$ and the centrifugal force a term $\omega_0^2(I_y - I_z)\theta_1$.

A number of important observations can be made by inspection of these equations. Except for the parametric excitation P_y, motion in pitch is uncoupled from that in roll and yaw, whereas the latter are crosscoupled through the terms in $\dot{\theta}_1$ and $\dot{\theta}_3$. No inherent damping is present about any axis. The motion is inherently stable, although undamped, if $I_z < I_x < I_y$. For stable motion, the restoring torques (the second term on the left of Eqs. [1, 2 and 3]) are very small, amounting to only a few hundred to a few thousand dyne-cm per degree for typical satellite vehicles, and hence the periods of oscillation are very long, the period in pitch being

$$0.577\sqrt{I_y/(I_x - I_z)}\,T_0$$

or more than 40 min (11). Here T_0 is the orbital period which is greater than 84.4 min for satellites of the Earth.

In order to use the gravity gradient or "dumbbell effect" (3) for satellite stabilization, it is first necessary to choose proper values for the moments of inertia about the principal axes so that the vehicle will have restoring torques about all three axes. The vehicle will tend to orient itself with the axis of minimum moment of inertia along the vertical and with the axis of maximum moment of inertia normal to the orbit plane. Next, since the restoring torques reach a maximum value at angles of about 45 deg from the reference orientation, when the satellite is put under the influence of gravity stabilization the initial conditions must be such that the vehicle will be constrained by the gravity gradient field and will not tumble. This means that when the satellite is released, the angular velocity and position deviation must be sufficiently small so that the vehicle will oscillate about the equilibrium position. Finally, since no inherent damping is present, it would be very desirable to introduce some source of damping torques to reduce these oscillations, eliminating the effect of transient disturbing torques such as meteor hits. Roberson (14) and Angle (8) have suggested the use of vibration absorbers or of variable speed inertial wheels driven from rate gyros to provide damping for a gravity stabilized satellite.

If a constant angular momentum flywheel is fixed in the satellite vehicle with its axis normal to the axis of minimum moment of inertia (the natural vertical axis), the vehicle on orbit will be subject to a torque tending to align the flywheel angular momentum vector with the angular momentum vector of the vehicle's rotation at orbital rate in inertial space, resulting from the gravity gradient constraint tending to keep the axis of minimum moment of inertia oriented to the verti-

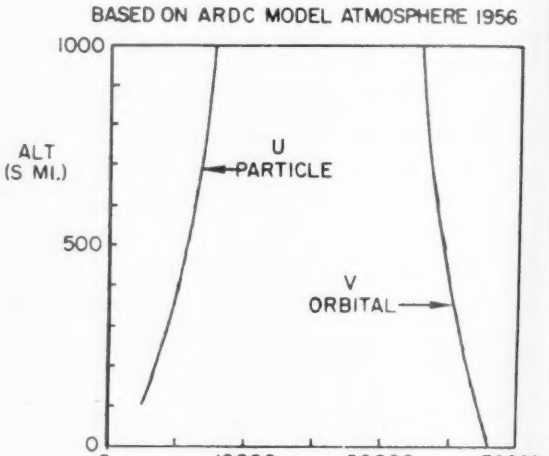

Fig. 1a Mean particle velocity of the atmosphere and velocity of vehicle in circular orbit vs. altitude

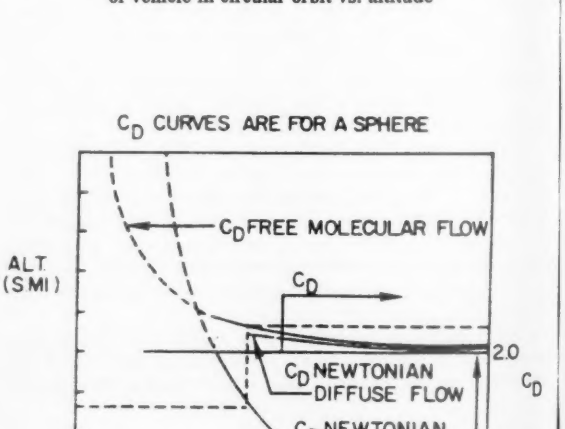

Fig. 1b Drag coefficient and altitude vs. molecular speed ratio

cal. Thus the axis of the flywheel will tend to be aligned normal to the orbit plane, and this effect can be used to provide a preferred yaw orientation to the vehicle as well as to augment the natural yaw and roll gravity and centrifugal restoring torques. The addition of such a "pitch wheel" has been proposed by several authors (6, 8). A natural result of the stiffening of the restoring torque in roll and yaw is the decrease in the natural period of oscillation about these axes.

Aerodynamic Stabilization

The possibilities of stabilization by aerodynamic forces which are not inappreciable at altitudes intermediate between the minimum for reasonable lifetime and the maximum for such forces to be usable have been discussed by DeBra and Stearns (15,16), and by Wall (17). An indication of the magnitude of these forces can be obtained when one computes the dynamic pressure on an orbiting vehicle: At 80 miles it is approximately 0.01 lb/ft², falling off to 3×10^{-8} lb/ft² at 350 miles. Sedov (27) reports drag forces on Sputnik III at perigee (226 km) of about 4 gr, leading to decelerations of 3×10^{-6} g. Figs. 1a and 1b show properties of the upper atmosphere and drag coefficients for orbiting vehicles. Natural stability is obtained by insuring that the center of pressure lies behind the center of mass relative to the direction of travel. At altitudes usually considered suitable for aerodynamic stabilization, between 80 and 300 miles (15–17), the aerodynamic forces provide no damping, so that some means of damping must be provided. Wall (17) has suggested viscous damping by means of a flywheel in oil or by a flexible joint coupling to a drag device.

Aerodynamic forces at the altitude of interest here (above 80 statute miles) are a study in themselves. The computation of drag based on free molecular flow is complex. A good approximation can be made assuming Newtonian flow, however, if the molecular speed ratio is sufficiently high. The assumption of Newtonian flow infers a drag coefficient of 2; so, when the drag coefficient based on free molecular flow approximates 2, the assumption of Newtonian flow yields reasonable results. Figs. 1a and 1b present a method of determining in what range of altitude this approximation can be used. The drag characteristic plotted is for a sphere, but the shape of the curve is characteristic. The assumption of Newtonian flow is therefore justifiable for altitudes less than 375 statute miles for accuracies on the order of 10 per cent. Theoretically, it is necessary that the Knudsen number (the ratio of particle mean free path to a significant vehicle dimension) be greater than 10 to justify free molecular flow. From experimental results, however, it appears that the flow is essentially free molecular for Knudsen numbers greater than 2.

DeBra and Stearns (15) have pointed out that gravity gradient stabilization and aerodynamic stabilization can be incompatible in that each may play the role of a disturbing torque for the other unless special designs are employed (17).

Radiation Pressure Stabilization

This method is similar to aerodynamic stabilization in that it depends on the presented area and the locations of the center-of-pressure and the center-of-mass. The sun's radiation is usually considered the source of pressure, and this amounts to 4.3 or 4.5×10^{-5} dyne/cm² (6,18).

The effect is quite small compared with other effects, but in addition to constituting a disturbing torque for some applications, it may play a useful role in interplanetary missions (19). In order to evaluate the effect of solar radiation pressure for attitude stabilization, consider the radiation falling on a body which is a right-circular cone with a mass protruding forward.[3]

The cone has the following properties (see Fig. 2):

Cone half angle, θ
Center of mass location, d — forward of vertex
Cone slant height, h
Surface area of cone, unity
Axis of cone, z-axis
Moment of inertia about Y-axis, I_y
Sun, in x-z plane such that incident radiation makes angle δ with z-axis

The torque acting on the cone which arises from radiation pressure is about the y-axis and is given by

$$L_Y = \frac{p_0 h^2}{2}\left[\left(\frac{2}{3}\right) h \cos^2\theta + d\right] \sin 2\theta \sin\delta$$

where p_0 is the radiation pressure.

The torque gradient with sun angle is

$$\frac{\partial L_Y}{\partial \delta} = \frac{p_0 h^2}{2}\left[\left(\frac{2}{3}\right)\cos^2\theta + \frac{d}{h}\right] \sin 2\theta$$

For all values of d/h, a unique value of $\theta \leq \pi/2$ will exist for which the torque gradient is a maximum.

The natural frequency of such a cone is given by

$$\omega_y = \sqrt{\frac{\partial L_Y/\partial\delta}{I_y}}$$

For a vehicle with the following properties

I_y = 90 slug ft²
d = 8 ft
θ = 70 deg
h = 6.0 ft

the natural frequency is computed to be $\omega_y = 1.5 \times 10^{-4}$ sec, and the period is about 12 hr.

The attitude of such a vehicle may, in principle, be con-

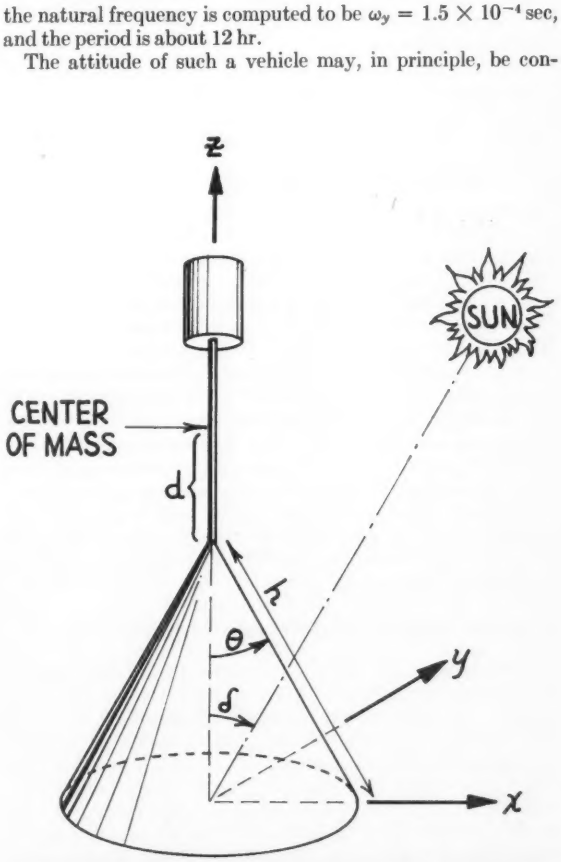

Fig. 2 Satellite vehicle stabilized by solar radiation pressure

[3] Although no specific reference exists, the contribution of R. H. Delp to the analysis of solar radiation stabilization must be acknowledged.

trolled using solar pressure if relatively small control surfaces which might be called "solarons" are added. By driving these surfaces from the servo error signals of a position and rate sensitive control system, the vehicle attitude may be completely controlled with the time constants as indicated.

Recent investigations have indicated the existence of a "solar wind." This is described as a motion of charged particles through the solar system; their motion is in the general direction radially outward from the sun (29). The exact nature of this solar wind is not well known, but it would appear that it is such as to reinforce the attitude control derived from solar radiation pressure.

The heat radiation from internal sources in the satellite vehicle can produce torques if radiated asymmetrically (6). Large amounts of power such as that from a nuclear reactor would be required to produce an appreciable effect. For example, the power radiated must be compared with solar energy falling on the vehicle; at the orbit of Earth this is about 130 w/ft^2.

Attitude Sensors

Among the various kinds of instruments and devices that have been proposed for sensing and controlling attitude from a satellite or space vehicle, one can list inertial devices such as gyros, including the rate sensitive type (20), instruments such as star trackers for establishing lines-of-sight to celestial bodies (21,22), equipment to measure the direction of the Earth's magnetic field (23), instruments for optical or radio sighting to or from the Earth, and even cosmic ray counters (24).

Of particular interest is the optical or infrared horizon scanner which, in addition to determining the local vertical (25), can also be used to give a rough measure of altitude by measuring the angle subtended by the Earth's disk (22,32), or the so-called dip-angle of the horizon. The use of microwave thermal radiations from the Earth to detect the local vertical might be of some interest.

Roberson (32) discusses the use of the horizon scanner for interplanetary guidance and examines the various sources of error, such as the effects of averaging and the oblateness of the planet.

Among the more unusual proposals for sensing attitude is that of Oberth (26) for pendulums to detect the gradient of the gravity field. Because of the extremely small accelerations arising from the very low frequency oscillations of a satellite vehicle, the feasibility of this technique is questionable.

Another interesting instrument reported under development is an "angle-of-attack" meter for intermediate altitudes, which measures the direction of motion relative to the residual atmosphere by means of sensitive microphones (28).

If used in conjunction with a local vertical attitude or reference, a gyroscope can be used to detect the direction of the orbital angular momentum and thereby provide an azimuthal reference in a satellite (33). This "gyrocompass" effect is related to that produced by the previously mentioned addition of a "pitch wheel" of constant angular momentum to the gravity gradient stabilization system to provide or augment yaw stability (6,8). In both cases, the vehicle or the sensing instrument must be stabilized to the local vertical (or horizontal) for proper operation.

Attitude Control Devices and Systems

The most popular methods discussed in the astronautical literature for providing control torques have been by means of reaction jets (8,34,35) and by rotating flywheels (6, 8, 14, 24, 36) or combinations thereof (8,41) in a configuration where rates due to disturbances are sensed and used to generate reaction torques which just counterbalance the disturbances. The reaction jets have the disadvantage of requiring matter to be ejected, thus limiting the useful life on orbit, whereas the accelerating flywheels can be saturated by unidirectional torques. In both cases, the limitations can be overcome or minimized by clever design, and much remains to be done to realize their full potential (6,14,22,37).

Roberson (6,14,23,37) has emphasized the importance of inertial control devices based on internal moving parts and has indicated the general methods of analysis (37). It can be anticipated that many ingenious mechanical designs for such inertial control devices will be evolved.

The Earth's magnetic field was mentioned earlier in connection with attitude sensing (23), and its effect on a spinning satellite has been examined in the literature (38,39). The interaction of the field due to a controlled current flowing in the satellite with the Earth field could form the basis of a control technique with no moving parts and might merit further investigation.

The generation of control torques is but one aspect of the overall servo control problem. Roberson (6,14,22,33,37) has pointed out the importance of a unified design approach and has proposed a synthesis methodology (6,14).

Sources of Disturbing Torques

All of the sources of stabilizing or control torques discussed can equally well act as potential sources of disturbing torques which must be taken into account when designing an attitude control system for a satellite or a space vehicle. In addition, because of the small magnitude of many of the control torques and forces that might be used, the effect of internal moving parts and machinery can be extremely serious, unless great pains are taken to balance out the resulting angular momenta by such means as counterrotating masses. Roberson (37,40) has given an exhaustive analytical treatment of the effect of internal rotating parts as well as a qualitative summary of the various sources of disturbing torques, which can be summarized as follows (6):

Earth's magnetic and electric fields. There is some uncertainty about the electrostatic field at satellite altitudes (6), but the magnetic field can cause eddy currents due to the varying components of the field which will interact with the field. Also, there will be torques on any paramagnetic or ferromagnetic material in the vehicle. In addition, there will be interaction with any electric currents flowing in the vehicle. Any electrostatic field will cause torques due to interaction with the induced electric field as well as with the electric field produced by the motion through the Earth's magnetic field.

Aerodynamic forces.

Sun's radiation pressure. These have both been discussed above in connection with stabilization.

Meteorite impacts. These hopefully will not be serious, except for the occasional catastrophic collision. Much more experimental data need to be collected and studied.

Cosmic ray impacts. These should be negligible in effect and small, even compared with the sun's radiation pressure.

Internal moving parts. Such things as inertia reaction torques from rotating parts, gyroscopic coupling torques, center of mass shifts and shift of principal axes of inertia can cause difficulties.

References

1 Laning, J. H., Frey, E. J. and Trageser, M. G., "Preliminary Considerations on the Instrumentation of a Photographic Reconnaissance of Mars," MIT Instrumentation Laboratory Rep. R-174, April 1958.

2 Routh, E. J., "Dynamics of a System of Rigid Bodies, Part II," Macmillan Co., Inc., 1905, 6th ed., chap. XII, pp. 369–384.

3 Klemperer, W. B. and Baker, R. M. L., Jr., "Satellite Librations," *Astronautica Acta*, vol. 3, 1957, p. 16.

4 Roberson, R. E. and Tatistcheff, D., "The Potential Energy of a Small Rigid Body in the Gravitational Field of an Oblate Spheroid," *J. Franklin Inst.*, vol. 262, 1956, p. 209.

5 Roberson, R. E., "Gravitational Torque on a Satellite Vehicle," *J. Franklin Inst.*, vol. 265, 1958, p. 13.

6 Roberson, R. E., "Attitude Control of a Satellite Vehicle—An Outline of the Problems," Proc. VIII Congress IAF, Barcelona, 1957, p. 317.

7 Roberson, R. E., "Attitude Control—Problems and Principles," *Navigation*, vol. 6, 1958, p. 59.

8 Angle, E. E., "Attitude Control Techniques," *Navigation*, vol. 6, 1958, p. 66.

9 Klemperer, W. B., "Satellite Libration," *Navigation*, vol. 6, 1958, p. 62.

10 Baker, R. M. L., Jr., "Passive Stability of a Satellite," *Navigation*, vol. 6, 1958, p. 64.
11 Davis, W. R., "Determination of a Unique Attitude for an Earth Satellite," Proc. Amer. Astronaut. Soc., 4th Annual Meeting, Jan. 1958.
12 Stocker, T. A. J. and Vachino, R. F., "The Two-Dimensional Librations of a Dumb-bell Shaped Satellite in a Uniform Gravitational Field," Proc. Amer. Astronaut. Soc., Western Regional Meeting, Aug. 1958.
13 Schindler, G. M., "On Satellite Librations," ARS JOURNAL, vol. 29, no. 5, May 1959, pp. 368–370.
14 Roberson, R. E., "Attitude Control," *Elect. Eng.*, vol. 77, 1958, p. 1086.
15 DeBra, D. B. and Stearns, E. V., "Attitude Control," *Elect. Eng.*, vol. 77, 1958, p. 1088.
16 DeBra, D. B., "The Effect of Aerodynamic Forces on Satellite Attitude," Proc. Amer. Astronaut. Soc., Western Regional Meeting, Aug. 1958.
17 Wall, J. K., "The Feasibility of Aerodynamic Attitude Stabilization of a Satellite Vehicle," ARS preprint no. 787–59, April 1959.
18 Buchheim, R. W., "Lunar Instrument Carrier-Attitude Stabilization," Rand Corp. Rep. RM-1730, June 4, 1956.
19 Sohn, R. L., "Attitude Stabilization by Means of Solar Radiation Pressure," ARS JOURNAL, vol. 29, no. 5, May 1959, pp. 371–373.
20 Draper, C. S., "Space-Flight Guidance," *Elect. Eng.*, vol. 77, 1958, p. 1081.
21 Eaton, E. P., "Star Trackers," *Navigation*, vol. 6, 1958, p. 24.
22 Gow, K. P. and Roberson, R. E., "Practical Considerations for Astronautical Guidance and Control," Proc. Amer. Astronaut. Soc., Western Regional Meeting, Aug. 1958.
23 Stockwell, R. E., "Sputnik III's Guidance System," *Missile Design and Development*, vol. 4, Sept. 1958, p. 12.
24 Stuhlinger, E., "Control and Power Supply Problems of Instrumented Satellites," JET PROPULSION, vol. 26, no. 5, May 1956, p. 364.
25 "Space Handbook," Rand Corp. Staff Report of the Select Committee on Astronautics and Space Exploration, U. S. Govt. Printing Office, 1959, pp. 62–66.
26 Oberth, H., "A Precise Attitude Control for Artificial Satellites," Vistas in Astronautics, Vol. I, Pergamon Press, 1958, p. 217.
27 Sedov, L. I., "Dynamic Effects on the Motion of Earth Sputniks," Proc. IXth IAF Congress, Amsterdam, Aug. 1958.
28 Dessler, A. J., Hanson, W. B., Hertzberg, M., McKibbin, D. D. and Wrigley, R. C., "A New Instrument for Measuring Atmospheric Density and Temperature at Satellite Altitudes," Proc. Amer. Astronaut. Soc., Western Regional Meeting, Aug. 1958; *also* JET PROPULSION, Dec. 1958, p. 837.
29 Parker, E. M., "Interaction of the Solar Wind with the Geomagnetic Field," *Phys. Fluids*, vol. 2, 1958, p. 171.
30 Press, S. J., "An Application of Solar Radiation to Space Navigation," *Aero/Space Engng.*, vol. 17, Nov. 1958, p. 51.
31 Garwin, R. L., "Solar Sailing—A Practical Method of Propulsion Within the Solar System," JET PROPULSION, vol. 28, no. 3, March 1958, pp. 188–190.
32 Roberson, R. E., "Optical Determination of Orientation and Position Near a Planet," JET PROPULSION, vol. 28, no. 11, Nov. 1958, pp. 747–750.
33 Roberson, R. E., "A Review of the Current Status of Satellite Attitude Control," *J. Astron. Sci.*, vol. 6, 1959, p. 25.
34 Sancrainte, W. A. and Schiavone, D. C., "Rocket Systems for Satellite Attitude Control," ARS preprint 790–59, April 1959.
35 Pistiner, J. S., "On-off Control System for Attitude Stabilization of a Space Vehicle," ARS JOURNAL, vol. 29, no. 4, April 1959, pp. 283–289.
36 George, M. B. T., "Attitude Control for Space Vehicles," ASTRONAUTICS, vol. 4, March 1959, p. 34.
37 Roberson, R. E., "Principles of Inertial Control of Satellite Attitude," Proc. IX IAF Congress, Amsterdam, Aug. 1958.
38 Rosenstock, H. B., "Effect of Earth's Magnetic Field on the Satellite Spin," *Astronautica Acta*, vol. 3, 1957, p. 215.
39 Bracewell, R. N. and Garriott, O. K., "Rotation of Artificial Earth Satellites," *Nature*, vol. 182, Sept. 20, 1958, p. 760.
40 Roberson, R. E., "Torques on a Satellite Vehicle from Internal Moving Parts," *J. Appl. Mech.*, vol. 25, 1958, pp. 196, 287.
41 Smith, F. A., "The Satellite Telescope," *J. Brit. Interplanet. Soc.*, vol. 16, 1958, p. 361.

Guidance Techniques for Interplanetary Travel

CHARLES D. BOCK and CHARLES J. MUNDO

**American Bosch Arma Corp.
Garden City, N. Y.**

The problem of guidance to near planets with low specific impulse engines is examined. Trajectories to which the vehicle must adhere in order to minimize fuel consumption are treated in order to evolve which measurable parameters are suited for guidance. Criteria are established for the judging of suitability of these measurement parameters. Various possible measurement techniques are catalogued into active electromagnetic techniques, passive electromagnetic techniques and inertial techniques. The merits of the individual methods and the classes are studied.

THERE appears to be little question that guidance techniques exist for controlling the flight of ballistic vehicles to other planets in the near future. The purposes of this paper are to survey these techniques, the hardware that appear suitable for implementing them, and to discuss their merits and limitations. To provide a basis for comparison of these techniques, a specific problem—the guidance of a vehicle to Mars—is treated. The guidance requirements for such a flight, needless to say, are dependent upon many parameters. For example, a system with a very high specific impulse, 10^6, and a very high thrust would require little more than the capacity to sight the target; at the other extreme, a vehicle with only marginal propulsive capacity to make good the mission would require a complex hybridization of highly accurate measurement and computational equipment. Therefore, it will be first necessary to develop an understanding of how system parameters are interrelated, and, further, of the specific requirements that must be fulfilled by the guidance hardware in terms of accuracy, range, speed of response, bandwidth, size and weight. To provide a wider scope of understanding of the capabilities and limitations of various techniques, trajectories resulting in two different orders of magnitude in the miss coefficients will be treated. The first, a hard impact upon Mars, falls within the realm of possibilities for current techniques for initiation guidance and ballistic flight. The second flight, a photographic graze of Mars and return to Earth, involves errors in our knowledge of the solar system and, therefore, is beyond what can be accomplished at initiation. Therefore, the aid of midcourse correction impulses will be required.

The guidance system is part of the whole Mars vehicle and, therefore, must interact with other elements of the spaceflight

Received Nov. 11, 1959.

system. To bound the system, the authors have limited the overall system to equipment that will be available before 1962. Therefore, exotic means of propulsion have been eliminated. This limits consideration of propulsion units to those in the specific impulse range of 300–400 sec and maximum thrusts of 10^6 lb. This implies, in turn, that the mission will be unmanned, and, hence, any equipment which is used must be automated.

The purpose of the guidance system is to control the vehicle so that it follows a trajectory and arrives at some predetermined target which is generally moving in space. The problem that is involved is fourfold:

1 Establish a set of trajectories that are suitable for fulfilling the mission.

2 Define what classes of measurements can be utilized to establish the vehicle on one of this set of trajectories.

3 Define the general problems that exist in making such measurements.

4 Establish what class of instrumentation is suitable for making these measurements.

Trajectories

The trajectory lies at the heart of the guidance problem. Trajectories define the set of possible solutions to which the guidance measurement and computing equipment keep the spacecraft so that its mission is achieved. In this section the problems that arise in the choice of trajectories will be examined. Then, how the various measurable quantities fit into the guidance picture will be treated. There has been extensive discussion of the general trajectory question in the literature by Battin (1,2),[1] Vertregt (3), Lawden (4–6), Preston-Thomas (7,8), Ehricke (9–11) and others. The choice of orbit is related to the complete spaceflight system. The nature of the propulsion available, in terms of both specific impulse and gross thrust, establishes definite bounds upon the set of trajectories that can be used. At the same time limits of guidance accuracies establish another set of limits upon the problem in terms of the miss coefficients.

As a consequence of the available propulsion, the trajectory, in the main, can be assumed to be a ballistic glide. The major element of the impulse will be applied at the beginning of the flight, while the spacecraft is within less than 2000 miles from Earth's surface. Minor correction impulses can be supplied if required after the vehicle has escaped from the Earth's gravitational field.

A poorly chosen trajectory could result in multiplying the gross weight of a vehicle many times. Compare, for example, the price paid in terms of fuel of applying the impulse required to transfer from the Earth's orbit to the Martian orbit before and after escape from the Earth's field. If the velocity required to transfer between the two orbits is V_{EM} and the velocity to escape from the Earth's gravity field is V_E, then the impulse $V_{T'}$ required to escape from the Earth's gravitational field would be $V_{T'} = V_E + V_{EM}$ if the two operations were accomplished successively. However, if the total impulse were to be applied at the beginning of the flight, this could be materially reduced. The initial velocity required to leave sufficient velocity after escape from the Earth's field to make good the Mars flight is given by

$$\frac{1}{2} V_T^2 - \frac{K}{r} = \frac{V_{EM}^2}{2}$$

whereas the velocity required to barely escape is

$$\frac{1}{2} V_E^2 - \frac{K}{r} = 0$$

Hence

$$V_T = \sqrt{V_{EM}^2 + V_E^2}$$

[1] Numbers in parentheses indicate References at end of paper.

Thus, the ratio of increase in impulse required when applied after escape from the Earth's field relative to that applied before is given by

$$\frac{V_{T'}}{V_T} = \sqrt{1 + \frac{2V_{EM}V_E}{V_{EM}^2 + V_E^2}} > 1$$

When this ratio is examined in the light of fuel requirements, it reflects an even larger price because of mass ratio, as shown in Table 1. This improvement in fuel performance that is attained by the early application of impulse, however, is paid for in terms of increasing guidance requirements by a factor of 4 to 1 as shown in Table 2 (11). However, a small correction impulse may be added after escape without an exorbitant cost in excess fuel. The ratio of the total escape velocities in this case is

$$\frac{V_T}{V_{T'}} = 1 + \frac{\delta}{V_s}\left(\frac{V_{EM}}{V_s} + 1\right)$$

where

δ = remaining impulse to be made good
V_s = total impulse initially imparted to the vehicle

A 30-fps deficiency in the Earth's orbit at escape would result in less than 4 per cent increase in mass even with a 300 specific impulse.

Table 1 Cost of transfer impulse above escape impulse, per cent

Transfer impulse	$I_{sp} = 300$	$I_{sp} = 400$
before escape V_T	30	20
after escape $V_{T'}$	160	115

Table 2 Miss coefficients Mars transfer orbit

Departure orbit	
satellite orbit (300 n. mile altitude)	21,947 n. mile/fps
Earth's orbit	5700 n. mile/fps

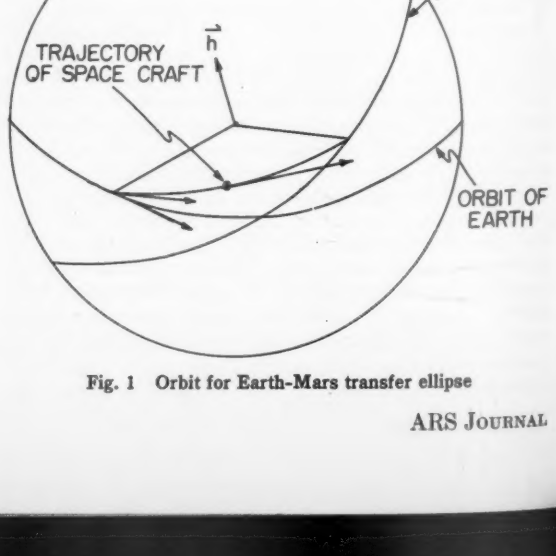

Fig. 1 Orbit for Earth-Mars transfer ellipse

The transfer orbits between Earth and Mars cannot be coplanar with the Earth's orbit because of the severe shooting time restrictions this would impose. However, an ample range of shooting times is available if an orbit plane is chosen defined by the sun, the Earth at the time of firing, and Mars at time of arrival (Fig. 1). If such an orbit is chosen, care must be taken to avoid those shots where the transfer plane makes large angles with the plane of the Earth, such as the condition when the vehicle leaves the Earth 90 deg before the line of nodes for the Earth-Mars ellipse and arrives at Mars 90 deg after, so that the transfer orbit must cross the pole of the Earth's orbit. Fig. 2 shows the high price in mass ratio for high angle orbits. By firing 10 deg and arriving 10 deg from these 90-deg points, this condition can be avoided. With the exception of Battin's work, the literature on three-dimensional interplanetary orbits is limited; particularly absent are miss coefficients studies (13).

The point where the trajectory studies play their most important role in the design of guidance equipment is in the decision of what parameters should be measured to establish the vehicle's trajectory. There are three sets of measurable quantities which can be utilized to guide the vehicle: A sequence of position measurements, a velocity measurement plus initial condition in position, and acceleration measurements plus initial conditions in both velocity and position. The choice of which to use is not a simple matter; there are a number of aspects to it:

1 The question of orthogonality of the measured parameters as they appear in the guidance solution heavily weights their value: To give a simple example of orthogonality, consider the problem of locating a point B based upon base line c-d with only the capacity to measure radial distance, and this with an error ϵR (Fig. 3). The error is given by ϵR. However, when the point moves to B', a large cross track uncertainty develops proportional to $\epsilon R/\sin A$. Such errors also may appear much more subtly in the guidance system.

2 The miss coefficients which result from the control of a particular set of parameters: It is through the miss coefficients that difficulty of measurement can be related to level of system performance.

3 The fact that the suitability of a particular set of measurement parameters varies throughout the flight.

4 The suitability of a particular parameter to make an orbit determination when the vehicle is accelerating, so that the orbit is continuously changing.

5 The accuracy of individual measurements alone may not be an adequate criterion for accuracy: Techniques which lend themselves to the generation of great quantities of data wherein the errors in the individual measurements are random in nature obviously result in greatly improved accuracy in the final data.

The guidance process is one of making the vehicle trajectory match one of the infinity of trajectories that pass through the target. To alter the current trajectory so that it matches a proper trajectory, a thrust is applied to effect an impulse of velocity on the vehicle. The direction of this thrust is such as to minimize the amount which must be applied in order that this match is effected. The magnitude of the velocity impulse is controlled by terminating the thrust at the appropriate time, called the cutoff. This cutoff determination gives rise to critical problems in guidance, since the accuracy of cutoff directly affects the accuracy of the missile.

With high impulses at termination, two problems arise:

1 The mechanical and chemical processes involved in terminating the impulse must be sufficiently predictable in their action and tailoff so that the error in added impulse after the termination signal is provided does not exceed the desired accuracy requirements for the mission.

2 The time required to accomplish a measurement, i.e., smoothing and data processing times, are sufficiently short so that the prediction of the terminal conditions do not vary from the actual terminal conditions by an amount in excess of the allowed error.

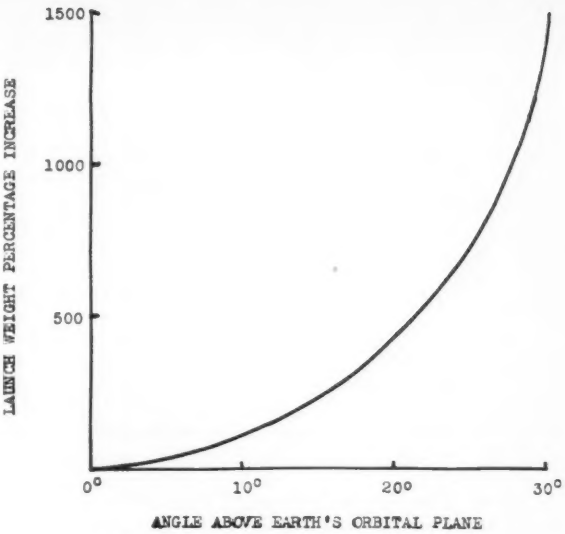

Fig. 2 Fuel cost for high angle transfer orbits

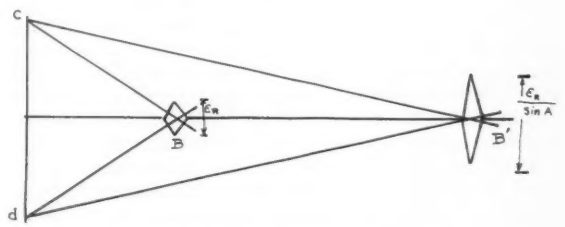

Fig. 3 Nature of orthogonality errors

Let us turn briefly to a comparison of the three kinds of measurables in the light of these system demands. The suitability of velocity measurement is made apparent from examination of the velocity miss coefficients. From Table 2, it is apparent that these are not beyond reasonable bounds of measurement if Mars is the target, and further that they vary materially during the progress along a given trajectory. Magness et al. (12) have shown that the miss coefficients depend critically upon the nominal trajectories and may be improved by a factor of 10 or more if the nominal trajectory is optimized.

Direct measurement of velocity has a positive advantage when the system is in dynamic transition. That is, if propulsion were terminated at this point, these conditions would represent the static energy orbit the vehicle would pursue. Unfortunately, many methods of velocity measurement are inherently noisy, and, as a consequence, a filter must be used. The result of the filter is a smoothing lag which means the system output indicates the condition of the system at some time in the past. In a static case, this is not serious because this error can be predicted. In the dynamic case, it obviously gives rise to a problem, particularly if the thrust and, consequently rate of change of velocity, is high. This can be overcome partially by use of low thrust correction intervals or propulsion system in which the performance is accurately predictable. Inertial measurements on the other hand derive velocity from integrating acceleration and do not suffer from this smoothing lag problem.

It should be pointed out that a high density of position measurements and their associated times are in effect also a good measurement of velocity. This is the case with many tracking radars.

Accelerations measurement also can serve as a basis for space guidance. This process is one which is really only adapted to measuring a change in the orbital state of the vehicle. While the vehicle is pursuing a static trajectory it undergoes no measurable accelerations, and, therefore, this approach cannot be used to measure what orbit a vehicle is on. If the initial conditions—that is, the orbit the vehicle is currently traveling—are determined, the measurement of acceleration is an excellent method for determining the change in orbit.

A sequence of position measurements can also be utilized to establish the trajectory of a vehicle in space. In this case, the vehicle must make good a segment of the trajectory which is being determined before the trajectory can be established. If the location of a target planet on its orbit is known simultaneously with that of the vehicle and two other position measurements for the vehicle, the miss of the spacecraft can be defined completely on a geometric basis. However, suitable position measurements are for establishing the trajectory a vehicle is pursuing; they are not at all adapted to metering out changes in velocity, and must be supplemented by a system which gives a good dynamic measurement of the correction increment.

In lieu of miss coefficients, Battin has studied particular trajectories using a position measuring system. In particular he has studied (13) the use of a 10-sec multifix astro-seeking position measuring system for the round trip to Mars. This is an extremely difficult guidance problem requiring a terminal accuracy of 250 miles which would require an accuracy of $\frac{1}{20}$ fps if accomplished by a velocity measuring method. This high precision is required to limit the errors caused by the Mars gravity deflection. His studies indicate that with an impulse of 1500 fps, this guidance problem can be solved. He points out that the clock is not critical in this problem if it is degraded from 1 to 2.5 parts per 10^5. The cost is only 4 per cent more fuel. However, a similar degradation in the guidance accuracy costs 30 per cent more fuel.

Before discussing specific kinds of equipment, it should be pointed out that even with perfect equipment the problem of errors that occur from uncertainties in the constants of our solar system will still arise. First, the scale of measurements used for calibrating our instruments on the Earth is calibrated in feet or meters, whereas astronomical distances are measured in astronomical units. A scale uncertainty of $\frac{1}{10,000}$ exists between the two systems of coordinates. This can be overcome in space only by the class of systems which makes angle measurements based upon base lines known in astronomical units. Perturbations from other planets will be small, that of Jupiter on the Earth being only 420 ft. However, the uncertainty in the moon perturbation will cause a sizable error in the initial launch phase, so that a correction must be made after the vehicle departs from its influence.

Measurement Techniques for Guidance

There are many ways in which position, velocity and acceleration can be measured in space. It is the purpose of this section to examine what these measurement techniques are and what attributes and limitations they have. These methods fall into four broad categories: Active electromagnetic, passive electromagnetic, inertial and contact.

Active Electromagnetic Techniques

Systems in this category measure position or velocity through the measurement of position increments and associated time.

Active electromagnetic techniques for guidance are those where the radiation used is generated within the system itself. These systems have part of their equipment located in the vehicle and part located on the ground. In principle, these parts will be interchangeable, but in practice, the equipment will be designed to place the heaviest elements on the ground. There are four principal types of systems that fall in this category:

1 Measurement of the direction from which the radiation is coming—for angle measurement.

2 Measurement of the transit time of energy from target to known reference point in space—for range measurement.

3 Measurement of the relative phase of coherent signals coming to or from the target along different paths for angle measurement.

4 Measurement of the shift in frequency caused by relative motion between the target and the observer which can be used for both range rate and cross range rate.

The first method involves only the ability to measure the angular direction from which the signal is coming. The last three methods are all synchronous and either explicitly or implicitly involve a clock. This clock may be the radiation itself.

Although each of these systems has its own problems, there is one set of problems common to all of these methods, that is, the tradeoff that exists between the signal-to-noise ratio, the bandwidth required to ascertain how the vehicle is moving in space, and the smoothing time required to obtain the accuracy level desired for the system. The signal-to-noise problem is treated in detail in another paper in this issue, "Radio Guidance," by Stodola. Briefly, however, the problem is that a certain bandwidth is required to measure the errors that arise in acceleration of the spacecraft. This error signal must compete with the noise background of space and the thermal noise of the input elements to the system, in order that the accuracy of measurement is maintained within certain bounds.

Some of the steps which may be taken to improve the signal-to-noise ratio are:

1 Use of a beacon aboard the spacecraft so that the distance attenuation for two-way reflected transmission $1/R^4$ is reduced to the one-way attenuation $1/R^2$.

2 Reduction of the bandwidth required by the system by simplifying the measurements, so that only the unpredictable elements of information are involved in the measurement.

3 Reduction of the noise input to the system by use of low temperature input devices, such as masers (14, 36) and high gain low spill over-feed (15) in the antennas.

4 Use of phase-coherent detection (16–18) systems which permit the realization of the narrow bandwidth systems that are compatible with the information content of the guidance signals.

Radio techniques have already and will continue to play an important role in space guidance. Obviously, their prime suitability is for the case when the vehicle is near the Earth. However, they are not limited to this region. It has been reported that the Russians have used these techniques in their recent high accuracy shot around the moon. Jet Propulsion Laboratory (19) has reported communication with the Pioneer space shot to a range in excess of 400,000 miles, and this with a radiated power of only $\frac{1}{4}$ w. Theoretically, this range can be extended indefinitely. The ability to sense dynamic state range tracking at these great ranges is open to question, and, as will be pointed out in the following discussion, large problems loom for obtaining any accurate cross range tracking data—an orthogonality problem.

The first category of active guidance methods is based upon the measurement of the direction of incoming radiation. It is accomplished in the same manner that is used for light. A parabolic surface causes the reflected plane wave front to arrive at the focus in phase when the axis of the parabola is normal to the wave front. However, because of diffraction, the antenna may be turned to either side of the normal by an angle 2.4 λ/d before the radiation is reduced perceptibly (d = size of reflector and λ = wave length of the radiation).

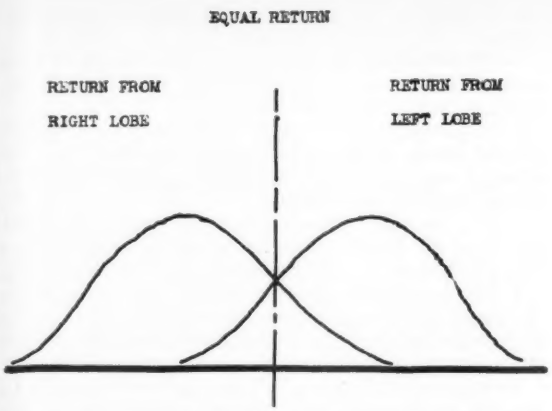

Fig. 4 Measurement of position by lobe comparison techniques

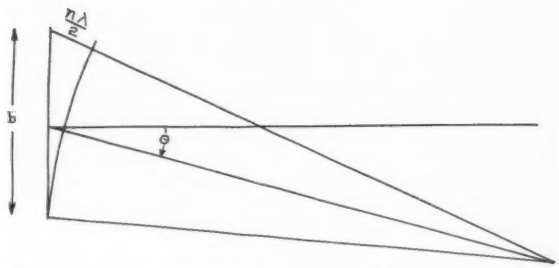

Fig. 5 Measurement of position by interferometer techniques

This angular accuracy can be improved by making a large number of readings so that the shape of the lobe can be accurately determined statistically. This means paying for greater angular accuracy by longer measuring time. One of the common methods for doing this is referred to as lobe switching, that is, perturbing the radiation pattern to look alternately to the right and the left of the target, then pointing the antennas, so that the two signal returns are equal when averaged over many pulses from the two returns (Fig. 4).

The problems in this approach arise primarily from the large size of the antennas and atmospheric refraction uncertainties. Antennas which have sufficient resolution for guidance far out in space generally fall in the 100- to 200-ft size range for the parabolic dish. This entails great difficulty in pointing the antennas toward the vehicle with any accuracy, in the light of normal outdoor factors, such as winds and temperature variations, and maintaining the shape of the parabola undistorted to sufficient accuracy. In addition, the energy must pass through a variable density variable thickness atmosphere at angles which vary materially from the zenith, and hence are unpredictably refracted. In the opinion of the authors, the best accuracies that can probably be expected are in the 1 mile per 5000 miles of range, although better results have been obtained in radio astronomy (20).

Measurement of transit time can be utilized with great precision to determine the range of a target (21). A coded pattern is transmitted to the target where a transponder picks up and retransmits the pattern. The transit time when the pattern is returned to the receiver is measured. The major problems that arise in this system are delays caused by ionization far out in space. In general, a simple pulse pattern is used in this type of system because the same signal-to-noise ratio for a given average power can be maintained if the energy is narrowed into a pulse and the bandwidth is increased to receive that pulse. If the trajectory of the target is known, information theory approaches can be used, in effect, to narrow the effective bandwidth of the system to a point where only the bandwidth required for error transmission is needed. This measurement and the associated range velocity measurements will be among the more accurate measurements that can be made in spaceflight. It should be pointed out that a space scale error will exist here.

The measurement of the Doppler frequency shift (22) of the returning radiation can be used to indicate the velocity of the spacecraft. This frequency will shift proportionally to the frequency times V/C, where V is the velocity of the spacecraft and C is the velocity of light. The primary problem that exists here is signal-to-noise ratio.

The interferometric method (23) of angle and angular rate measurement is based upon measuring the difference in path length to a target from two stations displaced from one another a distance b the base line (Fig. 5). The destructive interferences in the signal coming from the target result when the angle of deviation θ of the target from the centerline is given by $n\lambda/2b = \sin\theta$, where λ is the wave length of radiation used. The line of destructive interference defines the radiation lobe which is used to locate the vehicle angularly. Such a system, obviously, has many lobes so that some sort of fine-course system where the course system has a shorter base line must be used. If the paths are identical in their propagation characteristics and if the ground system can be balanced and maintained balanced, such a system is capable of providing great accuracy. Particularly for targets in the close-in region, great precision can be obtained; however, when a target moves into space and the ratio of base lines to distance is increased, many of the problems become critical. For example:

1 The variability of index of refraction along the two paths in space. If attempts are made to increase the base line to improve angular resolution, the atmospheric structure may alter the path length along the two paths, thus shifting the lobe pattern. At 1000 miles, a path difference of one part in 10^{-7} would lead to a 1-mile error.

2 The combination of the rotation of the Earth and the limited viewing angle requires either intermittent tracking or a large number of stations. When the tracked vehicle varies far from the plane perpendicular to the base line, the accuracy deteriorates because of the foreshortening of the base line as viewed by the target and because of refraction in the atmosphere.

3 The apparent cross base line motion of the target gives an apparent motion of about 300 fps per 1000 miles of range which must be subtracted from the measured motion of the target to give true cross track velocity. At 10^6 miles this velocity would be three times the total velocity of the vehicle and in a direction perpendicular to it.

Two-way transmission is not necessary if a precision clock such as an atomic clock is available aboard the spacecraft. In this case, the clock can transmit according to a pre-established plan, so that with a synchronized clock on the ground the difference in clock time can be measured which amounts to the travel distance. Fig. 6 shows the error in range as a function of clock precision.

This clock system offers the possibility of a very narrow bandwidth system where only the errors in trajectory position and velocity are sensed by the missile. A frequency signal

transmitted from one clock on the ground to a second synchronized clock in the vehicle differs in phase by an amount proportional to the distance of travel as shown in Fig. 7. If two frequencies are used, the second clock will have a difference in phase pattern proportional to distance. A phase comparison between these two frequency signals will give an interference pattern which changes more slowly with distance, so that we have, in effect, a fine-course system for measuring distance. If it is desired to convert this system to an error system, the ground-based frequencies can be shifted based upon the preplanned trajectory of the vehicle, so that the frequencies arriving at the spacecraft are always in phase with the spacecraft clock if the vehicle is following the preplanned trajectory. Deviations in phase and frequency are, then, error signals which can be used in series expansion to develop command signals to keep the missile on target.

Passive Electromagnetic Radiation

Guidance based upon measurement by passive electromagnetic means depend upon the measurement of the same type of physical phenomena as the active systems. They differ from the active systems in that the guidance system for the spacecraft utilizes the natural radiation from the sun or stars as a source of illumination for the reference bodies. The planets in this case will serve as the reference bodies so that the system is freed from the limitations of the Earth-based radiators. The general characteristics of this type of systems can be categorized as follows:

1 Sources of illumination—the sun and stars provide much more effective sources of illumination, so that signal-to-noise ratio is not such a serious problem.

2 In general, it will be found that the sources of illumination will shift to shorter wave lengths in the infrared and visible range; as a result, the beam widths for a given size of receiving aperture will be reduced.

3 The radiation patterns will not, in general, be controllable from the Earth, and as a result the measurements will not be reducible to a form in which errors are sensed directly.

4 No counterpart exists for systems which measure only the transit time of light between the reference object and the guided craft, because nature provides no sufficiently accurate and regular coding of its radiation.

5 The utility of this type of system will be, in general, low near the Earth but will increase as the vehicle moves out into space.

6 Individual measurements will have low accuracy in general because of the great distances that are involved. As a consequence large amounts of data will have to be gathered. This in turn involves a long smoothing.

The most practical and common type of passive guidance is the star tracker. The direction of the incoming radiation is measured by an automatic star tracking sextant and triangulation techniques based upon the precision astronomical knowledge of the relative positions of reference objects, such as planets, and the measured angles will permit a precise sequence of position measurements to determine the space trajectory. This method has been extensively examined in the literature. Stuhlinger (24) has suggested that the angles subtended by individual planets also be used to supplement this data. This method would be limited to close approach to planets, which probably could be better accomplished by active methods. Carroll (25) has suggested an excellent method of handling data in computing positions from star data which results in both position and error sensitivity outputs. Battin (13) has examined trajectories using this type of guidance and reported suitability for round trip flights to Mars and Venus.

This type of system will have greatly improved performance capacity over its active counterpart because of the combination of more intense source, the shorter wave length of incoming radiation and no problems from atmospheric refraction. These factors will result in an improved signal-to-noise ratio for the system. The shorter wave length of incoming radiation will permit a reduction in the receptor aperture and at the same time a narrowing of the system beam width. The latter results in the improvement of signal-to-noise ratio by reducing the space background total angle while maintaining the signal input constant. In changing from 3-cm radiation to red light, the beam width could be narrowed by a factor of 10^5 at the same time permitting a reduction of aperture size by 10^3. With this improvement in angular accuracy the limiting factor becomes the accuracy of the angular pickoffs. A reasonable accuracy for a pickoff which could measure the angular position of such stars might be expected to have an error of 10 sec, so that at 10^7 miles removed from a reference planet the error in a single line of position would be as high as 400 miles for a position.

It is difficult to design such an astro tracker to measure large angles to an accuracy of 1 sec. The reference circles must have errors the order of a few parts in a million. Either the stable reference must be held to fractional seconds or the telescopes arranged to measure several objects at once. Stuhlinger suggests a setup with 10 telescopes to cover five stars, the sun and four planets. Present star trackers have errors measured in minutes rather than seconds. Although these problems may not be insoluble, the more conventional star tracker systems do not promise the desired accuracy in a simple inexpensive instrument.

Fig. 6 Error in range as a function of clock precision

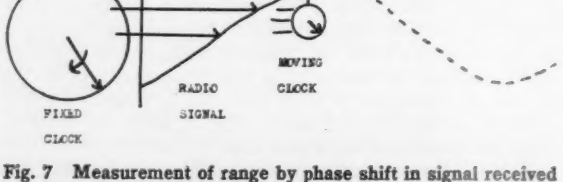

Fig. 7 Measurement of range by phase shift in signal received from a fixed clock with respect to the signal from a clock aboard the vehicle

Bock (26,27) has suggested a method of avoiding these pickoff errors. This method is referred to as occultation and is based upon establishing a line of position in space by locating a planet in relationship to its star background (Fig. 8).

By contrast with the conventional tracker, use of the already calibrated celestial sphere offers a natural solution to the measurement of large angles in space. If we assume a reference star half a degree away, 1 sec is only a part in 2000, for which conventional gearing, or micrometers, are easily made.

The question of what magnitudes of star we must be able to use determines the needed sensitivity. A look at the space distribution of stars of various magnitudes shows that to keep above a probable density of one star per square degree we must be able to use stars as weak as tenth magnitude. The stars are thinnest near the poles of our galaxy, with a distribution as shown in Table 3. Since the galactic pole is about 30 deg from the ecliptic plane, we must operate near minimum star densities.

Table 3 Star densities

Up to magnitude	Galactic latitude, deg 0	30	60	90
4	0.016	0.007	0.005	0.005
6	0.129	0.062	0.042	0.037
8	1.0	0.48	0.32	0.275
10	7.8	3.5	2.2	1.8

The light needed for tracking an eighth magnitude star can be collected by a 4-in. telescope provided a good photomultiplier tube is used. Such a star gives 10^{-1} w per in.^{2} at the Earth. An effective aperture of 1 in.^{2} would just meet the 1-cps threshold (8) of the 1P21 photomultiplier. Hence, reasonably good tracking should be possible with an 8-in. aperture at tenth magnitude. By using extra aperture and bandwidth, the need for special cooling of the sensor can be eliminated.

The telescope design seems to present no unconventional problems. (Fig. 9.)

The temperature compensation of magnification and focus must be given special attention. If good results at 2 deg are desired, scaling provision will be needed in addition to compensation. The stabilization requirements are severe. Movement around the mean pointing direction should be kept to a few seconds if the mean value is to be correct to a fraction of a second. This could be managed by making the inertial platform integral with the telescope.

This system has the advantages that it lends itself to the direct measurement of trajectory errors through measurement of displacement of the planet from its expected position against its star background at a particular time.

Let us examine some of the difficulties we must overcome to operate this system to obtain fraction of a second accuracy. They may be listed as follows, much as Larmore (28) has done:

1 Planets will appear crescent-shaped. Nonpredictable variations in albedo and moon illumination of the dark side will limit the accuracy of correction possible.

2 Sunlight must be kept off the lenses, since the bias would depend on the star magnitude.

3 Star proper motion must be corrected, along with velocity aberrations and planet position delay.

4 Double stars may give an average position.

5 Weaker stars in the field may give a bias, but this can be predetermined if they cannot be masked out.

6 Relative star magnitudes and background light will differ from that seen on Earth. Use of visual light only will minimize the differences due to atmospheric effects in calibration on the Earth.

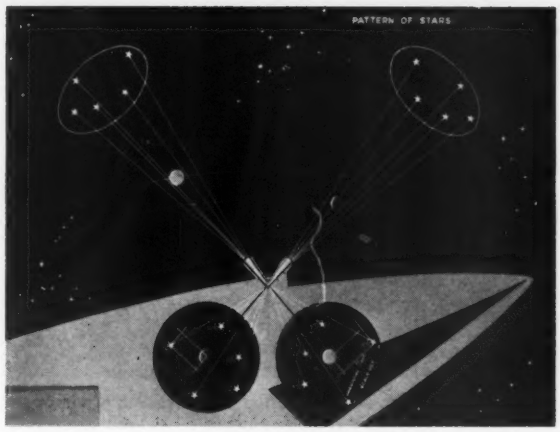

Fig. 8 Line of position in space established by planet position against star background

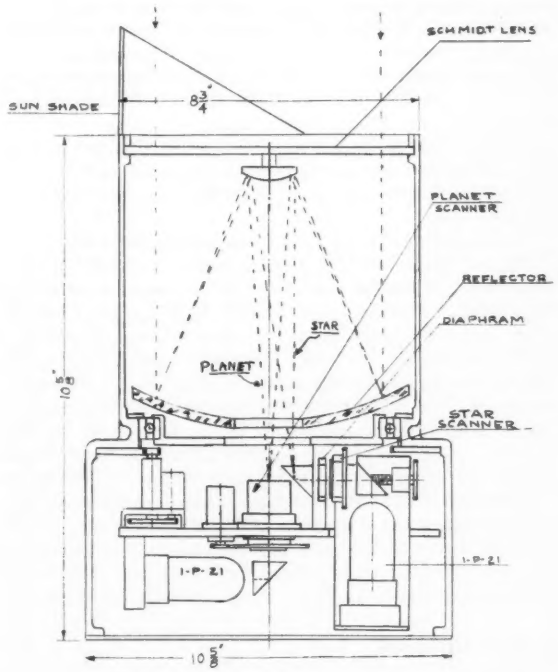

Fig. 9 Schematic diagram of occultation tracker

7 Long averages of the star position data, perhaps several minutes, will be needed to suppress the sensor noise.

8 Full symmetry of the optical system must be preserved; e.g., masking part of objective will offset the image too much.

Although straight transit time measurements of either source synchronous or bisynchronous-type are unlikely, other types of passive systems using correlation synchronous methods are possible. Zilczer (29) has suggested an interferometric type of system based upon a correlation comparison of direct sun signals and signals reflected from a planet (Fig. 10). This system depends upon frequent large nonrandom variations in the sun's emission, and the coherence of this with the pattern of reflected radiation from a planet. If a cross cor-

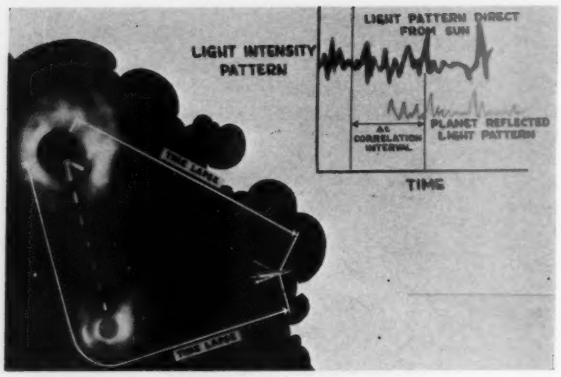

Fig. 10 Hyperbolic astronavigation by correlation of direct and reflected light

relation is made between the intensity of light from the planet and delayed light from the sun, and the delay is adjusted to yield a maximum value for the cross correlation, a measure of the time differential in path is available. The system has the advantage that it offers a broad base line. Zilczer has pointed out several possible problems that will arise with this type of system:

1 The uncertainty in length of base length arises because the correlatable events are point events on the surface of the sun. This results in a possible million mile uncertainty in the base line.

2 Smoothing of sun output by variable path length.

Doppler techniques can also be used to passively measure velocity (35). In this case, the bisynchronous sources are the Fraunhoffer absorption lines of the light coming from the star. This can be compared with spectral lines in an atomic source located on the craft. If visible light is used and a Fabry Perot interferometer, the limitations of the instrumentation would limit the accuracy to 20 fps provided, of course, that pressure broadening of the lines or the random velocity of the molecules did not provide a much higher bound. This technique may be more workable in the microwave region where the emission spectra from such large molecules as NH_3 in the atmosphere of Venus could be compared in a square law detector using the same microwave line from a local source with a sensitivity of 1-cps frequency shift per fps of reactive velocity at a frequency of 1 kilomegacycle (34).

Inertial Guidance

Inertial guidance is unique among the techniques that can be used for the guidance of spacecraft. It is the only method wherein changes of the trajectory are apparent as they take place; with all other techniques the knowledge of this change is delayed. In the radiative techniques which measure velocity, the velocity data must be delayed in a smoothing filter because of the poor signal-to-noise ratio which results in low precision of measurement before smoothing. In systems which measure position, an adequate deviation from the track is required to establish what the new track is—again; in a sense this is a signal-to-noise problem. The time constant associated with the measurement is of importance because of the precision of thrust termination required in spaceflight. In systems which require this smoothing lag either an increment or excess velocity is gained because of the impulse accumulated during the smoothing interval, or the thrust cutoff is based upon present rate of making good the velocity impulse needed to establish the new trajectory and no provision is made for thrust perturbations during the smoothing interval. The inertial system, on the other hand, has the ability to determine instantaneously the appropriate time for cutoff even at high thrust, because it directly senses the rate at which the trajectory is being altered. Unfortunately, the inertial system is subject to errors at the other end of the frequency spectra—bias and drift errors in the measurement of the total impulse. It is thus apparent that inertial and radio systems, rather than being in direct competition, can be used to supplement each other when high precision guidance is required.

An inertial system works very simply (30,31). It is based upon three perpendicular accelerometers which sense the components of acceleration. The coordinate orientation of the accelerometers is maintained by alignment to space references, such as free gyros or the stars. The accelerometers consist of a proof mass and a sensing constraint which forces the proof mass to follow the vehicle along its trajectory. It will follow the vehicle without any force being applied by the constraint, as long as no thrust is applied to the vehicle. If gravity is present, it accelerates the proof mass and the vehicle together. The constraint exerts no force upon the proof mass, and hence there is no accelerometer output. However, when a thrust acts on the vehicle, such as the propulsion, a force must be applied across the constraint to make the proof mass follow. Hence, it can be said that the accelerometers only sense thrust-caused accelerations.

These accelerations can be used to compute the change in trajectory of the vehicle. There are a number of different ways that this can be accomplished. For example, the output of the accelerometer can be corrected for the gravity and integrated once to yield velocity and a second time to yield position. The initial position and velocity of the vehicle must be provided as constants for this process. The computed position and velocity parameters are now available for a trajectory computer to establish the new orbit along which the vehicle is going to fly. The computer in this case will continue to compute the new position and velocity of the vehicle when the thrust terminates, even though there is no input to the computer, because the ballistic flight is itself an inertial process.

The errors that arise in inertial guidance are different from those that arise in the radiative-type guidance (32). Inertial errors are low frequency in character rather than the random noise type of error that can be expected in the radiative-type system. Their low frequency nature results from the fact that the sensed data are integrated, thus reducing its noise content in the high frequency part of the noise spectra. However, low frequency noise of the drift type tends to be accentuated if long thrust guidance periods are involved, because of the accumulation of otherwise small errors in the components. These errors will be introduced into the system through the accelerometers. They can be classified as bias errors, scale errors, linearity errors and alignment errors. These errors will depend greatly upon the way the velocity impulse is introduced into the system. Bias errors favor a short, high intensity impulse, since they depend upon time alone, whereas scale errors probably will favor slightly the short duration impulse because less total impulse will be required. Linearity errors tend to favor the long duration low intensity impulse, since they are acceleration dependent.

Briefly, the properties of inertial guidance can be summarized as:

1 It measures rate of change of orbital constants and therefore has excellent sensitivity to instantaneous changes.

2 It is subject to deterioration because of cumulative errors.

3 It requires input of initial conditions and is capable of correcting errors in its own initial condition.

4 It is self-contained.

5 It does not require the complex computing that is associated with a moving base line system, such as any Earth-based radio system would require.

Contact Navigation

Navigation over the surface of the Earth is frequently done by recognizing objects from maps at each point along the trajectory. It may be possible that recognizable landmarks precisely identify position in space, for example, magnetic fields, gravity fields, electrostatic fields, radiation density, etc. These methods are not treated here because the missions under consideration are proposed for the period before extensive mapping of space has taken place.

Problems in Synthesizing Guidance Systems

The principal problem in synthesizing a guidance system for the Mars flight lies in the area of attaining an overall balance in the design of the system rather than in the area of technological approaches, where there appear to be many suitable mechanisms. The engineer must look not only at the vehicle itself but also must take into consideration the scope of the associated ground equipment and its logistics against the price of increased vehicle size. The guidance equipment that is carried aboard the vehicle must justify the level of accuracy that it produces in terms of an appropriate reduction in fuel weight required to transport it. All of these factors must be studied in the light of carrying out the mission reliably in a high stress environment.

The trajectory of a space vehicle will be closely planned in advance of the flight. A nominal or ideal trajectory will be as established. However, minor variation in factors, such as mass flow rate and specific impulse, will cause the vehicle to deviate from this nominal flight path. Much can be done to simplify the system if full advantage is taken of this a priori knowledge so that there are only minor deviations from the nominal trajectory.

In the first place the guidance measurements should be based upon measuring the deviations from the preassumed trajectory which will lead to a reduction in the required bandwidth of the system and also reduce the precision of the measurements in that the full value of the parameter will not need to be measured. Certain of the guidance schemes lend themselves to this technique, such as the occultation technique and the radio guidance scheme that was proposed. The data processing can also be simplified if it is based upon small deviations from a nominal trajectory. The correction orders can be written in a series expansion (33) of the deviation from the nominal trajectory.

The guidance problem is one of dynamic trajectory conditions, so that in some way the impulse which is introduced to correct the flight will necessarily have to be introduced accurately in its direction. This requires accurate orientation information which must be remembered by an inertial system of some type.

The inertial system also affords the opportunity to utilize higher thrusts in the thermal period since it can directly sense what happens during the smoothing interval required for any of the electromagnetic techniques. In some cases it may prove sufficient in itself for pre-escape guidance. However, the inertial system alone is not sufficient to provide post escape corrections because it is an extrapolative type of system. That is to say, it must start its computation from a set of initial conditions. Therefore, at the beginning of the correction procedure in space, the inertial system will indicate that the system is flying on course to target. Some system which has the capacity to measure errors in this trajectory must be used to supplement the inertial system. The active radio type of system can accomplish this for the less precise guidance problems where the accuracy in relative velocity required is not beyond the scale accuracy considerations, such as the Mars flight. This method would lead to establishing the trajectory over a moderately short time. Although the system aboard the vehicle would be relatively simple, such a configuration would require relatively complex ground-based units which have a base line moving with respect to the vehicle. The cost of these units against the added size of missile that would be required to accommodate an astro tracker would be the determining factor in the configuration that was chosen.

When one turns to the problem of photographic graze and return to Earth, the margin of advantages is in the celestial guidance system primarily because the scale errors in the radio systems are too large to provide sufficient accuracy for the mission. The occultation method of star tracking has a substantial advantage over the conventional star tracker even if it is assumed to be heavier, because the accuracy gained more than makes up for the large price paid in excess weight. Battin has examined several Mars trajectories where a 10-sec astro tracker was used for guidance. He has found that a change of 2.5 times in the accuracy of the tracker results in a 30 per cent change in fuel requirements. The added accuracy of the occultation method is easily paid for in terms of fuel savings, even at the expense of added guidance weight, which seems unlikely.

References

1 Battin, R. H., "The Determination of Round Trip Planetary Reconnaissance Trajectories," *J. Aero/Space Sci.*, vol. 26, no. 9, Sept. 1959, pp. 545–567.

2 Battin, R. H. and Lanning, J. H., "A Navigation Theory for Round Trip Reconnaissance, Missions to Venus and Mars," Fourth Symposium on Ballistic Missile and Space Technology, Aug. 24–27, 1959, UCLA, Los Angeles.

3 Vertregt, M., "Interplanetary Orbits," *J. Brit. Interplanet. Soc.*, vol. 16, no. 6, March-April 1958, pp. 326–354.

4 Lawden, D. F., "Minimal Rocket Trajectories," JOURNAL OF THE AMERICAN ROCKET SOCIETY, vol. 23, no. 6, June 1953, pp. 360–367.

5 Lawden, D. F., "Fundamentals of Space Navigation," *J. Brit. Interplanet. Soc.*, vol. 13, no. 2, 1954, pp. 87–101.

6 Lawden, D. F., "Optimal Transfer Between Circular Orbits About Two Planets," *Astronautica Acta*, vol. 1, no. 2, 1955, pp. 89–99.

7 Preston-Thomas, H., "Generalized Interplanetary Orbits," *J. Brit. Interplanet. Soc.*, vol. 11, no. 2, 1952, pp. 76–85.

8 Preston-Thomas, H., "Two Aspects of the Time Element in Interplanetary Flight," Proc. 5th Int. Astronautical Congress, Springer Verlag, Vienna, 1954, pp. 150–156.

9 Ehricke, K. A., "Error Analysis of Keplerian Flights Involving Single Central Force Field Between Two Central Force Fields," *Navigation*, vol. 6, no. 1, Spring 1956, p. 22.

10 Ehricke, K. A., "Instrumented Comets: Astronautics of Solar and Planetary Probes," Proc. Eighth Astronautical Congress, Springer Verlag, Vienna, 1957.

11 Ehricke, K. A., "Interplanetary Operations," in "Space Technology," John Wiley and Sons, Inc., New York, 1959.

12 Magness, T. A., McGuire, J. B. and Smith, O. K., "Accuracy Requirements for Interplanetary Flight," Proc. Ninth Int. Astronautical Congress, Amsterdam, 1958, Springer Verlag, Wien, 1959, vol. 1, pp. 285–306.

13 Battin, R. H. and Laning, J. H., "A Navigation Theory for Round Trip Reconnaissance Missions to Venus and Mars," MIT Rep. R-240, Aug. 1959.

14 Wittke, J. P., "Molecular Amplification and the Generation of Microwave," Proc. IRE, vol. 45, no. 3, March 1957, pp. 291, 317.

15 Hansen, R. C., "Low Noise Antennae," *Microwave J.*, vol. 2, no. 6, June 1959, p. 19.

16 Nielsen, C. A., "Principles and Applications of Phase-Lock Detection in Phase-Coherent Systems," JET PROPULSION, vol. 28, no. 8, Aug. 1958, pp. 541–547.

17 Jaffe, R. M. and Rechtin, E., "Design and Performance of Phase Lock Circuits Capable of Near Optimum Performance Over a Wide Range of Signal and Noise Levels," Trans. IRE, Information Theory (IT), March 1955.

18 McAleer, H. T., "A New Look at the Phased Locked Oscillator," Proc. IRE, vol. 47, no. 6, June 1959, pp. 1137–1143.

19 Martin, B. D., "A Coherent Minimum Power Lunar Probe Telemetry System," Jet Prop. Lab. Rep. 610, May 12, 1959.

20 Fannin, B. M. and Jelin, K. H., "A Study of the Radar Elevation Angle Errors Due to Atmospheric Refraction," IRE Trans. on Antennas and Propagation, vol. AP-5, Jan. 1957, pp. 71–77.

21 Ridenour, T. N., "Radar Systems Engineering," McGraw Hill, New York, 1947, pp. 1–126.

22 Brown, R. R., Green, P. E., Howland, B., Manasse, R., Lerner, R. M. and Pettengill, G., "Radio Observation of Russian Earth Satellite," Proc. IRE, vol. 45, Nov. 1957, pp. 1552–1553.

23 Pickering, W. H., "Problems of Radio Guidance," in, "Space Technology," John Wiley and Sons, Inc., New York, 1959, pp. 23–29.

24 Stuhlinger, E., "Flight Path of Electrically Propelled Space Ship," JET PROPULSION, vol. 27, no. 4, April 1957, p. 410.

25 Carroll, J., "Interplanetary Navigation by Optical Resection and Inertial Systems," *Aero/Space Engng.*, vol. 18, no. 3, March 1959, pp. 53–56.

26 Bock, C. D., "Space Guidance," IRE L.I. Section, Fall Lecture, Series 1958.

27 Bock, C. D., "A High Precision Stellar Navigator for Interplanetary

Guidance," Fourth Symposium on Ballistic Missiles & Space Tech., Aug. 24–27, 1959, UCLA, Los Angeles.
28 Larmore, L., "Celestial Observations for Space Navigation," *Aero/Space Engng.*, vol. 18, no. 1, Jan. 1959, p. 37.
29 Zilczer, P., "Space Navigation by Correlation," Trans. Nat. Telemetry Conf., Denver, 1959.
30 Mundo, C. J. and Tooher, E. H., "Guidance for the Space Age," *Aero/Space Engng.*, vol. 17, no. 9, Sept. 1958, pp. 30–34.
31 Mundo, C. J., "Trade-off Considerations in the Design of Guidance Equipment for Space Flight," *Aero/Space Engng.*, vol. 18, no. 6.
32 Mundo, C. J., "Optimization of a Cello-Inertial Filter for Space Travel," Fourth Symposium on Ballistic Missiles & Space Tech., Aug. 24–27, 1959, UCLA, Los Angeles.
33 Baker, R. M. L., Jr., "Note on Interplanetary Navigation," Jet Propulsion, vol. 28, no. 12, Dec. 1958, p. 834.
34 Barrett, A. H., "Spectral Lines in Radio Spectroscopy," Proc. IRE, vol. 46, no. 1, Jan. 1959, p. 257.
35 Jenkins, F. A. and White, H. E., "Fundamentals of Physical Optics," McGraw Hill Book Co., Inc., New York, 1937.
36 Giordmaine, J. A., Alsop, L. E., Mayer, C. H. and Townes, C. H., "A Maser Amplifier for Radio Astronomy X Band," Proc. IRE, vol. 47, no. 7, pp. 1062–1069.

Radio Guidance

E. KING STODOLA

Reeves Instrument Corp.
Garden City, N. Y.

The radio methods of guidance depend upon communications to determine the navigational parameters of the vehicle and to command alteration in its course. In this paper a series of nomographs are developed which present the tradeoff between the communications parameters. A set of possible system configurations derived on the basis of these tradeoff curves are examined.

IT IS the purpose of this paper to discuss some aspects of radio guidance of space vehicles and to indicate some of the system requirements for any desired guidance range. The varieties of detail in such guidance systems make it necessary to limit this discussion to general considerations. This paper will be directed particularly to a discussion of the range to which present techniques may permit radio tracking.

A radio guidance system implies a radio communication over required distances, generally between one or more Earth-bound stations and the space vehicle being guided. Directions from one point to the other may be obtained by direction finding techniques, whereas range may be determined by measurement of time of travel of the signal between the stations. This time measurement may be made by determining the round trip travel time with a precise timing system at one end or, conceivably, by one-way measurement if precise clocks were available at each station to maintain sufficiently accurate synchronization over a long period. Doppler measurements on the transmissions may also be used to obtain velocity and acceleration data which may also be useful in a guidance system.

In still other variations of radio guidance systems, radio patterns are established in space by which it is possible in the vehicle to infer guidance by reference to these patterns.

However the guidance is accomplished in detail, it is necessary to provide communications between the guidance point and the vehicle. At present the most interesting possibilities for space vehicle guidance and communication involve relatively high frequencies and line-of-sight paths or, essentially, free space transmission. This subject can be approached using the concept of an isotropic antenna radiating in all directions uniformly with consequent spherical dispersion of energy from it.

It can be shown that if two isotropic antennas are located in free space P_R, the signal power available from the receiving member is related to P_T, the power transmitted by the radiating antenna by

$$\frac{P_R}{P_T} = 2.21 \times 10^{-4} \times \frac{1}{F^2R^2} \qquad [1]$$

where

F = radio frequency, mc/sec
R = spacing between antennas, statute miles

This equation is presented conveniently in the nomograms of Figs. 1 and 2 where P_R/P_T is given in decibels attenuation ($-10 \log_{10} P_R/P_T$).

These nomograms enable one to determine attenuation between two isotropic antennas located in free space. Actually, of course, one seldom uses isotropic antennas in such a situation, and, in fact, it usually proves most difficult to construct such an antenna when it is required. Generally, one or both of the antennas used is highly directive. Such directive antennas may consist of an array of properly phased radiators or an electromagnetic lens or a parabolic reflector properly illuminated. Generally the illumination is not uniform in order to concentrate the energy largely into a single "pencil" in the desired direction with "side lobes" minimized. (The matter of illumination will be discussed

Received Oct. 15, 1959.

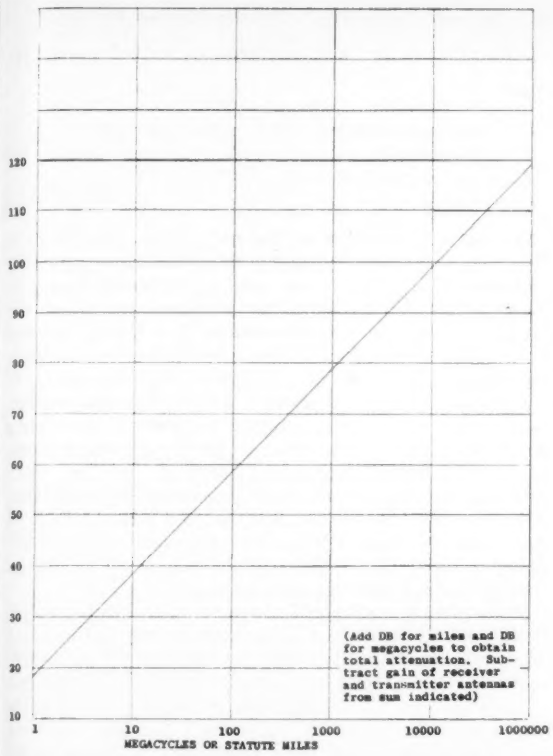

Fig. 1 Free space attenuation between transmitter and receiver antenna with antenna gains of unity (with respect to an isotropic radiator)

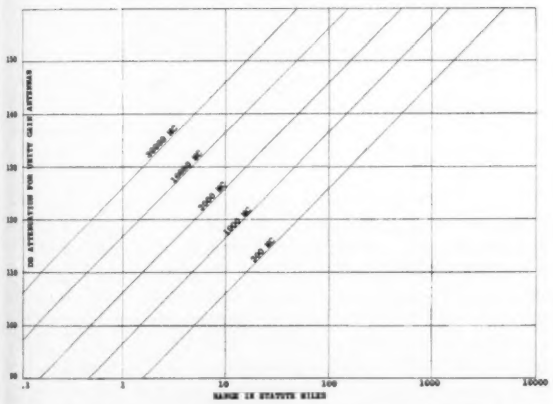

Fig. 2 Free space attenuation from transmitter to receiver for various frequencies with antenna gains of 1 (with respect to an isotropic radiator)

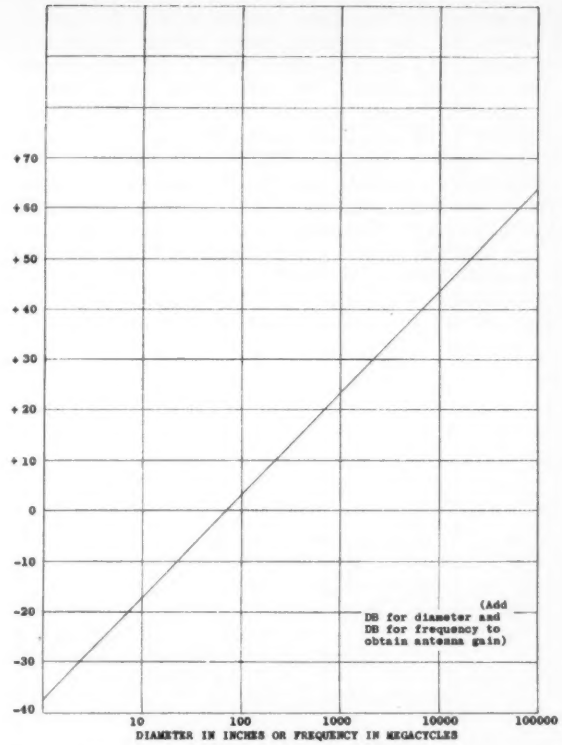

Fig. 3 Approximate gain for a parabolic dish or lens antenna with respect to an isotropic radiator

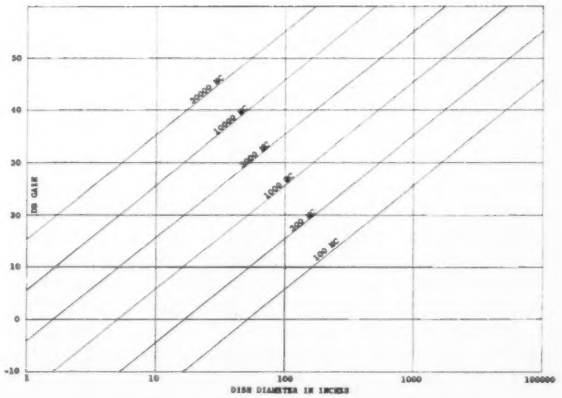

Fig. 4 Approximate gains for lens or parabolic antennas (gain referred to an isotropic antenna)

further at a later point in connection with noise.) The directivity of an antenna can be expressed as "gain," the ratio of the power at the receiving point to that which would have been received had the transmitting antenna been isotropic. Where the usual parabolic reflecting antenna is used, and assuming a 55 per cent efficiency factor to account for the usual nonuniform illumination of the aperture

$$G = D^2F^2 \times 3.9 \times 10^{-6} \qquad [2]$$

where

D = parabola diameter, in.
G = gain with respect to an isotropic antenna

The results of this with G expressed in decibels are given in the nomograms of Figs. 3 and 4.

Gain and beam width are directly related, since gain is but a measure of the concentration of the antenna's energy, and the half-power beam width of such an antenna is given approximately by

$$\theta = 8 \times 10^5/F \times D \qquad [3]$$

where θ is the beam width in degrees. The results of this equation are shown in the nomogram of Fig. 5.

In determining the attenuation from transmitter to receiver, the attenuation given by Equation [1] must be modified by

the receiving and transmitting antenna gain as indicated by Equation [2]. For example, assume 3000-mc operation at 400 miles range, a 100-in. diameter transmitting antenna and a 10-in. receiving antenna. We have: From Fig. 2, attenuation between isotropic antennas 158 db; from Fig. 4, gain for 100-in. antenna, 35.2 db, gain for 10-in. antenna, 15.2 db. Path attenuation is then $158-(35.2+15.2)=107.6$ db.

This gives the necessary data for determining path attenuation; we must now consider what attenuation is permissible from the viewpoint of transmitting and receiving systems.

The receiving antenna can be considered as a generator from the viewpoint of both signal and noise, with the signal power being determined by the considerations of the previous section, and noise corresponding to the equivalent temperature of the antenna. This noise is given by

$$P_n = KTB \qquad [4]$$

where

K = Boltzmann constant = 1.37×10^{-23} joules/C
T = absolute temperature, K
B = receiver bandwidth, cps
P_n = noise power, w

The result of Equation [4] is shown in nomogram form in Fig. 6 where powers are given in decibels with respect to 1 milliwatt (dbm). This noise shown is thermal noise inherent in the antenna and is the minimum with which the signal must compete. An antenna which is heavily coupled to the Earth's surface will show essentially the Earth surface temperature (about 290 K). If, however, the antenna is directed to outer space, its equivalent temperature may be much lower. This fact makes important the method of coupling the feed in a receiving antenna. If the illumination has substantial "spillover," appreciable coupling to the "hot" Earth may contribute undue noise even though the main beam of the antenna is directed toward cold outer space. It should also be realized that very appreciable noise in addition to temperature thermal noise may be picked up from the sun and other stars and sources.

Much of the work in radio astronomy is directed to the distribution of sources of radio noise in the universe. A Cosmic Noise Map giving data for 150 and 600 mc is now available from the Harvard College Observatory, Cambridge.

Unfortunately, the thermal noise in the antenna is not the only noise with which the signal must compete, since the receiving system adds a noise which may be characterized by the "equivalent receiver temperature." This can be defined as the temperature which a receiver input source at absolute zero appears to have when viewed through the

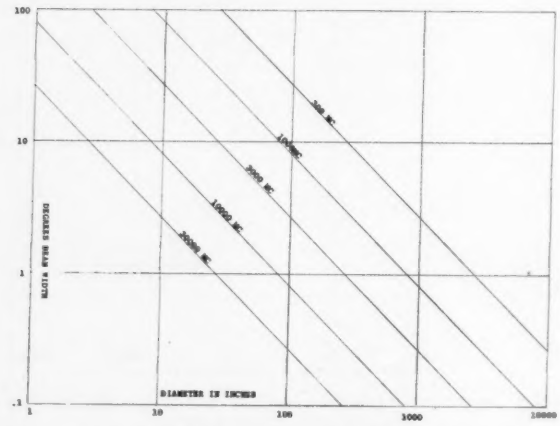

Fig. 5 Approximate half-power beam width for circular aperture antennas

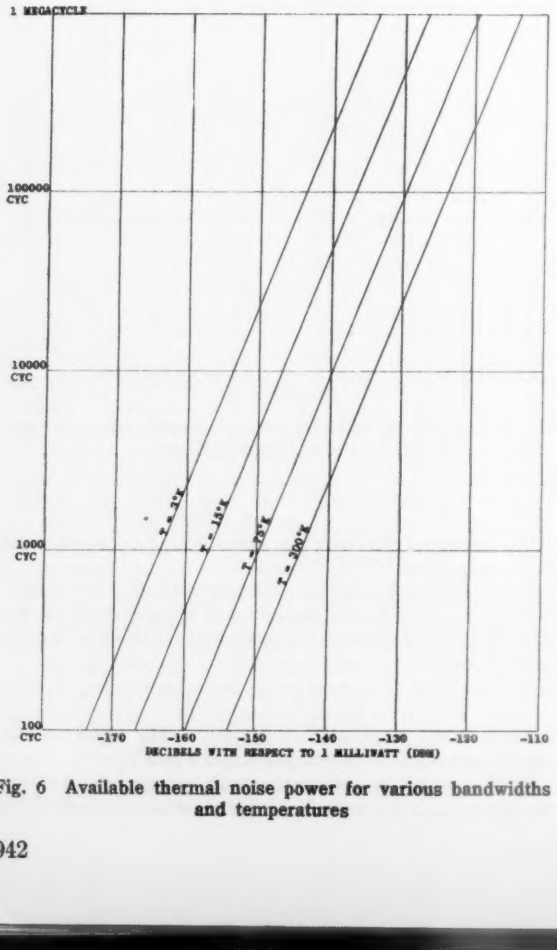

Fig. 6 Available thermal noise power for various bandwidths and temperatures

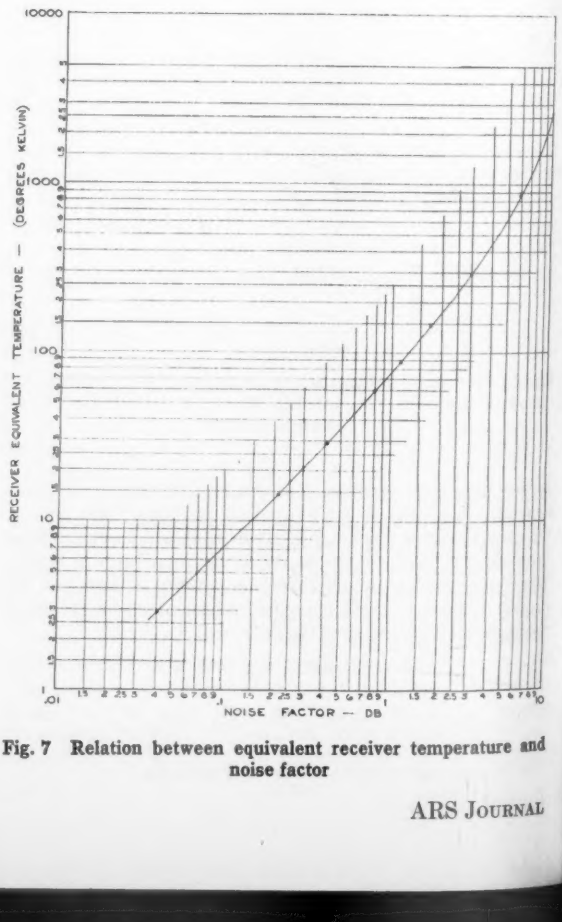

Fig. 7 Relation between equivalent receiver temperature and noise factor

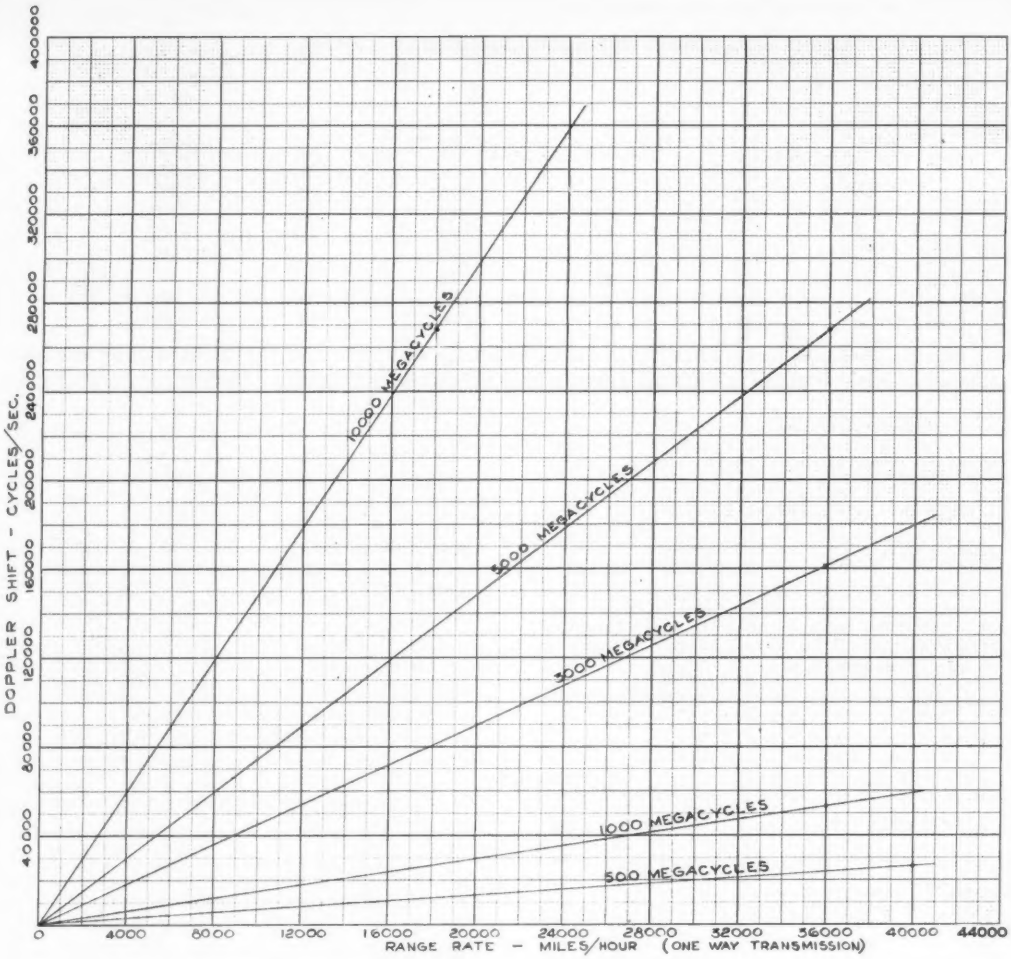

Fig. 8 Doppler shift in radio transmission

actual receiver. This receiver temperature must be added to the antenna temperature to evaluate the noise with which the signal must compete. (Receivers are also evaluated by the equivalent terms noise factor or noise figure (NF) which refer receiver performance to typical Earth temperature 290 K. For very low noise receivers used with low temperature antennas, the temperature concept is more useful. The relation between noise factor and equivalent receiver temperature is given by $T_R = 290\ (NF-1)$. Fig. 7 is a curve showing relation between T_R and NF, where the noise factor NF has been converted to decibels.)

It will be seen from Equation [4] that the noise power with which the signal must compete is proportional to bandwidth B. Actually the bandwidth required is determined by the character of the signal being used in the guidance system and may vary from a few cycles to many megacycles. It might superficially appear that the narrowest bandwidths might be most desirable, but the matter is not this simple. Wide bandwidths are required for pulse-type signals which, although they have high peak powers to compete with the relatively high noise level, prove to have low average power because of the low duty factor involved. Conversely, a narrow band system involves lower signal peak powers, but because of the necessarily high duty factor, the average power can be expected to be comparable. (See, for example, Haeff, Proc. IRE, Nov. 1946.)

In consideration of system bandwidth, Doppler effect must not be overlooked. It can be employed for radial velocity measurement, and inferences as to range and position may be drawn from it. On the other hand, in a system where it is not directly utilized, sufficient bandwidth or frequency control must be allowed to cover the difference between received signal and transmitted signal frequency. Doppler effect shifts the frequency in the ratio of the vehicle velocity to propagation velocity

$$\Delta F = F(V/C) \qquad [5]$$

where

ΔF = frequency shift
F = operating frequency in same units as ΔF
V = rate of change of radial path length
C = velocity of propagation in same units as V. (Average value approximately 186,200 miles/sec)

It should be noted that V is the rate of change of path length, and that this may be either one or two times the rate of change of radial range, depending on the nature of the signaling system. If the transmitted signal is fixed in frequency independent of the frequency of any interrogating signal, the unity factor applies as, for example, in a (presently) conventional radar transponder. On the other hand, when the transmitted frequency depends upon that of the

Table 1 Velocity of propagation, miles per sec

Per cent relative humidity → Temperature, C	0	20	40	60	80	100
−40	186,213	186,213	186,213	186,213	186,213	186,213
−30	216	216	215	215	215	215
−20	218	218	218	217	217	217
−10	220	220	219	219	218	218
0	222	221	220	219	218	217
+10	224	222	220	218	216	214
+20	226	222	219	215	212	208
+30	228	222	216	209	203	197
+40	229	221	209	200	189	180

Taking 186,219 miles per sec as the velocity (a recommended average value), the delay is 10.74 microsec per mile range (two-way transmission). In determining actual range, delays in local transmission and transducer circuits must be accounted for.

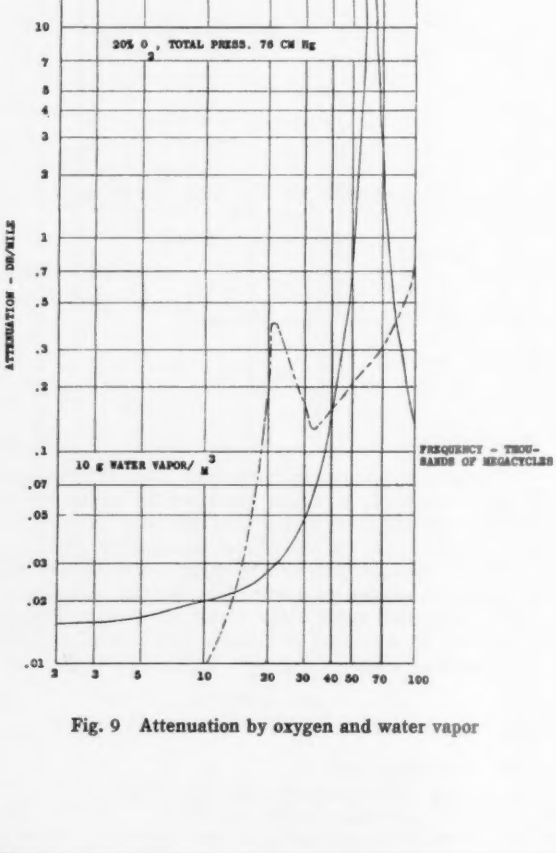

Fig. 9 Attenuation by oxygen and water vapor

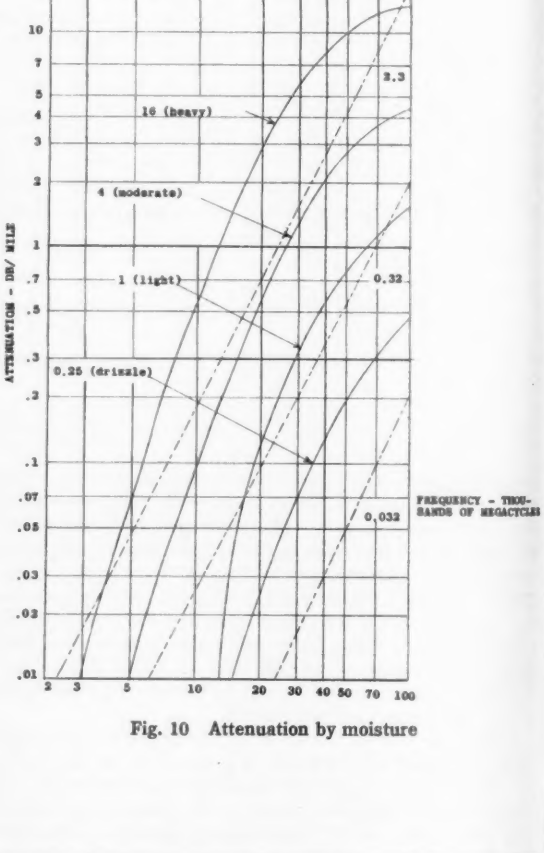

Fig. 10 Attenuation by moisture

Table 2 State of development of elements of a 3000-mc communication system

Status	Ground antenna diameter, ft	Ground receiver sens, dbm	Space trans, kw	Space receiver sens, dbm	Space station antenna
Well within present art	10	−98	2	−72	isotropic
Near limit of present art or reasonable practical limit	60	−110	10–250	−98	10-ft diam

Table 3 Approximate ranges for space communication and tracking at 3000 mc

Ground antenna diameter, ft	Vehicle antenna diameter	Ground transmitter power	Vehicle transmitter, kw	Ground receiver, dbm	Beacon receiver, dbm	Range, miles
10	isotropic	250 kw	2	− 98	−70	8000
10	2 ft	250 kw	10	−110	−90	10^6
60	isotropic	250 kw	2	− 98	−70	7×10^5
60	2 ft	250 kw	10	−110	−90	9×10^7
60	isotropic	10 megawatts	250	−110	−98	10^8
60	10 ft	10 megawatts	250	−110	−98	5×10^9

received signal, as in the case of a radar reflection, the Doppler effects in both directions must be added. This gives a factor of 2 if both paths are at substantially the same frequency. Fig. 8 is a plot of Doppler effect to indicate its magnitude.

It will be seen that at 20,000 mph radial speed, a Doppler shift of about 100 kc/sec occurs for an operating frequency of 3000 mc.

Range can be measured in guidance systems by measuring time of travel over the path and using velocity of propagation. Velocity of propagation is quite constant, but is affected slightly by material in the path. Table 1 gives velocity of propagation as a function of temperature and humidity.

In utilizing radio range data in a radio guidance system, account must be taken of the fact that the data obtained relate to the time at which transmission from the vehicle occurred, rather than the time at which it is received, an important consideration when time of travel reaches many seconds or minutes.

It should also be mentioned that oxygen and water vapor in the atmosphere produce attenuation of signals in a manner shown in Figs. 9 and 10.

The previous discussion has set forth some of the considerations which are vital to a high frequency radio guidance system. In order to indicate the possibilities of such systems some constants which would be practicable for a particular system will be assumed and the range capabilities assessed.

Suppose a ground system involving a pulse transmitter and receiver operating at 3000 mc and a vehicle-borne transponder beacon having a suitable receiver and transmitter. Assume a pulse width of 2 microsec and a receiver bandwidth of 1 mc. The possibilities of other constants are summarized in Table 2.

Various combinations of these possibilities are set forth in Table 3 which shows the possibilities of such systems from satellite tracking range all the way to the nearer planets.

It should be noted that the figures given are only approximations and will be affected by many system details. However, they give an indication of the kind of ranges available with minimum signal margins. To provide additional signal margin, ranges of one half to one quarter of those given should be considered more realistic.

Bibliography

Joint Board on Scientific Information Policy, "Radar, A Report on Science at War," Govt. Printing Off., Washington, D. C., Aug. 1945.

Smith-Rose, R. L., "Radiolocation, Principles and Origins," *Wireless World*, vol. 51, no. 2, Feb. 1945; vol. 51, no. 3, March 1945, p. 66; Dorset House, London.

Colton, R. B., "Radar in the United States Army," Proc. IRE, vol. 33, Nov. 1945, p. 740.

DuBridge, L. A., "History and Activities of the Radiation Laboratory of the Massachusetts Institute of Technology," *Rev. Sci. Instr.*, vol. 17, Jan. 1946, p. 1.

"Evolution of Radar," *Engineering* (London), Aug. 24 to Oct. 12, 1945.

Tuska, C. D., "Historical Notes on the Determination of Distance by Timed Radio Waves," *J. Franklin Inst.*, Jan.-Feb., 1944.

Nyquist, H., "Thermal Agitation of Electric Charge in Conductors," *Phys. Rev.*, July 1928.

Haeff, A. V., "Minimum Detectable Radar Signal and Its Dependence Upon Parameters of Radar Systems," Proc. IRE, vol. 34, Nov. 1946, p. 857.

North, D. O., "The Absolute Sensitivity of Radio Receivers," *R.C.A. Review*, Jan. 1942.

Friis, H. T., "Noise Figures of Radio Receivers," Proc. IRE, July 1944.

Ridenour, L. N., "Radar in War and Peace," *Elec. Engng.*, vol. 65, May. 1946, pp. 202–207.

Watson-Watt, Sir Robert, "Evolution of Radiolocation," *Engineer*, vol 151, April 5, April 12, 1946, pp. 319, 330.

"I.R.E. Standards on Electron Devices: Methods of Measuring Noise," Proc. IRE, July 1953, p. 891.

DeWitt, J. H., Jr. and Stodola, E. K., "Detection of Radio Signals Reflected from the Moon," Proc. IRE, March 1949, p. 229.

Ridenour, L. N., "Radar System Engineering," MIT Radiation Laboratory Series, McGraw-Hill Book Co., New York, 1947.

Fink, D., "Radar Engineering," McGraw-Hill Book Co., New York, 1947.

Cosmic Noise Map, Harvard College Observatory, Cambridge, Mass.

Pawsey, J. L. and Bracewell, R. N., "Radio Astronomy," Oxford University Press, New York, 1955.

Kerr, D. E., "Propagation of Short Radio Waves," MIT Radiation Laboratory Series, McGraw-Hill Book Co., New York, 1951.

Locke, A. S., "Guidance: Principles of Guided Missile Design," Van Nostrand Co., Inc., 1956.

"Optimum Frequencies for Outer Space Communications," U. S. Army Radio Frequency Engineering Office, Office of the Chief Signal Officer, Wash., D. C., July 1958.

"Tentative Evaluation of Transmission Factors for Space Vehicle Communication," U. S. Army Signal Radio Propagation Agency, Project 664, Fort Monmouth, N. J., Sept. 1958.

Burgess, E., "Satellites and Space Flight," The Macmillan Co., New York, 1957.

Bean, B. R. and Abbott, R., "Oxygen and Water Vapor Absorption of Radio Waves in the Atmosphere," *Geofisica Pura E Applicata*, Milano, vol. 37, 1957, pp. 127–144.

Radio Astronomy Issue, Proc. IRE, vol. 46, no. 1, Jan. 1958.

Norton, K. A., "Maximum Range of a Radar Set," Proc. IRE, Jan. 1947.

Castruccio, P. A., "Communications and Navigation Techniques of Interplanetary Travel," IRE Trans. on Aeronautical and Navigational Electronics, Dec. 1957.

Recent Progress in Inertial Guidance[1]

JOHN HOVORKA,
JOHN W. HURSH,
E. J. FREY,
WILLIAM G. DENHARD,
LESTER R. GROHE,
P. J. GILINSON Jr. and
W. E. VANDER VELDE

MIT Instrumentation Laboratory
Cambridge, Mass.

Introduction and Survey

NAVIGATION is traditionally the art of steering a vehicle from an origin to a destination over a mapped course; inertial navigation is a mechanization of this art. In inertial navigation, the force in the vehicle is measured with accelerometers in a gyro referred coordinate system. Thus, during certain intervals, navigation is carried on without reference to the environment of the vehicle. From the measured force and a foreknowledge of the gravitational field through which the vehicle moves, the acceleration of the vehicle through the field is deduced. Part of this acceleration may be due to the rotation of the Earth, which must then be accounted for; thus sidereal time is also an input to the navigation system. The acceleration on course is doubly integrated to indicate the displacement along the course, or position; these data are then used for steering.

Inertial navigation's beginnings, involving partial inertial guidance systems, go back to the first practical marine gyrocompass by Anschütz of Germany early in the present century (1).[2] The next development pertinent to inertial navigation was the artificial horizon for air navigation, a long period pendulous gyroscope. As this device was improved it became a *nonpendulous* gyro coupled, through a pneumatic control system, to separate single axis pendulums. Thus, the general principles of today's inertial navigation devices emerged: The measurement of force with single axis accelerometers in coordinates determined by gyros. This type of system was the basis of the guidance of the German V-2 rocket during World War II (2).

After the war, reports from abroad (3), plus the technological improvements developed during the war, stimulated fresh approaches, and the method was investigated for various airborne, marine and missile applications in this country. Most of the present system principles were in use in the designs of the mid-1950's (4) and successful tests were recorded. In 1953, for example, the MIT Instrumentation Laboratory was responsible for the first fully inertially guided coast to coast airplane flight. During this period, several other groups were also working on this problem: Among the earliest work may be mentioned that of the Autonetics Division of North American Aviation, Inc., and also that of the Army Ballistic Missile Agency. Engineers in the USSR also appear to have been interested in the navigation system problem (5) and particularly in the design of gyros (6).

The distinctions between airborne, marine and missile applications of inertial navigation are drawn in terms of two circumstances: The force environment to which the navigation system is subjected, and the expected time of operation as a purely inertial device. With respect to the force environment, the burden is, first, on the accelerometers, in that they must have the desired precision (this includes precision of analog to digital data conversion, if digital computation is used) and range of operation; and second, on the computer, the interpretive mechanism that yields position data as an output with accelerometer data, gravitational field data and time as inputs. Thus, gravity is apt to be the dominant force in airborne and marine systems, whereas thrust is apt to be the dominant force in missile systems during powered flight. With respect to operating time, the behavior of the gyros raises certain limitations; that is, gyro drift will sooner or later cause the axes in which the force is being measured to depart far enough from their reference directions to seriously impair navigation accuracy. This is clearly a less serious matter in missiles and satellites, where the time of powered flight is relatively short, than in, say, marine navigation, where there may be a need to retain reference coordinates mechanically simulated by gyros for several days.

A group of engineers at the Instrumentation Laboratory at MIT present their views, in the short papers to follow, of certain recent aspects of inertial guidance. The authors see these developments from the point of view of the wide variety of research efforts that are under each man's supervision. In the first paper, by Hursh, airborne inertial systems, i.e., for use in the atmosphere, are discussed from the point of view of a type of system developed at MIT for long range flights, which is contrasted with a short time of flight system indicating geographic coordinates—north, east and vertical.

In the second paper, Frey considers missile and space vehicle guidance problems, where "navigation" in the traditional sense of the interpretation of measurements to provide data for steering gives way to the view of guidance as a problem in classical mechanics modified by the use of control mechanisms. Both views, of course, amount in the end to the same thing, but the second more easily merges guidance with astronomy, which is the principal background science in space technology.

In the third paper, Denhard provides a view of recent gyro development, with particular attention to performance criteria and testing. Thus, after a preliminary discussion of design and materials choices, the author proceeds to detail the test procedures with which he is familiar, examining the concept of "gyro drift," both as a physical quantity to be graphed against time and as a figure of merit.

In the fourth paper, Grohe discusses accelerometer development, particularly in missile applications where the problems are toughest. Accelerometer calibration is characterized generally by a dependence on the elastic properties of a material, since accelerometers in general are devices which indicate the applied force as a displacement, i.e., in terms of elasticity. Even the pendulous integrating accelerometer, in which the applied force causes a gyro to exhibit its unbalance as an angular velocity proportional to the force (so that the angular displacement is proportional to the integral of the force, or, making due allowance for the gravitational field, the integral of the acceleration), does not escape this limitation entirely, because of the gimbal bearing material requirements.

In the fifth paper, Gilinson takes up the problem of elec-

Received Nov. 4, 1959.
[1] Edited by John Hovorka.
[2] Numbers in parentheses indicate References at end of paper.

tromechanical converters for torquing gyros and accelerometers, for deriving signals from them, and also—a related but distinct problem—the torquing of the gimbals on which the gyros and accelerometers are mounted.

In the next paper, Vander Velde contrasts analog and digital computers, with particular emphasis on recent developments in the latter.

The last paper is a brief statement of the problem of marine navigation, where inertial techniques started, and where they appear in a highly refined form today. The application of inertial guidance to submarines has, in fact, made the Polaris missile possible. By putting the problem in reverse, so to speak, marine inertial techniques can also be used in oceanographic research.

The objective which we hope has been achieved is to give a broad view of recent developments in these specialties which, while necessarily brief and therefore somewhat superficial, will nevertheless be stimulating. To this end, an extensive bibliography is appended to the set of papers.

—JOHN HOVORKA

Recent Developments in Airborne Inertial Systems

All airborne inertial systems developed to date use gyros to establish physically a set of reference axes isolated from aircraft rotational motion. Three single degree of freedom gyros or two two degree of freedom gyros have been used, the single degree of freedom design being preferred for highest accuracy over long periods of time. The gyro signals are resolved along the drive motor axes of the gimbals which support the gyro platform. The resolved signals are amplified and applied to the gimbal drive motors, forming a closed loop system that isolates the gyro package from aircraft motion. Inertial systems may be divided into the following three categories depending on the gyro reference coordinate system used:

1 Inertially fixed system.
2 Earth fixed system.
3 Local vertical fixed system.

Systems may be further subdivided according to the disposition of the sensitive axes of the specific force measuring instruments (accelerometers) with respect to the gyro reference axes (4).

The purpose of the nonrotating gyro coordinate system is to provide reference directions with respect to which specific force measurements can be made. The specific force (force per unit mass) measured by the accelerometers is equal to the force of gravitation acting on the unit mass minus the acceleration of the unit mass with respect to inertial space. Gravity, as distinguished from gravitation, is defined as the accelerating force acting on a mass stationary in Earth space. The direction of this vector defines local vertical. Using appropriate angular rate and position vectors, the specific force may be expressed analytically in terms of gravity and acceleration with respect to any one of a number of coordinate systems. A wide choice faces the designer, and since the rate and position information needed can be obtained from the indicating system, the selection of accelerometer coordinates is made on the basis of expected accuracy of measuring and computing instrumentation. In order to avoid computing the force of gravitation or gravity to a high order of accuracy, most airborne systems built to date have been designed with the sensitive axes of the accelerometers perpendicular to one or the other of these forces.

In one inertial system design, both the gyro reference axes and the accelerometer input axes are fixed with respect to local vertical. Three gyros are used with their sensitive axes orthogonal, two in a horizontal plane and a third along local vertical. Two accelerometers are mounted with their sensitive directions also in the horizontal plane perpendicular to each other. The accelerometer outputs are integrated and fed into the gyro torque motors. The sensitivities are adjusted such that the platform is precessed at precisely the same rate as the vehicle moves over the surface of the Earth. Thus, the sensitive directions of the accelerometers are driven toward perpendicularity to the vertical and a condition in which no component of gravity is sensed. Angular rate may be obtained directly from the gyro torquing signals, but position computation requires an external open loop integration of the rate signals. Earth rate must be resolved along the gyro axes using the position thus obtained in order that the gyros may be torqued to compensate for rotation of the Earth. In addition, compensations must be computed and subtracted from the accelerometer outputs. The resulting system has the advantage of being relatively simple (except for the resolution of Earth rate) and of being small in size and weight, for a given performance level and over a relatively short time of flight. A disadvantage is that after a few hours, errors in the resolution of Earth rate and in the open loop integration to obtain position cause the overall system errors to diverge rapidly.

A system design (7) which has been developed and tested in the MIT Instrumentation Laboratory over relatively long times of flight extending over many hours falls under category 1 above rather than category 3, which includes the system just described. The reference gyros are inertially fixed, Earth rate being removed by physically rotating the outer gimbals about the gyro package by means of a time drive. The sensitive directions of the two integrating accelerometers are maintained perpendicular to the local vertical by means of precision drives under the control of the indicating system. A single integration in each channel of the indicating system generates the accelerometer platform positioning signals. Thus, the accelerometers are maintained perpendicular to the gravity vector and the gyros are left untorqued. Accelerometer compensations must be computed, but Earth rate computations based on indicated present position are not necessary. Time of operation is therefore not limited by such computations, although the gimbal system is necessarily somewhat larger and more complicated than that of the local vertical fixed system of category 3.

It should be noted that in those systems described in the foregoing, undamped indicators are described. Internal damping can be used together with velocity compensation using airspeed or groundspeed information which may be available aboard the aircraft. Relatively low damping ratios are used since presently available accelerometers have dynamic range sufficient for the system to be set in operation on the ground prior to flight, keeping initial condition errors small. The indicators are null systems, a design which tends to minimize errors due to computing instrumentation inaccuracies. Flight performance tests of the Instrumentation Laboratory system showed that undamped operation over relatively long periods of time was entirely feasible. Forced errors due to wind changes in the damped system using airspeed compensation may well be more serious than long term error buildup due to nonideal instrumentation in the undamped system.

The trend of inertial system design in all three categories is toward reduced size and weight, made possible through the use of smaller and lighter inertial and electronic components. Digital computing techniques have high accuracy capability compared to the analog techniques previously used, and have made possible advancement in inertial system design concepts. For example, since resolutions may be performed by the digital computer with extreme accuracy, a system has been designed under category 1 above (inertially fixed gyro reference frame) employing three accelerometers, also inertially fixed. The vertical is indicated in the gyro coordinates as a set of numbers in the computer. The use of digital computers has accelerated a trend toward the development of inertial components capable of producing digital outputs and

accepting digital inputs. Much progress has been made in the development of integrating accelerometers with digital outputs. Some success has been achieved in digital torquing of inertial gyros units as well. The use of integrating accelerometers eases the speed of computation requirement on the digital computer.

At the present time effort is being directed toward the integration of the inertial guidance system into the overall weapon system of which it forms a part. The inertial system is used directly as an attitude reference and to provide stabilization information for other equipment in the weapon system in addition to performing its navigational functions of position and velocity indication.

—JOHN W. HURSH

Application of Inertial Navigation to Ballistic Missile Guidance and Launch Guidance of Space Vehicles

A function that must be performed by a ballistic missile guidance system is the solution of a fire control problem involving some rather unusual interior ballistics. As the name ballistic missile implies, at the point where the final rocket has cut off and the missile is in free fall, the guidance job is complete. In other words, a ballistic missile guidance system is concerned primarily with establishing a velocity vector which will carry the missile in free fall to its target; thus such a guidance system is primarily a velocity control system. The "gun barrel" may be several hundred miles in length and the projectile may spend several minutes in its course through the flexible gun barrel which ends at whatever point the last propulsion is shut off.

The launch guidance of satellites and space vehicles is essentially similar, as long as propulsion consists of chemical rockets burning over short periods of time. In this case, too, one is interested in solving a boundary value problem, whether it be placing a satellite in orbit or sending out a space probe. In satellite and space vehicle launchings the periods of propulsion may be separated by intervals of free fall, the precise nature of the trajectory depending upon the propulsion system employed and the nature of the mission to be accomplished. Although the specific equations may change, the general principle of establishing a suitable velocity vector still applies.

With this broad background in mind, let us consider the nature of a ballistic missile flight. First, an intercontinental ballistic missile with a free fall range of 5000 miles must have a velocity with respect to the Earth of well over 20,000 fps. This velocity is accumulated by means of chemical rockets providing substantial accelerations over a period of several minutes. Since the guidance system is fundamentally concerned with velocity measurement and control, the sensitivity of the overall system to velocity error must first be determined. For example, at a 5000-mile range a velocity error of 1 fps provides a target miss of approximately 1 mile. Hence, for such a mission if, for example, 22,000 fps were the required velocity, velocity error of one part in 1000 means a target miss of approximately 20 to 25 miles. Obviously then, velocity measurement is a critical portion of this job. In addition, since large rocket engines are not yet capable of being constrained to follow precisely some specified thrust history, the guidance mission must be accomplished while both missile parameters and Earth parameters, such as atmospheric winds, depart from nominal values. One may assume that the rocket can be controlled by means of swiveled rocket engines and by means of staging or cutting off rocket engines upon command. If, however, one assumes that one cannot throttle a large rocket engine, it then becomes impossible to constrain the initial flight path to nominal conditions if the propulsion system parameters vary from nominal. Even if the rocket flew a nominal path through space, it could pass through each point along the path either ahead or behind time depending on the variations of the thrust profile of the engines.

Consider first what sort of computation must be done in these circumstances. Obviously, since the guidance system is a velocity control system, in at least an implicit form one must first compute missile velocity and compare it to some desired velocity which will achieve the job, and second, take such control action as will insure that missile velocity becomes equal to desired velocity. At this point propulsion is shut off and the missile is in free fall to the target. The computation of actual velocity and desired velocity as well as the other parameters that may be required, such as time and position, is done by the indication system; the zeroing of the difference between desired and actual velocity is done by the flight control system. The computation and control actions performed should be of the highest degree of simplicity consistent with satisfying the mission. Additional constraints may be placed upon the flight profile, for example, by the need to rise vertically initially, so that the missile velocity will not be too high while the missile is still surrounded by a relatively dense atmosphere, or by constraints which may be implied by the launching of the missile for an underwater submarine. These constraints, together with the constraints originating in the nature of the propulsion and airframe, form a set of "ground rules" under which the guidance system must work. Both indication and control may be solved in a variety of ways; those ways are best which keep the amount of airborne equipment to a minimum.

When one considers the demands made on velocity computations, it becomes apparent that, at least at long ranges, digital computation techniques must be used. Certainly it is far from easy to make analog equipment perform with the accuracies mentioned in the foregoing; in addition, analog equipment of such accuracy is ordinarily far more complex than is desirable. Hence the modern trend is to digital computers for inertial guidance of ballistic missiles. Either special purpose or general purpose computers may be employed, depending upon a number of considerations. When the equations to be handled by the computer are exceedingly simple, there can be distinct advantages to a special purpose computer such as the digital differential analyzer. As the equations become more complex such a computer, in which each extra equation means extra equipment, becomes less efficient in comparison with the general purpose computer with a central arithmetic element. It should be pointed out, however, that both types of computer must communicate with other equipment and such communication is always in the form of special purpose input and output equipment. Thus, whatever the nature of the computer, the virtues of airborne simplicity are once again apparent, since the greater the number of elements with which the computer must exchange information, the greater the complexity that is involved in the computer itself, regardless of its type. In general, the logic involved in all such computers is currently constructed of solid state elements. A variety of different storage elements are used.

In putting together a guidance system, it is appropriate to consider next the special demands that the ballistic missile mission makes upon the basic sensing elements, that is, upon the gyroscopes and accelerometers. Consider first the case of the gyro and compare the demands made upon it with the demands of the navigation mission of a manned craft, such as an aircraft or submarine.

Aside from the environmental conditions of acceleration, vibration, special thermal conditions, shock, etc., which may be inherent in a ballistic missile flight, the basically new demands made upon the gyroscope relate primarily to its relatively short period of use in the high acceleration environment. In the flight of a ballistic missile, those disturbing torques which over a course of hours or days in a manned craft would seriously affect the performance of the gyro and the reference held by the gyro, will have considerably less time in which to

act. Hence, gyros designed for the navigation of a manned aircraft over a period of hours are, in certain respects, overdesigned for the ballistic missile mission. For example, the effect of unbalanced torques which are proportional to the specific force or g vector, will be more important to the navigation of an aircraft over a period of many hours than to navigation of the ballistic missile over a period of several minutes even though the specific force vector is considerably larger in the ballistic missile. Compliance effects which produce torques proportional to the square of the specific force vector do become more important for the ballistic missile. It is this type of effect which is one of the reasons for the increasing use of beryllium as a structural material in gyros. The particular virtue demanded here is the extreme stiffness of beryllium which presents one possible means of reducing an isoelastic compliance. Currently both one degree of freedom and two degree of freedom gyros are in use, and floated gyros and air supported gyros are also in use. Both ball bearings and air bearings are used for spin axes. The relative virtues of one design over another will become apparent only from actual test.

The demands upon the accelerometer presented by the ballistic missile guidance are totally different from those which had been presented by earlier navigation systems for aircraft and submarines. In general, the specific force receivers for the earlier navigation systems were designed for relatively steady and moderate levels of force. In addition, they were ordinarily used in coordinate systems which moved with their location on the surface of the Earth so that the average was a steady 1 g. Here too a variety of accelerometers have come to the fore. Currently the pendulous integrating gyro accelerometer (2), the vibrating string (8) and various forms of restrained pendula are in use. Most of these instruments are now designed so that they can have a digital or a quasi-digital output. Many of them also feature an integration so that the output of the instrument is something with the dimensions of velocity. However, all of the designs are similar in that they are attempts to provide a specific force transducer for high and changing levels of force. In general, the more accurate guidance requires that the accelerometers be oriented with their input axes along a set of coordinates different from missile coordinates. The accuracy demands of intercontinental missile guidance were mentioned earlier. One part in one thousand for a 4000-mile flight will produce over 20 miles miss at the target. If the accelerometer has a digital output, the granularity of this output must also be sufficiently fine to permit computation of the trajectory indication system with adequate accuracy.

The inertial sensors or gyros and accelerometers are customarily mounted in a base motion isolation system. In general, this base motion isolation system is designed to hold a set of coordinates in inertial space physically, although it may be designed to follow some other reference, for example, a rotating Earth set of coordinates. In general, however, only modest motion of the stabilized package is involved. This relates primarily to the fact that at the present stage of development both gyros and accelerometers are not performing at their best when their axes are rotated at large rates. In other words, we cannot yet build highly accurate accelerometers that retain their accuracy when their sensitive axes are rotated at rapid rates. The same fact is essentially true for gyros. In the design of base motion isolation systems, various approaches are taken. There are the classical gimbal systems and the "inside out" or Hooke's-joint systems, both in widespread use. In order to provide good base motion isolation in a vibrating, turning and bending missile, gear drives are being replaced by direct drives with a view to the elimination of backlash (11). In the electronics which drive such systems, tubes are being replaced by solid state elements, both at the signal and power level. In order to withstand the high acceleration and high vibration environment encountered in ballistic missile flights, design of gimbal systems and packaging of electronics has taken a variety of directions, but all are primarily aimed at increasing reliability, increasing structural integrity and reducing size and weight. The course of this development is not within the scope of this paper.

A final word should be said about the nature of the control system which constrains the missile to its mission on the basis of information supplied to it by the indication system. Here, too, a variety of approaches are possible, but all approaches emphasize two features: First, simplicity and second, the avoidance of large angular motions. This last is desirable both from the standpoint of fuel efficiency and from the standpoint of keeping equipment working around a null rather than having the equipment go through major motion during a critical period of control.

Inertial guidance systems of various designs have been tested in a number of missiles: The Redstone, the Jupiter and the Thor. Inertial guidance systems are currently being designed and built for the Polaris, the Atlas, the Minuteman and the Titan as well. It is merely a matter of time before all of these systems, some of drastically different approaches, will have been tested in actual missile flight.

—E. J. Frey

Gyros Used in Inertial Navigation

In an inertial navigation system the gyro serves as a coordinate reference, or memory. The perfect gyroscope, when properly coupled into a servo system, will perfectly hold or stabilize a reference alignment for itself and, therefore, for the inertial navigation system of which it is a part. Since three orthogonal reference coordinates must be stabilized in inertial space, there must be three servo systems and three gyro stabilized lines of reference. In autopilot, fire control or panel instrument applications, the gyro must again stabilize a navigation (or fire control) reference line. However, the accuracy required is considerably less than that required of an inertial navigation gyroscope. In the case of the autopilot, for example, when more accuracy is required, there is a correcting override on the autopilot fed in by the pilot, radar or inertial navigation system, etc. Such combinations use the autopilot for maneuver without upsetting the inertial navigation system coordinate reference lines.

Nearly all gyros used for these purposes are either the single degree of freedom gyro or the two degree of freedom gyro; these are shown schematically in Fig. 1. The single degree of freedom gyro has only one defined axis of freedom for precession and, therefore, may be used to stabilize only one axis. The gyro will respond to the vector component of angular velocity that lies along its *input axis*, which is perpendicular to the precession axis - spin axis plane. Three of these gyros are required to provide a set of three orthogonal reference coordinates.

In some applications, the two degree of freedom gyro has two defined axes of freedom for precession and, therefore, may be used to stabilize two axes. In other applications, the axes of precession are not defined as such, but the gyro is still limited to stabilizing two axes and no more. Either type of two degree of freedom gyro is a so-called "free gyro." By proper servo control and gimballing, two two degree of freedom gyros can provide a navigation system with three inertial coordinate reference axes (10, 11).

It should be noted that for precision navigation equipment, emphasis has been placed on the single degree of freedom type gyro—the type used in the Thor, Titan, Redstone, Jupiter and Vanguard missiles, and planned for the shipboard navigation system and the missile itself of the Polaris system. Certain autopilots use single degree of freedom gyros, as do fire control systems involving high angular rates of the line of sight. This is mainly because of the difficulty of consistently achieving low drift rates with the two degree of freedom gyro. Ideally, the gyroscope is a precisely balanced mass supported by frictionless gimbals. Since the single degree of freedom

type has one less gimbal than the two degree of freedom type, gimbal bearing uncertainty torques, which cause gyro drift, are less of a problem. In addition, precise balance is easier to achieve in the single degree of freedom unit, where the only unbalance that can affect performance is that which causes a torque about the precession axis. Therefore, precise balance is necessary only about the precession axis. (Actually, the gimbal is also balanced longitudinally to equalize loading of the end supports, but this balance is not nearly as critical as the balance about the precession axis.) In contrast, a two degree of freedom gyro's performance is affected by any unbalance at all, so that precise balance must be achieved—with considerable difficulty—about the intersection of two axes, or a point. Thus, in spite of the fact that three single degree of freedom gyros are necessary to define a set of inertial reference coordinates as opposed to only two two degree of freedom gyros, the single degree of freedom type is widely used where high performance specifications must be met.

The categories of effort in the design of gyros include reducing their size, investigation of new materials, methods of driving the wheel, temperature control, methods of mounting, signal pickoffs and biasing torquers. However, the most intense development efforts have been concentrated on low friction shaft support, i.e., various forms of bearings. A summary of types of bearings is given in the following.

Wheel Support

Ball Bearings. This is the most commonly used means, although to date very little research effort has been put into perfection of bearings for this purpose.

Autolubricated Air Bearings. Although this is an old and long used method of supporting a spinning wheel, it is only recently that it has begun to find any favor in precision gyro design. A primary reason for this is that only recently have the required dimensional tolerances been achievable by anything other than hand methods, and the same applies to measurement for inspection purposes.

Electrostatic Field. This is not a new idea in itself, but its potential feasibility has been demonstrated only recently.

Magnetic Field. The interest in this means of support is concurrent with increased knowledge and success in cryogenic work, because a suitable working unit could not normally be obtained if large magnetic losses occurred.

Newer Laboratory Approaches. These include the use of spinning electrons, atomic particles, etc. Not much information is available for publication on these methods.

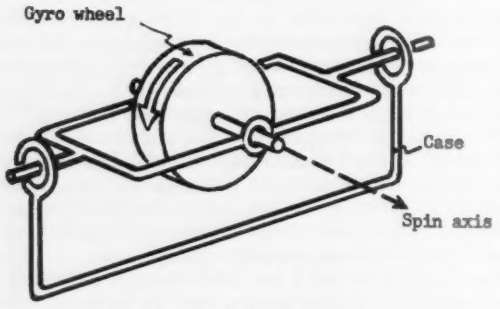

SINGLE DEGREE OF FREEDOM GYRO

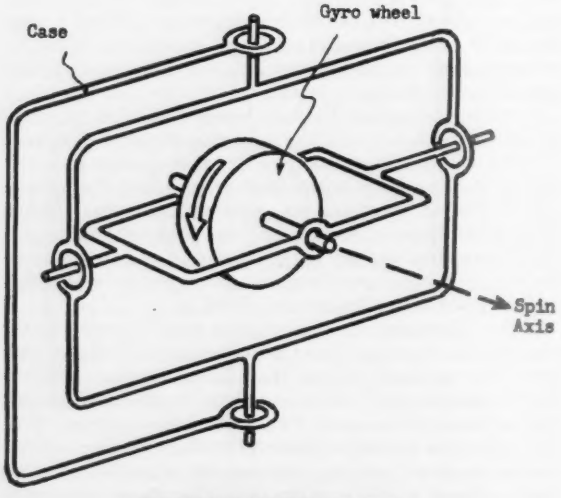

TWO DEGREE OF FREEDOM GYRO

Fig. 1 Line schematic diagrams showing basic differences between single degree of freedom and two degree of freedom gyros

Support of the Spinning Member Assembly About the Precession Axis or Axes

Flotation in a Liquid. Most high precision gyros use this means of support, as do a major percentage of the gyros for less accurate applications. The gyro wheel is sealed in a can, which is as nearly neutrally floated as is feasible. There is no energy fed via the fluid for support.

Pressurized Air Bearing. External air under pressure is supplied to the clearance between the housing and the can containing the wheel, using orifices to establish stable support.

Ball Bearings. These are not used for this particular purpose in highly accurate gyros, but are found in applications calling for considerably reduced accuracy in a relatively low acceleration environment.

Torsion Wire. This has very minor application. (See also discussion in next section.)

Electrostatic Field. With this means of support, a spinning ball is all that is needed, and, therefore, the electric field support of the ball is identical with that for the precession axes. In this case, the axes are defined by the pickoff system only.

Magnetic Field. This is the same as for the electrostatic field case.

Means of Defining the Precession Axis or Axes

Pivot and Jewel Bearings. This method has been used for a major percentage of instruments employing the flotation principle. Each bearing is simply a pin (the pivot) in a clearance hole (the jewel) to provide radial support with low friction. The pivot end can also be used as part of the axial thrust bearing.

Pressurized Fluid Bearings. This method is also used with floated instruments and provides a positive energy consuming radial (and axial) support bearing.

Torsion Wires. Again, this means is used with floated instruments but, as indicated, not extensively. Torsion wires provide both radial and axial support, but the wires must be in line and in tension for the results to be successful.

Crossed Reeds. This is a means of placing three reeds (or wires) in tension radial to the precession axis with one set at each end of the axis. By proper adjustment, it is at least theoretically possible to get a zero-restraint zero-friction support, but success depends on a critical adjustment. This method is generally used only with floated instruments.

Pressurized Air Bearing. This bearing uses energy and can be used to define the precession axis, but it may exert unwanted torques about it, due to the energy in the air.

Ball Bearings. The ball bearings mentioned in the foregoing can define the precession axis as well as support the

spinning-member assembly, but ball bearings in this application have high friction torques compared to other bearing types.

The subject of defining gyro uncertainty or drift (12,13) is broad enough to fill a nonpocket edition, and the controversy over the validity of various tests in terms of operating conditions, if converted into Btu, could operate the Nautilus for a year. The basis of the controversy seems to hinge on whether tests on a gyro in a constant-g field are truly indicative of instrument reliability and whether the tests are applicable to installations involving varying-g and/or high-g field. At the MIT Instrumentation Laboratory testing in a varying-g field is emphasized. The Laboratory has actual data showing that inferior caliber gyro units can pass tests made in a constant-g field and yet fail those in a varying-g field. Figs. 2 and 3 show test configurations for the two cases. The gyro in each case is operating in a closed loop positional servo.

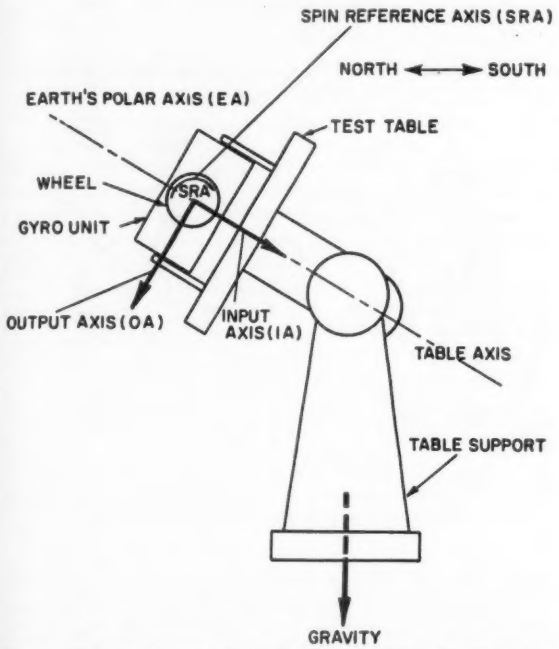

Fig. 2 Unit positioned with input axis parallel to Earth's polar axis and controlling servo to fix platform in inertial space

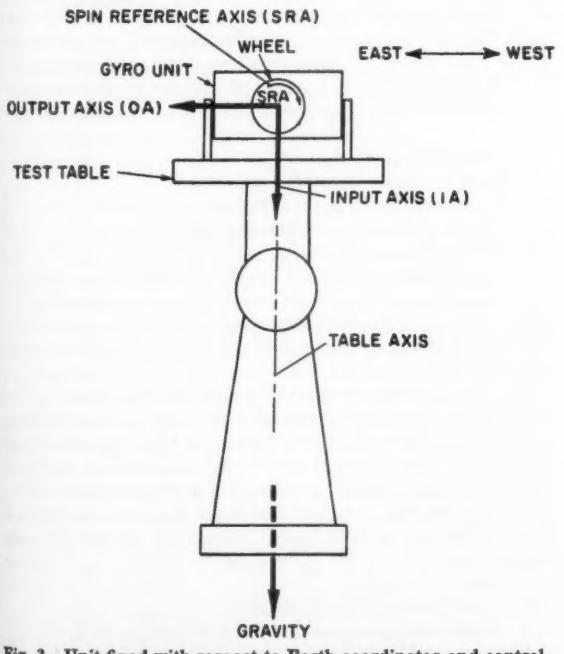

Fig. 3 Unit fixed with respect to Earth coordinates and controlling servo to fix platform with respect to the Earth (input axis vertical, output axis horizontal) (vertical component of Earth rate compensated)

The definition of gyro uncertainty is generally based upon the ability of the gyro to react either consistently with time to a given input (linear acceleration and angular velocity, where one or both factors may be chosen as zero or compensated out) or to react consistently with repeated tests under the same conditions.

Under the test conditions of Fig. 2, the gyro will stabilize the turntable in inertial space and, therefore, take out Earth rotation. In doing so, the component of the Earth's gravity field parallel to the turntable top will sweep around the gyro in the spin reference axis-output axis plane. This varying gravity component will tend to dislocate or move any mass free to move in this plane. Such mass shifts will, of course, affect the balance of the gyro and thereby the ability of the gyro to stabilize the turntable against the Earth's rotation correctly and repeatedly. By recording the rate of rotation of the turntable for repeated cycles of rotation and comparing it to Earth's rate, the uncertainty or drift of the gyro can be determined. Such drift can be defined as a time history of the deviation, as in Fig. 4, or can be defined in terms of a single number (but less usefully) as the mean rate of drift which produces either the final or peak displacement error during the time of test as shown in Fig. 4. The drift also may be defined as the rms of the ordinates of Fig. 4.

Under the test conditions of Fig. 3, the turntable will stand still with respect to the Earth as it also would do if everything were turned off. Therefore, this test can be misleading. However, the data resulting might also appear as in Fig. 4 and be described in the manner of the preceding paragraph.

Other methods of testing used elsewhere include variations on Fig. 3, i.e., output axis vertical and table shaft horizontal, as well as so-called "cogging" tests where the configuration might be as in Fig. 3, but with Earth rate not compensated out. Here the reaction of the gyro to the vertical component of Earth rate results in rotation of the turntable. Data are taken for repeated sweeps through a given azimuth angle. The average is removed to allow an rms analysis of the remainder for the series of runs. These tests are short and inexpensive but are unreliable indication for high caliber varying-g inertial performance.

Variations on the cogging test of a more severe nature have been introduced (or at least introduced to MIT) by British engineers. For these, the table shaft is horizontal and the tests are run for various inclinations of the output axis to the horizontal. Some analysis is required to correlate the data but this test gives more reliable results. It is not, however, of itself considered accurate enough for determining highest caliber inertial performance.

The type of gyro designed, built and tested at the MIT Instrumentation Laboratory (14,15) is the Draper floated

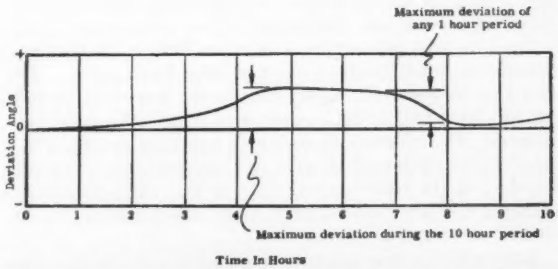

Fig. 4 Typical plot of gyro deviation angle vs. time for an inertial gyro in laboratory test

single degree of freedom integrating gyro unit shown in the line schematic diagram of Fig. 5 and the pictorial schematic diagram of Fig. 6. Fig. 5 shows, in simple form, the principles and functional parts of the unit. The synchronous (16) gyro wheel, providing the angular momentum, is carried in a sealed unit called the float gimbal structure. This is referred to as either the float or the gimbal, depending on whether operational or structural characteristics are emphasized. The single degree of freedom construction is shown by the single pair of pivot and jewel bearings located at either end of the float. The axis passing through the pivots is the output axis of the gyro.

The wheel, rotating on its own spin-axis ball bearings, is sensitive to angular velocities of the supporting case about any axis that is radial to the wheel shaft. Because of the single degree of freedom construction of the MIT gyro unit, the float is free to precess only in response to the components of angular velocity received along the gyro unit input axis.

The output signal of the gyro unit is produced by a signal generator, an electromagnetic reluctance bridge device called a microsyn. The microsyn rotor is mounted on one end of the float and the stator is mounted concentrically with the rotor on the gyro unit case. The signal generator detects rotation of the float with respect to the case and produces a polarized voltage signal proportional to the angle of rotation.

The torque generator, which is also a microsyn, is mounted at the other end of the float in a similar manner. The torque generator is a two winding element, similar to the signal generator, which responds to the in-phase product of the currents in the two windings. The torque generator can be excited so as to create controlled torques about the output axis, giving a means for correcting any predictable errors in the gyro unit, such as those due to mass unbalance.

In addition to performing the function of signal or torque generator, each microsyn is a magnetic suspension device that senses any radial displacement of the rotor with respect to the stator and changes the magnetic flux distribution in the air gap, so that a force acts on the stator, tending to return it to perfect centralization with respect to the stator gap. Since the sealed float gimbal structure is supported by a fluid film that supplies a buoyant force approximately equal to the weight of the float, the magnetic suspension microsyns are required to support only the unfloated portion of the total float weight. Note that the buoyant force as well as the float weight is proportional to the applied acceleration, thereby reducing to a negligible amount the load on the output axis bearings at all times. The function of the pivot and jewel bearings is to provide radial limits of travel of the float during storage as well as axial thrust limits at all times.

The highly viscous supporting fluid serves also as a damping fluid. High damping is obtained by the small thickness of the film of fluid between the float outside diameter and the case inside diameter. High damping increases the speed of response of the gyro unit to such inputs as step functions and makes the response time of the order of a few milliseconds. The unit composed of the float and the torque generator and signal generator rotors is called the torque summing member (13). The rotation of the torque summing member, and hence the gyro output signal, is proportional to the sum of the torques about the output axis.

The gyro unit case supports the gyro float in the fluid and provides the restricted clearance necessary for damping. The case also supports the signal and torque generator stators, and the fixed half of both jewel pivot combinations. Other elements are necessary to complete the gyro design, but a detailed description of them is not necessary for an understanding of the basic instrument. In this category, for example, are balance adjustments, power lead baffles, thermal control devices, etc.

Although this description is of a specific gyro design, some combination of the elements listed in the foregoing performing functions similar to those described here will be found in any

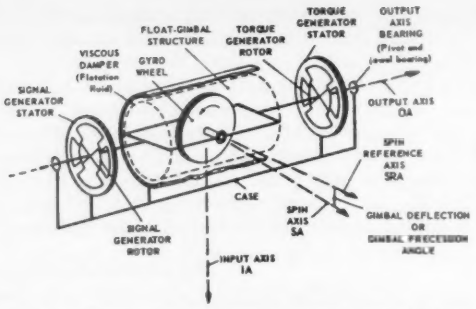

Fig. 5 Line schematic of the floated, single degree of freedom, integrating gyro

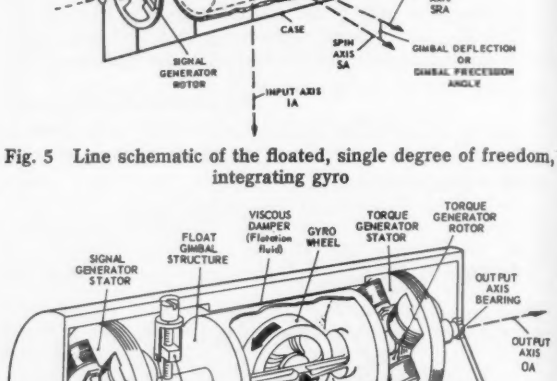

Fig. 6 Pictorial schematic of an early MIT design of the floated, single degree of freedom, integrating gyro

single degree of freedom integrating gyro (17). Note that, by simply adding the additional gimbal shown in Fig. 1, the description in this section would apply equally well to the two degree of freedom gyro design.

—William G. Denhard

Accelerometers

The basic elements of any acceleration measuring device evolve from the application of the principle of force or torque balance, which may be simply expressed as torque is proportional to the product of inertia and angular acceleration, or force is proportional to the product of mass and linear acceleration.

The basic elements are:

1 Mass or inertia element.
2 Force or torque summing member suspension.
3 Linear or angular displacement indicator.
4 Controlled force or torque restraint device.

A mass or inertia element usually consists of a concentrated mass of some high density material securely mounted in a rigid frame. Efficient design often permits the same structure to support components of the displacement indicator and torque restraint.

The force or torque summing member suspension serves to maintain the acceleration sensitive element in a single plane and determine the axis of measurement. The support should be passive in that it should contribute a minimum of coulomb friction or unpredictable forces. There are numerous ways to accomplish this, some of which are described in further detail elsewhere in this paper. Examples of output axis bearings are:

1 Magnetic bearings.
2 Fluid bearings (liquid or gas).
3 Elastic support (cross reed or torsion filament).

Displacement indicators are often chosen from the following:

1 Microsyn signal generator.
2 Capacitive.

3 Optical.
4 Moving vane.

Signal-to-noise ratio, i.e., signal resolution and selectivity, stability of nonpassive reaction forces and signal transmission line coupling problems, usually influence the choice of a pickoff.

The controlled force or torque production device is the subject of intense research activity because the ultimate linearity and range of the accelerometer are limited by its action. Some currently used restraint devices are:

1 Constant speed gyro wheel.
2 Controlled variable speed rotor.
3 Microsyn torque generator.
4 D'Arsonval torque generator.
5 Electrostatic torque generator.
6 Eddy current torque generator.
7 Elastic restraint.

The choice of restraint method gives the instrument designer considerable opportunity for ingenious application of new or unusual engineering materials. The objective is always to minimize disturbances resulting from temperature, pressure deflection and coulomb friction (18,19).

It is the manner in which the four basic elements of an accelerometer are combined that produces variations in the basic theme; these variations may be likened to the subject matter of a patent application in that any originality present is apt to be in a reassembly of familiar objects rather than in a new principle. What happens to the output of the measuring device, i.e., the mechanical or electrical operations performed, depends on the guidance system requirements. The decision to single integrate for velocity information or double integrate for distance information depends on the degree of accuracy attainable in the integration technique.

Ballistic missile applications require the range of acceleration measurement to extend over several decades, and furthermore it is desirable that any acceleration within this range be known to high precision. The linearity and repeatability requirements represent a significant challenge to an instrument builder when one considers the shock vibration and thermal environment to be encountered during the measuring process in flight. Although sufficient accuracy and stability are attainable in laboratory instruments, there is fierce competition among guidance system manufacturers for the reduction in size, weight and complexity. A review of current literature shows that accelerometer builders are striving to miniaturize prototypes which, though presumably meeting the specifications, remain too large and heavy.

The forward strides in today's accelerometer development are not the result of any new concepts of physical principles but are the result of basic research in the fields of chemistry and metallurgy. This research provides new engineering materials: Metals, fluids, potting compounds, bearing steels and dielectric materials, etc.

The ultimate utilization of these new materials depends on an increasing recognition by designers of devices which embody linear, nonsaturating torques employing feedback arrangements to minimize cross coupling errors. In addition, an accelerometer should contain elements with inherently good signal-to-noise ratios, matched thermal expansion coefficients, high ratio of structural stiffness to weight and, above all, good dimensional stability.

To describe the many types of accelerometers under consideration or manufacture would entail extensive space and time; however, the current approaches to the problem of acceleration and velocity measuring, fall into three categories (20):

1 Torque restrained pendulum or force restrained slug.
2 Vibrating string.
3 Pendulous integrating gyro.

The torque restrained pendulum is simple and economical in design and construction, but it suffers from its inherent susceptibility to cross coupled acceleration forces. It must therefore be constrained to a small dynamic displacement angle thus imposing a stringent displacement indicator resolution requirement at low accelerations. In order to accommodate high accelerations the torque motor must deliver a high torque level linearly, i.e., without saturating.

Some interest has been stirred in the direction of pulse torquing a pendulum in order to alleviate the magnetic linearity problem. This technique provides digital information to the computer, thereby making this class of instrument a strong contender for future accelerometer use. If the electronics associated with the pulse torquing can be made simple and reliable as well as compact, a very neat reduction in instrument complexity and size will result.

In the vibrating string accelerometer (8) the change in frequency of a tautly stretched wire is proportional to the square root of the tension of the wire. This in turn depends on the wire's obeying Hooke's law; i.e., strain is proportional to stress in a perfectly elastic material. The sensitivity, size reduction and tendency to average cross coupling effects makes this accelerometer attractive at first glance. The stability of calibration depends on the metallurgy of the wire. History shows that high unit stress is not conducive to low creep or drift characteristics in metal crystal groups. Frequent calibration coupled with compensation devices and networks may be employed to offset the short time instability.

The pendulous integrating gyro accelerometer is an outgrowth of the basic integrating accelerometer used in the German V-2. Certain techniques developed by MIT Instrumentation Laboratory and others have extended this philosophy to a high degree of perfection to produce the current accelerometers in missile guidance systems. Its great virtue as an acceleration measuring device lies in the fact that it does not use any restraint device which is limited by Hooke's law. A linear, unsaturable torque generated by a rigid pendulous element is balanced by a similar linear, unsaturable torque developed by the gyroscopic precessional torque as it responds to the angular velocity of a high performance servo.

One other aspect of the integrating accelerometer that makes it attractive is its linearity and accuracy as an integrator. Other types of accelerometers (with the exception of the vibrating string) must depend on external mechanical or electrical integrators, which are limited in precision, are very complex and require extra weight and space.

—Lester R. Grohe

Electromechanical Components Used in Inertial Navigation

The electromechanical components discussed here are used in inertial navigation as transducers for converting information from shaft rotation form to electrical signals or power, and vice versa. The information may be differentiated or integrated in the conversion process. The most interesting of these applications are devices called angular displacement signal generators, angular velocity signal generators and torque generators. There is a corresponding class of linear, rather than angular, displacement transducers which operate on the same principle.

The design objectives may be summarized broadly as follows:

1 High output-input sensitivity with low null signal giving good resolution for signal generators.
2 Minimum reaction or residual torque on both signal and torque generators.
3 When necessary, good linearity over a large range of input for both signal and torque generators.

These devices have two categories of use in inertial guidance systems: *Within* gyro and accelerometer components to convert their input and output quantities from electrical to me-

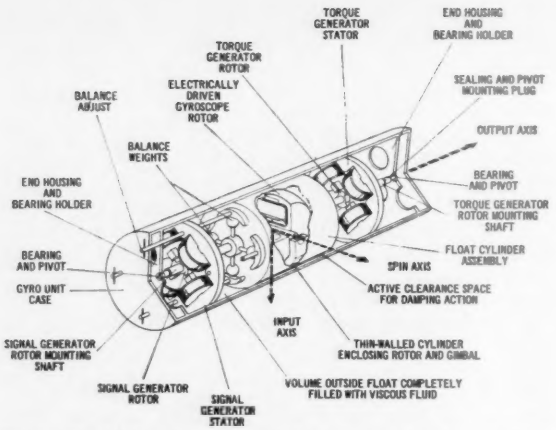

Fig. 7 Single degree of freedom floated gyro showing microsyn signal and torque generators

chanical form or vice versa, and *externally*, with similar functions, on the gimbal systems to which the gyros and accelerometers are mounted. The internal use category is discussed first.

An electromagnetic variable reluctance bridge type device called the "microsyn" (22) lends itself to many gyro and accelerometer applications in inertial navigation systems for the following reasons:

1 High signal-to-noise ratios over commonly used frequency ranges and high angular resolutions.

2 Input and output winding impedances are very flexible and can be obtained in manufacture over a wide range by simply using appropriate numbers of turns and wire sizes in the microsyn coils.

3 No flexible lead-in wires needed to attach to the output axis with its resultant error torques.

4 Extremely rugged and self-contained.

The microsyn consists of a high permeability stator core of 4, 8, 12, or 16 salient poles each with a primary and secondary winding, and a rotor core (with no windings) so shaped that a rotation of the rotor with respect to the stator increases or decreases the mutual inductance of the primary and secondary windings, relative to a quiescent or zero angular value.

In the microsyn signal generator, the primary coils serve as the excitation winding and the secondary coils serve as the output signal winding whose terminal voltage is proportional to the excitation current and frequency and the rotor displacement angle from the zero or null voltage position.

In the microsyn torque generator, the primary coils serve as the reference excitation winding, and the secondary coils serve as the control current winding. The output torque is proportional to the scalar product of the primary reference and secondary control currents.

The microsyn has a further advantage in that it can be used in such a manner as to magnetically support its own rotor core in the center of its stator bore when used in a floated type single degree of freedom gyro or accelerometer. The gyro or accelerometer float is held by a radial elastic magnetic force with respect to its outer case even under large case accelerations such as are found in missile applications. This is called the microsyn magnetic suspension (21).

The microsyn can identically be used as either an angular displacement signal generator or a torque generator for applying any desired torque or sum of torques to the gyro or accelerometer output shaft. Each microsyn type can be used to magnetically support its own rotor and the float in a floated type single degree of freedom instrument.

Microsyns have the disadvantage of having residual or reaction torques due to core assymmetries, and hysteresis torques in the torquers, if used with direct current excitation.

The use of two similar microsyns mounted "back to back" as a signal generator and a torque generator at both ends of a floated gyro or accelerometer shaft, as shown in Fig. 7, assures that residual or reaction torques due to environmental changes or stray fields will compensate to some extent. Also the use of two microsyns to lend elastic support to the floated gyro or accelerometer prevents the float from moving radially and axially while under the influence of high accelerations. The combination of the elastic magnetic support and the axial and radial damping of the viscous liquid make up a dynamic "shock absorber" on the instrument float.

Electrodynamic devices (22) with a fixed and moving coil can be used as both an angular displacement signal generator and torque generator, but this necessitates a delicate moving coil structure on the output shaft together with flexible lead wires.

The electrodynamometer type of torque generator, with two coils and no iron core, has the advantage of having no uncertainty torques due to hysteresis effects. Its big disadvantage is its low maximum torque per unit current density in the wire coils, because of the low permeability of air.

A widely used torquer, which combines the advantages of the microsyn torquer, which has a relatively high maximum torque with little or no hysteresis or reaction torques and excellent current input torque output linearity, is the d'Arsonval or "voice coil" type of torquer. This consists of one movable control current coil in a permanent magnet field. It has another advantage in that no power is required nor dissipated by the fixed or permanent magnet field. It has the disadvantage in gyro or accelerometer torquing of having to bring current lead wires to the moving coil on the instrument output shaft. These lead wires exert an uncertainty torque analogous to the magnetic reaction torque in microsyn type torquers.

Optical types of instruments are sometimes used as signal generators, but signal voltage generation in gyros and accelerometers may be difficult. Electrostatic devices with a fixed and moving set of vanes have been used for some time as capacitive signal generators and torquers. They avoid the lead-in difficulty to the instrument shaft but they have the disadvantages of high impedance and high voltage circuits.

Most torquers of the electromagnetic type discussed are limited in maximum torque due to heating or magnetic core saturation or both. Torquers of the electrostatic type are limited in maximum torque because of dielectric rupture of the air due to excessive voltage.

The second use category for electromechanical transducers is, as mentioned in the foregoing, their use on gimbal drive systems external to the gyros and accelerometers. These gimbal drive system components include, as before, angular displacement signal generators and torquers, of the following general types (23):

1 Signal Generators: Resolvers, synchros, microsyns and other miscellaneous inductive devices.

2 Torquers: a-c two-phase induction motors and d-c permanent magnet field motors.

These signal generators are required to have good angular resolution. The resolver and synchro type may be used over a range of multiples of one revolution whereas the microsyn can only be used over a limited range. The torquers may be used with gear trains or as direct coupled drives (9). Heating rather than magnetic saturation limit the maximum control torque in gimbal drive torquing.

Most modern inertial gyro spin motors are driven by the so-called hysteresis motor (24,25) which is a synchronous polyphase motor. It is very rugged and reliable and can be built to have a relatively high efficiency resulting in low heat dissipation to the gyro float. It consists of a silicon-iron stator core with a polyphase winding fixed to the float, a gimbal and a hard magnet material for the rotor. The rotation of the polyphase electromagnetic field causes magnetic poles to be

set up in the rotor at synchronous speed. The rotor will continue to rotate at synchronous speed until its maximum torque limit is reached.

—P. J. Gilinson Jr.

Computer Subsystem

The computer subsystem of the inertial guidance system may be thought of as the assembly of equipment which takes the data from the inertial instruments as inputs and supplies outputs to the flight control and other operating subsystems. Thus the computer has a data processing job to do which may involve converting the data form, solving sets of equations and performing logical and other functional operations.

Application of Analog Computers

The computer designer has the immediate choice between analog and digital instrumentation for the computer subsystem. The choice is by no means unique, and there may well be subjective as well as objective arguments employed in practical design situations. In general, however, one may think of the analog computer as having appropriate application to situations in which a single, specified computation is to be carried out—that is, situations in which the ability to time-share computing equipment over different computations would be of little advantage, and in which a computing precision of one part in 1000, or in certain cases one part in 10,000 is adequate. The precision required in a given computational situation depends to a marked degree upon how the equations are formulated and upon the nature of the other equipment to be used with the computer. One might conclude that analog computation is not applicable to IRBM guidance. Actually, analog computation can be used if the accelerometer is of the integrating type such as the pendulous gyro integrating accelerometer. In that case the nongravitational acceleration is integrated to a velocity by the inertial instrument itself, and the computer need supply only a small increment to the velocity indication—that which is due to perturbations from the nominal trajectory.

If analog instrumentation is to be used, the designer still has the choice between d-c and a-c signal levels—or perhaps a combination system. The d-c computer normally performs integration with a chopper stabilized d-c integrating amplifier, multiplication with a servo driven potentiometer, and trigonometric operations with sine-cosine plots or with a resistance card with wipers carried over a circular path. The a-c computer normally performs integration with a motor-tachometer integrator, multiplication with a servo driven potentiometer, and trigonometric operations with induction resolvers. The problems of d-c drift and the reliability of brushes and commutators which are inherent in d-c systems may be balanced against the problems of phase shift of the carrier and harmonic generation which are inherent in a-c systems. The d-c systems are the more common choice for analog computers used in laboratory situations and a-c systems are probably the more common choice for computers used in operating systems such as guidance systems.

The analog computer currently enjoys one distinct advantage over the digital computer: Many more engineers and technicians are familiar with analog technology than with digital. For this reason, no more will be said here about analog computers, although much remains unsaid.

Application of Digital Computers (26-29)

Some factors which point toward digital instrumentation of the computer subsystem are the following.

1 Accuracy. If a computing precision of one part in 1000 or perhaps a little better is clearly inadequate, then no choice exists in today's technology—a digital computer must be used. This is the case, for example, in the guidance of ballistic missiles of intercontinental range.

2 Flexibility. The digital computer can more easily be arranged to use the same equipment to perform different tasks at different times. This kind of flexibility is especially true of the arithmetic type of computer.

3 Compactness. The basic elements of which digital computers are composed have steadily become smaller and lighter, so that it is now possible in almost every case to construct a more compact digital than analog computer to perform a given task.

4 Reliability. Although very little is ever proved regarding reliability, one has the general feeling that the digital computer offers promise of greater operational reliability. This is due to the lack of dependence upon stable voltages and careful balancing. Usually the only critical quantity in a digital computer is the basic clock frequency, and for years the engineer has been able to effect more precise control over frequency than any other quantity.

Types of Digital Computers

If digital instrumentation is to be used, the designer still has a basic choice between two types of digital computers which will be referred to here as the *arithmetic* and *incremental* computers.

The arithmetic digital computer is like the common general purpose laboratory computer, which solves problems numerically in essentially the same way a human would using a desk calculator. This computer processes whole-number information; that is, a number being used in the arithmetic unit might represent to a known scale the velocity of the vehicle at that instant. Fundamentally, this machine simply adds numbers and performs certain logical comparisons. Integration is accomplished numerically, using an integration rule or quadrature formula of the designers choice. Multiplication is performed numerically by repeated shifting and adding. Trigonometric functions are usually evaluated using power series expressions. This computer solves a stated problem by carrying out one basic operation after another under the control of the program. The program is a sequence of coded instructions which usually are stored in the computer memory together with the required data. Thus the task which this computer performs can be changed just by causing the computer to follow a different program which also is stored in the memory. The arithmetic digital computer is then the most flexible of computers.

The incremental digital computer usually takes the form known as the digital differential analyzer or DDA. This computer processes incremental information; that is, the only information which it would receive from an inertial instrument which indicates velocity due to nongravitational acceleration would be a sequence of pulses—each one signifying that the velocity had changed by a prescribed increment. The basic element of the DDA is the DDA integrator or increment multiplier. This device yields an output pulse rate ΔZ proportional to the product of a whole number Y and a pulse rate ΔX. This increment multiplier is sometimes called a DDA integrator, because each output pulse ΔZ is proportional to $Y\Delta X$ which is an element of the integral of Y with respect to X using the rectangular integration rule. The accumulation of these ΔZ pulses then represents the integral of Y with respect to X. Trapezoidal and higher ordered integration rules can be instrumented with increment multipliers if desired. Products and trigonometric functions are determined by solving for the increment in the desired quantity in terms of known quantities and their increments. The computer processes all of the increment multipliers in a time known as the cycle time of the computer. Usually the cycle time and increment values are chosen in such a way that no variable changes by more than one increment in one cycle time. The problem which a DDA solves is defined by the interconnection of the increment multipliers; it is thus not so flexible in the changing of its program as is the arithmetic computer.

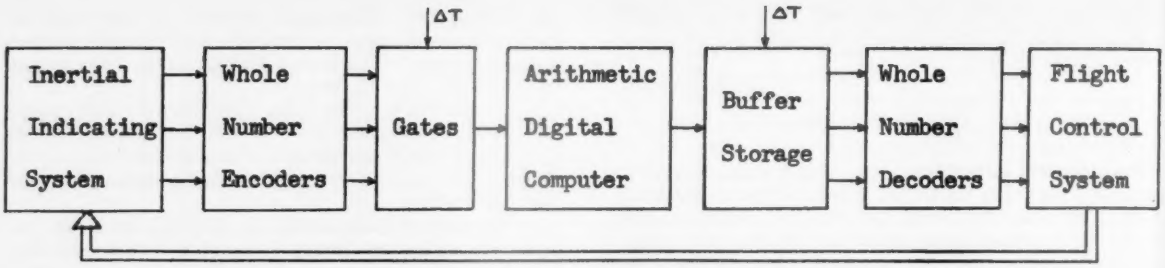

Fig. 8 General system configuration using an arithmetic digital computer

System Configurations Using Digital Computers

The general system configuration for an inertial guidance system using an arithmetic digital computer is shown in Fig. 8. At fixed time intervals ΔT, the current indications of the interial instruments, encoded into whole numbers, are gated into the computer memory. The computer then steps through its program solving the given equations. When the computer has executed the entire program it reads the output data into buffer storage and stops. At time ΔT later, fresh data are read in and the program is repeated. At the output end, whenever a new number appears in buffer storage, it is decoded into an analog signal for use by the flight control system.

For an operating system such as this the encoders may very well be repeater servos, if needed, and whole number shaft angle encoders. The computer probably would use a magnetic drum memory, which is the most compact storage medium in today's technology when all required auxiliary equipment is considered. The main disadvantage of drum storage is that instructions and data must be carefully placed on the drum if waiting time for required words to appear under the real heads is to be minimized. This is a severe limitation for a general purpose laboratory computer, but is less so for a special purpose computer which always will operate with a single program. To minimize waiting time, the computer will use a two-address instruction code or perhaps a relative address system, and parallel arithmetic will probably be required. The buffer storage may be flip-flop registers, and the decoders may well be servos with shaft angle encoders used in feedback loops.

The general system configuration using an incremental digital computer is shown in Fig. 9. In this case the computer operates almost continuously, accepting input pulses whenever they occur and putting out output pulses whenever required. The incremental encoders may be incremental shaft angle encoders, which are considerably smaller than whole number encoders. The computer may use magnetic drum memory or, if the problem is too small to warrant the use of a drum, magnetic core shift registers may well be used. The incremental decoder is smaller than a whole number decoder; it may be a stepping motor with an analog signal generator on its shaft, or in some cases, a simple smoothing of the output pulses yields directly the appropriate d-c analog signal.

Characteristics of the Systems

The choice between the arithmetic and incremental computers is by no means clear. Nor is the design procedure in either case a simple matter. Having a statement of the problem to be solved and the accuracy required, there is no obvious way of determining the best values for cycle times and increments for the variables. The world is still waiting for some inspired graduate student to provide some answers. One might expect in general, however, that the smaller problems can be solved in a more compact computer of the incremental type; if significantly different problems are to be solved at different times by the same computer, the arithmetic computer is probably indicated; in a complicated problem, a combination of the two types of computer might very well be of advantage.

—W. E. Vander Velde

Marine Inertial Navigation

Marine inertial navigation was initially conceived in 1950 in terms of a system for submarines which would replace the gyrocompass and the dead reckoning position indicator. Two requirements sharply distinguished the problem from other forms of inertial navigation proposed at that time: The initial alignment of the gyros relative to the Earth's polar axis, and the long operating time, during which the behavior of the gyros was expected to be less and less predictable. The first problem was solved by making the system track the Earth's polar axis in a manner broadly analogous to the way a gyrocompass tracks north—the inertial navigation system tracking the Earth rate vector, while a gyrocompass tracks the horizontal component of this vector.

The second problem involved realignment while the system was in use, without external references. The first system attempting to answer these requirements was tested by the MIT Instrumentation Laboratory in 1955; since that time, both the Sperry Gyroscope Co. and the Autonetics Division of North American Aviation, Inc., have entered the field. The latter group is responsible for the systems used in the recently famous subpolar explorations.

The impetus for recent effort in this field stems from the launching requirements of the IRBM Polaris. The ship's inertial navigation systems (SINS) provides Polaris with firing

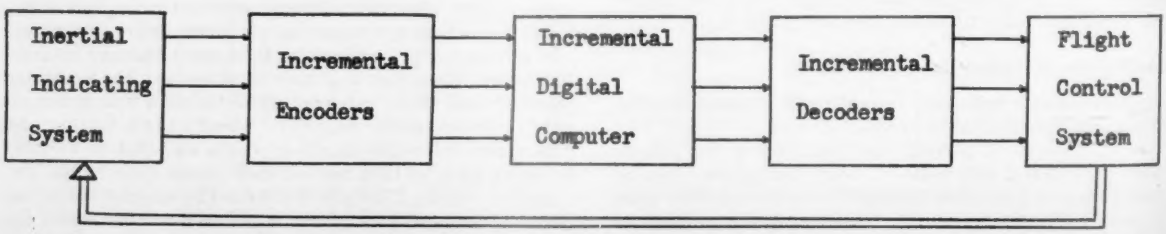

Fig. 9 General system configuration using an incremental digital computer

data. The role is probably the most taxing, in terms of accuracy and stability, that has thus far been assigned to an inertial guidance system.

—JOHN HOVORKA

References

1 Rawlings, A. L., "Theory of the Gyrocompass," Macmillan Co., New York, 1944.

2 Kooy, J. M. J. and Uytenbogaart, J. W. H., "Ballistics of the Future," McGraw-Hill Book Co., New York, 1946, pp. 280 ff.

3 Reisch, S., "Reports on Absolute Navigation No. 1," Royal Aircraft Establishment Translation 75, Vienna, 1945.

4 Wrigley, W., Woodbury, R. B. and Hovorka, J., "Inertial Guidance," SMF Fund Paper no. FF-16, New York, IAS, 1957.

5 Ishlinsky, A. Yu., "Equations for the Problem of Determining the Position of a Moving Object By Means Of Gyroscopes And Accelerometers," *Prikladnaya i Mekhanika*, Moscow, vol. XXI, no. 6, Dec. 1957, pp. 725–39.

6 "Floating Gyros and Their Application" (from Slavic Library, Battelle Memorial Institute), Moscow, 1958.

7 Wrigley, W., "Theoretical Background of Inertial Guidance Systems," Rep. 6398-S-5, MIT Instrumentation Laboratory, March 1950.

8 Gilbert, R. L. G., Proc. Phys. Soc., London, vol. B-62, 1949, p. 445.

9 Nelson, S. G., "Application of Direct-Drive Servomotors to Gyro Platforms," Proc. Nat. Electronics Conf., vol. 14, 1958, p. 498.

10 Osband, S. and Mundo, C. J., Jr., "A Two Degree of Freedom Gyro and Its Application," paper presented at ARS Meeting, Detroit, Sept. 1958.

11 Denhard, W. G., "Some Physical Configurations and Typical Data Form Encountered in Laboratory Testing of Inertial Gyros," R-112, MIT Instrumentation Laboratory, April 1956.

12 Denhard, W. G., "Laboratory Testing of a Floated, Single-Degree-of-Freedom, Integrating Inertial Gyro," R-105, Parts I, II and III, MIT Instrumentation Laboratory, Sept. 1956. (*Confidential*)

13 Denhard, W. G., "The Floated Gyroscope a "Canned" Signpost for Space Flight on Earth or in Outer Space," GY-166, Inertial Gyro Group, MIT Instrumentation Laboratory, Sept. 1958.

14 Draper, C. S., Wrigley, W. and Lees, S., "Inertial Guidance—A Monograph," MIT Instrumentation Laboratory, Aug. 1957. (*Secret*)

15 Denhard, W. G., "Notes on Hysteresis Motor Theory and Operation with Emphasis on Their Use in High-Performance Gyros," R-100, MIT Instrumentation Laboratory, Feb. 1956. (*Confidential*)

16 "Bibliography of Components Used in Gyroscopic Instruments," R-106, MIT Instrumentation Laboratory, Nov. 1956.

17 Sirri, N. and Fant, J., Jr., "Accelerometer Testing Procedures," California Institute of Technology, Jet Propulsion Laboratory, Pasadena, Calif.

18 Fellows, W. E., "Vibration Effects on Gyroscopes and Accelerometers," Minneapolis-Honeywell Regulator Co., Inertial Guidance Facility, St. Petersburg, Fla.

19 Grohe, L. R. and Kirk, J., "Instrumentation Components for Orbital and Satellite Vehicles," Summer Program Notes, Dept. of Aeronautics and Astronautics, MIT, Aug. 1956.

20 Mueller, R. K., "Microsyn Electromagnetic Components," MIT Instrumentation Laboratory, Dec. 1952.

21 Gilinson, P. J., Jr., "Microsyn Magnetic Suspension Elementary Principles," E-597, MIT Instrumentation Laboratory, Nov. 1956.

22 Draper, C. S., McKay, W. and Lees, S., "Instrument Engineering," McGraw-Hill Book Co., New York, 1955, vol. III, Part I, Chap. 35.

23 Greenwood, I. A., Jr., Holdam, J. V., Jr. and Macrae, D., Jr., Editors, "Electronic Instruments," Radiation Laboratory Series 21, McGraw-Hill Book Co., New York, 1955.

24 Roters, H. C., "The Hysteresis Motor," AIEE Trans., 1947, vol. 66, pp. 1419–1430.

25 Teare, B. R., Jr., "Theory of Hysteresis Motor Torque," AIEE Trans., 1940, vol. 59, pp. 907–912.

26 Chow, C. K., "Contactor Servomechanisms Employing Sampled Data," Ph.D. Thesis, EE Dept., Cornell University, 1953.

27 Martin, F. H., "Transient and Limit Cycle Behavior of a Mixed Analog-Digital System," MIT Instrumentation Laboratory Rep. T-210, June 1959.

28 Salzer, J. M., "Frequency Analysis of Digital Computers Operating in Real Time," "Proceedings of the IRE," vol. 42, no. 2, 1954, pp. 457–466.

29 Truxal, J. G., Ed., "Control Engineers' Handbook," McGraw-Hill Book Co., New York, 1958, Chap. 5.

Doppler Radars for Guidance—Design Techniques and Performance

WALTER R. FRIED

General Precision Laboratory, Inc.
Pleasantville, N. Y.

The fundamental principles of self-contained Doppler velocity measuring radars and Doppler guidance systems are described. A comparison of the various design techniques for Doppler radars and the advantages and limitations of each are presented. The overall configuration of a typical Doppler radar is described. The performance characteristics of Doppler radars, with regard to accuracy and range capabilities are discussed. It is shown that basic velocity information with a probable error of near 0.1 per cent is obtainable from Doppler radar. The use of a Doppler radar as one element of a complete guidance system is discussed. It is shown that the overall system accuracy of such a system is a function of the accuracies of all of the sensor and computation elements and, in many cases, can be no better than that of the weakest element. The nature of some of the system errors are described, including the effects of the directional and attitude references. Some recent advances in Doppler radar techniques and applications to space guidance problems are discussed.

ONE OF the basic pieces of information needed for the guidance of any vehicle is its velocity vector. In one form of application, the velocity, once determined, is combined with directional information and integrated to obtain miles traveled so as to compute the position of the vehicle. In addition, the velocity information can be used to determine other elements of guidance information which are a function of the vehicle's velocity, or to compensate the information from sensors which inherently require velocity correction.

In 1842 the Austrian physicist Christian Doppler predicted an effect in connection with sound waves which was destined to make a tremendous impact on the guidance field over 100

Received July 17, 1959.

years later, by providing an accurate means for the determination of the velocity of a vehicle. This effect, known as the Doppler effect, can be described as the observed change in frequency due to the relative motion of the source and the observer. When the velocity of motion is small compared to that of the propagating medium this change in frequency, the Doppler shift, exhibits a direct proportionality relationship to the relative velocity between the source and the observer, and hence represents a direct means of measurement of this velocity.

Christian Doppler dealt with sound waves in the 1840's; the Doppler effect was demonstrated in connection with microwaves in 1938 by workers at the U. S. Naval Research Laboratory. The use of the effect for the determination of velocity for navigational purposes by means of Doppler radar was first proposed in the 1940's by W. J. Tull and J. J. Hibbert at the MIT Radiation Laboratory (1).[1] Subsequently, the U. S. Air Force, General Precision Laboratory Inc. and other organizations began an extensive research program in the field of Doppler radar navigation. The results of this work clearly demonstrated that a Doppler radar, located on a vehicle, provides a highly accurate means of determining the velocity of the vehicle with respect to the Earth or other reflecting body from which the energy is backscattered. Thus, self-contained, i.e., vehicle-borne, Doppler radar emerged as a new sensor of great value for the accurate guidance of airborne vehicles without the need for any ground based stations. Continued effort has lead to many new developments in the field of Doppler radar techniques for navigation and guidance and to a tremendous growth and progress in this field.

It is the purpose of this paper to present a detailed discussion of the theory and practice of Doppler radar techniques for guidance. The fundamental principles of a Doppler velocity measuring radar will be described. This will be followed by a critical comparison of the different design techniques for Doppler radars and the advantages and limitations of each. The performance capabilities, as regards range and accuracy, and the various sources of error of a Doppler radar will be discussed. The interrelationship of the Doppler radar sensor with the other components of a guidance system is of considerable importance. It will be shown that, in general, the overall accuracy of a complete integrated Doppler guidance system can be no better than that of the poorest of the components of the system. Moreover, possible interconnections with other velocity and position sensors and typical methods of application of Doppler radar for the guidance of aircraft, missiles and spacecraft will be discussed. A comprehensive bibliography is given at the end of the paper.

[1] Numbers in parentheses indicate References at end of paper.

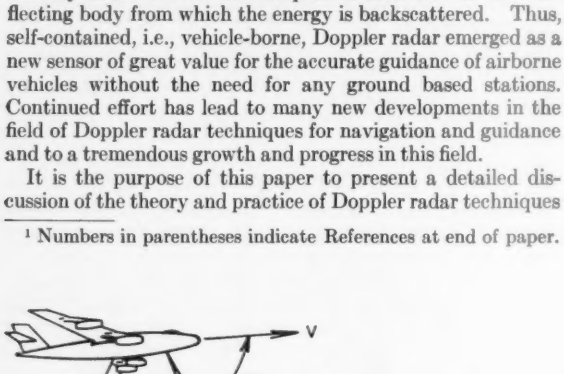

Fig. 1 Basic Doppler beam configuration

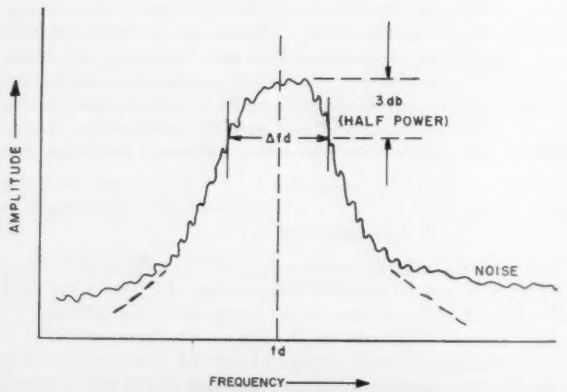

Fig. 2 Typical Doppler spectrum

Fundamental Principles of Doppler Radar

If one mounts a radar transmitter *and* receiver on a vehicle so that it transmits energy toward the ground and receives the backscattered energy, the difference between the received and transmitted frequencies is the Doppler shift. This shift exists since the transmitter and also the receiver are moving with respect to the Earth from which the energy is backscattered. If one measures this Doppler shift and knows the frequency of transmission, the velocity of light and the angle of radiation, one can determine the only unknown quantity, the velocity of the vehicle. The velocity can then be combined with directional information and integrated to measure the miles traveled and to compute the vehicle's position. This is illustrated schematically in Fig. 1. The basic output of a Doppler radar is therefore in the form of frequency, and, in general, the observed Doppler shift is given mathematically by the Doppler equation

$$f_d = \frac{2vf}{c} \cos \gamma = \frac{2v}{\lambda} \cos \gamma \qquad [1]$$

where

f_d = Doppler shift
v = velocity of the vehicle
c = velocity of light
γ = angle between the velocity vector and the direction of propagation
f = frequency of radiation
λ = wave length of radiation

Since the antenna beam has a finite width and since the scattering from the Earth is of random-like nature, the information received from the ground is not a single frequency, however; rather it is in the form of a noise-like frequency spectrum, like the one shown in Fig. 2. A certain amount of smoothing time is therefore required to determine the velocity to a given accuracy, with the accuracy increasing with smoothing time. A velocity smoothing time constant must be chosen, and its value usually represents a compromise between the velocity accuracy and rate of information required on one hand and the dynamics, e.g., maximum acceleration, of the vehicle on the other hand. If too large a smoothing time constant were selected, the Doppler radar would not be able to follow the vehicle accelerations or only with too great a lag. However, the effective smoothing time for average velocity or distance measurement is the total time flown and for typical systems it turns out that the fluctuation error due to the random-like nature of the information is completely overshadowed by certain instrumentation errors after only a few miles of flight (3 to 5).

It is the function of the frequency tracker of the Doppler radar, which will be discussed later, to determine the center of area of the Doppler spectrum, i.e., to determine the *single frequency* which is proportional to the desired velocity component. The half-power width of this spectrum Δf_d is quite

important with regard to velocity accuracy considerations. It is dependent on the antenna beam width and several other radar parameters, and is given mathematically by the expression

$$\Delta f_d = (2v/\lambda) \sin \gamma \Delta\gamma \qquad [2]$$

where

Δf_d = half-power spectrum width
$\Delta\gamma$ = two-way beam width of the antenna in the γ direction

In order to measure the total velocity vector three noncoplanar beams are required. However, it is possible to measure two horizontal velocity components with respect to the vehicle axis with only two beams radiating energy toward the ground, provided information on the vertical component is furnished by another source, such as a barometric device. This is shown schematically in Fig. 3. In a fixed antenna system, the longitudinal (along-heading) velocity component can then be obtained by adding the Doppler shifts obtained from the two beams. The lateral (cross-heading) velocity component can be obtained by taking the difference between the Doppler shifts from the two beams. In a gimballed antenna system, the drift angle or ground track angle can be obtained directly by servoing the antenna until equal Doppler shifts are obtained, and the ground speed by using the Doppler shifts from either one or both of the beams. It is clear that the measurement of along-heading and cross-heading velocity components is equivalent to the measurement of ground speed and drift angle, since the former two are simply components of the ground velocity vector, of which the ground speed is the magnitude and the drift angle is the angle of the vector with reference to the vehicle longitudinal axis. The hyperbolas appearing on the right side of Figs. 3 and 4 are contours of constant Doppler shift on the ground plane ("isodops") for a velocity vector which is coincident with the longitudinal axis of the vehicle. By considering these contours, one can see how the Doppler shifts from the left and right antenna of a fixed antenna system will be different, if the velocity vector is not coincident with the longitudinal axis, i.e., when a drift angle exists. The difference between these two Doppler shifts is then proportional to the cross-heading component of velocity.

For a number of reasons it turns out that the use of two beams is not optimum for most applications, rather the use of three or four beams, as shown schematically in Figs. 4 and 5. This configuration has been given the name Janus configuration, after the Roman god who was said to have the facility of looking forward as well as backward. Such a two-way looking or Janus system has the following advantages at the cost of one extra beam, over the one-way looking or non-Janus system (2 to 5):

1 It provides for inherent cancellation of the vertical velocity components when the forward and rearward looking beams are combined to measure horizontal velocity components, and hence information on the vertical velocity component from another source is not required.

2 The measurement of the horizontal velocity components is highly insensitive to errors in the vertical reference (pitch and roll) for both horizontal and nonhorizontal flight.

3 Measurement of the vertical velocity component, and hence of the total velocity vector, is possible, whereas it is not possible in the two-beam (non-Janus) case. In fact, in the non-Janus case it is necessary to furnish vertical velocity information from an external source as a correction signal.

The mathematical expressions showing this difference in dependence on the vertical attitude and vertical rate are easily derived (5) and are shown in the following for the somewhat simplified case of no drift and roll

$$E_v = \delta v/v = \tan \gamma(\delta\gamma) \qquad \text{non-Janus (pitch only)} \qquad [3]$$

$$E_v = \delta v/v = 1 - \cos(\delta\gamma) \qquad \text{Janus (pitch only)} \qquad [4]$$

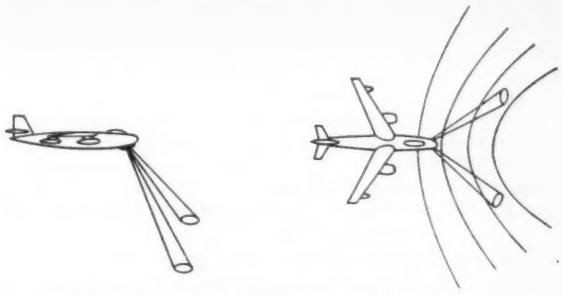

Fig. 3 Two-beam Doppler system configuration

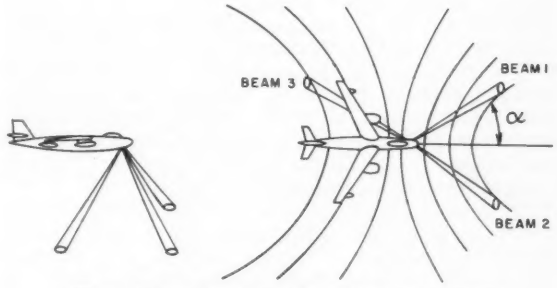

Fig. 4 Three-beam Doppler system configuration

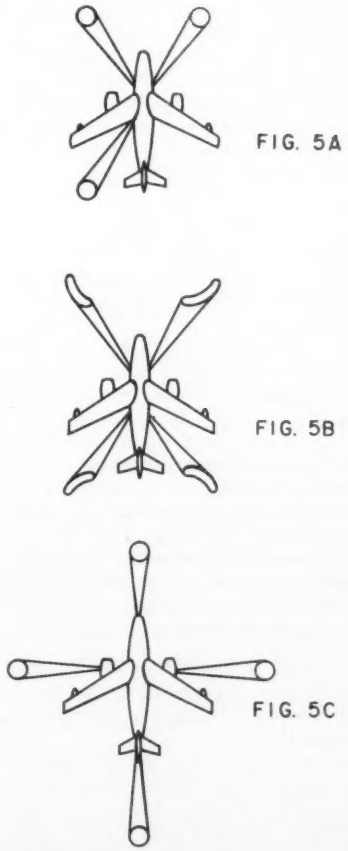

Fig. 5 Typical Doppler Janus system beam configurations

$$E_v = \delta v/v = 1 - \cos(\delta\gamma) + \sin\delta\gamma \tan\epsilon$$
Janus (pitch and vertical velocity) [5]

where

E_v = fractional velocity error
δv = error in velocity
v = velocity
$\delta\gamma$ = uncertainty in pitch angle
γ = angle between the horizontal velocity component and the direction of radiation
ϵ = angle of climb or descent

It is seen from these expressions that for a γ angle of 70 deg (a typical value for many Doppler radars) the non-Janus system suffers approximately a 4.7 per cent velocity error for 1 deg of uncertainty in pitch angle, whereas the Janus system suffers approximately a 0.014 per cent velocity error for a 1-deg error in pitch angle. Similarly, the error due to vertical velocity is very small in the Janus case, while it must be compensated for in the non-Janus case, with uncertainty in vertical velocity appearing as a direct factor. Janus systems use three or four beams of radiation; four beams are used in some systems primarily because of the symmetry of this configuration, which usually results in greater computer simplicity, and also because four beams are naturally produced by certain types of antennas, such as planar arrays.

In a Janus system the Doppler shift obtained with the forward beam is effectively added to the Doppler shift obtained with the rearward beam. For the condition of no pitch and roll, so that the forward and rearward Doppler shifts are equal, the equation for the total Doppler shift from two beams takes the form

$$f_d = (4v/\gamma)\cos\gamma \qquad [6]$$

where the symbols are the same as those defined earlier.

The particular beam configuration shown in Fig. 4 has been called λ configuration. Since it is a Janus system using three noncoplanar beams, all three components of vehicle velocity, i.e., the along-heading, cross-heading and vertical components of velocity can be obtained with it. For the condition of no pitch and roll, the mathematical expressions for the computation of the three velocity components are

$$\bar{V}_H = \frac{(\bar{f}_{d_3} - \bar{f}_{d_1})}{4\lambda\cos\theta\cos\alpha} \qquad [7]$$

$$\bar{V}_C = \frac{(\bar{f}_{d_1} - \bar{f}_{d_2})}{4\lambda\cos\theta\sin\alpha} \qquad [8]$$

$$\bar{V}_V = \frac{(\bar{f}_{d_3} + \bar{f}_{d_2})}{4\lambda\sin\theta} \qquad [9]$$

where

$\bar{V}_H$ = along-heading velocity component
$\bar{V}_C$ = cross-heading velocity component
$\bar{V}_V$ = vertical velocity component
$\bar{f}_{d_n}$ = Doppler shift of beam n
θ = depression angle of the antenna beams
α = azimuth angle of antenna beams (smallest angle between projections of longitudinal axis of vehicle and antenna beam on the ground plane)

Since a condition of no pitch or roll was assumed for the foregoing expressions, the quantities V_H, V_C and V_V can be described as the three orthogonal velocity components in vehicle coordinates.

The choice of γ angle for a Doppler system represents a compromise between high velocity sensitivity (cps per knot) which increases with smaller γ angles, and high signal return over the sea which increases with larger γ angles (or at least with larger antenna depression angles, which generally increase with γ angles). Most early equipment designers adopted a γ angle of 70 deg as the optimum compromise value. Another disadvantage of γ angles larger than this value has been a larger land-to-water bias error (which is discussed in more detail in a later section); however the use of land-sea calibration methods have reduced the importance of this factor to a very considerable extent, resulting in the selection of larger γ angles in later designs.

The choice of the α angle depends largely on the application of the system and certain technical considerations such as drift angle sensitivity and signal return. Typical α angles range all the way from 20–90 deg. Fig. 5 shows three examples of azimuth beam configurations for typical Janus systems. Figure 5a is the λ configuration already discussed. Fig. 5b is a typical four-beam configuration particularly suited for certain planar array antenna systems. Fig. 5c is a configuration which is suitable for Doppler systems requiring a complete ± 180-deg drift angle range.

In a practical Doppler radar the Doppler shift obtained is the beat between the transmitted and received signal. In order for such a system to function it is necessary that the received and reference signals be phase coherent with one another. This can be accomplished by a number of methods, depending on the type of transmission, and these will be discussed in some detail in the next section.

A block diagram of a typical Doppler radar is shown in Fig. 6. It consists of four major components; the antenna system, a radar transmitter, a radar receiver and one or more frequency trackers. In general, the outputs of the Doppler radar are frequencies, voltages or pulse rates representing the orthogonal velocity components of the vehicle.

Comparison of Design Techniques for Doppler Radars

Type of Transmission

The types of transmission for Doppler radars can be divided into three general categories:

1 Pulse.
2 Pure continuous wave (CW).
3 Frequency modulation continuous wave (FM-CW).

Pulse systems can be further subdivided into incoherent and coherent systems, and into low duty ratio (5 per cent or less) and high duty ratio (25–50 per cent) systems. Low duty ratio pulse systems are normally found in the incoherent class, whereas high duty ratio pulse systems are found in both the incoherent and coherent classes.

The low duty ratio incoherent pulse type of transmission employs techniques most similar to those used in conventional radars. In common with all of the pulse and FM-CW systems, but contrary to pure CW systems, this type of transmission exhibits high receiver-transmitter isolation. Because of its low duty ratio, this type of transmission is the least efficient of the types of pulse systems mentioned in the foregoing. However, primarily because of the state of the art of techniques and the availability of components at the time, this is the type of transmission used in the earlier Doppler radars (16,17).

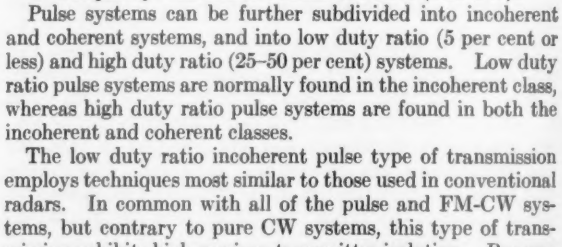

Fig. 6 Block diagram of typical Doppler radar

The high (25–50 per cent) duty ratio pulse systems exhibit high spectrum utilization efficiency, in some cases approaching that of CW systems, and at the same time they have the high transmitter-receiver isolation lacking in the pure CW systems.

Incoherent pulse systems (of high or low duty ratio) normally use an incoherently pulsed magnetron and achieve the coherence required for Doppler radar operation by beating the returns from forward and rear beams, which are themselves coherent with one another. The method has been called self-coherence and inherently requires a condition of at least partial time overlap. This type of system exhibits a certain simplicity through the use of a single magnetron transmitter as compared to typical coherent pulse systems, as will be seen later. Also, in contrast to both CW and coherent pulse systems, incoherent pulse systems impose no severe requirements on transmitter frequency stability. In such systems the frequency needs to remain only within the receiver IF-pass band, and the frequency deviation during a transmitted pulse must not be large compared to the reciprocal of the pulse duration. The incoherent pulse system has the limitation that backward velocity information (sense of direction) and the vertical velocity component cannot normally be obtained, since the separate frequency shifts of the echoes from the individual beams are not available. Also, at high altitudes, the signal-to-noise ratio (S/N) falls off somewhat faster with increasing altitude than in CW, coherent pulse and FM-CW systems, primarily because of certain effects of the time spread of the echoes, and, at very high altitudes, because of certain undesirable signal and noise products. At the lower altitudes, however, the rate of S/N falloff is approximately the same for all of the types of transmissions mentioned here (20,21).

The coherent pulse transmission systems, which are usually found in the high (25–50 per cent) duty ratio class, obtain the required coherence through the use of a free running CW oscillator, which is also used as the source for the reference signal, and whose output is fed to some form of pulse modulator and then to one or more klystron amplifiers. The pulse modulation process can be performed by means of a crystal modulator, gridded klystron, or synchrodyne, or a combination of these. The coherent local oscillator reference signal is usually obtained by means of a so-called side-step local oscillator arrangement, in which a small amount of energy from the CW oscillator is mixed with energy from an oscillator at intermediate frequency so as to produce the local oscillator signal. A coherent pulse system is capable of determining backward velocity (sense of direction) and vertical velocity and hence the total velocity vector, since the Doppler shifts of the echoes in the individual beams are available separately. At high altitudes, the S/N falloff of coherent pulse systems can be made better than that of incoherent pulse systems, remaining at 6 db per octave (twice the altitude) throughout, provided no loss of coherence occurs. At high altitudes the high duty ratio coherent pulse system thus represents the most efficient of the various pulse systems. One of the disadvantages of the coherent pulse system, as compared to the incoherent pulse system, is considerably greater complexity, since it normally requires specialized microwave modulation and gating devices and a multiklystron transmitter chain, as compared to the simple magnetron of incoherent systems. Furthermore, the frequency stability requirement for the free running CW oscillator of such systems is very stringent, namely it is a function of the maximum echo return time (or altitude), as compared to the much less stringent requirement for incoherent pulse systems which was described earlier. Also, in such systems, care must be taken to suppress coherent carrier leakage to avoid undesirable effects in the receiver (23).

All types of pulse systems are subject to so-called "altitude holes," which exist at periodic altitudes at which the return pulse arrives near or at the time of the next transmission pulse and can therefore be gated out, unless special steps are taken. The method normally used to reduce or completely eliminate this problem is to vary the pulse repetition rate (PRF) either continuously or in discrete steps, so that energy is received at all altitudes, including those at which a "hole" would exist if the PRF were fixed at one value.

Pure continuous wave (CW) transmission is inherently the simplest and most efficient type of transmission. No modulators of any kind are required, and, ideally, the spectrum utilization efficiency is 100 per cent. Also, no altitude hole problems of any kind exist in such a system. However, pure CW transmission systems are faced with the problem of difficulty of transmitter-receiver isolation and an inherent lack of discrimination against echoes from nearby objects. The lack of isolation can result in large undesirable carrier and noise leakage signals which can lower the receiver gain and increase the effective noise level, thus greatly reducing the signal-to-noise ratio. This is of particular importance for operation at high altitudes, where the backscattered signal is, of necessity, relatively small. Also, in this case, an increase in transmitter power will be accompanied by a proportional increase in leakage power and therefore will not produce any increase in signal-to-noise ratio. Similarly, reflection and backscattering from nearby objects, such as stationary or vibrating structural members like the radome, nearby turbulent air (supersonic shock waves) and precipitation, will cause undesirable noise power which is in the frequency band of interest and whose level is proportional to the transmitted power. To improve basic transmitter-receiver isolation, dual antennas (space duplexing) are usually employed, resulting in larger antenna cutouts. Moreover, in general the installation of a CW system is precarious and troublesome because of the problems of achieving rigidity and avoiding vibration and leakage paths. The problem of lack of discrimination against echoes from noise producing scatterers in the vicinity of the vehicle itself is inherent with CW systems and virtually unavoidable. These factors represent a severe limitation of CW systems with respect to high altitude operation and have discouraged many designers from choosing this type of transmission. CW systems are inherently coherent in view of their continuity of transmission and reception. The stability requirements of the transmitter of typical CW systems is essentially the same as that of coherent pulse systems; i.e., it is a function of the total echo time, such that partial loss of coherence usually results in spectrum broadening and an increase in S/N falloff to values greater than the ideal of 6 db per octave (18,24,36).

The frequency modulation continuous wave (FM-CW) type of transmission attempts to combine some of the advantages of pulse and pure CW systems. The problems of transmitter-receiver isolation and discrimination against nearby echoes are eliminated in such a system on a frequency basis, much as they are eliminated in pulse systems on a time basis. In an FM-CW system the transmitter is frequency-modulated, and the receiver is designed to accept and use only the Doppler shift of a particular sideband, other than the zero-order sideband, of the beat between the received and transmitted signals. Since the modulation index of the beat spectrum, and hence the amplitude of all but the zero-order sidebands, decreases very rapidly with decreasing range, becoming zero at the receiver terminals, high transmitter-receiver isolation and suppression of returns from nearby objects is achieved. Since such a system requires only one transmitter klystron and a simple low power sine-wave modulator, it tends to resemble the simplicity of a pure CW system. One of the disadvantages of the system is a relatively low spectrum utilization efficiency, since the power in all of the other sidebands is not used. Another, even more serious, problem of typical single antenna FM-CW systems is the fact that the full transmitter power feed-through of the duplexer, which is determined by the duplexer isolation characteristics obtained in practice (frequently from 20–30 db maximum), is continuously applied to the receiver crystals. This can result in severe crystal deterioration and hence in a significant loss and accompanying

reduction in receiver sensitivity. This fact prevents the use of higher powers over and above some maximum value (a few watts or so) and represents a severe limitation of FM-CW systems with regard to very high altitude operation. Also, in such systems, the requirement for maintaining the transmitted modulation index is reasonably critical. FM-CW systems are inherently coherent in view of their continuity of transmission. However, the requirement on the stability of the transmitter is different for the two possible types of Janus FM-CW systems. In one type, in which mixing is done after tracking, the stability requirement is similar to CW and coherent pulse systems, and any incidental FM in the transmitter can result in considerable spectrum broadening and a lowered S/N ratio (27). In the other type of FM-CW system, mixing is done before tracking and undesirable effects of incidental FM in the transmitter are inherently eliminated by cancellation through self-beating, so that the frequency stability requirement of the transmitter is lowered considerably.

FM-CW systems are subject to altitude hole problems in a manner equivalent to the one discussed for pulse systems (though for different reasons), and these problems can be solved in FM-CW systems by somewhat similar techniques as those discussed earlier in connection with pulse systems (26,27,33–35,38,39).

Frequency of Transmission

As seen from Equation [1] the sensitivity of a Doppler radar in cps per knot increases with increasing frequency of transmission. On the other hand, if the frequency selected is too high, the absorption and backscattering effects of the atmosphere become objectionably large (7) and satisfactory radar components are less available. Thus, the choice of frequency becomes a compromise based on the foregoing factors and at the present time Doppler radars use frequencies in the X band, specifically 8800–10,000 mc/sec, and in the K_E band, specifically 13.25 – 13.5 mc/sec.

Polarization

The types of polarizations presently used for Doppler radars are linear and circular-odd (opposite rotation received), although cross-linear and circular-even (same rotation received) have also been considered. The main advantage of circular-odd polarization has been more efficient duplexing, although ferrite duplexers have largely removed this advantage over linear polarization. The same is true for cross-linear polarization; however the scattering loss is quite considerable for this polarization. To date, there is no experimental evidence of any appreciable difference in backscattering characteristics between linear or circular-odd (opposite rotation received) polarization. Circular-even polarization (same rotation received) has very desirable and well-known rain discrimination properties. However, as cross-linear polarization, it suffers from an appreciable scattering loss, particularly over water, which has discouraged designers from using this polarization.

Antennas

Antennas used for Doppler radars include phased linear arrays producing partial fan-shaped beams and a variety of antennas producing pencil beams or near pencil beams such as those shown in Fig. 5. Among the latter types are phased planar slotted arrays, parabolas and cut parabolas, and dielectric and metal-plate lens antennas fed by horns. Linear and planar arrays are normally considerably thinner than equivalent lenses or parabolas, thus requiring less height within the vehicle. These antennas are also more adaptable to beam shaping and can be designed to make the Doppler calibration constant completely independent of transmitter frequency. Both phased planar arrays and lenses can provide multiple beams with a single aperture. In general, the size of the antenna aperture is determined by the desired beam width. The latter has a marked effect on the velocity fluctuation error and on the over-water bias error. One-way beam widths chosen for modern Doppler radars range from 3–7 deg, with the majority of systems having adopted a value near 5 deg.

Stabilization

As indicated previously, all Doppler radars are sensitive to some degree to a knowledge of the attitude (pitch and roll) of the vehicle, although Janus systems less so than non-Janus systems. Some correction or stabilization for the pitch and roll of the vehicle must therefore be made by means of information from a vertical reference, and the two ways of accomplishing this are antenna stabilization and data stabilization. Systems using fan-shaped beam configurations tend to favor physical ground track stabilization, because of the shape of the constant-Doppler hyperbolas shown on Figs. 3 and 4. Roll and pitch stabilization can also be done by physically moving the antenna; this is referred to as antenna stabilization. Data stabilization, on the other hand, constitutes pitch angle and roll angle correction of the data in some form of computer, and allows the use of fixed antennas. This generally requires somewhat less radome cutout size and weight than stabilized antennas, but at the expense of the stabilization computer. Antenna stabilization results in somewhat greater accuracy in some cases, particularly for drift angle determination over water, and it eases the tracking rate requirement of the frequency trackers in certain types of systems. It also permits considerably larger roll and pitch excursions over water without loss of signal, since it avoids large increases in incidence angle with resulting decreases in scattering coefficient.

Receivers

Doppler radar receivers can be classed into the two categories of crystal video (zero frequency IF) and intermediate frequency (IF) receivers. There are further differences determined largely by whether the system is CW or pulse, non-Janus, RF Janus or IF Janus, as discussed elsewhere in this paper. Zero frequency IF receivers heterodyne a portion of the transmitted energy directly with that of the received energy, thus producing an audio Doppler signal at the crystal of the receiver. Although this system is by far the simplest and also eliminates one of the carrier leakage problems, it suffers from the poor noise characteristics of crystals at audio frequencies resulting in an inherent reduction of signal-to-noise ratio by 15–20 db. Intermediate frequency systems require the necessary local oscillators, mixers and filters, but exhibit the resulting 15–20-db signal-to-noise ratio improvement over crystal video receivers.

Frequency Trackers

As mentioned earlier, the function of the frequency tracker is to determine the center of area of the noise-like frequency spectrum obtained from the ground echo. The generic forms of practical frequency trackers are the axis crossing counter and the closed loop frequency discriminator. Practically all modern Doppler radars use some form of closed loop frequency discriminator as the frequency tracking device. The Doppler signal is usually fed to one or more modulators which modulate it with a signal from a variable frequency oscillator (tracking oscillator) and feed the output to the device which performs the discriminator function. The output from the latter is smoothed in an integrator and used to control the frequency of the tracking oscillator. The tracking oscillator can then provide the frequency tracker output. Mechanically tuned discriminators have also been employed, although they appear to have less accuracy capability (3,17,35). A discriminator type of frequency tracker can assume different forms, depending on whether the tracking operation is done at audio (d-c) or

at some intermediate frequency. Furthermore, a frequency discriminator can employ a sweeping operation, a comparison of two nearby filters, some form of autocorrelation technique or a combination of these methods. Practice appears to show that there are no large differences in the performance of most of the existing frequency trackers either as regards accuracy or sensitivity, although conclusive comparisons have not yet been made.

Performance Considerations

Altitude Range

The altitude range capability of a Doppler radar is primarily dependent on the following factors:

1 The radar system parameters.
2 The scattering properties of the target area.
3 The attenuation (absorption) and backscattering properties of the atmosphere.
4 The velocity of the vehicle.
5 The efficiency of the particular type of system.
6 The design practices employed to solve the critical system problems.

The radar parameters include such factors as the transmitter power, antenna gain, looking angle, receiver noise figure and wave length of transmission.

The scattering surface fills the entire antenna beam in Doppler radar operation, and the value of the backscattering coefficient of the terrain is an important factor in determining the signal power available at the receiver. Since the scattering coefficient of water surface is approximately 5–15 db worse than that of land surface (8–11) depending on incidence angle and sea state, the operation of a Doppler radar over water represents the most severe condition from the viewpoints of the type of target area and the altitude capability.

If the atmosphere through which the energy must travel has significant attenuation (absorption) and scattering properties at the wave length in question, the useful signal power available at the receiver is proportionately reduced. At the wave lengths generally used for Doppler systems (2.2–3.0 cm) these effects are normally quite small, however.

The velocity of the vehicle is involved in the altitude performance of a Doppler radar in view of the spectral nature of the Doppler signal and the narrow banding property of Doppler receivers. The noise bandwidth in which the Doppler signal is measured is the width of the Doppler spectrum. Since this Doppler spectrum width is proportional to the vehicle velocity, as shown by Equation [2], the noise power in the bandwidth of interest increases linearly with velocity, and the available signal-to-noise ratio decreases by the same factor. Stated differently, for a given spectrum power content the signal power per cps decreases with increasing velocity.

The characteristics of the particular system, such as the type of transmission, type of antenna, form duplexing, sensitivity of the receiver and sensitivity of the frequency tracker, which were discussed in previous sections, have, of course, a significant bearing on the altitude capability of the system.

The final item listed in the foregoing deals with the design practices employed in the solution of the system design problems. Although these factors are frequently not amenable to ready calculation, they can be of extreme importance with regard to the altitude capability of the system. An example of these would be the requirement for extreme rigidity of construction in the case of a pure CW system, in view of the undesirable effects of vibration of structural members which are located anywhere in the path of the transmitted or received energy. Vibration of this type can cause large noise levels in the bandwidth of the desired Doppler information and thus reduce the signal-to-noise ratio at the receiver. This assumes particular significance at high altitude at which the backscattered signal is relatively small. Another important example of this type of problem is the frequency stability of the free running oscillator in CW, coherent pulse and certain types of FM-CW systems. Lack of sufficient frequency stability of the oscillator which can be due to such factors as power supply ripple, microphonic pulling or temperature effects, causes partial loss of coherence and can result in appreciable broadening of the Doppler spectrum and correspondingly lower signal-to-noise ratios.

Quantitatively, the altitude capability of a Doppler radar can be expressed as a function of the available Doppler signal-to-noise ratio at the highest altitude, highest velocity and over the worst terrain, as compared to the sensitivity of the frequency tracker. The latter is expressed as the minimum Doppler signal-to-noise ratio required by the frequency tracker for acquisition and tracking of the signal.

The following is an expression for the first of these two parameters: The Doppler signal-to-noise ratio. The expression given is valid for coherent non-Janus systems and coherent Janus systems using post tracker mixing. It is derived from the radar equation which can be found in any radar text (6)

$$\left|\frac{S}{N}\right|_d = \frac{P_t G_0 W_{rf} E f(\psi) \lambda^2 A F L \cos^2\psi}{(NF) K T \Delta f_d (4\pi h)^2} \qquad [10]$$

where

$\left|\frac{S}{N}\right|_d$ = Doppler signal-to-noise ratio (Doppler S/N). (Ratio of the total Doppler signal power to the noise power in the bandwidth of the Doppler spectrum. The bandwidth of the Doppler spectrum is measured at the 3-db points)
P_t = average transmitted power per beam
G_0 = one-way maximum antenna gain relative to an isotropic radiator
W_{rf} = RF attenuation in the plumbing of the transmitter and receiver paths, including duplexing and wave guide losses
E = efficiency factor (ratio of available Doppler S/N to the Doppler S/N which would be available if all of the received signal were converted to Doppler information. This includes spectrum utilization in pulse and FM-CW systems, gating improvements and noise foldover losses)
$f(\psi)$ = scattering coefficient at the given ψ angle. $f(\psi) = \frac{1}{2}\sigma_0 \sec \psi$, where σ_0 is the average radar cross section per unit area)
(NF) = RF noise figure
K = Boltzmann's constant
T = absolute temperature
Δf_d = bandwidth in which the noise is measured, i.e., the bandwidth of the Doppler spectrum. (See Eq. [2] for the coherent single beam case, for example)
L = attenuation in the atmosphere
A = antenna efficiency
ψ = angle of incidence, i.e., angle between the vertical and the direction of radiation
F = antenna pattern parameter (normally between 0.5 and 0.67)

From the foregoing expression the Doppler S/N can be calculated. The actual or measured Doppler S/N may be smaller in some cases because of the effects of certain of the design practices referred to under item 6 at the beginning of this section.

To obtain an expression for the Doppler S/N ratio for coherent Janus systems using pretracker mixing, Equation [10] must be modified to take into account the so-called signal suppression effect, which becomes significant only at extremely small IF S/N ratios and causes the S/N altitude falloff to increase to as much as 12 db per octave (double the altitude). For the case of coherent and incoherent pulse

Janus systems using pretracker mixing, Equation [10] must be further modified to include the effects of the time spread of the echoes, which becomes significant at medium altitudes and can cause the S/N altitude falloff to increase from the 6 db per octave value for low altitudes to 9 db per octave. For the case of incoherent pulse systems using pretracker mixing a final modification of Equation [10] is required to take into account the so-called pulse overlap noise which can occur at very high altitudes due to second detector noise produced by the beating of the returns from successive transmitter pulses. [See reference (20) and reference (3) cited therein.]

The other important parameter, the minimum Doppler S/N required by the frequency tracker of course depends on the performance characteristics of the particular frequency tracker. Modern frequency trackers have been built in production which will acquire the signal at a Doppler S/N of 2–4 db and which will track the signal at a Doppler S/N of less than 0 db.

On the basis of the foregoing considerations and the present state of the art, it can be shown that Doppler radars can be designed to operate at the highest altitudes required for current commercial and military aircraft and cruise missiles, and over smooth water, using average transmitter powers of less than 15 w.

It can also be shown that for certain terminal guidance spaceflight applications, for example for a landing on the moon, which is believed to have no water surfaces, a range of 100 miles can be obtained with a high duty ratio coherent pulse system using currently known techniques and having an average transmitter power of 50 w. Recent work seems to indicate that only one third of this power would be needed over land for a coherent pulse system using a pulse length which corresponds to the echo return time and which is large compared to the Doppler correlation time, as is the case for extremely high altitude operation. For shorter range lunar landing applications, Doppler radars using other types of coherent transmissions can be shown to provide satisfactory solutions.

Accuracy

Although the basic velocity accuracy achievable with a Doppler radar is extremely high, there are a number of sources of error which contribute to the error in velocity measurement. Following is a list of the major errors, and a discussion of each of them. Some of these are clearly random errors; some are clearly systematic (i.e., are amenable to being "calibrated out"), and some of the errors contain both random and systematic components:

Doppler Fluctuation Error σ_{d_f}. This random error is due to the noise-like nature of the Doppler signal spectrum, and is a function of the smoothing time, the velocity and the spectrum width. The latter is in turn dependent on certain basic radar parameters, such as beam width, wave length and looking angle. Since the expression describing the fluctuation error involves the smoothing time and the velocity only as a product (2,5), the fluctuation error is a function only of distance traveled, observing an inverse square root dependence. Thus, the fluctuation error decreases very rapidly with distance traveled. For instance, it is shown in (5) that for a typical Doppler radar, the standard deviation of this error is 0.045 per cent after 10 miles and 0.02 per cent after 50 miles of travel. Hence, the Doppler fluctuation error is usually swamped by other instrumentation errors of the guidance system with regard to distance and position determination. However, it must be considered for short term velocity measurement.

Errors in the Beam Direction σ_{ϵ}. (Antenna and Bore Sighting Errors). As seen from Equation [1], an error in beam direction directly effects the value of the measured Doppler frequency. This is clearly a systematic or bias error, however, and in many cases it can be removed by some form of calibration procedure. Moreover, Janus-type systems are much less sensitive to any misalignment in the installation of the entire antenna because of the nature of the Janus self-compensation discussed previously.

Error in the Transmission Frequency σ_f. It is also seen from Equation [1] that an error in the transmission frequency directly affects the value of the measured Doppler frequency. However, when the frequency stability of existing microwave tubes is considered in the light of Equation [1], it is seen that this error is normally quite small. Moreover, as discussed earlier, phased linear and planar array antennas can be so designed as to make the Doppler calibration constant completely independent of transmission frequency (3, 22).

Error in Frequency Measurement σ_m. (Frequency Tracker Error). This error is, of course, a function of the instrumentation of the frequency tracker. The error can normally be expressed as a fraction of the Doppler spectrum width and hence as a percentage of velocity. Frequency trackers having errors less than 0.02–0.05 per cent are within the present range of achievement.

Error in Data Conversion σ_c. In many systems it is necessary to convert the Doppler frequencies representing the desired velocity components into some other form, such as analog voltages for instance, in order that the information can be operated upon in a computer or used by other equipments in the vehicle. This data conversion can deteriorate the accuracy of the velocity information. The error has been particularly significant in the earlier Doppler radars, which used relatively inaccurate tachometers in the conversion device. Recently, however, electronic frequency to analog conversion devices have been developed which exhibit errors less than 0.05 per cent. In addition, airborne digital computers are finding increasingly more widespread use, and conversion devices which transform Doppler frequency data into binary digital form can be designed with negligible error, or with an error which is limited only by the number of binary bits used.

Error of Stabilization or Conversion From Vehicle to Ground Coordinates σ_s. Since the basic Doppler velocity information is obtained in vehicle coordinates and is generally required in ground or other coordinates, a conversion from the former to the latter is usually required. For normal flying, this conversion amounts to stabilization about the pitch and roll of the vehicle. In antenna stabilized systems the information furnished by the Doppler radar is in the desired coordinate system, and the stabilization error is primarily a function of the errors of the vertical reference and of the servo which controls the antenna. In fixed antenna systems the Doppler velocity information is furnished by the Doppler radar in vehicle coordinates and the data are corrected for the pitch and roll of the vehicle in some form of computer which again receives pitch and roll information from a vertical reference. In this case the resulting error consists of the error of the vertical reference system and of the computer error of the stabilization computer. As was shown earlier, the basic error due to pitch and roll uncertainties is quite small for Janus systems (0.014 per cent per 1 deg of uncertainity in pitch for instance). Reduction of this error to extremely small values can be achieved through the use of an accurate vertical reference system and a high precision servo or stabilization computer.

Error Due to the Nature of the Target Area σ_t. For operation over land this error is negligibly small. It is caused by a very small change in scattering coefficient with looking angle over the finite beam width, by range difference effects over the beam width and by nonlinearities in converting ray angles to Doppler frequencies. For operation over water, however, this error can assume very appreciable values, primarily because now the change in scattering coefficient with looking angle over the finite beam width can be quite large (3–5,9). This phenomenon has the effect of producing a somewhat skewed and shifted Doppler spectrum, which results in a so-called water calibration shift error. Al-

though this error is a systematic error for a given sea state, it varies for different sea states (3–5). Thus, it can be reduced to a considerable degree, although not completely, by a land-water calibration change based on an average sea state. The water calibration shift error is primarily a function of beam width, beam shape, incidence angle and sea state. Assuming a properly selected mean for the sea state calibration correction and a random (gaussian) distribution of occurrence of sea states about the mean, the error can be reduced to a peak value of ± 0.7 per cent and possibly a 1σ value near 0.25 per cent for typical systems and for a range of sea states defined as Beaufort 1 to Beaufort 4 (4,5). For sea states smoother than Beaufort 1, the error would be somewhat greater. New techniques (of which details are still classified) are being investigated, however, which are aimed at further progress in this area. This work is greatly justified since this error represents one of the largest errors in velocity measurement by a Doppler radar (4,5). Water surface droplet motion and water current motion also cause Doppler velocity errors; however (unlike the calibration shift error discussed above), these errors decrease, percentage-wise, as the vehicle velocity increases, and therefore tend to become acceptably small for most modern vehicles (4, 5).

On the assumption that the systematic errors have been removed by some form of calibration procedure, the total nonsystematic Doppler velocity error σ_{v_f} can be obtained by combining the Doppler fluctuation error σ_{d_f} (for a desired distance or velocity and smoothing time) and the nonsystematic components of the other errors discussed above in a root-sum-squared manner as follows

$$\sigma_{v_f} = \sqrt{\sigma_{\ f}^{\ 2} + \sigma_{m_f}^{\ 2} + \sigma_{c_f}^{\ 2} + \sigma_{s_f}^{\ 2}} \qquad [11]$$

where the subscript f denotes the nonsystematic (fluctuation) component of the error in question.

For typical high performance systems, this results in a total 1σ Doppler velocity error over land of less than 0.1–0.3 per cent and an equivalent error in drift angle or cross-heading velocity. A considerable amount of statistically significant measured flight data, in many yet unpublished and in some published papers (4,5,12), have clearly demonstrated Doppler radar velocity accuracy of this quality.

For operation over water, the calibration shift error discussed in the foregoing must of course be taken into consideration as an additional source of error.

System Considerations

In many applications Doppler radar velocity information is fed to some type of computer which combines it with information from a directional (heading) reference, integrates the velocity to produce miles traveled and computes position and steering information. In this case, the Doppler radar, the computer and the directional reference constitute the three major components of a complete guidance system. It is important to note that the overall accuracy of such a guidance system can be no better than that of the poorest of the three major components. In fact, the overall along-track (range) error is obtained by combining, in a root-sum-squared manner, the range components of the errors of the Doppler radar and the computer, and the cross-track (transverse) error is obtained by combining the transverse components of the errors of the Doppler radar, the computer and the error of the directional reference (13). The importance of the directional reference is easily appreciated in this connection, when one observes that a 1-deg directional error results in a 1.75 per cent error in position. Because of the difficulty of obtaining accurate directional references, it is the error of the directional reference which controls the overall system error in many present-day systems (4, 5, 12, 13).

Typical directional references are the gyro-magnetic compass (40), the free gyro (41), the astro-compass and the north seeking gyro-compass (42, 43).

The north seeking gyro-compass is perhaps the least known of the four devices mentioned; it appears to have considerable potential. It is an inertial device which inherently seeks north by finding an Earth rate signal null, and it does not exhibit a drift error which accumulates with time, as does a conventional inertial platform or free gyro (41–43). Successful operation of this device requires accurate information on the vehicle's velocity, which is available from Doppler radar. It also requires at least one gyro with drift rates of the order of 0.01 to 0.1 deg per hr. Gyros having such quality have recently become practical. It also requires vertical stabilization, which can become an important design problem if the vehicle can be subjected to large attitude excursions. If the proper design techniques are used, the north seeking gyro-compass operated in conjunction with Doppler radar is capable of very high, sustained, azimuth (heading) accuracy (4, 5, 42, 43).

The effect of the vertical reference error on the Doppler system error was discussed previously and was shown to be of lesser importance than the directional reference error, particularly for Janus systems. This is especially true for applications in aircraft and cruise missiles. Vertical stabilization may assume greater importance in connection with Doppler radar applications in space vehicles, since large excursions of the vehicle are possible and cannot be tolerated beyond certain limits in view of the nature of the Doppler radar backscattering requirements. However, equipment which is designed to accurately stabilize such vehicles is being developed for other purposes and should, hopefully, provide sufficient performance to permit Doppler radar operation.

The accuracy of the computer of a complete self-contained guidance system is also of importance, since it provides the function of velocity integration, and position and steering error computation. However, the development of high precision analog and digital computers is so far advanced that a computer of almost any desired accuracy compatible with those of the Doppler radar and directional reference can be designed. It becomes necessary only to select a computer design which does, in fact, have performance characteristics which are properly compatible with those of the sensors.

On the basis of the foregoing considerations, i.e., over-land 1σ Doppler velocity errors of 0.1 to 0.3 per cent, computer errors of the same order and directional errors two or three times that value, typical high performance Doppler navigation systems exhibit overall rms position errors somewhere less than 1 per cent of distance traveled (4, 5, 12, 13).

Since approximately 1954, Doppler navigation systems have found widespread application in military aircraft (5, 47, 48), have been evaluated for certain cruise missile applications, and, more recently, have been designed for use in commercial aircraft (49–51). The characteristics of many of these systems have been described in the literature (3–5, 16–39). The weight of the lightest of the Doppler radars in present-day production is approximately 60 lb, and the weight of the lightest complete systems is somewhere near 100 lb. However, extensive efforts toward further reduction of weight and size of Doppler radars are being carried on at the present time.

For some applications extremely accurate short term velocity information is required, in addition to accurate vertical, attitude and position information. In this case, the interconnection of a Doppler radar and an inertial platform represents an ideal solution, since such a system combines in a complimentary fashion the highly accurate long term velocity information furnished by the Doppler radar, useful for airborne erection and damping of the inertial system, and the highly accurate short term velocity and vertical information of the inertial platform, which can in turn aid the Doppler radar tracking and provide dynamic inertial memory. Hence, such a combined system is capable of providing very accurate velocity and vertical information (45,46). If highly accurate position, and hence directional, information is required for long periods, as in the case of long range vehicles,

an ideal Doppler-inertial interconnection is a system which employs a Doppler radar as part of a so-called Doppler-inertial compass, i.e., with a platform, which is interconnected so as to operate in a north seeking gyro-compass mode. In this mode of operation the platform is kept pointed north at all times through use of the basic principle discussed earlier in connection with the north seeking gyro-compass. The necessary vehicle ground velocity information is of course available in the system from the Doppler radar. Such a system provides accurate information on long term velocity from the Doppler radar and short term velocity, verticality and long term azimuth from the inertial platform, and thus permits the computation of highly accurate position for long ranges and periods of time (46).

Another possible combined system configuration is a so-called Doppler-inertial-stellar system, which uses a Doppler radar for long term velocity, an inertial platform for short term velocity and an astro-compass for accurate directional information and position correction. Various forms of such self-contained combined systems using Doppler radar have found application in military vehicles and their uses are destined to increase rapidly in the future.

Doppler radars can also be used advantageously in other forms of combined systems, such as in conjunction with certain ground based radio guidance systems. In such systems, the Doppler radar provides continuity of information but with an error which accumulates with distance, whereas the ground based radio system provides intermittent, but instantaneously highly accurate, position fix information (44, 51).

Recently, considerable work has been done in connection with the application of Doppler radar techniques for the guidance of satellites and space vehicles (52–54). The nature of Doppler radar operation makes it particularly suitable for such terminal guidance applications as the establishment of a precise "parking" orbit at a destination planet with respect to its center of gravity and the safe reduction of vehicle velocity for a soft landing. A coherent, long pulse, Doppler system using a fixed thin planar array antenna appears to represent one possible configuration for a Doppler radar to be used for the determination of velocity in space vehicles (52). Other types of lightweight coherent Doppler systems have also been considered for such applications. Some of the design problems to which particular attention must be paid for such applications are sufficient frequency stability of the reference oscillator in the Doppler radar and the stabilization of the vehicle. The former is required to assure coherence between the reference signal and the received signal in certain types of Doppler radars, considering the large ranges involved, and the latter is required to assure proper orientation of the radiated beams. Fortunately, highly stable microwave sources are either available or under development, and equipment capable of accurately stabilizing such vehicles is already being developed for a number of purposes. The successful development of low noise receivers should also greatly facilitate the design and increase the range and hence the potential usefulness of Doppler radars for space applications.

Conclusions

Self-contained Doppler radar represents a highly accurate means of measuring the velocity of a variety of vehicles, without the need for any ground stations. The Doppler velocity can be combined with directional information and integrated to provide continuous information on the vehicle's position; it can be employed by itself as a guidance sensor; it can be used to compensate other equipments requiring velocity correction, and it can be interconnected with other velocity and position sensors to optimize overall system performance. Vehicle-borne Doppler radar appears destined to find continued usefulness for the guidance of aircraft, missiles and spacecraft for many years to come.

References

Doppler Radar Theory and Practice

1 Hall, J. S., "Radar Aids to Navigation," MIT Radiation Laboratory Series, McGraw-Hill Book Co., New York, vol. 2, 1947, p. 110.

2 Berger, F. B., "The Nature of Doppler Velocity Measurement," IRE Trans., vol. ANE-4, Sept. 1957, pp. 157–175.

3 Berger, F. B., "The Design of Airborne Doppler Velocity Measuring Systems," IRE Trans., vol. ANE-4, Dec. 1957, pp. 176–196.

4 Fried, W. R., "Principles and Performance Analysis of Doppler Navigation Systems," IRE Trans., vol. ANE-4, Dec. 1957, pp. 176–196.

5 Fried, W. R., "Doppler Navigation Systems—Principles and Practice," Wright Air Dev. Center Tech. Note 57-175; Wright Patterson Air Force Base, Dayton, Ohio, ASTIA no. AD-118271, Dec. 1957.

Radar Theory and Propagation

6 Ridenour, L. N., "Radar System Engineering," MIT Radiation Laboratory Series, McGraw-Hill Book Co., New York, vol. 1, 1947.

7 Kerr, D. E., "Propagation of Short Radio Waves," MIT Radiation Laboratory Series, McGraw-Hill Book Co., New York, vol. 13, 1951.

8 Davies, H. and Macfarlane, G. G., "Radar Echoes from the Sea Surface at Centimeter Wavelengths," Proc. Physical Society, vol. 48, Nov. 1946, pp. 717–729.

9 Campbell, J. P., "Back-scattering Characteristics of Land and Sea at *X*-Band," Proc. 1958 National Conference on Aeronautical Electronics, IRE, Dayton, Ohio, May 1958.

10 Grant, C. R. and Yaplee, B. S., "Back-scattering from Water and Land at Centimeter and Millimeter Wavelengths," Proc. IRE, vol. 45, July 1957, pp. 976–982.

11 Wiltse, J. C., Schlesinger, S. P. and Johnson, C. M., "Back-scattering Characteristics of the Sea in the Region from 10 to 50 KMC," Proc. IRE, vol. 45, no. 2, Feb. 1957, pp. 220–228.

Doppler System Performance

12 Berger, F. B., "Summary of AN/APN-66 Flight Test Accuracy Data," General Precision Laboratory Internal Rep. #161, May 17, 1955.

13 Fried, W. R., "Performance Profiles and Future Outlook of Doppler Navigation Systems," IRE Trans., vol. ANE-5, Dec. 1958.

14 Thorne, T. G. and Billings, J. A., "The Performance of Doppler Navigation Systems," British Communications and Electronics, March 1959, pp. 176–179.

15 Harder, D. and Strell, J., "Reliability Analysis of AN/APN-81 in a Field Operation," Proc. 1958 East Coast Conference on Aeronautical and Navigational Electronics of the IRE, Baltimore, Md., Oct. 1958, pp. 85–94

Doppler Radar Equipment

16 Tull, W. J., "Doppler Navigation," Proc. 1957 National Conference on Aeronautical Electronics, IRE, Dayton, Ohio, May 1957.

17 McMahon, Frank A., "The AN/APN-81 Doppler Navigation System," IRE Trans., vol. ANE-4, Dec. 1957, pp. 202–211.

18 Condie, M. A., "Basic Design Considerations—Automatic Navigator AN/APN-67," IRE Trans., vol. ANE-4, Dec. 1957, pp. 197–201.

19 Walker, E. G., "Factors in the Design of Airborne Doppler Navigation Equipment," *J. Brit. IRE*, vol. 18, July 1958, pp. 425–442.

20 McKay, M. W., "The AN/APN-96 Doppler Radar Set," 1958 IRE National Convention Record, Part 5, pp. 71–77.

21 McMahon, Frank A., "The Radan Model PC-221A," vol. 4, GPL Technical Series, General Precision Laboratory Inc., Pleasantville, N. Y.

22 Saltzman, H. and Stavis, G., "A Dual Beam Planar Array Antenna for Janus Type Doppler Navigation Systems," IRE Convention Record 1958, Part I, p. 241.

23 Laschever, Norman L., "AN/APN-78, a Doppler Navigator for Helicopters," Proc. 1958 National Conference on Aeronautical Electronics, IRE, Dayton, Ohio, May 1958, pp. 117–122.

24 Bowden, John J., "Continuous-Wave Doppler Navigation," Proc. 1958 National Conference on Aeronautical Electronics, IRE, Dayton, Ohio, May 1958, pp. 123–127.

25 Bussey, H. C. and Zielinski, C. A., "The AN/APN-79 Navigation System CW Doppler Radar Groundspeed Sensor," Proc. 1958 National Conference on Aeronautical Electronics, IRE, Dayton, Ohio, May 1958, pp. 128–132.

26 Glegg, K. C. M., "A Low Noise CW Doppler Technique," Proc. 1958 National Conference on Aeronautical Electronics, IRE, Dayton, Ohio, May 1958, pp. 133–144.

27 Brown, R. K., "The Canadian Lightweight Doppler Navigation Radar," Proc. 1958 East Coast Conference on Aeronautical and Navigational Electronics, IRE, Baltimore, Md., Oct. 1958, pp. 117–121.

28 Gray, T. and Moran, J., "Decca Doppler and Airborne Navigation," *Brit. Comm. and Electronics*, vol. 5, Oct. 1958, pp. 764–771.

29 Beck, G. E., "Airborne Doppler Equipment," *J. Inst. Navigation*, Great Britain, vol. XI, no. 2, April 1958, pp. 117–124.

30 Houghton, P. A., "The Future Development of Doppler Navigation," *J. Inst. Navigation*, Great Britain, vol. XI, no. 2, April 1958, pp. 130–137.

31 Durst, C. S., "The Sea Surface and Doppler," *J. Inst. Navigation*, Great Britain, vol. XI, no. 2, April 1958, pp. 143–149.

32 Brown, R. K. et al., "A Lightweight and Self-contained Airborne Navigational System," Proc. IRE, May 1959, pp. 778–780.

33 Wulfsberg, P. G., "A Coherent High-Performance FMCW Doppler Radar Navigation System," Proc. 1959 National Aeronautical Electronics Conference, May 1959, pp. 343–347.
34 Tollefson, R. D., "Application of Frequency Modulation Techniques to Doppler Radar Sensors," Proc. 1959 National Aeronautical Electronics Conference, May 1959, pp. 683–687.
35 Stryker, E. M., Jr., "The Use of a Tuned Discriminator in Tracking a Doppler Navigation Radar Spectrum," Proc. 1959 National Aeronautical Electronics Conference, May 1959, pp. 228–231.
36 Miller, G. M., "Design Considerations for the APN-79 Airborne Doppler Navigation System," *Navigation*, vol. 6, no. 3, Autumn 1958, pp. 147–156.
37 Lawton, L. M., Jr., "Evolution of Modern Doppler Navigation," to be published in Proc. June 23–26, 1959 Meeting of the Ausschuss für Funkortung, Haus der Technik, Essen, Germany.
38 Glegg, K. C. M., "The CMA 620 Series of Doppler Sensors," to be published in Proc. June 23–26, 1959 Meeting of the Ausschuss für Funkortung, Haus der Technik, Essen, Germany.
39 Bath, C. C., "Modern FM/CW Doppler Techniques," to be published in Proc. June 23–26, 1959 Meeting of the Ausschuss für Funkortung, Haus der Technik, Essen, Germany.

Directional References

40 Shapiro, A., "Precision Azimuth Reference Systems," Proc. 1957 National Conference on Aeronautical Electronics, IRE, Dayton, Ohio, May 1957.
41 Harmon, W. L. and Goldman, C. C., "Gyro Heading Reference for High Latitudes," Wright Air Dev. Center Tech. Note WCLN 54-4, Wright Patterson Air Force Base, Dayton, Ohio, May 1954.
42 Cudaback, J. L. R., "Earth Rate Directional Reference for Aircraft," U. S. Air Force Inst. of Technology Masters Thesis; Wright Patterson Air Force Base, Dayton, Ohio, March 13, 1956.
43 Atwood, D. J. and Best, F. A., "Airborne Earth Rate Directional Heading Reference," 1958 Proc. National Conference on Aeronautical Electronics, May 1958, pp. 457–462.

Combined Systems

44 Galbraith, H. J. and Braverman, N., "The Practical Combination of Air Navigation Techniques," IRE Trans. on Aeronautical and Navigational Electronics, March 1956.
45 Duncan, B. D., "Combined Doppler Radar and Inertial Navigation Systems," *Navigation*, vol. 6, no. 5, Spring 1959.
46 Dworetzky, L. M. and Edwards, A., "Introduction to Doppler-Inertial System Design," ARS JOURNAL, vol. 29, no. 12, Dec. 1959, pp. 967–972.

Doppler Radar Applications to Airborne Flight

47 Whiting, R. E., "The Use of Doppler by the United States Air Force," *Navigation*, vol. 6, no. 3, Autumn 1958.
48 Moorhen, C. N., "The Navigational Applications of Doppler Equipments," *J. Inst. Navigation*, Great Britain, vol. XI, no. 2, April 1958, pp. 125–130.
49 Myers, J. S., "The Significance of Doppler in Jet Transports," *Navigation*, vol. 6, no. 3, Autumn 1958, pp. 135–137.
50 Fraser, D. O., "Doppler and Civil Aviation," *J. Inst. Navigation*, Great Britain, vol. XI, no. 2, April 1958, pp. 138–143.
51 Fried, W. R., "On the Application of Doppler Navigation Equipment in the Air Traffic Control Environment," Proc. 1959 National Aeronautical Electronics Conference, IRE, Dayton, Ohio, May 1959, pp. 502–517.

Doppler Radar Applications to Spaceflight

52 Silberberg, M. Y. and Campbell, J. P., "Space Vehicle Applications of Self-Contained Doppler Radar," Proc. 1959 National Aeronautical Electronics Conference, IRE, Dayton, Ohio, May 1959, pp. 104–109.
53 Campbell, J. P., "Doppler Techniques for Space Vehicle Guidance," Proc. Third National Convention on Military Electronics, IRE, Washington, D. C., July 1959.
54 Berger, F. B., "Use of Doppler in Space Navigation," to be published in *J. Inst. Navigation*.

Principles of Doppler-Inertial Guidance

L. H. DWORETZKY and A. EDWARDS

**General Precision Laboratory, Inc.
Pleasantville, N. Y.**

The principles of Doppler-inertial system theory and design are developed following a description of the characteristics and limitations of individual Doppler radar and inertial navigation systems. It is shown that the combined system provides improved accuracy and the capability of in-flight vertical and heading alignment.

A DOPPLER-inertial navigation system is composed of a Doppler radar, an inertial navigation system and combining equipment. An individual Doppler or inertial system is capable of making an independent determination of the velocity of the vehicle in which it is carried. Each of the velocity measurements has some desirable and some undesirable characteristics, and it is the role of the combining equipment to process the information obtained from these two measurements to enable the system to indicate a velocity which contains as many of the desirable features as possible and as few of the undesirable features of each measurement as possible.

One of the most important features of the combined system is that it can establish its orientation in a navigational reference frame without ground alignment or dependence upon a magnetic compass. It erects itself to the vertical and can align itself to true north while in flight.

Received July 17, 1959.

Doppler Radar

A Doppler radar measures the velocity with respect to the Earth (ground velocity) of the vehicle in which the radar is carried by measuring the Doppler frequency shift in the return from beams of microwave energy aimed at the ground and reflected back to the moving vehicle. The Doppler frequency so measured is proportional to ground velocity.

Most systems operate with three or four beams and thus are potentially capable of measuring the total ground velocity vector in three dimensions. For normal aerial navigation, the two dimensions in the horizontal plane are of principal interest, and consequently, in Doppler design the vertical velocity measurement has not been stressed. However, with the advent of high performance vehicles and helicopters the importance of the three-dimensional capability will increase. Since the ground velocity is obtained in aircraft coordinates, auxiliary vertical and heading references are required to obtain the velocity in Earth coordinates to provide a self-contained navigation capability.

Because the Doppler radar beams have finite width, the return is composed of energy reflected from a group of random scatters on the ground, and instead of a single Doppler frequency the return contains a spectrum of Doppler frequencies. The process of determining ground speed consists of averaging over a time interval to find the center frequency of the spectrum. Because of this averaging process, the Doppler measured velocity is not highly accurate instantaneously. However, the long term average is very accurate.

Inertial System

An inertial navigation system measures velocity by integrating the outputs of accelerometers whose sensitive axes are directed along the axes of a three-dimensional coordinate system defined by the mutually orthogonal reference axes of three single-degree-of-freedom rate-integrating gyros. The gyros and accelerometers are mounted in a structure which is isolated from the roll, pitch and azimuth motion of the vehicle by servo controlled gimbals. This configuration is called an inertial platform. Synchros or resolvers on the gimbal axes provide a direct measure of vehicle attitude with respect to the platform. If the platform is maintained level with respect to the Earth only two accelerometers are generally required to perform the basic navigation function in the horizontal plane. The comments relative to the three-dimensional Doppler apply as well to the three-dimensional inertial system.

It should be pointed out that since the accelerometers measure acceleration with respect to inertial space, their integrated outputs give velocity with respect to inertial space. It is necessary, therefore, to correct for the effect of Earth's angular velocity in order to obtain ground velocity for navigation over the Earth's surface.

The gyros will sense any tendency of the platform to change its orientation in inertial space, and electrical pickoffs on the gyro sensitive axes provide signals to the gimbal servos to return the platform to its original attitude. If the gyro sensitive axes are torqued at the proper rate, a platform whose plane was originally tangent to Earth's surface can be maintained tangent as the vehicle is translated over the surface of the Earth. Furthermore, if one of the gyro reference axes originally pointed north, this axis can be maintained north. An inertial system can thus provide a heading reference and a vertical reference as well as velocity.

It can be shown that the proper torquing rates to keep a platform level and to keep the reference coordinate axes respectively pointed east, north and up along the vertical are

$$\omega_E = -\frac{V_N}{R} = -\frac{V_{IN}}{R} \qquad [1]$$

$$\omega_N = \frac{V_E}{R} + \omega_e \cos\lambda = \frac{V_{IE}}{R} \qquad [2]$$

$$\omega_z = \frac{V_E}{R}\tan\lambda + \omega_e \sin\lambda = \frac{V_{IE}}{R}\tan\lambda \qquad [3]$$

where

$\omega_E, \omega_N, \omega_z$ = torquing rates supplied to the east, north and heading gyros, respectively
ω_e = Earth's angular velocity (assumed uniform)
V_{IE}, V_{IN} = east and north components, respectively, of vehicle linear velocity with respect to inertial space
R = Earth's radius (Earth assumed spherical)
λ = latitude of the vehicle
V_E, V_N = east and north components, respectively, of vehicle linear velocity with respect to the Earth

In these equations it has been assumed that the vehicle altitude above the Earth's surface is small compared with the Earth's radius.

It is well to remark at this point that in many applications the heading gyro is left untorqued and the platform is not slaved to north. The heading is then computed from initial heading plus the integral of the rate given by Equation [3]. The north slaved configuration has been chosen for this discussion because it is easier to understand.

It may also be shown that the outputs of the east and north accelerometers for a platform torqued at the rates given by Equations [1, 2 and 3], if the platform is leveled so that its plane is normal to the local vertical, are

$$a_E = PV_{IE} - (V_N V_{IE}/R)\tan\lambda \qquad [4]$$

$$a_N = PV_N + (V_{IE}^2/R)\tan\lambda - R\omega_e^2 \cos\lambda \sin\lambda \qquad [5]$$

where $P = d/dt$. It has been assumed here that the vehicle is traveling at constant altitude above the Earth's surface.

The second terms on the right sides of Equations [4 and 5] are Coriolis accelerations, and the third term on the right of Equation [5] is a centripetal acceleration. These terms can be computed and subtracted from the accelerometer outputs. Assuming this is done, it is clear that the resultant term on the right side of Equation [5], if integrated and divided by R, can be used to torque the east gyro according to Equation [1]. The resultant term on the right side of Equation [4], if integrated and divided by R, can be used to torque the north gyro according to Equation [2]. Furthermore, since

$$V_N/R = P\lambda \qquad [6]$$

if the north accelerometer output is integrated twice and divided by R, it is possible to use the resulting value of λ to derive the heading gyro torquing rate (Eq. [3]), and to compute the centripetal and Coriolis accelerations to correct the accelerometer outputs. In addition, the vehicle longitude can be derived from the relation

$$\frac{V_{IE}}{R}\sec\lambda - \omega_e = P\phi \qquad [7]$$

where ϕ is vehicle longitude. Fig. 1 is a block diagram of the inertial navigation system just described.

The pure inertial system provides an accurate and simple means of obtaining velocity, heading, position and vertical references. Furthermore, the velocity instantaneously indicated by the system does not suffer the degree of dynamic lag which is characteristic of the Doppler radar indicated velocity. There are, however, some important disadvantages. To see what these are will require a more detailed analysis of a closed loop containing an accelerometer, a velocity integrator and a gyro. Such a loop is called a Schuler loop, and a thorough understanding of it is necessary as a reference point from which to consider the combined Doppler-inertial system.

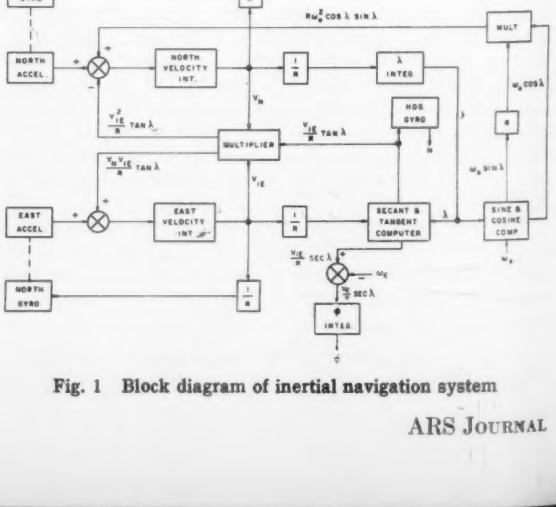

Fig. 1 Block diagram of inertial navigation system

Schuler Loop

In the material presented thus far, no consideration has been given to what happens when there is an error in the vertical (i.e., when the platform is not level). Nor has any consideration been given to the effects of gyro drift, accelerometer error and instrumentation errors in the computations. An error in the vertical will cause a component of g the gravitational acceleration to appear in the accelerometer outputs. This component when integrated will lead to an error in velocity and subsequently to errors in the gyro torquing rates, the heading and the position. Gyro drift and errors in computation of Earth rate lead to errors in the torquing rates and the ground velocity, respectively. Accelerometer errors have the same effect as a gravity component. These errors or noises are shown in Fig. 2, which is a more detailed block diagram of the Schuler loop containing the east gyro, the north accelerometer and the north integrator.

The dynamics of the problem have been shown on the block diagram of Fig. 2. It has been assumed that μ, the error in the vertical, is small, so that the component of g in the accelerometer output can be approximated by $g\mu$.

The equations which describe ϵV_N, the error in north velocity, and μ may be derived as follows:

1 The error in the torquing rate to the gyro is equal to the rate of change of the error in the vertical. This may be expressed as

$$-\frac{V_N + \epsilon V_N}{R} + N_G + \frac{V_N}{R} = P\mu \quad \text{or} \quad -\frac{\epsilon V_N}{R} + N_G = P\mu \qquad [8]$$

where N_G is gyro drift rate.

2 The integrated accelerometer output is equal to the north component of velocity plus the error in the north component of velocity. This may be expressed as

$$PV_N + g\mu + N_A = P(V_N + \epsilon V_N) \quad \text{or} \quad g\mu + N_A = P\epsilon V_N \qquad [9]$$

where N_A is the accelerometer error.

3 If Equations [8 and 9] are solved for μ and ϵV_N, the result is

$$[P^2 + (g/R)]\epsilon V_N = gN_G + PN_A \qquad [10]$$

and

$$\left(P^2 + \frac{g}{R}\right)\mu = PN_G - \frac{N_A}{R} \qquad [11]$$

Equations [10 and 11] indicate the basic difficulties with a pure inertial system. It will first be noticed from the left sides of Equations [10 and 11] that there is no damping term inherent in the system. Consequently, initial errors in velocity will persist indefinitely and oscillate with a period given by

$$T_S = 2\pi\sqrt{R/g} \qquad [12]$$

T_S is the so-called Schuler period (approximately 84 min), and an inertial system with this period is said to be Schuler tuned. Even if there are no initial errors in vertical and velocity, the gyro and accelerometer noises on the right side of Equations [10 and 11] act as forcing functions causing oscillations to occur and errors in velocity and vertical. It is also clear that a Schuler tuned pure inertial system cannot be leveled from a cold start in a moving vehicle due to the absence of initial velocity information, and that velocity and vertical errors, while oscillating at the Schuler frequency, must continually increase in amplitude due to imperfections in instrumentation. In addition, the increasing error in the torquing rate to the heading gyro, coupled with heading gyro drift rate, contributes to the ever increasing rate of buildup of position error.

It can be said, then, that a Schuler tuned pure inertial system has good high frequency characteristics and poor low frequency characteristics in its response to changes in velocity. It is apparent that some form of damping is needed, and an obvious choice is to try feedback around the velocity integrator.

Self-Damped Inertial System

Fig. 3 is a block diagram of the Schuler loop with degenerative feedback through a gain γ added at the input of the velocity integrator. By the methods used in the previous section, the equations for the error in the velocity and the vertical are found to be

$$[P^2 + \gamma P + (g/R)]\epsilon V_N = gN_G + PN_A - \gamma PV_N \qquad [13]$$

and

$$\left(P^2 + \gamma P + \frac{g}{R}\right)\mu = (P + \gamma)N_G - \frac{N_A}{R} + \frac{\gamma}{R}V_N \qquad [14]$$

The loop now has damping, and the platform can be leveled, after a fashion, in a moving vehicle. However, the loop is dynamically inexact. That is, the steady-state errors are functions of velocity and acceleration. The steady-state errors assuming the vehicle undergoes a uniform acceleration a (i.e., $V_N = V_{NO} + at$), are

$$\epsilon V_{N_{s.s.}} = R\bar{N}_G - \gamma Ra/g \qquad [15]$$

$$\mu_{s.s.} = \frac{\gamma R}{g}\bar{N}_G - \frac{\bar{N}_A}{g} + \frac{\gamma}{g}V_{NO} + \frac{\gamma}{g}at \qquad [16]$$

where $\bar{N}_G$ and $\bar{N}_A$ are the bias values of gyro drift rate and accelerometer error. It can be seen from Equations [15 and 16] that an acceleration will cause a lag in the velocity and the vertical, and that even a uniform velocity will cause a lag in the vertical. The latter error can be removed by replacing γ with a high pass filter, but the acceleration dependent error cannot be removed.

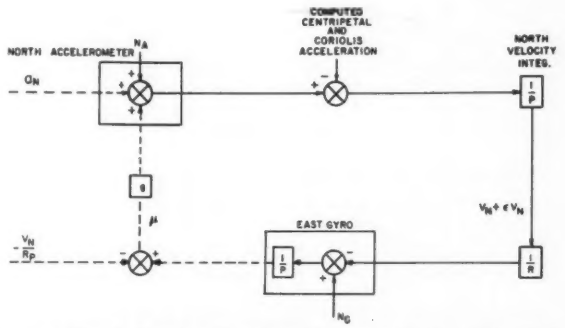

Fig. 2 Block diagram of Schuler loop showing dynamics and noise sources

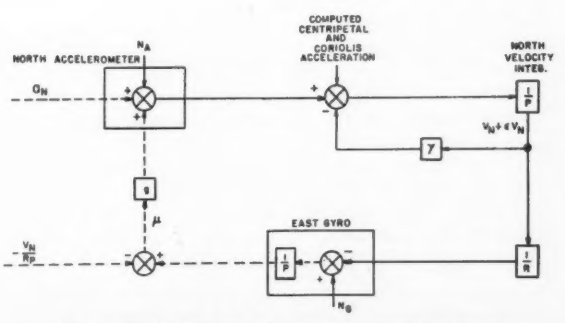

Fig. 3 Block diagram of self-damped Schuler loop

Apparently damping from an external source of velocity is required.

Second-Order Doppler-Inertial System

Fig. 4 is a block diagram of one loop of a Doppler-inertial system. As can be seen from the figure, the inertially derived and Doppler derived velocities are compared and the difference signal fed back around the velocity integrator for damping. For reasons which will become apparent, the difference signal is also amplified and fed to the gyro torquer. Since this changes the natural period of the loop, it is called tuning. The velocity output of the system is taken at the output of the velocity integrator. The equations for errors in velocity and vertical are

$$\left[P^2 + \gamma P + (1 + \alpha)\frac{g}{R}\right]\epsilon V = gN_G + PN_A + \left(\gamma P + \alpha\frac{g}{R}\right)N_D \quad [17]$$

and

$$\left[P^2 + \gamma P + (1 + \alpha)\frac{g}{R}\right]\mu = (P + \gamma)N_G - \frac{(1 + \alpha)}{R}N_A + \frac{(\alpha_P - \gamma)}{R}N_D \quad [18]$$

where N_D is Doppler error.

It can be seen from Equations [17 and 18] that damping is now inherent in the system and that the errors in velocity and vertical are not subject to lags caused by aircraft motion (i.e., the system is dynamically exact). Furthermore, the presence of the damping implies that the platform can be erected or leveled from a cold start while airborne. This last is possible

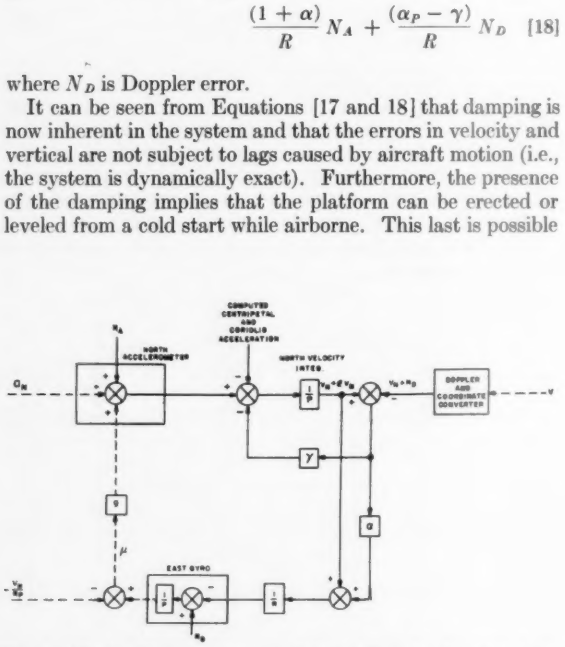

Fig. 4 Block diagram of second-order Doppler-inertial loop

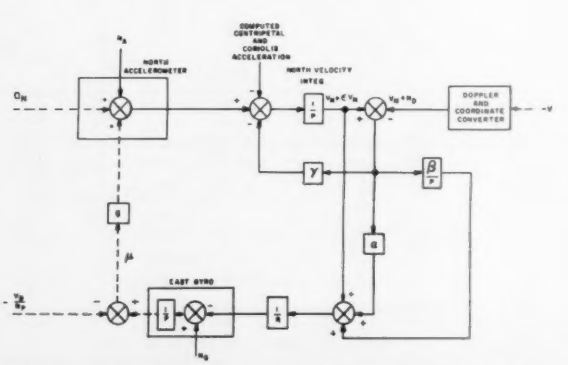

Fig. 5 Block diagram of third-order Doppler-inertial loop

because the Doppler radar, which makes an independent direct measurement of ground velocity, supplies initial conditions to the velocity integrator outputs.

The bias errors in the output, or Doppler inertially derived velocity, and in the vertical reveal a bit more about a second order Doppler-inertial system. These errors are found to be

$$\overline{\epsilon V} = \left(\frac{R}{1 + \alpha}\right)\bar{N}_G + \left(\frac{\alpha}{1 + \alpha}\right)\bar{N}_D \quad [19]$$

and

$$\bar{\mu} = \left[\frac{\gamma R}{g(1 + \alpha)}\right]\bar{N}_G - \frac{\bar{N}_A}{g} - \left[\frac{\gamma}{g(1 + \alpha)}\right]\bar{N}_D \quad [20]$$

from which it can be seen that by proper choice of α and γ the bias errors in velocity and vertical caused by bias gyro drift and Doppler velocity bias error may be minimized. For example, if the steady gyro drift rate is large compared to the bias error in Doppler measured velocity, the choice of a relatively large value of α will tend to minimize the bias error in output velocity.

Third-Order Doppler-Inertial System

A third-order Doppler-inertial configuration is shown in Fig. 5. This loop differs from the second-order loop of Fig. 4 in that the difference between the two velocities, besides being used for tuning and damping, is amplified, integrated, and added to the gyro torquing rate. The equations for the errors in velocity and vertical for the third-order system are

$$\left[P^3 + \gamma P^2 + \frac{g}{R}(1 + \alpha)P + \beta\frac{g}{R}\right]\epsilon V = gPN_G + \left(\gamma P^2 + \alpha\frac{g}{R}P + \beta\frac{g}{R}\right)N_D + P^2N_A \quad [21]$$

and

$$\left[P^3 + \gamma P^2 + \frac{g}{R}(1 + \alpha)P + \beta\frac{g}{R}\right]\mu = (P^2 + \gamma P)N_G + \left[\frac{\alpha P^2}{R} + \frac{(\beta - \gamma)P}{R}\right]N_D - \left[\frac{(1 + \alpha)P}{R} + \frac{\beta}{R}\right]N_A \quad [22]$$

The bias errors for the third-order system are

$$\overline{\epsilon V} = \overline{N_D} \quad [23]$$

$$\bar{\mu} = -\overline{N_A}/g \quad [24]$$

It can be seen from Equations [23 and 24] that the extra integrator has functioned to cancel the bias gyro drift from the velocity and both gyro and Doppler bias from the vertical. This configuration is very useful when the gyro bias is large compared to the Doppler bias.

The third integrator output, which in Fig. 5 is added to the gyro torquing terms, could instead be added to the Doppler output. When this configuration is used, it will be found that the Doppler bias no longer appears in the output velocity bias error. In its place, the gyro drift bias appears. The vertical bias error is unchanged. This configuration is useful if the gyro bias is small compared to the Doppler bias.

Doppler-Inertial Compass

It was pointed out briefly that velocity error and heading gyro drift rate would produce an increasing error in heading. However, thus far no mention has been made of a means of correcting or bounding this heading error. It turns out that a Doppler-inertial system provides such a means.

An inertial system determines the velocity of the vehicle with respect to inertial space. A Doppler radar determines velocity with respect to the rotating Earth. The two velocities differ, therefore, only by the eastward velocity of the

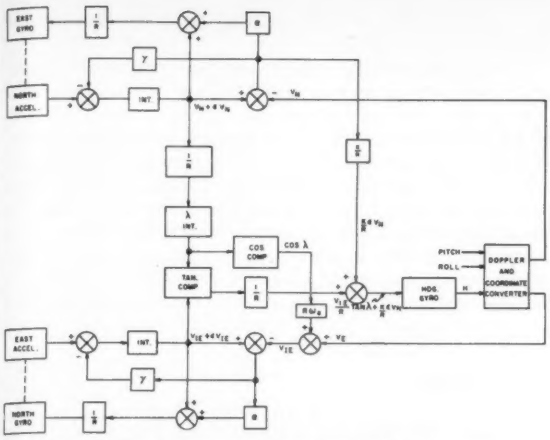

Fig. 6 Block diagram of Doppler-inertial compass

point on the Earth directly below the vehicle. It follows that the north components of the two velocities should be identical. Any difference which actually exists between the north components of the velocities reported by the two systems can be attributed to an error in heading plus errors contributed by the noise sources. If the difference signal between the two north velocity components is amplified and added to the heading gyro torquing rate, the error in heading can be reduced to a value determined by the system noise sources. Fig. 6 is a block diagram of a Doppler-inertial system in which a Doppler-inertial compass interconnection has been made. The Coriolis corrections and the longitude computation have been omitted for the sake of clarity. These are the same as in Fig. 1.

No attempt has been made here to give an analysis of the heading loop in a Doppler-inertial compass. The dynamic coupling between the vertical and the heading in the general case leads to a set of differential equations with time variable coefficients which are more difficult to handle than the simple linear equations discussed thus far. A detailed analysis is consequently a large subject in itself and requires more space than is available here. An approximate formula for the bias error in heading is given for reference, however. This is

$$\overline{\epsilon H} = \frac{1}{\omega_e \cos \lambda}\left[\bar{N}_{GE} + \frac{\bar{N}_{DN}}{R} + \frac{(1+\alpha)}{K}\bar{N}_{GH}\right] \qquad [25]$$

where

$\overline{\epsilon H}$ = bias heading error, radians
$\bar{N}_{GE}$ = east gyro bias drift rate
$\bar{N}_{DN}$ = north component of Doppler velocity bias error
$\bar{N}_{GH}$ = heading gyro bias drift rate
α, K = system parameters (see Fig. 6)

Equation [25] indicates that for a given latitude the bias error in heading is bounded by the north component of Doppler error, east gyro bias drift rate, and heading gyro drift rate to an extent dependent upon system parameters. As latitude increases, however, the bias error increases and there will be a practical upper latitude limit beyond which the Doppler-inertial compass ceases to be useful, as such. It is, however, possible to use a Doppler-inertial compass interconnection up to a given latitude and then go into an untorqued heading gyro mode of operation. If an integrator has been placed in the heading loop during the Doppler-inertial compass mode, it will serve to cancel out the error due to heading gyro bias drift rate. If the integrator is left connected to the heading gyro after the loop is opened, the bias will continue to be compensated, and only the heading gyro random drift rate will contribute to the error.

Three-Dimensional Doppler-Inertial Systems

The preceding sections have concentrated on interconnections of two-dimensional inertial and Doppler systems. The same basic approach may be applied to synthesize a Doppler-inertial interconnection in the vertical axis as well as in the horizontal axes, and the benefits are similar. The high frequency vertical velocity components are accurately measured by the vertical accelerometer, whereas the long-term error is bounded by the Doppler. Bounding of the velocity error is particularly important because of the excessive error obtained in a pure inertial system due to accelerometer bias and errors in the computation of gravity, which enter the vertical acceleration computation at full value.

With increasing need for three-dimensional dynamic and position information, there will be a corresponding increase in applications for complete three-dimensional Doppler-inertial systems.

Optimal Design

The choice of the best configuration for the Doppler-inertial interconnection is generally made from among the three basic forms that have been presented, all of which are dynamically exact.[1] These are:

1 Second-order damped and tuned system.
2 Third-order system that compensates for Doppler velocity bias error.
3 Third-order system that compensates for gyro bias drift rate.

The appropriate interconnection for a given platform and a given Doppler is suggested in most cases by a comparison of the relative magnitudes of their respective bias errors. The comparison is straightforward, i.e., 1 knot of Doppler bias is equivalent to 1 arc min per hr, or $\frac{1}{60}$ deg per hour, of gyro bias drift rate. If the sensors are roughly equivalent in accuracy by this standard, the second-order system would be a logical first choice since there is little gained in going to the more complex third-order interconnection. On the other hand, one sensor may contribute an error several times larger than the other, which may justify use of one of the third-order configurations. Inasmuch as present-day Dopplers have bias errors of 1–2 knots, or 0.02–0.03 deg per hr, their performance has been equal to or superior to most gyros, and the third-order system that compensates for gyro drift and the second-order system have found widest application.

The choice of values for the damping, tuning and third-order integrator gains in the combining equipment is based on consideration of the transient response to disturbances, particularly errors in the inertial system's initial conditions, and consideration of the effects of system noise and bias errors on the outputs.

Regarding the transient response, it is desirable that the initial errors be reduced to the noise level in a short time and with a minimum of oscillation. With respect to noise and bias errors, the effects must be held to a minimum. Of course these objectives are conflicting in that fast response implies noise amplification, and hence some compromise is indicated. The effects of this tradeoff on final performance can be minimized by providing one or two fast slew modes in which initial condition errors are quickly reduced to reasonable levels before switching to the final, relatively slow mode.

With the provisions for initial erection and alignment slewing modes included, one may then proceed to choose the optimum parameters with emphasis on system noise and bias errors, subject now to the restriction that the system be relatively well-damped, rather than both well-damped and fast.

The main sources of noise and bias errors in a well-designed system are the Doppler velocity measurement, the drift rate

[1] Study of nondynamically exact systems indicates there is probably no practical advantage in a configuration more general than one which is dynamically exact.

of the gyros and the accelerometer output. The distinction between noise and bias errors, for the purposes of analysis, is made as follows: Bias errors are those which are essentially constant for periods much longer than the response time of the system; noise errors are those which fluctuate in time periods less or comparable to the system response time.

The effects of bias errors on system outputs are rather simply related to system parameters, as indicated in the previous development, and in many cases the nature of the interconnection is such that the effects are completely independent of the choice of parameters. It is at this point, namely consideration of bias errors, that the analysis of an inertial system by itself or a Doppler by itself quite often ends, because the bias errors are generally so far above the noise level that they are the significant factors in system performance. In the Doppler-inertial case, however, a particular bias error may have little or no effect on the outputs, and consideration of the noise becomes important if one desires to obtain near optimum performance and take full advantage of the potential accuracy of the Doppler-inertial system.

The noise generated by the Doppler, gyros and accelerometers is properly treated as a random quantity in each case. The Doppler velocity measurement is inherently a statistical process, as has been mentioned previously, and one would expect a more or less completely random error.[2] The fluctuations in gyro drift rate, although related to quite specific mechanical and temperature effects, are so variable and indeterminate that a statistical approach is also required. The situation is comparable for an accelerometer.

The technique of handling statistical variables in linear systems has been well developed and, although the relation between output error, system parameters and noise is more complicated than in the case of bias errors, results can be obtained in a straightforward manner. Briefly, one must know the amplitude of the input noise power as a function of frequency, that is the power spectrum, or know the autocorrelation function of the noise. Both characterizations of the noise contain the same information, and one may be derived from the other by Fourier transformation.

Most physical processes generate random noise power spectra which are constant at low frequencies and exhibit decreasing amplitude at higher frequencies. The decay of the Doppler and accelerometer random noise occurs at such high frequencies that the spectra may be assumed flat over the low frequency range applicable to Doppler-inertial systems, and the noise calculations are simplified. The gyro drift rate spectrum, on the other hand, often decays at frequencies comparable to the natural frequency of the Doppler-inertial system, and the calculations as a result are somewhat more complicated.

The power spectra or autocorrelation function data for the sensing elements can be obtained by computation from strip chart data taken during bench tests of the sensor equipment. For lengthy tests the computation is best accomplished by an automatic calculator. The noise measurements on the Doppler can be obtained by suitable flight tests as well to provide more realistic data, but this approach is practically excluded for the inertial elements.

The output error due to noise and bias error inputs is generally expressed as an rms amplitude and is computed for a variety of system parameters, the choices of which are subject to the restraint of a well-damped transient response. Optimum constants may be chosen, for example, based on the criterion of a minimum for the root-sum-square of the errors due to all sources. The group of parameters which minimizes the error in vertical will not usually be the same group which minimizes the error in velocity or in heading, but for an appropriate selection of the basic configuration, a choice of parameters can be made which is very nearly optimum for all outputs of interest.

[2] This statement must be qualified at the higher frequency ranges, but is appropriate for the limited bandwidth of a D.I. system for optimization purposes. Circuit design must of course take into account the full spectrum including periodic noise associated with switching and demodulation to avoid saturation effects.

Bibliography

1 James, H. M., Nichols, N. B. and Phillips, R. S., "Theory of Servomechanisms," MIT Radiation Laboratory Series, vol. 25, McGraw-Hill Book Co., Inc., 1947, pp. 262–370.

2 Greenwood, I. A., "The Theory of Combined Doppler-Inertial High-Precision Navigation Systems," Internal Technical Rep. no. 150, May 10, 1951, General Precision Laboratory, Inc., Pleasantville, N. Y. (*Confidential*)

3 Blumenthal, I. S., "Design of a Two-Integrator Doppler-Inertial Track-Keeper," Northrop Aircraft Co. Memorandum, March 7, 1952. (*Confidential*)

4 Clemens, J. E., Kerris, W. and Waxelt, F., "Navigational Systems Combining Inertial and Ground Velocity Vector Information," WADC Technical Rep. 52-76, April 1952. (*Confidential*)

5 Goldman, C. C. and Hayden, M. L., "Linearly Combined Doppler-Inertial Navigation Systems," WADC Technical Rep. 52-120, June 1952. (*Confidential*)

6 Armstrong, J. W. and Dodd, J. M., Jr., "Doppler-Inertial Mixing Systems," Convair Rep. no. FZA-4-089; contract no. AF 33(038)-21250, April 30, 1953. (*Secret*)

7 Interim Engineering Report no. 2, Phase 2, Sept. 12, 1952–May 2, 1953, Advanced Electronics Center, General Electric Co., Ithaca, N. Y.; contract no. AF33(600)-9248, May 15, 1953. (*Confidential*)

8 Taylor, J. E. and Lang, P., "Doppler-Inertial Navigator, Model 1," Final Engineering Rep. (Rep. no. 100R4), M. Ten Bosch, Inc., Pleasantville, N. Y.; contract no. a(s)53-230-6, Nov. 30, 1953. (*Confidential*)

9 Yachter, M., "Generalized Optimum Transfer Function of a Linear Doppler-Inertial System," High Speed Electronic Automatic Ground Position Indicator, Engineering Rep. A14-7 for Feb. 18, 1954 to April 18, 1954, Part 5, pp. 1–15, General Precision Laboratory, Inc., Pleasantville, N. Y.; contract no. AF33(616)-435, June 10, 1954. (*Confidential*)

10 Hall, B. A. and Zweig, F., "Doppler Inertial Navigation," Twentieth Progress Report, General Precision Laboratory Research, SAR/AF33(616)-435-GPL-PO-52495, Dunham Laboratory, Yale University, New Haven, Conn., May 1955. (*Confidential*)

11 Berger, F. B. and Heath, W. H., "Doppler-Inertial Systems: Basic Principles, Characteristics and Their Applications to Bombing," Internal Rep. no. 160, May 2, 1955, General Precision Laboratory, Inc., Pleasantville, N. Y. (*Confidential*)

12 "High Speed Electronic Automatic Ground Position Indicator," Phase II Final Rep., vol. 1, General Precision Laboratory, Inc., Pleasantville, N. Y.; contract AF33(616)-435, Oct. 24, 1955. (*Confidential*)

13 "Study of Inertia—Velocity Navigation Systems," Phase I Final Engineering Rep., Oct. 15, 1954, Phase II Final Engineering Rep., Dec. 31, 1955, New York University, College of Engineering; contract no. AF33-(616)-2291. (*Confidential*)

14 "Development Program for Inertial Extrapolator," Sperry Gyroscope Final Engineering Rep. no. 5297-2305-22; contract no. AF33(038)-15636, July 1956. (*Secret*)

15 "Study of a Doppler-Inertial Subsystem," General Precision Laboratory, Inc., Pleasantville, N. Y.; contract no. AF33(600)-31315, IBM P.O. W-17387-299, Nov. 1956. (*Secret*)

16 Stevens, F. and Lynch, F. W., "Aids to Inertial Navigation," Institute of Aeronautical Sciences, Nov. 1957. (*Unclassified*)

17 "Feasibility and Flight Test Program," Interim Engineering Rep. I, Sept. 11, 1956 to March 15, 1957, Interim Engineering Rep. II, March 16, 1957 to Jan. 5, 1958, Final Engineering Report, Sept. 11, 1956 to Oct. 24, 1958, General Precision Laboratory, Inc., Pleasantville, N. Y.; contract no. AF33(600)-31315, IBM P.O. no. W-12573-525. (*Secret*)

18 Cole, R. D., "Inertial and Doppler-Inertial Navigation, Fixed-Pole System," Naval Ordnance Test Station, China Lake, Calif., NOTS TP2057, NAVORD Rep. no. 6376, June 19, 1958. (*Confidential*)

19 Cole, R. D. and Seeley, R., "Inertial and Doppler-Inertial Navigation, Free-Azimuth System," Naval Ordnance Test Station, NOTS TP2058, NAVORD Rep. no. 6377, July 10, 1958. (*Confidential*)

20 Duncan, D. B., "Combined Doppler Radar and Inertial Navigation Systems," *Navigation*, vol. 6, no. 5, Spring 1959, pp. 321–327.

Infrared Tracking

R. W. POWELL

Aerojet-General Corp.
Azusa, Calif.

The state of the art of infrared tracking and range detection capability is reviewed. Particular emphasis has been placed upon the rapid advance made in recent years. The improvement of cell detection in larger wave length range and resultant higher scan speeds is examined. New optical materials and systems are treated. The development of space filtering is discussed.

AT THE present state of man's knowledge, the long range detection and tracking of airborne and spaceborne objects is accomplished almost exclusively with electromagnetic radiation—visible light, radio (or radar) and infrared (or "heat") radiation. Of the three, visible light and radiofrequency radiation were the most widely used in long range detection equipment before World War II. Before this, the exploitation of infrared radiation for this purpose proceeded slowly, owing to the lack of a suitable detector. Early infrared detection equipment was too slow and insensitive to be very useful. However, near the end of World War II, new types of infrared detectors were developed which largely overcame the earlier problems. The ranges achieved were a small fraction of those that have been achieved in the last few years. There are two major reasons for this.

First, the objects of interest are flying faster and higher. We are now looking for Mach 2.0 and Mach 3.0 targets, as well as various ballistic missiles. To attain these increased speeds, extreme amounts of power are needed. This results in increased heat, which greatly increases the ranges that can be obtained with passive infrared equipment. For example, the radiation from an intercontinental ballistic missile may be a million times the infrared radiation of a subsonic aircraft, with the higher speed aircraft somewhere in between. The greater altitudes of today result in considerably less scattering and absorption of the radiated energy.

The second reason is that recent advances in the state of the art have resulted in equipment of much greater performance. The improvements have been mainly concerned with the following.

1 Modern detectors respond to longer wave lengths than did the early postwar detectors, and, since they have greater information capacity, they are able to scan at higher speeds. Not only is there generally more energy being radiated from most targets at the longer wave lengths, but the interference from the background is considerably reduced. Part of the detector development program has been concerned with the development of very small cooling systems which are required to maintain the new types of longer wave length responding detectors at required operating temperatures of −78 to −269 C.

2 New refracting materials of excellent transmission and low dispersion have become available. They make high efficiency, catadioptric systems feasible, and provide materials for high transmission windows required for environmental protection. Some of the new materials have excellent physical properties.

3 In order to obtain optimum, spectral pass bands for best transmission of target energy in the presence of background radiation, new absorption filter materials and interference filter techniques of high transmission efficiency and sharp cutoff are available.

Received July 30, 1959.

4 Not only is background interference being reduced by choice of wave length, but advantage is being taken of the different spatial characteristics of the target, as compared to the background. Since the target at a distance is very small and background objects are relatively large, cross correlation of the image plane with a finely spaced grid pattern or reticle results in background discrimination based on spatial relationships. This technique of "space filtering" has been developed to a high degree.

5 Improved optical systems using aspheric techniques reduce the number of elements. This increases the efficiency and provides the very fine image quality required for the very fine grid patterns of the space filters. New techniques of scanning have produced much higher efficiencies.

6 The importance of infrared in many applications permits the use of relatively large size optical systems in comparison to those permitted earlier. This is because many of the early systems were in the category of retrofit. Today, the carrying equipment is being designed with the infrared equipment installation requirements in mind.

Long range detection systems are either cooperative (with the detected equipment carrying a beacon to aid the detection station) or noncooperative (with no special provisions made in the detected equipment to aid the detector). Of course, in military equipment, extensive measures are taken to make detection by the enemy difficult.

An example of a cooperative system is found in the use of running lights on automobiles, boats and aircraft to aid in the detection by the human eye and prevent collision with another vehicle at night. Part II of Fig. 1 is a block diagram of a typical cooperative system that may use either visual, radio or infrared wave lengths.

Noncooperative detection is more difficult. However, it is more reliable, even in nonmilitary applications, since beacon failure ruins any cooperative system. Part IA of Fig. 1 shows that noncooperative visual equipment is semi-active—i.e., the detection set requires an external beacon, such as the sun or a searchlight, to illuminate the target.

Noncooperative radio or radar equipment may be either semi-active or fully active. As shown in Part IB of Fig. 1, most radar equipment is fully active—i.e., the detection set "sees" the target by detecting the target reflected energy that originally was emitted by a beacon near the detector and interconnected to it. In fact, most radar sets use the same antenna to transmit the beacon energy and to receive the reflected signal.

One of the unique features of infrared detection is that it is entirely passive—i.e., it can operate by detecting the self-emitted radiation of the target (see Part IC of Fig. 1). All objects above absolute zero in temperature emit infrared radiation in varying intensities and at varying wave lengths, depending upon their temperature and their surface characteristics. Except in a few special cases, very little visible or

radar energy is emitted. So, infrared detection can be considered the only passive method of detection.

Performance Criteria

Several characteristics can be used to express the performance of an infrared system. In military equipment, where the most important factor is long detection ranges, the ability of the equipment to detect the target in the presence of noise determines performance. In other words, the major criterion is the minimum signal that can be detected. Since this is almost always limited by extraneous signals (noise) that mask the desired signal, the important factor, then, is the ratio of the signal to the noise instead of the output response produced by the signal.

Because of the very short wave length involved, infrared systems are not bothered by the most troublesome noises of radar, such as angle noise. Side lobes are virtually nonexistent in well-designed infrared systems. The noise is generally due to two separate effects. System noise is noise distributed in time. It may be due to noise generated in electronic circuitry, in mechanical vibration or by servo systems. In well-designed systems, most system noise is generated in the detector.

A second source of noise is due to radiation gradients in the atmosphere, the sky or the Earth background on which the desired target is tracked. These gradients are either the result of direct emission, or reflection and scattering of solar energy. Although there are relatively slow temporal variations (particularly in the turbulent atmosphere and hydrosphere), the primary characteristic of the background is that it is distributed in space.

Neglecting the background noise for a moment, the range achievable by an infrared system of spectral response $\Gamma_{(\lambda)}$, observing a target of spectral radiant intensity $J_{(\lambda)}$, through an atmosphere of transmission $t_{(\lambda,s)}$, is expressed by the following equation for systems that perfectly cancel signals caused by background and reticle radiant emittance

$$\frac{S}{N} N_{(\omega)} = V_{(\omega)} = \frac{RA}{s^2} \int_0^\infty J_{(\lambda)}\, t_{(\lambda,s)}\, \Gamma_{(\lambda)}\, d\lambda$$

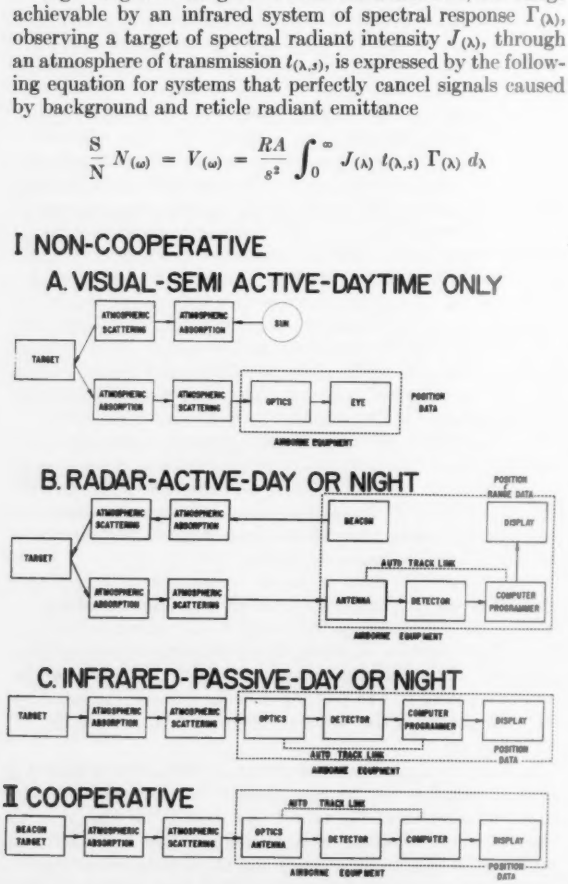

Fig. 1 Detection systems

where

- S/N = required signal-to-noise ratio
- N = rms noise within the pass band referred to the detector
- V = rms signal out of the detector within the pass band
- R = proportionality constant of the normalized responsivity of the detector in volts rms per watt of radiant flux in the scanning system used
- A = area of the aperture
- s = range to the target
- λ = wave length of radiation

Although this equation is complicated by the fact that the transmission $t_{(\lambda,s)}$ is a complex function of range due to differential absorption and scattering of the atmosphere, it can be seen that to achieve a desired range is to vary the optical aperture, the detector parameters or the spectral pass band. This would be true in the absence of a spatially distributed background.

Because long range infrared systems are passive, there is no possibility of eliminating even distant background gradients by range gating, as with radar systems. Consequently, the background noise generally is the predominant noise in most modern, well-designed systems. Any increase in signal by such stratagems as increasing the aperture will also increase the background noise in direct proportion. Since the backgrounds vary in space, in time, in spectral characteristics and in different situations, and since a variety of different targets must be considered, the best design for different applications may vary widely.

System Noise

Terms like "noise equivalent power" (NEP) and "noise equivalent power density" (NEPD) are commonly used to express the performance of detection equipment. The NEP (or NEPD) is defined as the signal power (or power density) that will produce a signal equivalent to the noise. (The usual units are watts or watts per cm^2.) For this definition, it can be seen that these terms cover essentially the same concept as the term "resolution," which may be defined as "the least change which can be made in the input to a device and produce a measurably different output." The term "threshold" is used as a descriptive, qualitative term to express any one of the resolution-like quantities.

Because of the confusion with electrical circuit terms that occurs when the input radiant flux is spoken of as power, McFee has recommended that "noise equivalent flux" (NEF) and "noise equivalent flux density" (NEFD) are preferable to NEP or NEPD. Therefore, it is suggested that NEF and NEFD be adopted.

Inherent in the concept of threshold is the implication that the smaller the value obtained, the better the instrument. Although physicists and engineers may be able to tolerate this inverted concept, it is not easy to explain to the uninformed why a piece of equipment having a small value is better than one with a large value. Jones has suggested that the NEF (NEP) and NEFD (NEPD) terms be inverted and designated by a coined term, "detectivity."

The terms NEF, NEFD and detectivity are useful primarily as figure of merit terms for detectors. But, since most practical infrared systems involve other sources of noise and can operate usefully only at signal-to-noise ratios substantially greater than unity, the term "minimum acquisition flux density" (MAFD) has been suggested as useful for search sets. The term "minimum tracking flux density" (MTFD) has been suggested for tracking sets.

The relationship between the NEFD and the MAFD (or MTFD) of a piece of equipment is the lowest useful signal-to-noise ratio with which the equipment is operable, as defined by the equipment specification, and is also a function of the design of the information processing circuitry or servomechanism. For example, one piece of equipment produced by

Aerojet-General has a "sensitivity" specification expressed in terms of the aperture flux density that permits an average noise pulse density of $1\frac{1}{2}$ per sec. Obviously, a different specification would result in a different MAFD. A NEFD could be determined and the MAFD be obtained by multiplying by the signal-to-noise ratio required to obtain the desired subjective result. However, this would be involved and relatively profitless because the subjective result is the desired effect. A reduction in the required signal-to-noise ratio by clever circuitry would be equally as satisfactory an improvement as a reduction in the NEFD.

Defining the threshold terms is only part of the requirement of defining the performance of an infrared system. In general, the source radiation and the spectral characteristics of the receiver are broad bands which usually do not coincide. Furthermore, the atmosphere has several absorption resonances which must be computed, even for measurements over very short distances.

It has been common in the past to expose the system to the radiation of a heat source, using a short path length and a known atmospheric transmission. By knowing the temperature, the effective emissivity, and the aperture size of a blackbody (which is very hot compared to its surroundings), the total energy emitted can be directly calculated by means of the Stefan-Boltzmann law, provided the radiation pattern of the blackbody is known. Generally, the spatial radiation pattern of the blackbody furnace closely follows a cosine function for small angles off the aperture axis; hence, there is little probable error if the axis of the blackbody-furnace aperture and the optic axis of the equipment are closely aligned. If the path length is short and the equipment is not sensitive to energy falling within any of the severe atmospheric absorption bands, the response to the total radiation of a blackbody at the temperature chosen can be determined with reasonable accuracy, after corrections have been made for the existing atmospheric absorption.

However, this type of measurement cannot generally be used to predict performance. This is immediately apparent when the response of a wide band pass receiver is compared to that of a narrow band pass receiver. When a source with a broad energy spectrum (such as a blackbody furnace or an emissive liquid or solid) is viewed, the broad band pass system can yield the greatest response. However, the broad band pass system could easily be much less effective than the narrow band pass system for practical application: (a) because targets, in general, do not radiate like a blackbody, (b) because of greater and different atmospheric absorption, and (c) because the background radiation conditions will probably create considerably more noise in the wide pass band system. It is clear that rating the threshold of a system in terms of the total radiation at any blackbody temperature usually gives a poor criterion of performance.

In an attempt to provide a better criterion of performance, the concept of "equivalent" or "effective" radiation has been used. With this scheme, the same measurement techniques used for total radiation are used to obtain the raw data. However, in addition to the correction for atmospheric absorption, a correction is made for the spectral response of the equipment measured.

This correction is accomplished in the following manner. A spectral-responsivity curve for the equipment is either computed from individual component characteristics or is measured by a spectrometer (the latter is by far preferable). From the response curve, the "spectral-cutoff" wave lengths are determined from the following equations

$$\lambda_1 = \lambda_p - \frac{\int_0^{\lambda p} \Gamma(\lambda)\, d\lambda}{\Gamma(\lambda p)}$$

and

$$\lambda_2 = \lambda_p + \frac{\int_{\lambda p}^{\infty} \Gamma(\lambda) d\lambda}{\Gamma(\lambda p)}$$

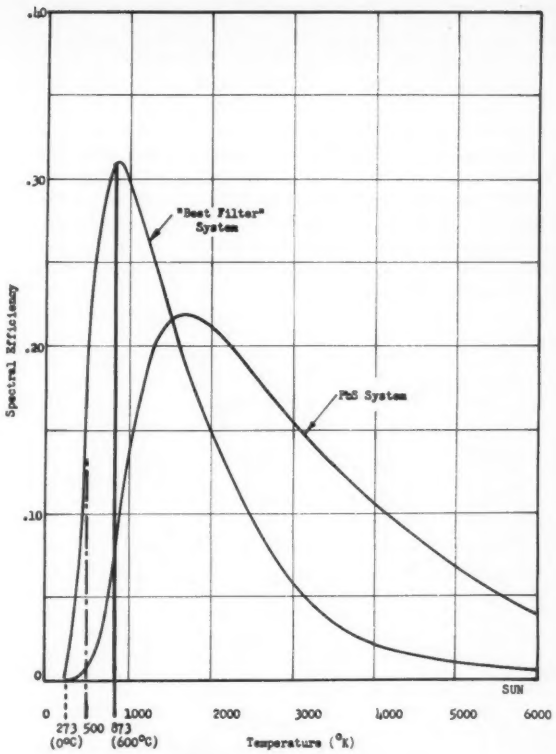

Fig. 2 Blackbody spectral efficiency

where

λ_p = wave length at the peak spectral response
λ_1 = short wave length cutoff
λ_2 = long wave length cutoff

The simplified assumption, then, is that the response of the system is equal to the peak spectral response everywhere within the spectral region between λ_1 and λ_2, and is equal to zero outside this pass band.

The effective-radiation concept is logical in case of a "white" (or flat) source spectrum $J_{(\lambda)}$ or when the source spectrum peaks near the wave length of the peak spectral response of the equipment. However, in practice, great errors are encountered due to the slopes and asymmetries and variable nature of the power spectra of the source (which almost never behave in the manner assumed in the effective-radiation concept).

The effective-radiation concept breaks down almost completely when the performance of the equipment against a single gas emission line is to be determined. In this case, the peak spectral threshold and the responsivity curve are required.

The radiant flux from a source is controlled primarily by the temperature, but it is also a function of the size of the emitter, its distance, the emissivity of a hot target and the reflectivity of a reflecting target. For example, the power in the image of a distant hot target may prove less than that in the image of a nearby or large cool object, due to image quality, reticle detail, etc. Furthermore, although a cloud scattering sunlight has essentially the 6000-K sun spectrum, it is several thousand times less bright. Because of such complexities, most experimenters think of target and background radiation in terms of watts per cm² at the aperture instead of in terms of an equivalent blackbody temperature. This concept makes a criterion based upon the efficiency of utilization of the source spectrum feasible and informative.

Fig. 2 illustrates the criterion of performance in which the ordinate is the fraction of the total blackbody radiation to which the system is responsive, and the abscissa is the temperature of the source. It can be seen that the system used in this example (hereafter called the PbS system) is most sensitive to sources having a temperature of about 1700 K, since it receives 22 per cent of the total energy at this temperature. The system does not respond to self-emission from clouds (273 K), and it is a poor receiver for low temperature targets (500 K). Although it responds much better to high temperature targets, such as modern turbojet tailpipes, it is almost as sensitive to the reflected energy of the sun; hence, it would have trouble with backgrounds.

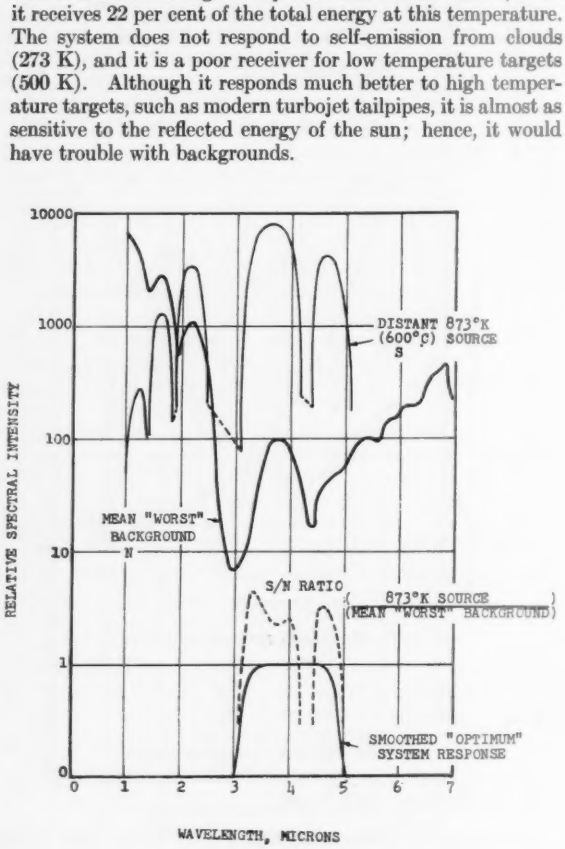

Fig. 3 Spectral design parameters

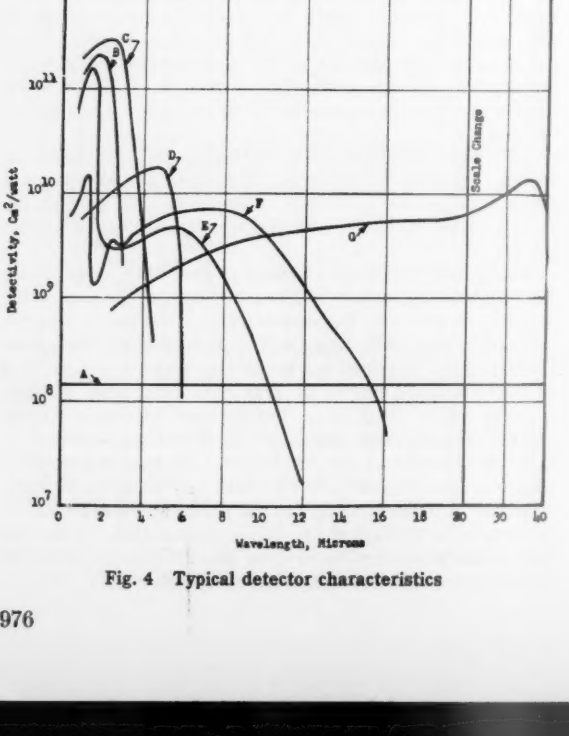

Fig. 4 Typical detector characteristics

The process of designing a receiver for the most effective detection of an 873 K (600 C) target, with maximum rejection of the background from a spectral standpoint, involves the application of Wiener's best-filter theory, as illustrated in Fig. 3. The N curve is a typical "worst"-background-gradient spectrum such as might occur in the image plane of a receiver. The S curve is the signal power spectrum that might be received from a distant source of 873 K (600 C) equivalent temperature, showing considerable atmospheric absorption. The signal-to-noise curve constructed to the Wiener criterion should yield the best filter. Smoothing this curve to a physically realizable filter, the second spectral efficiency curve of Fig. 2 is obtained, showing an expected peak of 31 per cent at an effective temperature slightly greater than peak response at 873 K.[1] Although this system is much more sensitive to cloud self-emission than the PbS curve,[2] cloud emission is still quite negligible. But of most importance is the considerably reduced sensitivity to reflected solar energy. At a glance, this can be seen to be a near optimum system for its intended purpose from a spectral point of view. However, it should be emphasized that the best design for each application depends on the operational parameters.

Until recently, however, there was no great latitude of design available. Perhaps the greatest recent advance has been in the development of a wide variety of sensitive detectors.

Detectors

Until World War II, designers of infrared equipment were forced to use thermal detectors having characteristics poorer than those shown in curve A of Fig. 4.

The invention of the PbS photoconductor detector during World War II (curve B of Fig. 4) allowed the designer considerably better sensitivity and shorter time constants than the thermal detectors shown in curve A. The major difficulty with the PbS detector was the long wave length cutoff at 3 μ. For applications involving targets similar to that shown in Fig. 3, the sulfide detector is not a good solution. Cooling the detector to the temperature of dry ice (−78 C) improved both the response and the cutoff wave length, as shown in curve C. But the time constant also greatly increased with this detector, making the cooled PbS detector difficult to use in high speed trackers. Research on the phenomenon of photoconductivity has yielded a variety of detectors having a response characteristic similar to that shown in curve D, which represents a diffuse junction indium antimonide detector cooled to −196 C, the temperature of liquid nitrogen. Slightly less sensitive are the lead selenide and the lead telluride detectors which also must be cooled to −196 C. Other work on doped-germanium-crystal detectors has resulted in detectors in the curve E class. Recently, detectors of extraordinarily long wave length characteristics, as shown in curves F and G have been developed. They require cooling to near absolute zero. One of the major advantages of this new series of detectors is that they all exhibit extremely short time constants, from $\frac{1}{10}$ to $\frac{1}{10000}$, or less, of that of the lead sulfide detector (curves B and C). To a large extent, this compensates for the lower detectivity, due to the fact that detector noise tends to diminish with frequency. Consequently, for any given application, where the pass band is fixed being a function of the information requirement, the system response is improved through using these detectors at very high modulating frequencies. Because most detector noise is generated at the terminals of the photoconductor, the

[1] The curve peaks at temperatures greater than 873 K because of the skewness of the background and the differential effects of atmospheric absorption.

[2] The greater sensitivity to low temperature objects would mean, however, that the system would be more sensitive to its own radiation; hence, more pains would have to be taken to shield the detector from moving parts to prevent a large amount of self-induced noise.

General Bronze Corp. has proposed and built a terminal-less detector which operates by detuning a microwave cavity. However, all of the newer detectors have very much lower noise voltage than that of a lead sulfide detector, making it difficult for the detector noise to predominate in a system. (Fig. 4 is based upon the comparison of signal voltage to detector noise voltage.)

Developments in physical arrangements of the detectors have also been an important factor. For example, since the signal-to-noise ratio of a detector varies inversely as the square root of the area of the detector, the ability to make very small detectors provides much greater system sensitivity where the optical system and search and tracking kinematics permit smaller detectors to be used. In this latter connection, detector manufacturers have recently been able to provide a wide variety of shapes and arrays of multiple detectors which have permitted infrared systems to search much larger fields than ever before, and to track with very much smaller fields. The result is much higher optical gains and therefore greater sensitivity.

The refractive index of most detector materials is very high. This means that the infrared energy striking the detector through air or vacuum must be at an angle near the normal to the detector surface to be absorbed. However, by forming the detector directly on an optical element, such as a condensing cone or the final element of a field lens, the change in refracting index between the optical material and the detector is much less, resulting in much lower reflection losses. Depending upon the particular optical system design, increases in detectivity of several times can be achieved by this technique known as detector immersion.

In addition to the detectors described, there are a number of others being developed which may have similar characteristics. The future development of infrared masers may greatly increase the efficiency of infrared trackers.

Although some lead selenide and indium antimonide, as well as other long wave length detectors, can operate uncooled, their detectivities are very much lower than the cooled detector. Consequently, their use is restricted to applications where the greater detectivity is not required. Consequently, the development of cooling systems has been a major factor in making long wave length detectors usable.

There are very few problems encountered in cooling when detectors are to be tested and used in the laboratory. Dry ice (CO_2) and acetone mixtures will produce temperatures of about −78 C. Liquid nitrogen can be used for cooling to lower temperatures since its boiling point is at −196 C. Again, on a laboratory basis, temperatures below −196 C can be achieved through the use of liquified neon (−245.9 C), hydrogen (−252.7 C) or helium (−268.9 C). Usually, a vacuum flask can be designed around a detector in such a manner that a reservoir of the refrigerant can be provided to maintain low temperatures. Such a flask, having double walls, would have the detector mounted on the cooled inner wall and an infrared transmitting window incorporated as part of the outer wall. Normally, if the flask is of a small size (1 in. OD × 2 in. long) the reservoir is quite small and must be used in an upright position. The best cooling time that can be expected from a glass, vacuum flask, as described, is about ½ hr. per filling.

Cooling detectors that are to be placed in infrared systems in aircraft and missile applications present an entirely different picture. The detector assembly may be buried deep within the infrared system which, in turn, may be well inside an aircraft or missile and still be capable of being cooled on demand. The equipment providing cooling must be light in weight, especially in comparison with the infrared system. The period of cooling may vary from several minutes to several days, without allowing the refrigerant to be recharged. The cooling system must be capable of operation at any altitude or temperature, or in any position an aircraft or missile may assume. Also, the detector assembly itself may be in gimbals which must not be unduly encumbered. Finally, a high degree of reliability is required.

The first approach to cooling of long wave length detectors for infrared systems came in the form of a miniature cryostat. This is a lightweight piece of equipment about the size of a standard cigarette. It consists of a length of finned metal tubing of very small size, wound around a mandrel. This assembly is inserted into a close fitting tube which makes up the inner portion of a small vacuum flask. Nitrogen gas under pressure is passed through the finned tubing toward the back of a detector. As the gas emerges from the fin tubing, it is cooled by Joule-Thomson expansion. The expanded gas is then passed back over the coil of this tubing, thereby producing regenerative cooling. Although a long period of cooling is possible by this method, the problem of contaminants in the gas is acute.

To limit the problems in the operation of a cryostat cooling system, two methods have been used. Both are designed to reduce weight and possible contamination. One system, a liquid nitrogen converter, has been used in several applications.

The second system for operating a cryostat is a closed loop unit using a noncontaminating compressor. Piston-type compressors have had their lubricants cause plugging of the cryostat. Bellows and diaphragm-type compressors have been attempted or are under development.

An alternate to the use of cryostats for cooling to −196 C is the direct, liquid nitrogen transfer system. In this technique, a well-insulated flask is used to store liquid nitrogen as well as maintain a small pressure, usually less than 15 psig. The pressure forces liquid nitrogen through a withdrawing tube which transports the liquid to the area of the detector.

Developmental work is being carried out in two new areas. These are the miniaturization of both the expansion engine and the gas liquifier. Both systems are operational and available in larger sizes. Both may be capable of cooling below −196 C.

The expansion engine is usually employed in the liquification of helium. By compressing helium gas and causing it to lose energy in expansion by doing work, its temperature is reduced. Further Joule-Thomson expansion causes liquification.

Temperatures in the range of dry ice are not particularly difficult to achieve. CO_2 passed through a small coil and cooled regeneratively, similar to the cryostat and vacuum flask configuration, produces dry ice at the rear of the detector. There have been similar techniques developed for other gases, such as freon 13, to give the same temperature range. Most of these techniques rely on the expansion of the gas, and phase change from gas to liquid, for cooling. Miniature refrigerators are also being developed using freon gases.

Peltier thermoelectric coolers have been developed giving a temperature drop of 30 to 40 deg below ambient. Through the use of different junction materials, it is expected that the temperature drop may be increased.

Optical Materials

The need for choice of wave length for each particular application requires optical transmitting materials useful in the longer wave lengths, although pure reflecting systems are not wave length sensitive. They cannot be used within the Earth's atmosphere without transmitting materials. Such materials must be used in any window, and to transmit the energy through the Dewar to the cooled detector.

However, although energy is lost at every reflecting and refracting surface as well as absorbed during transmission through the refractor, many designs (even in spaceborne applications) can be greatly improved by the addition of refracting elements. Further, in many applications the shape and size requirements make the pure refracting system the best choice. The use of catadioptric (combination reflecting and refracting optics) systems is, generally, by far the best choice for highly sensitive long range trackers. The reason this is

generally true is that in order to space-filter in favor of the target very fine image quality is required upon the reticle or space-filter. To achieve this, a large f/no. system is superior, since the image quality is better and the image is larger, making the reticle dimensions more manageable. Of course, when this is done the detector cannot be placed directly behind the space filter to collect the energy, since its large size would result in very low system sensitivity. Instead, a relay optical system or field lens is generally placed behind the reticle to collect the transmitted energy and condense it onto a very small detector. The aperture blocking losses and the difficult geometry required of field reflecting optics make it almost necessary to use a refracting system. Since good image quality is not required on the detector, extremely small f/nos. are feasible, resulting in extremely high system optical gain and system sensitivity. An added advantage of relay catadioptric optical systems is that variations in detectivity over the surface of the detector do not produce spurious modulation noises.

The optical silica glasses are generally not useful for wave lengths beyond 3 μ. Although quartz, flint, crown and special infrared silica glasses are extensively and successfully used for PbS systems, their poor long wave length transmission makes them useless for equipment designs at longer wave lengths.

The choice of transmitting materials is greatly limited beyond 3 μ. Commonly employed materials include arsenic trisulfide, silicon, sapphire, germanium, calcium aluminate and strontium titanate. Other than calcium aluminate, these show little absorption, and transmission is independent of the thickness.

Many of the materials have a high index of refraction. This permits spherical surfaces of less curvature for the same power, compared to conventional glasses. Monochromatic aberrations are readily minimized. Low reflectance coatings are used to overcome surface reflection losses.

Unlike materials for short wave lengths, materials transmitting longer wave lengths are limited in size and are usually expensive. For the larger aperture systems, windows or domes must be segmented from pieces. The most pressing need in infrared systems development is for a satisfactory material obtainable in large sizes at an economical price.

Filters

The necessity of optimizing the system response to the conditions of use generally requires filters having very sharp cutoff and high transmission efficiencies. A large variety of interference filters have become available. These filters are made from multiple layers of materials of different index, evaporated on a suitable substrate. The individual layer thicknesses must be very carefully controlled. These filters have the ability to cut off from 80 per cent transmission to 5 per cent transmission within a wave length region 0.09 of the cutoff wave length. Almost any desired response can be obtained at reasonably high transmission efficiency. However, interference filters operate properly only when the angle of incidence is near normal, making them useful primarily in applications where near parallel light is used. Absorption materials such as germanium (long pass 1.8 μ), silicon (long pass 1.4 μ), indium arsenide (long pass 4.0 μ), and sapphire (short pass 5.5 μ) are insensitive to angles of incidence, and are used extensively in applications of large-angle convergence, such as in field lenses and detector windows.

Background Noise

Because the infrared tracker is a passive system receiving incoherent energy, it cannot filter in range as a radar system and must accept all of the radiation from the background as well as the target.

General background characteristics can be arbitrarily categorized into two classes, reflective and self-emitting. The former includes the reflection and scattering of solar radiation by clouds during daylight operation. The spectral pattern of reflective radiation simulates that of the sun and is most intense in the shorter wave lengths from 1 to 4 μ. Self-emitting backgrounds include both atmosphere and clouds which have significant thermal emission, both day and night, at wave lengths greater than 4 μ.

Special background phenomena include the sun and moon, self-emissive sources which require special consideration because of their intensity. The moon is an important radiator, not only because of its reflected sunlight, but also because of emission from its high temperature surface, approximately 100 to 150 C on the illuminated side.

A target can be considered as a point source, and irradiance at the instrument will be a function of viewing distance. The irradiance due to the large background areas will be independent of range and will depend on the space discriminating ability of the detecting system.

A typical sky in the Earth's atmosphere, viewed in the infrared, exhibits a random spatial pattern of radiance. This radiance arises from diffuse reflection, and scattering of radiation from other sources, principally the sun. It is also from self-radiation by clouds, hilltops, gases, vapors and dusts carried in the atmosphere. The radiance patterns depend on the time and season of the year, on geographical location, on the direction of the sun and on the observer's altitude and direction of observation.

The exact configuration of the background is not reasonably predictable in advance of any one mission of a piece of equipment; indeed, the equipment must usually be designed to operate against a great variety of patterns to give some best average performance.

The particular value of radiance "seen" at any particular angle at one time is random-variable predictable only by some probability distribution. The several values of radiance seen in a set of directions, or at a set of times, form a set of random variables in two space dimensions and one time dimension. The most complete description possible of such a stochastic process would be given by the joint probability density function for all resolvable points in the object surface of the telescope. It would not, of course, be possible to obtain such a description nor, in general, feasible to use it if it were available. It is, therefore, necessary to use a similar approximate description which is a sufficient indication that the results of analysis and optimization based upon it are satisfactory for their purposes. A two-dimensional autocorrelation function or a Wiener spectrum are two such descriptions for the process.

It can be shown mathematically that a reticle may be considered as a combination of band pass and low pass filters selecting energy at certain space wave numbers. The analogy is developed between space filtering and the reduction of electronic noise by time filtering. The space mean-square-radiance spectrum (watts/cm^2-steradian)^2 per (wave/radian) against waves per radian may be considered as a cross section of a three-dimensional model which would have the units (watts/cm^2-steradian)^2 per (wave/radian)^2. This three-dimensional model represents the univariate, two-dimensional analogy of the normal univariate, one-dimensional energy-density spectrum used in electronic noise problems. Multiplication of such an energy-density spectrum by the wave number domain, two-dimensional transfer function for a reticle, followed by integration and taking a square root, yields the rms background voltage expected at the output of a detector, except for a constant relating the rms radiation to rms voltage through the detector.

In a Fourier transformation of time functions, a pulse of very short duration contains components extending out to high frequencies. Similarly, in taking two-dimensional transforms of distributions of radiant source distributions, a source such as a typical target which has a very small subtend in one direction will have an extensive spectrum in that direction in the wave number domain. Also, sources which have a large

extension in the image plane exhibit a narrow spectrum in the wave number domain.

The fine image of an optical system may often be considered circular and small, so that it is an approximation of a two-dimensional Dirac delta function. Because it has a nonzero diameter, however, it will have a transform which does not extend out to all wave numbers but will fall off at a radius close to the reciprocal of twice the image diameter.

Fig. 5 illustrates portions of the two-dimensional transfer functions of a typical reticle. The most significant features of these transfer functions are indicated. It will be observed that each transfer function shows a peak of transmission at the origin corresponding to the d-c energy transfer from backgrounds, and two or more other peaks corresponding to particular orientations of gradients which produce a large response.

The result of moving an irradiance function across a reticle is a convolution integral. The most useful property of the Fourier transform is that it converts a convolution operation to the multiplication of two transforms. Thus, the target output transform of the reticle can be found by multiplying the image transform by the reticle transfer function and by the electronic band pass transform. Taking the inverse transform of this product yields the output of the system.

The two-dimensional transform approach is not only able to aid in qualitative understanding, but it is also capable of giving quantitative evaluations of merit when the background-energy-density spectrum is known. In order to use this method of computing the system numbers, measurements are being made which will define the background-energy-density spectrum in waves per radian to the finest image quality of systems that will be used in the near future.

Although this technique of background discrimination was developed in the early 1950's by NOTS, Aerojet and others, its application to effective space filter design has been limited until recently because of a great lack of background data. Although reliable data are still not available in quantities which would be required for a good statistical model (this is particularly true in the longer wave lengths), data have recently become available which permit a very much more intelligent approach to the engineering compromises required in space filter design. Some experimental evidence on the Wiener spectra of cloud backgrounds based on the assumption (in measuring as well as interpreting data) of isotropicity suggest that the spectra between about 11 and 200 waves per radian fall off with about the 2.7 power of wave number.

Another advance of particular importance has been the development of fine reticles. It can be shown that the space filtering ability of a reticle is seriously hampered if either the average transmission departs greatly from 50 per cent or if the bar dimensions are uncontrolled. Since the fineness of the bar spacing is the prime factor in space discrimination, very good optical imagery requires extremely fine patterns which must be held to extremely close tolerances. Advanced photographic techniques are providing the required tolerances on transparent substrate and in etched, shim stock. Fig. 6 is a typical reticle pattern.

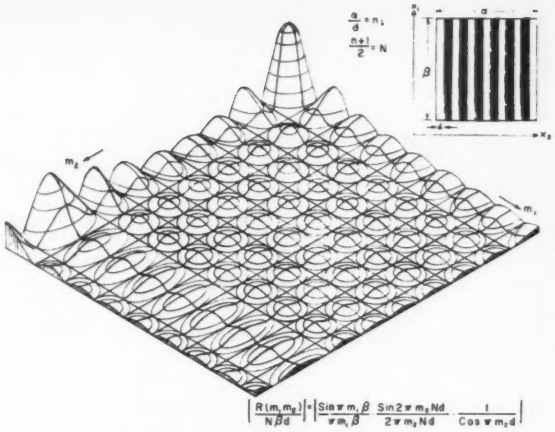

Fig. 5 Picket fence reticle transform

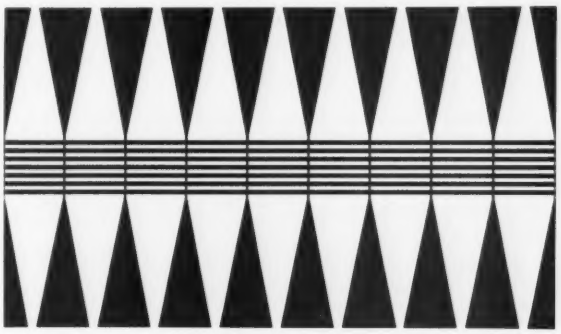

Fig. 6 Reticle pattern

Optical Systems

The discrimination of background energy is accomplished by using an extremely small, instantaneous field of view or by placing a reticle in the imaging plane of the optical system of the equipment to modulate the target energy. In order to obtain optimum space or size discrimination, the diameter of the target image focused on the reticle must be equal to, or smaller than, the distance between the reticle bars, thereby causing modulation to occur only of that energy emitted from a source equal to, or smaller than, the anticipated targets. It is, therefore, necessary for the optical collection system to be able to focus the energy from a target within the smallest possible space on the reticle. Since any practical optical system is limited in its resolving power, the ability of an infrared system to perform size discrimination against backgrounds is ultimately limited by the image quality or resolving power of its optics.

A usual technique in visual systems is to use spherical optical elements which are corrected to the high resolution required for any application by additional refracting optical elements. There are two reasons why this technique becomes very difficult to use in the longer wave length infrared. First, the wide variety of optical materials of different indexes and dispersion which are available to the visual optical system designer do not exist for the infrared optical designer as was discussed earlier. Secondly, although relatively low transmission efficiencies are satisfactory for many visual systems, the infrared system designer finds it difficult to tolerate similar losses since, for any given sensitivity requirement, any transmission loss must be compensated for by a linear aperture increase. Consequently, the multiple surface reflection losses and the multiple element absorption losses that the visual system designer accepts, cannot be accepted by the infrared system designer, particularly in the primary optical system. It has long been known that aspheric optical surfaces, correctly designed and polished, can provide the excellent image quality with only one or two elements. The use of these techniques has not been extensive in visual systems because of cost of fabrication. A great amount of highly skilled hand work and testing is required to attain the optical contour and polish required by visual wave lengths. However,

the longer wave lengths of infrared give some relief in surface finish. This, then, permits fabrication of complex aspheric shapes by replication processes which, for quantity production, are relatively inexpensive. In many cases, not only are aspheric infrared systems more efficient than a corrected spherical system, they are cheaper and more reliable (in production quantities, of course) since a fewer number of optical elements are required.

Conclusion

After a relatively long and slow period of development of infrared detection and tracking devices, starting at the time of World War II, highly successful equipment has become operational. The most notable examples are the seekers of the Sidewinder and Falcon missiles, and the infrared fire control tracker of the F-104. These successes, coupled with great recent advances in the state of the art in detectors, coolers, optical materials, and technique, and in information processing, indicate that extraordinary increases in the tracking ranges of infrared equipment may be expected in the future.

In addition, future targets should radiate considerably more energy, further enhancing the range of infrared detection. It appears that these factors will make infrared detection and tracking equipment an essential part of any modern weapons system.

Bibliography

1 Aroyan, G. F., "Space Filtering by Reticles," Proc. IRIS, vol. 3, no. 4, Dec. 1958, pp. 108–120.

2 Baker, J. G., "Family of Flat-Field Cameras, Equivalent in Performance to the Schmidt Camera," Proc. Amer. Phil. Soc., vol. 82, 1940. pp. 339–349.

3 Ballard, S. S. et al., "The Optical and Other Physical Properties of Infra-Red Optical Materials," Baird-Atomic, Inc., Final Rep. on Contract no. W-44-009-eng-473, June 1949.

4 Ballard, S. S. and McCarthy, K. A., "Optical Materials for Infrared Instrumentation," *Nuovo Cimento, Suppl.*, vol. 2, Series X, 1955, pp. 648–652.

5 Ballard, S. S., McCarthy, K. A. and Wolfe, W. L., "Optical Materials for Infrared Instrumentation," University of Michigan, Willow Run Laboratories Rep. no. 2389-11-S, Jan. 1959, pp. 1–115.

6 Betz, C. R., "Infrared Radiation Materials," *Electric Equipment Engng.*, May 1959, pp. 49–52.

7 Betz, C. R., "Properties of Infrared Radiation," *Electric Equipment Engng.*, Feb. 1959, pp. 48–52.

8 Beyen, W., Bralt, P., Davis, H., Johnson, L., Levenstein, H. and MacRae, A., "Cooled Photoconductive Infrared Detectors," *J. Opt. Soc. Amer.*, July 1959, vol. 49, no. 7, p. 686.

9 Blau, H. H., "Glass to Transmit Infrared Radiations," Ohio State University, Interim Reps. nos. 1–14 on Contract no. DA-44-009-eng-658, Sept. 1951 to June 1956.

10 Bouwers, A., "Achievements in Optics," Elsevier Publishing Co., New York, 1946, 2nd ed., 1950.

11 Couder, A., "Cellular Construction of Telescope Mirrors," *Comptes Rendus*, vol. 201, 1935, pp. 595–597.

12 Couder, A., "Deformation of Large Astronomical Mirrors," *Bull. Astron.*, vol. 7, 1932, pp. 201–281, 283–312, 353–381.

13 Couder, A., "Execution of Non-spherical Optical Surfaces; Schmidt Telescope," *Comptes Rendus*, vol. 40, 1940, pp. 327–329.

14 Crowley, D. E., "An Annotated Bibliography of the Emissivity and Reflectivity of Materials in the Infrared," Air Force Cambridge Research Center, Technical Memorandum to the Director, GRD-TM-57-23, June 1957.

15 Crowley, D. E., "Emittance and Reflectance of Materials in the Infrared," University of Michigan, Willow Run Laboratories, Rep. no. 2389-15-S, April 1959.

16 Cussen, A. J., "A Comparison of Photoconductive Detectors," Proc. IRIS, vol. 1, no. 1, June 1956. (*Confidential*)

17 DeGrott, W., "Optical Aberrations in Lens and Mirror Systems," *Philips Tech. Rev.*, 9, 1947/1948, pp. 301–308.

18 "Development of Materials for Transmitting Infrared Energy," WADC Technical Rep. 54-457, March 1955.

19 Elias, P. and Grey, D. S., "Fourier Treatment of Optical Processes," *J. Opt. Soc. Amer.*, vol. 42, no. 2, Feb. 1952, p. 127.

20 Holter, M. R., Nudelman, S., Suits, G. H., Wolfe, W. L. and Zissis, G. V., "Fundamentals of Infrared Technology," University of Michigan, College of Engineering, Summer Session, 1959.

21 Fusca, J. A., "Satellite Optics Limited by Atmosphere," *Aviation Week*, Jan. 1959, p. 75.

22 Glaze, F. W., "Development of Glasses for Transmitting Infrared Energy," NBS Reps. 2993, 3173 and 3359 on Contract AF33(616)-53-16, Dec. 1953 to June 1954.

23 Glaze, F. W., Blackburn, D. H. and Capps, W., "Development of Materials for Transmitting Infrared Energy," National Bureau of Standards, WADC Technical Rep. 54-457 on Contract AF33(616)-53-16, March 1955.

24 Hass, G. and Jenness, J. R., Jr., "Method for Fabricating Paraboloidal Mirrors," *J. Opt. Soc. Amer.*, vol. 48, no. 2, Feb. 1958, pp. 86–87.

25 Hekker, F., "On Concentric Optical Systems," Delftsche Uitgevers-maatschappij—DELFT, 1947.

26 Hoesterey, H. F., "Materials for Infrared Windows, Domes, Lenses," *Electronics*, Jan. 16, 1959.

27 Irvine, N. L. and Davis, L., "Simulation by Modeling," Proc. Western Joint Computer Conf., 1955.

28 Jamieson, J. A., "Proposed Study of Infrared Background Fluctuations," Aerojet-General Corporation Rep. no. 1557, 1959. (*Confidential*)

29 Jeffries, D., "Configuration of Available Lead-Sulfide Detectors," Proc. IRIS, vol. 3, no. 2, June 1958.

30 Jenness, J. R., Jr., "The Development of Irdomes," Naval Air Development Center, Rep. no. NADC-EL-53112, Aug. 1953.

31 Jones, R. C., "Detection of Targets Against the Sky Background," Polaroid Corp. Rep. 535, April 12, 1954.

32 Jones, R. C., "Methods of Rating the Performance of Photoconductive Cells," Proc. IRIS, vol. 2, no. 1, June 1957.

33 Jones, R. C., "On the Theory of Scanning Reticles (Episcotesters)," Polaroid Corp. Rep. 542, May 25, 1954.

34 Jones, R. C., "Performance of Detectors for Visible and Infrared Radiation," L. Morton, Ed., vol. 5, Academic Press, Inc., New York, 1953, pp. 2–96.

35 Karr, P. R., "Mathematical Study of Background Noise," Proc. IRIS, vol. 2, no. 2, Dec. 1957, pp. 47–56.

36 Kovit, B., "Microwave IR Detector Has High S/N, Broad BW," *Space Aeronautics*, April 1959.

37 Kovit, B., "Design Digest," *Space Aeronautics*, April 1959, pp. 147–149.

38 Kreidl, N. J., "Investigation of Infrared Transmitting Materials," Bausch & Lomb Optical Co., Reps. 1–4, 1955. (See also quarterly reps. for 1956, 1957 and 1958.)

39 Kreidl, N. J. et al., "Fabrication of Infrared Transmitting Materials by Hot Pressing Techniques," WADC Technical Rep. 58-275, Part 1, on Contract AF33(616)-5123, WADC, Oct. 1958.

40 Kreidl, N. J. et al., "Investigation of Infrared Transmitting Materials," Bausch & Lomb Optical Co., WADC Technical Rep. 55-500, on Contract AF33(616)-2769, Part 1, July 1957; Parts 2 and 3, Oct. 1958.

41 Larson, M. H., "Multiple Frequency Reticles," Aerojet-General Corporation Rep. no. TM 510:57-9-222, Jan. 1957. (*Confidential*)

42 Lasser, M. E., Cholet, P. and Wurst, E. C., *J. Opt. Soc. Amer.*, vol. 48, 1958, pp. 48–468.

43 McFee, R. H., "Missile Guidance by Infrared," Astronautics, May 1958, pp. 33–36.

44 Michelsen, A., "Sensitivity of IR-Reticle and No-Reticle Systems," Aerojet-General Corporation Rep. no. TM 520:58-8-384, Jan. 1958.

45 "Photoconductivity Conference," Edited by R. G. Breckenridge, E. E. Hahn and B. R. Russell, John Wiley & Sons, Inc., New York, 1956.

46 Nicolosi, S. J., Devaux, L. H. and Strauss, A. J., "New Intermetallics Offer Wide Infrared Response," *Electronics*, July 4, 1958, p. 48.

47 Peterson, E. W., "Demonstration of Lead Selenide Cell & Cryostat Unit," Proc. IRIS, vol. 2, no. 1, June 1957. (*Confidential*)

48 Petrits, R. L. and Humphrey, J. U., "Research on Photoconductive Films of the Lead Salts," Proc. IRIS, vol. 3, no. 2, March 1958.

49 Phillipi, C. M. and Beardsley, N. F., "Infrared Window Studies," WADC Tech. Note 55-194, Parts I and II, Dec. 1956.

50 "Photoconductor Infrared Detector Exhibits Wide Spectral Response," *Aviation Week*, April 13, 1959, p. 82.

51 Powell, R. W., "Criteria for the Performance of Infrared Systems," Aerojet-General Corp. Special Rep. no. 1610, June 1959.

52 Powell, R. W., "Infrared Detection Systems," Aerojet-General Corp. Special Rep. no. 1362, Dec. 1957.

53 Powell, R. W. and Kauffman, W. M., "Infrared Applications to Guidance and Control," *Aero/Space Eng.*, vol. 17, no. 5, May 1958, pp. 66–71.

54 Schwalow, A. L. and Townes, C. H., "Infrared and Optical Masers," *Phys. Rev.*, vol. 112, no. 6, Dec. 15, 1958, pp. 1940–1949.

55 Smith, R. A., Jones F. E., and Chasmar, R. P., "The Detection and Measurement of Infrared Radiation," Oxford University Press, New York, 1957.

56 Sumnicht, H. I., "Infrared 'Effective' Radiation," Proc. IRIS, vol. 4, no. 1, March 1959, pp. 52–56.

57 Talley, R. and Petrits, R., "Some Considerations of Infrared Photoconductive Detectors as Power Transducers," Proc. IRIS, vol. 4, no. 1, March 1959.

58 Turner, F. A., "Infrared Transmission Filters," Bausch & Lomb Optical Co., Quarterly Tech. Reps. nos. 1–8, on Contract DA-44-009-eng-1113, 1952–1954.

59 "Two Approaches for Cooling IR Detectors," *Missiles & Rockets*, Feb. 16, 1959, p. 23.

60 "Unit Cools IR Gear as Low as 60°K," *Missiles & Rockets*, May 25, 1959, p. 32.

61 Weinstein, A. I., "Cooling of Long Wavelength Infrared Detectors," *Electronics*, McGraw-Hill Book Co., New York, Aug. 1959, pp. 36–37.

62 Whitney, T. R., Eisele, R. E., Mascaro, F. G., Pesterre, J. A. and Rollauer, A. M., "Infrared Sky Background Investigation; Second Semiannual Report," Contract AF33(600)-30489, Rep. no. RW 1631.84, Nov. 30, 1956, pp. 1–80.

63 Wiener, N., "The Extrapolation, Interpolation, and Smoothing of Stationary Time Series," Technology Press & Wiley, New York, 1949.

64 Williams, V. Z., "Infrared the Frontier Frequency," *Research & Engng.*, May 1957, pp. 10ff.

Celestial Guidance

R. B. HORSFALL

Autonetics Division,
North American Aviation, Inc
Downey, Calif.

This paper treats the problems that underlie celestial guidance for cruise vehicles. The equations for the error signals are derived from star tracking based on an assumed position and local vertical reference. The problem of distinguishing a star from a noise background is also treated, and the problem of directing the telescope from a reference is examined both from the point of view of astronautics and cruise missile guidance.

SOME background on navigation in general is desirable for an understanding of automatic celestial navigation. In the broadest terms, navigation may be defined as the process of locating one's position with reference to a desired objective. As has been pointed out by Bell (1),[1] this problem may be considered an application of a theorem of projective geometry which defines the location of one unknown point by its relationships with four known points of which at least one must be at a finite distance.

As a practical matter, three properly chosen points usually suffice, because other information is available to distinguish the proper choice between alternate solutions. The requirement that at least one point be "near" implies a knowledge of distance as well as direction, either between the one near point and the observer, or between at least two near points.

In the practical application of navigation, it is customary to subdivide the field broadly into three categories: Piloting, dead reckoning and celestial navigation.

In piloting, position is determined by reference to landmarks (known points) all of which are at a finite distance. As in all ordinary navigation on the surface of the Earth, the Earth's center is one of the known points; furthermore, the distance from the point is known, although its direction is not. In a crude form, piloting has been in use for as long as intelligent life has existed. In more refined forms, it is still used for all modes of transportation today. In air transport, the various forms of radio range and hyperbolic navigation aids are clearly recognized as refined forms of piloting. The interpretation of control of a railroad train as an example of piloting is left as an exercise for the reader.

Dead reckoning is nearly as old as piloting. In this case, the point of departure is known. Direction of travel from the point of departure (relative to other points) is measured, and an estimate of distance traveled in this direction is made; to the accuracy with which these two items can be determined, the present position is known. This was the only technique available in ancient times for travel beyond sight of land and was used extensively by the Phoenicians, Greeks and Romans. Present-day pure inertial navigation and Doppler navigation are the most refined versions of dead reckoning so far developed.

Celestial navigation as practiced on the Earth's surface is the most abstract of the three broad divisions of navigation. It involves only the Earth's center as a local point and requires the determination of direction to two other points (properly selected) treated as infinitely distant. These points are represented by astronomical objects, such as fixed stars and planets. In one degenerate case the geometric situation is such that a single star will give a location of position on the Earth's surface (when the star is directly overhead). This situation was known and used by the Polynesians in navigating between island archipelagoes. During the past decade, the principles of celestial navigation have been applied to automatic missile and aircraft guidance. Many details of these applications are still under security classification, but the broad picture can be presented.

One may ask why it is necessary to consider automatic celestial navigation. For high accuracy work the answer is twofold. Pure inertial (dead reckoning) navigation should be entirely satisfactory if we were only able to produce equipment of sufficient stability. All such systems depend on gyroscopes for equipment stabilization. To date, it has not been possible to build gyroscopes capable of maintaining the accuracy required for inertial navigation for more than a few hours without external aid. Consequently, navigation over extended periods requires additional information. Application of more conventional celestial navigation techniques becomes less and less reliable as vehicle speed increases. Consider a vehicle traveling in the low supersonic range, at 500 m per sec. Suppose that this aircraft instead of flying straight is actually turning so that the radius of the turn is 25,000 km. This rate of turn is sufficient to give nearly 4 miles of error in a celestial navigation system depending on a conventional bubble level or pendulum for vertical reference. This corresponds to a rate of turn of the aircraft of only 4 deg per hr, which would be impossible to detect without accurate instrumental references. Thus, for slow speed aircraft or for surface vessels, inertial navigation must be supplemented by other aids to give sufficient accuracy over the time of operation. For high speed aircraft, a better means of determining the vertical is required for celestial methods to be useful. Unless the speed is sufficiently high to keep the duration of an entire mission within the useful operating time of an all-inertial system, a combination or so-called stellar-inertial system is required. Of course, piloting in its various forms may also be used. During clear weather, visual means are available, but under overcast conditions only active methods, such as radar, are possible. For military applications these are frequently counterindicated because radiation from the vehicle might reveal its presence to the enemy.

Historically, use of stars as an aid in automatic navigation has been considered from two different points of view. The first of these involves mechanization of the conventional means of celestial navigation, which has been applied for many years by human navigators aboard ships and in aircraft. The second considers astronomical references as the most nearly ideal inertial base and uses them to correct the performance of the stabilizing gyros of an inertial navigation system. In this capacity the astronomical reference serves to eliminate the effects of the gyro drift from the performance of the navigation system.

Received July 16, 1959.

[1] Numbers in parentheses indicate References at end of paper.

Mechanization of Conventional Celestial Navigation

In its fundamental form, conventional celestial navigation involves the solution of the so-called astronomical or celestial triangle (Fig. 1). There are many fine points involved in detailed application in this technique for which reference may be made to standard works on navigation (2,3). The most usual technique involves assuming a position based on dead reckoning or other approximate methods and determining for a particular star what its altitude and bearing angle should be at the time an observation is to be made. Measurement of the actual elevation of the star (normally accomplished by a sextant) provides a figure usually different from the predicted value. The difference is interpreted as an error in the assumed position along the azimuth line to the star. By making two such determinations from stars at different azimuths, corrections in two coordinates are obtained which provide a complete position determination or fix. Evidently, the more nearly the azimuths to the two stars differ by 90 deg the more accurate the fix will be. If no information were available to indicate an approximate position, observation on two stars could only provide an indication that the observer is at one of two more or less widely separated geographic positions. In such a case, observation of a third star would permit identification of which of the two was the correct fix. A third star is frequently used to provide a check on the two-star fix, even though dead reckoning is accurate enough to eliminate one of the two alternate positions.

Mechanization of this technique normally involves the same principles of assuming a position and using star sights to provide correction information. Some form of gyro stabilized platform is used as a reference in place of the natural horizon or bubble used with the conventional sextant. Inertial navigation techniques are normally used to provide the dead reckoning information which carries the automatic navigator from one star fix to another. It is usually possible to provide for nearly continuous stellar information when the sky is clear. In most applications, periods of overcast must be allowed for and the inertial system must be adequate to carry operation through these periods (4–6). A system which is adequate as an inertial navigator for this purpose provides the best available vertical reference for the astronomical sights when the vehicle is subject to appreciable and unknown accelerations.

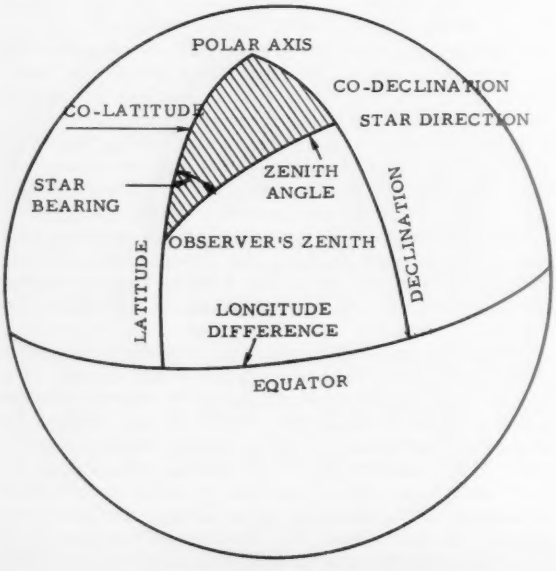

Fig. 1 Celestial triangle

System Involving Correction of Gyro Drift

The alternate technique is based on the theory of using astronomical sights as a fundamental inertial reference against which drift errors of the stabilizing gyroscopes may be measured and corrected. Because gyro drift is one of the major sources of autonavigator error, during long missions such stellar corrections should lead to markedly improved navigation accuracy and greatly extended range of operation. In this case, it is also evident that a minimum of two star sights are necessary to obtain complete supervision of gyro performance. An observation on one star alone is capable of indicating drift errors about any axis at right angles to the line of sight, but gives no information with respect to orientation about the line of sight. Inclusion of a second star in a different direction provides the necessary additional information to detect errors about the line of sight of the first star.

For any long range or long duration flight it is not possible to observe the same two stars all the way. Consequently, there is a problem in retaining control during the operation of switching from one pair of stars to another. If a third star is included, information for position determination or platform control is redundant. However, this redundancy permits continuation of complete control during switching from one set of stars to another.

For terrestrial navigation, tracking of planets or other objects in the solar system is undesirable. In general, they are confined to a rather narrow band in the neighborhood of the plane of the ecliptic, so that geographical limitations would be inevitable if they were used exclusively. Their motions are more complex than those of fixed stars, so that more information would be required in the automatic navigation system to permit their use. Moreover, they appear as finite disks rather than points of light, so that a further uncertainty in pointing may result. The sun and the moon are both so large and bright as to require special provisions to reduce the signal level and determine the center of the image if they are to be employed.

System Applications

It is interesting to note that both lines of attack lead ultimately to the same fundamental result and that residual differences are those of engineering and mechanization rather than of fundamental principles. Because the inertial portion of the equipment used in mechanization of the conventional celestial navigation problem must be Schuler-tuned to perform adequately, either as a vertical reference or as an inertial extrapolator, the overall system proves to behave as an 84-min pendulum with respect to error propagation. Use of the astronomical reference prevents drift-type error buildup. Similarly the all-inertial system is basically an 84-min pendulum but is subject to the accumulation of drift-type errors. Introduction of stellar references for correction of gyro drift eliminates these errors and gives the resultant system characteristics identical to those of the mechanized celestial navigator. Because of the potential of nearly continuous stellar observation in both cases, and the fact that accumulation of error during periods of overcast must be small if the system is to operate, the general solution of the celestial triangle is not normally utilized as a position-finding method. The triangle is solved in terms of the assumed position and known star coordinates, and the tracker telescopes are used only to detect small-angle errors.

Telescope Complement

In the practical construction of a system employing stellar

references, the use of three separate star tracker telescopes permits complete stellar control as long as the stars are not obscured by weather. With such a system it would theoretically be possible to do without gyroscopes entirely. However, as long as stars may be obscured, if only for a very short period, some form of gyroscope equipment is essential. If even elementary gyroscopes are provided, they will serve to carry the system through a period of switching from one star to another so that only two telescopes are required.

In general, it has been found that moderately long periods without visibility of the stars must be allowed for. A system needs to be able to start under overcast and climb above the clouds before picking up the stars. Also, unless flight at extremely high altitude is all that is required, some areas of cloud cover must be expected. When gyroscopes are sufficiently improved to handle such periods, adequate performance can be obtained by the use of a single star tracker telescope, which alternates observations between the two stars of the necessary pair and steps forward to a new pair whenever required.

Error Determination

The use of a single telescope leads to problems in handling of star error signals which are not met in multiple telescope systems. These become evident when the possible solutions for corrective torques are analyzed. In general, the telescope may be characterized by a set of orthogonal axes ξ, η, ζ, with ζ along the optical axis. Its orientation with respect to an x, y, z platform coordinate system (z toward zenith when platform is level) may be defined by the direction cosines

$$\| C_{a\alpha} \| = \begin{Vmatrix} C_{x\xi} & C_{y\xi} & C_{z\xi} \\ C_{x\eta} & C_{y\eta} & C_{z\eta} \\ C_{x\zeta} & C_{y\zeta} & C_{z\zeta} \end{Vmatrix} \qquad [1]$$

Note the use of a and α as "typical indexes." These direction cosines may be evaluated in terms of telescope gimbal angles when the mounting has been defined.

An error in platform orientation must be small if the system is to function at all. Consequently, it may be represented by a vector related by the right-hand screw convention to the axis about which the error exists and to the sense of the error. Thus

$$\epsilon = \sum_a \mathbf{1}_a \epsilon_a = \sum_\alpha \mathbf{1}_\alpha \epsilon_\alpha \qquad [2]$$

where

$a = x, y, z$
$\alpha = \xi, \eta, \zeta$

If all three ϵ_α were known, a straightforward solution for ϵ_a could be written

$$\epsilon_a = \sum_\alpha \epsilon_\alpha C_{a\alpha} \qquad [3]$$

By applying corrective torques proportional to the negative of ϵ_a to the corresponding gyroscopes, the platform could be forced to precess directly back to its proper position. Unfortunately, a telescope is unable to detect misalignment about its optical axis, so ϵ_ζ is not observable. Thus it is necessary to make use of a second star. If the two were observed simultaneously, the four observable quantities ϵ_ξ^1, ϵ_ξ^2, ϵ_η^1, ϵ_η^2 would be redundant for solution of Equation [2] for the ϵ_a. Here the superscripts refer to the two stars. A straightforward mathematical procedure is to write the inverse of Equation [3] for the four observable quantities

$$\begin{aligned} \epsilon_\xi^1 &= \sum_a \epsilon_a C_{a\xi}^1 \\ \epsilon_\xi^2 &= \sum_a \epsilon_a C_{a\xi}^2 \\ \epsilon_\eta^1 &= \sum_a \epsilon_a C_{a\eta}^1 \\ \epsilon_\eta^2 &= \sum_a \epsilon_a C_{a\eta}^2 \end{aligned} \qquad \ldots\ldots\ldots\ldots\ldots\ldots\ldots\ldots\ldots\ldots [4]$$

Any three of these equations may be solved simultaneously for ϵ_a to give equations for the required corrective torques. For example, let the telescope be connected to the platform through level, cross-level axes as shown by the unit sphere diagram (Fig. 2); then the direction cosines may be written in matrix form (Table 1). The last pair of Equations [4] becomes

$$\epsilon_\eta^1 = \epsilon_y \cos \phi^1 + \epsilon_z \sin \phi^1 \qquad \epsilon_\eta^2 = \epsilon_y \cos \phi^2 + \epsilon_z \sin \phi^2 \qquad [5]$$

Because these contain only two of the unknowns, they may be solved directly to give

$$\epsilon_y = \frac{\epsilon_\eta^1 \sin \phi^2 - \epsilon_\eta^2 \sin \phi^1}{\sin (\phi^2 - \phi^1)} \qquad \epsilon_z = \frac{\epsilon_\eta^2 \cos \phi^1 - \epsilon_\eta^1 \cos \phi^2}{\sin (\phi^2 - \phi^1)} \qquad [6]$$

Choosing the first of Equations [4] and substituting from Equations [6] gives

$$\epsilon_x = \frac{\epsilon_\xi^1}{\cos \theta^1} + \frac{\epsilon_\eta^2 \tan \theta^1}{\sin (\phi^2 - \phi^1)} - \frac{\epsilon_\eta^1 \tan \theta^1}{\tan (\phi^2 - \phi^1)} \qquad [7]$$

It is evident that this solution requires $\phi^1 \neq \phi^2$ to keep the values finite.

If it is assumed that the platform has already been corrected to bring it in line with star 2, then $\epsilon_\eta^2 \doteq 0$, and it may

Table 1 Direction cosines for telescope pointing angles

	x	y	z
ξ	$\cos \theta$	$\sin \theta \sin \phi$	$-\sin \theta \cos \phi$
η	0	$\cos \phi$	$\sin \phi$
ζ	$\sin \theta$	$-\cos \theta \sin \phi$	$\cos \theta \cos \phi$

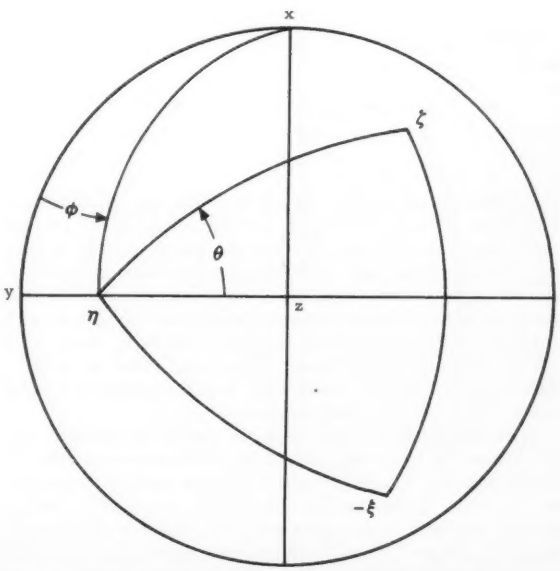

Fig. 2 Unit sphere diagram for telescope pointing angles

be neglected in the mechanization of corrections while observing star 1. Assuming no material buildup of errors during the tracking cycle and no imperfection in mechanization, it then suffices to put conditions on $\phi^2 - \phi^1$ and $\theta^2 - \theta^1$ to prevent loss of stars when they are first picked up after a period of overcast. It turns out that $\theta^2 - \theta^1$ must be materially less than $\phi^2 - \phi^1$ if use of the approximation $\epsilon_\eta{}^2 = 0$ is not to result in an increase of error on the second star.

Physically, these restrictions do not appear serious, but they are artificial. It is evident that accuracy of control will depend on the angle between the two star directions, but it should not depend on the location of this angle relative to the platform. Moreover, it has been found that this mechanization results in rocking of the platform about the x axis if pointing drive errors are present on either gimbal axis. The explanation for this is evident if the errors observed on the second star are evaluated after correcting on one star only. Writing

$$K_1 = \frac{1}{\sin(\phi^2 - \phi^1)} \qquad K_2 = \frac{\tan\theta^1}{\tan(\phi^2 - \phi^1)}$$

Equations [6 and 7] become

$$\begin{aligned}
\epsilon_x &= \frac{\epsilon_\xi{}^1}{\cos\theta^1} - K_2\epsilon_\eta{}^1 + (K_1\tan\theta^1)\epsilon_\eta{}^2 \\
\epsilon_y &= K_1(\epsilon_\eta{}^1\sin\phi^2 - \epsilon_\eta{}^2\sin\phi^1) \\
\epsilon_z &= K_1(\epsilon_\eta{}^2\cos\phi^1 - \epsilon_\eta{}^1\cos\phi^2)
\end{aligned} \qquad \ldots\ldots [8]$$

or, approximately, neglecting $\epsilon_\eta{}^2$

$$\begin{aligned}
\epsilon_x &= \frac{\epsilon_\xi{}^1}{\cos\theta^1} - K_2\epsilon_\eta{}^1 \\
\epsilon_y &= K_1\epsilon_\eta{}^1\sin\phi^2 \\
\epsilon_z &= -K_1\epsilon_\eta{}^1\cos\phi^2
\end{aligned} \qquad \ldots\ldots [9]$$

After making corrections according to Equations [9] and assuming no new errors, the residual platform errors are

$$\begin{aligned}
\epsilon_x{}^* &= (K_1\tan\theta^1)\epsilon_\eta{}^2 \\
\epsilon_y{}^* &= -(K_1\sin\phi^1)\epsilon_\eta{}^2 \\
\epsilon_z{}^* &= (K_1\cos\phi^1)\epsilon_\eta{}^2
\end{aligned} \qquad \ldots\ldots [10]$$

Transforming to telescope coordinates and simplifying, it is found

$$\begin{aligned}
\epsilon_\xi{}^* &= K_1\epsilon_\eta{}^2[\tan\theta^1\cos\theta^2 - \sin\theta^2\cos(\phi^2 - \phi^1)] \\
\epsilon_\eta{}^* &= \epsilon_\eta{}^2
\end{aligned} \qquad \ldots\ldots [11]$$

Note that the operation has left the telescope misalignment about the η^2 axis unchanged, but has replaced the original error about the ξ^2 axis with one dependent on the original $\epsilon_\eta{}^2$. Drive errors will show up as faulty values of the ϕ and θ angles. Consideration of Equations [11] shows that such errors may produce hunting about the x axis, both as a result of direct errors in ϕ, and as a result of errors in θ which otherwise would show only a small effect on y and z axes. Such hunting contributes to autonavigator system noise, and is therefore undesirable.

A second method of handling the correction problem may be derived by inspecting the plane of the two stars (Fig. 3). If the platform has been aligned with the number 2 star, then ϵ is $\mathbf{1}_\xi{}^2\,\epsilon_\xi{}^2$. Note that the measurable errors when looking at star number 1 lie in a plane perpendicular to ζ^1, and in fact, must be along r. Thus the measurable errors may be written

$$\epsilon_r{}^1 = [(\epsilon_\xi{}^1)^2 + (\epsilon_\eta{}^1)^2]^{1/2} = \epsilon_\xi{}^2\sin\psi \qquad [12]$$

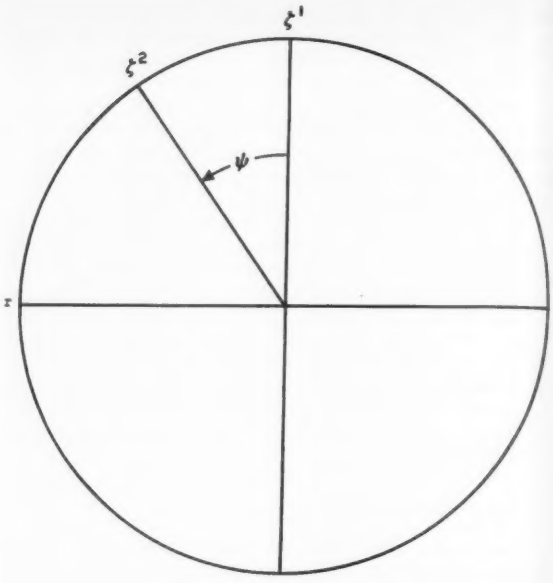

Fig. 3 Two-star plane

Note also that the unobservable error must be

$$\epsilon_\xi{}^1 = \epsilon_\xi{}^2\cos\psi \qquad [13]$$

Combining Equations [12 and 13] it is found that

$$\epsilon_\xi{}^1 = \epsilon_r{}^1\,\mathrm{ctn}\,\psi \qquad [14]$$

Equation [3] may then be written

$$\epsilon_a = \epsilon_r(\cos\beta\,C_{a\xi} + \sin\beta\,C_{a\eta} \pm \mathrm{ctn}\psi\,C_{a\zeta}) \qquad [15]$$

where β is the phase angle of the measured ϵ_r relative the ξ, η axes. The sign of the last term must be the same as that of $C_{\zeta r}{}^2$ in order to apply the ζ correction in the right direction. To the extent that alignment on the "other" star is perfect, Equation [15] will give an ideal solution for the corrections. However, the synthetic value of $\epsilon_\zeta{}^1$ may be violently wrong if these equations are applied on the first star observed. Thus special provisions must be made to eliminate this term when first acquiring stars.

A third scheme which avoids the possibility of erroneous drive on star acquisition is obtained by correcting by a combination of a rotation about the line of sight to the star not under observation, and a rotation about the common normal to the two stars. Defining

$$\mathbf{A} = \mathbf{1}_\zeta{}^2 \times (\mathbf{1}_\zeta{}^2 \times \mathbf{1}_\zeta{}^1) \qquad [16]$$

the corrective torques (or drives) are expressed as

$$\mathbf{L} = -K(\boldsymbol{\epsilon}_p + B\mathbf{1}_\zeta{}^1) \qquad [17]$$

where

$$\boldsymbol{\epsilon}_p = \boldsymbol{\epsilon} - \mathbf{1}_\zeta{}^1\epsilon_\zeta{}^1$$

is the observable component of the error angle at right angles to the line of sight, and B is so defined as to make

$$\mathbf{L}\cdot\mathbf{A} = 0 \qquad [18]$$

Substituting in Equation [18] from Equations [16 and 17] leads to

$$(\boldsymbol{\epsilon}_p + B\mathbf{1}_\zeta{}^1)\cdot\mathbf{1}_\zeta{}^2 \times (\mathbf{1}_\zeta{}^2 \times \mathbf{1}_\zeta{}^1) = 0 \qquad [19]$$

or

$$(\epsilon_p + B1_\zeta^1)\cdot[1_\zeta^2(1_\zeta^1\cdot 1_\zeta^2) - 1_\zeta^1] = 0 \qquad [20]$$

whence

$$B = \frac{-\epsilon_p\cdot 1_\zeta^2(1_\zeta^1\cdot 1_\zeta^2)}{(1_\zeta^1\cdot 1_\zeta^2)^2 - 1} \qquad [21]$$

This is equivalent to

$$B = \frac{\epsilon_p\cdot 1_\zeta^2\cos\psi}{\sin^2\psi} \qquad [22]$$

Therefore

$$\mathbf{L} = -K\left(\epsilon_p + \frac{\epsilon_p\cdot 1_\zeta^2\cos\psi}{\sin^2\psi}\ 1_\zeta^1\right) \qquad [23]$$

Expressed as scalar equations

$$\begin{aligned} L_\xi &= -K\epsilon_\xi^1 \\ L_\eta &= -K\epsilon_\eta^1 \\ L_\zeta &= -K(\cos\psi/\sin^2\psi)\,(\epsilon_\xi^1 C_\xi^1{}_\zeta^2 + \epsilon_\eta^1 C_\eta^1{}_\zeta^2) \end{aligned} \qquad [24]$$

Both the functions of ψ and the direction cosines may be expressed explicitly in terms of the gimbal angles, and the corrections may be transformed to give L_a. The resultant expressions are too complex to include here, and if analog equipment is used in mechanization, the explicit forms are not needed.

Telescope Pointing

So far, nothing has been said about the method of pointing the telescope toward the expected star position. Mechanically, gears, tangent screws, direct angle measurement, etc., may be considered for control of gimbal angles. Choice is a matter of engineering to provide acceptable accuracy. However, the determination of the proper angles is another matter.

In general, a straightforward procedure is to express the direction cosine matrix (Table 1) connecting platform and telescope axes in two forms. First, it may be expressed in terms of the desired gimbal angles as in Table 1. Second, it may be written in terms of the astronomical coordinates of the star, the orientation of the platform relative to the Earth and the sidereal time. Comparison of the two then permits expression of gimbal angles in terms of the other quantities. As a practical matter, it is usually not necessary to write out the complete matrix in either case. For the chosen example it may be noted that

$$\theta = \sin^{-1} C_{x\zeta} \qquad \phi = -\tan^{-1}(C_{y\zeta}/C_{z\zeta}) \qquad [25]$$

Only the $C_{a\zeta}$ need be evaluated in terms of known quantities in order to derive the gimbal angles θ and ϕ. A similar procedure is possible for any two-axis telescope mount. The only excuse for a three- (or more) axis mount is to provide axes parallel to geographic or astronomical coordinate axes. Doing so simplifies the determination of gimbal angles at the expense of mechanical complexity and resultant accuracy and reliability problems. To continue the example for a two-axis mount, let it be assumed that the axis is located by conventional latitude λ and longitude Λ angles, modified to agree with the right-hand rule by measuring longitude Λ positive to the east through the full 360 deg from the Greenwich meridian. In addition, a further rotation about the z axis might be included, but is of no advantage in displaying the computational principles involved. The star is located by right ascension ρ, declination δ and Greenwich hour angle of Aries γ. Fig. 4 shows these relations. Note that γ, ρ and Λ are all about the same axis, so only their algebraic sum σ is involved

$$\sigma = \gamma + \Lambda - \rho + 90 \text{ deg} \qquad [26]$$

Note that some violence has been done to the right-hand screw convention in the interests of customary usage for certain quantities. It is possible now to write the desired direction cosines in terms of λ, σ and δ

$$\begin{aligned} C_{x\zeta} &= \sin\delta\cos\lambda + \cos\delta\sin\lambda\cos\sigma \\ C_{y\zeta} &= \cos\delta\sin\sigma \\ C_{z\zeta} &= \sin\delta\sin\lambda + \cos\delta\cos\lambda\cos\sigma \end{aligned} \qquad [27]$$

If Equations [27] are substituted into [25], the telescope pointing angles become

$$\begin{aligned} \theta &= \sin^{-1}(\sin\delta\cos\lambda + \cos\delta\sin\lambda\cos\sigma) \\ \phi &= -\tan^{-1}\frac{\cos\delta\sin\sigma}{\sin\delta\sin\lambda + \cos\delta\cos\lambda\cos\sigma} \end{aligned} \qquad [28]$$

It is clear that other choices of gimbal angles or coordinate orientations will modify the detailed form of these equations, but no major simplification is possible with a two-axis telescope mount. In fact, they may be considerably more complex.

With certain choices of coordinates it is possible to formulate the equations equivalent to Equations [28], so that for a trajectory of predetermined type the gimbal angles are algebraic sums of geographic position angles and angles which are functions only of time and constant parameters. Such a choice permits the precision computation to be performed on the ground in advance, and the recording of the results in a form that may be played back by chronometer driven analog equipment in the airborne autonavigator. A particularly elementary (and equally useless) form occurs, if with the foregoing choice of coordinates, it is desired to travel a purely equatorial course. In this case the x axis coincides with X, so that ϕ combines algebraically with the other

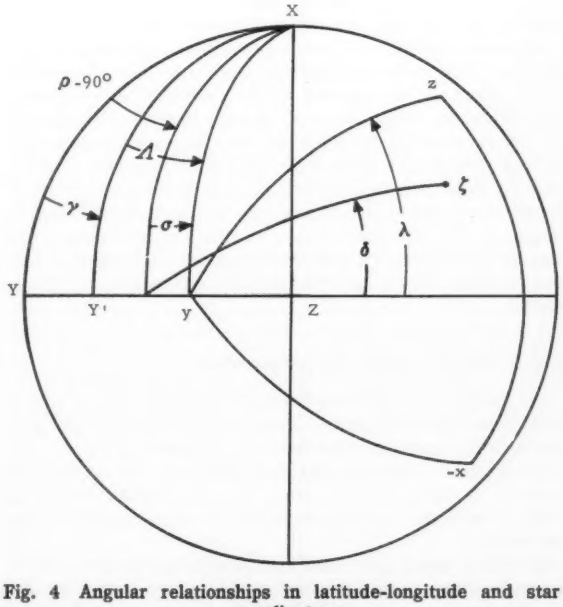

Fig. 4 Angular relationships in latitude-longitude and star coordinates

angles. With a bit of juggling, or by inspection, Equations [28] may be seen to reduce to

$$\theta = \xi \qquad \phi = (\rho - 90 \text{ deg} - \gamma) - \Lambda \qquad [29]$$

Because γ is a function of time only, ϕ is a simple difference of a time function and one of the position coordinates, whereas θ is a constant, and evidently satisfies the condition for precomputation. Other selections of coordinate systems can be made in which similar simplifications lead to useful results.

In general, residual errors in pointing the telescope and in detecting the star position, together with errors in correcting position or platform orientation in response to star information are random in nature. Thus such errors may be treated as system noise, which causes an error amplitude buildup proportional to the square root of time. If this effect becomes serious in an actual system, damping can prevent its occurrence. Meanwhile, use of the star information prevents accumulation of errors corresponding to gyroscope drift.

Astronautics

If we consider the extension of star tracker systems to astronautics, several possible changes occur. Once a vehicle is in interplanetary space it is free from sudden random disturbing influences of large magnitude, such as wind gusts; and particularly if it is in free motion, it may be a good stable platform in itself. Possibly the use of gyroscopes can be dispensed with entirely for this situation.

Secondly, for use within the solar system, planets are essential as elements of the navigation problem. During the midcourse phase of a trip between planets, the departure and destination planets are probably two of the most useful objects to observe. When moderately close to either one, a technique of stadiametric ranging may be used to determine the distance and rate of change of distance to the planet. On still closer approach, this stadiametric technique goes over continuously into a technique which may be called horizon scanning as a means of determining direction and distance to the center of the planet. It is probable that tracking at least a third object will be necessary. This is certainly true if complete position determination is required at all phases of the flight. Either the sun or a star may be suitable for this purpose. If the sun is selected, it is still subject to the limitations previously mentioned which result from its finite size and high light output.

In connection with the practical problems of mechanization for the astronautics application, two things must be considered. First, the equipment must be capable of functioning for extremely long periods as compared with the time required for terrestrial navigation. Second, resistance to high energy radiation is likely to be of major importance. The vehicle is no longer shielded by the atmosphere from intense solar radiation, which may be critical. Also, it is almost certain that some form of nuclear reactor will be essential for interplanetary vehicles, and radiation from the reactor must be allowed for in the design of the navigation equipment.

General Telescope Requirements

Automatic star trackers for use as components of stellar inertial navigation systems intended for terrestrial use must be capable of meeting the following requirements:

1 They must be capable of operation in full daylight as well as at night. This is required because operational flexibility would be seriously impaired if either condition were ruled out.

2 They must have sufficient sensitivity to give reliable operation on a group of stars which will permit unlimited flexibility of operation. This number is determined in part by the limited cone of view which may be seen through the necessary window in the airframe. Because of optical and aerodynamic limitations, such a window is usually flat and restricts the cone of view to about 90 or 100 deg. Under these circumstances, approximately 100 of the brightest stars must be trackable. This is equivalent to saying that the star tracker must operate on stars of approximately 2.5 magnitude. Order of brightness and limiting magnitude depend on the spectral sensitivity curve of the photoelectric element used, so they do not necessarily correspond to the usual visual case.

3 They must be capable of a high order of accuracy because errors of position are related to tracker errors by a factor of approximately 100 ft/sec.

4 Finally, they must be moderately durable, to provide reasonable service life in flight and to allow for the considerable time which will normally be expended in test and calibration operations.

For applications in the field of astronautics, star tracker requirements are somewhat different. Durability becomes a paramount consideration because continuous operation for a period of $1\frac{1}{2}$ to 3 years may be required even for exploration of the inner regions of the solar system. On the other hand, sensitivity is not such a critical matter. Once past the initial takeoff boost, an interplanetary vehicle will be outside the atmosphere and therefore free from aerodynamic limitations. Thus the tracker may be designed to cover a full hemisphere or more without window restrictions. Multiple windows can be provided if the system must be sealed in a pressurized compartment. Because this allows a wider choice of astronomical objects, a smaller number of the brighter stars and planets will serve the purpose. It is also probable that accuracy requirements may be relaxed for astronautics, because the problem approximates a lead-pursuit situation.

Most of the problems associated with star tracker design are more critical for terrestrial use than for interplanetary service. A major problem in this case is the background illumination during daytime operation. This problem arises primarily as a result of scattering of sunlight in the atmosphere. The result is the usual blue of the clear sky, because such scattering is more prominent in the short wave region of the spectrum. The brightness of the daytime sky is such that one square second of clear sky supplies as much light as some of the weaker navigational stars which must be used. For a star tracker of reasonable size the image of a star may occupy a circle 10 to 15 sec in diameter. Thus it is evident that the amount of light reaching a photosensitive detector from a field whose size is just sufficient to pick up the majority of the light from the star will be at least 100 times as great as the starlight.

Another problem that must be considered is the relationship between telescope focal length and pointing accuracy. For example, if a focal length of 200 in. is possible, an error of 0.001 in. in determination of star image location in the focal plane will correspond to a 1-sec pointing error. For a 20-in. focal length the same 0.001-in. tolerance corresponds to a 10-sec pointing error. Consequently, a suitable compromise must be selected between focal length, mechanical accuracy and detector dimensions.

Finally, the accuracy of pointing drive requires high precision. The same factor occurs here as in the relation between angular accuracy and position accuracy in navigation, and between focal length and sensing precision. One second of arc is approximately $\frac{1}{200,000}$ radian so a 10-μin. error on the tooth of a final drive gear 4 in. in diameter corresponds to 1-sec drive error.

Sensing Techniques

In general, it is necessary to convert a signal resulting from star light into an electrical signal to permit its use in automatic navigation. There are numerous possible photoelec-

tric elements which may be considered. These include photoemissive cells, both the simple diode-type and photomultiplier cells. Photoconductive cells are also available. The earliest type commonly known is the selenium cell. More recently lead sulfide cells have been developed to give better performance than the selenium units, and still other types are available for special purposes. The majority of the others operate too far in the infared for practical use in star tracking. Other photosensitive devices include such solid state photodetectors as phototransistors and thermistors. Finally, there are television pickup tubes, such as the image orthicon and videcon. With the exception of the television tubes, the only photosensitive device which has proved capable of satisfactory performance in daytime star trackers is the photomultiplier. For astronautical use, however, it is possible that some photoconductive or other solid state device may prove preferable.

It is evident from the relation between star and sky light that for terrestrial use some means of modulation of the incoming light will be required. The obvious first thought is to provide beam splitters and multiple photocells. This scheme is hopeless with background illumination so many times the available star signal. Even for astronautical use, however, such a scheme would be ruled out because of its bulk and the known secular variability of photocells. Modulation techniques which have been considered include as the simplest what is known as a Kron disk (7). This amounts to a circular shutter, half transparent and half opaque, rotated about the center of the dividing line. For nighttime use this gives an approximate square wave signal whenever a star appears off center. As the star image is brought into coincidence with the axis of rotation, the square wave begins to decrease in amplitude as soon as the axis of rotation encroaches on the star image, and decreases to zero when alignment is accomplished. It is evident that a simple Kron disk will also modulate light coming from a nonuniform background. Thus, in the daytime such a scanner would tend to drive the star tracker toward the sun even if a fairly bright star were within its field of view. To minimize this effect a compensating Kron disk has been devised which makes use of a semiannular clear zone opposite to the clear area of the regular disk. By making the centroid of the total clear area coincide with the axis of rotation, compensation for all odd-order terms in the sky gradient may be accomplished. A compensated Kron disk was used as the signal modulator in the first successful daytime tests of a stellar inertial navigation system.

Another system which has been proposed makes use of a pattern like a spoked wheel in the telescope focal plane (8). By moving either the wheel or the entire telescope so that the image of a star follows a circle of half the wheel diameter, a signal is obtained which is frequency-modulated when the star is decentered. Under these circumstances the circular path of the star image approaches the rim of the wheel on one side and the hub on the other, thus giving a frequency swing once per cycle of the nutating motion.

Still another way of reducing the effect of sky gradient on the detection system is to chop the typical Kron disk signal at a higher frequency. This has been done by modifying the basic Kron disk with spokes in the normally clear area, and also by a modification of the frequency modulation wheel in which the wheel is spun on its own axis and the nutating motion is such that the star image follows the rim of the wheel when on center. All of the modulation techniques discussed expose the photocell to light from an area of sky comparable with the entire scan field. The result is a relatively high noise background.

Various types of flying spot scanners have been developed, which result in much smaller total light on the photocell and consequently in lower noise levels. Mechanical schemes which have been developed have the effect of moving a pinhole over the desired scan field in a suitable pattern. It is obvious that a similar result can be obtained electronically if a television tube is used as the sensing element. Possible patterns include the raster type commonly used for television pictures, a PPI type similar to the pattern used in mapping radars, a Palmer scan (prolate epicycloid) and a simple spiral scan.

Pointing Coordinates

Three main types of mount have been considered for star tracker use. The first of these may be called an equatorial mount. In general, it incorporates three drive axes, the innermost of which corresponds to a declination axis, the next to the polar axis, and the outermost usually to a latitude axis. This mount has the advantage of providing simple mathematical relationships for determination of the necessary drive angles. On the other hand, the additional axis is an extra source of potential mechanical error in pointing. Furthermore, the structure is such that it tends to pose a clearance problem in practical application to an airborne autonavigator.

The second arrangement may be called an alt-azimuth mount. In this mount the outer axis is a vertical or azimuth axis and the inner a horizontal or elevation axis. The mathematical relationships required for computing the drive angles for this mount are relatively complex. This arrangement also suffers from gimbal lock at zenith and cannot be used with a line of sight too near the vertical. On the other hand, the alt-azimuth mount provides a direct tie to conventional celestial navigation practice, in which elevation and bearing are the usual measurements made. In addition, the alt-azimuth scheme may permit design with a smaller flat window than the other types which have been considered. Finally, it should be noted that the two drives require entirely different ranges of motion. The azimuth drive must operate over an unrestricted 360-deg range, whereas the elevation drive will normally have to cover only 45–50 deg.

The third system is the level, cross-level system previously discussed. The level, cross-level system avoids the zenith gimbal lock problem of the alt-azimuth system. Depending on the nature of the optical system, the range of motion in the two coordinates may be one to one with each requiring 90 to 100 deg, or two to one with the smaller requiring only 45 to 50 deg.

Signal-to-Noise Considerations

For night use there is relatively little difficulty in securing an adequate signal from a sufficient number of navigational stars. Likewise, for the astronautics application it is probable that signal-to-noise ratios will be high enough without special precautions. It is in the case of terrestrial daytime operation that noise becomes a limiting factor and the major problem in production of a useful star tracker. Noise may arise either from modulation of background light or from "misbehavior" of the electrical and electronic elements themselves.

An example of the first type is the signal arising from a nonuniform sky when a Kron disk scanner is used. In general, such noise would be absent if the sky were absolutely uniform. Under the actual conditions usually found, the magnitude of such noise may be several thousand times the magnitude of the star signal for any of the scanners which expose a major fraction of the tracker field at one time. For this reason, even with the compensated Kron disk, additional tricks were necessary to balance out residual modulated sky signal in order to provide successful tracking in the earliest complete system tested.

With flying spot scanners, nonuniform sky background produces a smaller signal, but one which is still comparable to the star signal in magnitude. In general, noise of this type will have predictable frequency characteristics; and with suitable choice of scanner design, these frequency charac-

teristics can be differentiated from those of the star signal to permit separation by filtration.

Electronic sources of noise include shot noise which results from the discrete nature of photo current in a photoemissive cell. Thermal noise resulting from agitation of electrons in resistance is another type, which is of importance in photoconductive detectors. Both of these sources produce essentially white noise which therefore cannot be completely eliminated by filtering. Shot noise varies with the square root of cathode current and therefore with the square root of total illumination. Thus its magnitude can be reduced by limitation of the area of sky seen at any instant, which favors the use of the flying spot scanner. Thermal noise on the other hand is independent of incident illumination and varies essentially with the square root of the absolute temperature of the resistance element in which it occurs. It also varies directly with the resistance. Unfortunately, the signal itself also varies directly with resistance, so that change in resistance value is not available as a means of improving signal-to-noise ratio. Where thermal noise is a problem, the only available means for reducing it is refrigeration of the critical resistances.

As a practical matter, it has been found that photoemissive cells with their associated equipment show so little thermal noise that it can be neglected in design of a star tracker system. Conversely, photoresistive cells show no shot noise of any importance. Unfortunately, the thermal noise in such detectors has proved to be too high for practical use without refrigeration. Consequently, successful tracker systems have employed photoemissive cells almost exclusively.

The problem of separating star signals from the noise background is largely one of eliminating modulation noise and separating the star signal from the residual shot noise. For trackers whose dimensions are capable of giving satisfactory performance, modulation noise can be reduced to a negligible value by making the diameter of the scanning aperture approximately equal to the star image size. The latter is determined by diffraction and residual aberrations in the optical system. If the smoothing time of the detection system is then made of the same order of magnitude as the duration of a star pulse, the separation of star signal and shot noise will be optimized. Under these circumstances the probability P that a noise pulse will occur during one scan period is given approximately by

$$P = \frac{k_1 D^2 p^{1/2}}{d^2 A T^{1/2}} \exp\left(-\frac{k_2 A^2 T}{D^2 p}\right)$$

where

D = diameter of the field of view
d = diameter of the scanning aperture in the same units as D
T = scanning period
p = external air pressure
A = objective aperture
k_1, k_2 = constants

This relation depends on the use of nonlinear detection techniques including narrow band filtration corresponding to the assumed smoothing time followed by base clipping to eliminate all but the highest pulses in the output signal. Use of a resonant output or correlation techniques applied to the final output signal may be shown to be equivalent in effect to increasing the scan period with a corresponding decrease in bandwidth.

References

1 Bell, F. C., "Report on the Geometric Basis of Celestial Navigation," Northrop Aircraft Co., Rep. no. GM-503, April 1, 1947.

2 Dutton, B., "Navigation and Nautical Astronomy," U. S. Naval Institute, Annapolis, Md., 1943.

3 Bowditch, N., "The American Practical Navigator," U. S. Hydrographic Office.

4 Schuler, M., "Die Storung von Pendel und Kreiselapparaten durch die Beschleunigung der Fahrzeuges," *Physikalische Zeitschrift*, vol. 24, 1923, p. 344.

5 Slater, J. M. and Duncan, D. B., "Inertial Navigation," *Aeron. Engng. Rev.*, vol. 15, 1956, p. 49.

6 Wrigley, W., Woodbury, R. B. and Hovorka, J., "Inertial Guidance," IAS Preprint no. 698, presented at 25th Annual Meeting, Jan. 1957.

7 Whitford, A. E. and Kron, G. E. "Photoelectric Guiding of Astronomical Telescopes," *Rev. Sci. Instr.*, vol. 8. 1937, p. 78.

8 Thorne, T. G. "The Automatic Guiding of Astronomical Telescopes,' *Engineering*, vol. 169, 1950, p. 197.

RESEARCH SCIENTISTS and ENGINEERS with MS, PhD or ScD

The Academic Approach to Research

...can it be transplanted to an industrial laboratory?

YES...in its environment of free inquiry and in scholarly consideration of the work of qualified colleagues.

This attainment is the experience of members of the Scientific Research Staff at Republic Aviation. Here, the initiation of original research is encouraged and generous support is provided to demonstrate the validity of theoretical concepts.

A preference exists for theoretical and experimental studies related to the many and varied disciplines of aeronautics and astronautics. These cover a wide spectrum of scientific research in its most active and interesting aspects.

At the same time, more emphasis is placed upon bringing new theories into the realm of feasible engineering than would normally be found at an academic institution.

THE PRACTICAL RESULTS OF THIS POLICY

The fruitfulness of the research environment at Republic is evidenced by the advancements and developments continually resulting. One well-known example is the current research and development of the Plasma Pinch Engine (for interplanetary travel) conceived by members of the Scientific Research Staff. Other wide-ranging research programs concern such subjects as the theory of lifting fans, new sophisticated methods of structural analysis, advanced electronic systems and techniques, space mechanics and nuclear physics, among others.

SCIENTISTS AND ENGINEERS ARE INVITED TO JOIN OUR STAFF AS NEW RESEARCH CENTER NEARS COMPLETION

Early in 1960, a new Research Center, including 7 modern laboratories, will be completed to support Republic's expanding effort in research and advanced development. Existing areas of investigation are being enhanced and new ones will be initiated.

If your interests coincide with the work of such a group and you feel you can contribute to progress in any of the physical and engineering sciences related to aeronautics and astronautics — Republic would like to talk with you. Salaries are high, commensurate with talent and expert knowledge.

IMMEDIATE OPPORTUNITIES EXIST FOR SCIENTISTS WITH APPROPRIATE RESEARCH EXPERIENCE AND ADVANCED DEGREES IN:

- Navigation and Communication Systems
- Electronic Theory
- Electronic Circuits and Components
- Nuclear Physics
- Nuclear Power
- Nuclear Propulsion
- Aerodynamics and Fluid Mechanics
- Theory of Lifting Fans
- Applied Mechanics
- Space Environment
- Missions and Trajectories
- Space Flight Control
- Applied Mathematics
- Hypersonics
- Plasma Dynamics

Write in confidence directly to:
Dr. Theodore Theodorsen
Director of Scientific Research

REPUBLIC AVIATION
Farmingdale, Long Island, New York

Technical Literature Digest

M. H. Smith, *Associate Editor*
The James Forrestal Research Center, Princeton University

Aerodynamics of Jet Propelled Missiles

Forebody Drag Characteristics of an Ogive Cylinder, by W. T. Strike and Jack D. Whitfield, *J. Aero/Space Sciences*, vol. 26, June 1959, p. 383.

Wind-Tunnel Investigation at Mach Numbers From 0.40 of the Static Aerodynamic Characteristics of a Nonlifting Vehicle Suitable for Reentry, by Albin O. Pearson, *NASA Memo* 4-13-59L, May 1959, 14 pp.

A Study of the Motion and Aerodynamic Heating of Ballistic Missiles Entering the Earth's Atmosphere at High Supersonic Speeds, by H. Julian Allen and A. J. Eggers, Jr., *NACA Report* 1381, 1958, 16 pp.

Investigation of the Drag of Various Axially Symmetric Nose Shapes of Fineness Ratio 3 for Mach Numbers from 1.24 to 7.4, by Edward W. Perkins, Leland H. Jorgensen and Simon C. Sommer, *NACA Report* 1386, 1958, 17 pp.

Hypersonic Flow Over an Elliptic Cone: Theory and Experiment, by Robert L. Chapkis, *Calif. Inst. Tech., Guggenheim Aeron. Lab., Hypersonic Res. Proj., Mem.* 49, May 1959, 44 pp.

Water-Landing Characteristics of a Reentry Capsule, by John R. McGehee, Melvin E. Hathaway and Victor L. Vaughan Jr., *NASA Memo* 5-23-59L, June 1959, 27 pp. (Film suppl. available on request.)

On the Rotational Motion of a Body Re-Entering the Atmosphere, by T. B. Garber, *J. Aero/Space Sci.*, vol. 26, July 1959, p. 443.

An Investigation of the Pressure Distribution on Conical Bodies in Hypersonic Flows, by Victor Zakkay, *J. Aero/Space Sci.*, vol. 26, July 1959, p. 457.

Heat Transfer and Fluid Flow

Digital Computer Solution of Equations for Transient Heating of Porous Solid, Including Effects of Longitudinal Conductions, by F. A. Creswick, *Indus. Math.*, vol. 8, 1957, pp. 61–69.

Thermal Stresses Caused by Heating Thick-Walled Hollow Cylinders, by W. Endres, **Brown-Boveri Rev.,** Jan. 1958, p. 21.

Transient Temperature Distribution in Aircraft Structures, by Irving Frank, *J. Aeron. Sci.*, vol. 25, no. 4, April 1958, p. 265.

Vertical Re-Entry of Very Light-Weight Bodies Into the Earth's Atmosphere, by R. D. Linnell, *Convair Sci. Res. Lab. RN* 9, Oct. 1957, 30 pp.

Aerothermoelasticity, by M. Rogers, *Aero/Space Engng.*, Oct. 1958, pp. 34–38.

Heat Transfer and Pressure Drop Across Banks of Finned Tubes, by D. J. Ward and E. H. Young, *Chem. Engng. Prog.*, vol. 54, no. 10, Oct. 1958, pp. 87–93.

Heat Transfer Between Fluidized-Solids Beds and Boundary Surfaces—Correlation of Data, by L. Wender and G. T. Cooper, *J. AIChE*, vol. 4, 1958, pp. 15–23.

Effects of Ultrasonics on Heat Transfer by Convection, by G. C. Robinson, C. M. McClure III and R. Hendricks Jr., *Amer. Ceramic Soc. Bull.*, vol. 37, no. 9, Sept. 1958, pp. 399–404.

Heat Transfer to Boundary Layers with Pressure Gradients, by R. A. Seban and H. W. Chan, *Wright Air Development Center, WADC Tech. Rep.* 57–111, *ASTIA AD* 118075, May 1958.

Effect of Free-Stream Turbulence on Heat Transfer from Flat Plate, by S. Sugawara, T. Sato, H. Komatsu and H. Osaka, *NACA Tech. Memo* 1441, July 1, 1958, 21 pp.

Tabulation of Coordinates for Hypersonic Axisymmetric Nozzles—Part 1—Analysis and Coordinates for Test Section Mach Numbers of 8, 12, and 20, by Robert J. Cresci, *Polytechnic Institute of Brooklyn, Dept. Aeron. Eng. and Appl. Mech., WADC TN* 58–300 Part 1 (*ASTIA AD* 204 213), Oct. 1958.

Differential Equations for Cylindrical Shells with Arbitrary Temperature Distribution, by P. P. Bijlaard, *J. Aero/Space Sci.*, Sept. 1958, pp. 594–602.

Heat and Mass Transfer Bibliography with Selected Abstracts, by W. J. Christian and T. H. Schiffman, *Wright Air Development Center, WADC Tech. Rep.* 58–186 (*ASTIA AD* 151199), May 1958.

A New Approach to the Measurement of Convection Heat and Mass Transfer, by R. A. Cranville and A. Sigalla, *Research*, vol. 11, no. 8, Aug. 1958, p. 326.

Effects of Thermal Relaxation and Specific-Heat Changes on Measurements with Pneumatic-Probe Pyrometer, by P. W. Kuhns, *NACA TN* 4026, July 1957, 67 pp.

Supersonic Two-Dimensional Magnetohydrodynamic Flow, by F. Fishman, J. Lothrop, R. Patrick and H. Petschek, *Avco Mfg. Corp., Res. Rep.* 30, Feb. 1959, 49 pp.

Visualization of Cylindrical Shock Waves, by F. D. Bennett and D. D. Shear, *Aberdeen Proving Ground, Ballistic Res. Labs, Mem. Rep.* 1199, March 1959, 8 pp.

Operation and Performance of a Shock Tube with Heated Driver, by Robert C. Evans, *Calif. Inst. Tech., Guggenheim Aeron. Lab., Hypersonic Res. Proj. Mem.* 48, Feb. 1959, 29 pp.

Influence of Diaphragm Opening Time on Shock Tube Flows, by Donald R. White, *General Electric Res. Lab. Rep.* 58-RL-1999, June 1958, 17 pp.

An Experimental Investigation of the Effect of Ejecting a Coolant Gas at the Nose of a Blunt Body, by Hugh C. Warren, *Calif. Inst. of Tech., Guggenheim Aero. Lab., Hypersonic Res. Proj. Mem.* 47, Dec. 1958, 43 pp.

Heat Transfer from Cylinders in Transition from Slip Flow to Free-Molecule Flow, by Ronald J. Cybulski and Lionel V. Baldwin, *NASA Memo* 4-27-59E, May 1959, 49 pp.

Recent Developments in Convective Heat Transfer, by Rolf H. Sabersky, ARS JOURNAL, vol. 29, May 1959, pp. 325–331.

Hypersonic Shock Tunnel, by H. T. Nagamatsu, R. E. Geiger and R. E. Sheer Jr., ARS JOURNAL, vol. 29, May 1959, pp. 332–340.

Similarity Parameters for Surface Melting of a Blunt Nosed Body in a High Velocity Gas Stream, by Lester Lees, ARS JOURNAL, vol. 29, May 1959, pp. 245–253.

Use of a Catalytic Probe for Detection of Dissociated Nonequilibrium States in Hypersonic Flow, by Stuart A. Hoenig, ARS JOURNAL, vol. 29, May 1959, pp. 361–362.

Velocity of Tank Fragments, by Saunders B. Kramer, ARS JOURNAL, vol. 29, May 1959, pp. 363–364.

Generalized Solution for the Problem of Pipe Flow With Friction Heat Addition, by R. W. McJones and M. L. Caplan, ARS JOURNAL, vol. 29, May 1959, pp. 366–367.

Mechanism of Cratering in Ultra High Velocity Impact, by Melvin A. Cook, *J. Appl. Phys.* vol. 30, no. 5, May 1959, pp. 725–735.

Ablation Studies in a Shock Tube, by R. W. Nicholls, W. H. Parkinson and H. Van Der Lann, *J. Appl. Phys.* vol. 30, no. 5, May 1959, p. 797.

Electron Mobility in Partially Ionized Atomic Hydrogen, by Mahendra Singh Sodha, *Phys. Rev.*, vol. 113, March 1, 1959, pp. 1163–1164.

General Approach to the Study of Electrical Conductance and Its Relation to Mass Transport Phenomena, by Richard W. Laity, *J. Chem. Phys.*, vol. 30, March 1959, p. 682.

A Simple Construction for the Determination of the Magnetohydrodynamic Wave Speed in a Compressible Conductor, by Nicholas Rott, *J. Aero/Space Sci.*, vol. 26, April 1959, p. 249–250.

Concise, Systematic Jacobin Thermodynamics for High-temperature Real Gases, by Russell J. Arave, *J. Aero/Space Sci.*, vol. 26, April 1959, pp. 250–253.

On the Heating Effect in a Resonance Tube, by I. M. Hall and C. J. Berry, *J. Aero/Space Sci.*, vol. 26, April 1959, p. 253.

Laminar Jet Mixing of Electrically Conducting Fluid in a Transverse Magnetic Field, by S. I. Pai, *J. Aero/Space Sci.*, vol. 26, April 1959, pp. 254–255.

General Characteristics of Binary Boundary Layers With Applications to Sublimation Cooling, by Joseph F. Gross, David J. Masson and Carl Gazley Jr., *Rand Corp.*, P-1371, May 1958. 52 pp.

Influence of Large Positive Dihedral on Heat Transfer to Leading Edges of Highly Swept Wings at Very High Mach Numbers, by Morton Cooper and P.

EDITOR'S NOTE: Contributions from Professors E. R. G. Eckert, J. P. Hartnett, T. F. Irvine Jr. and P. J. Schneider of the Heat Transfer Laboratory, University of Minnesota, are gratefully acknowledged.

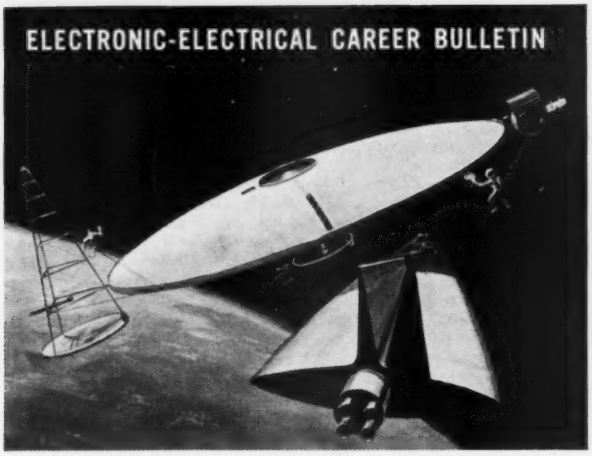

MARS VEHICLE. Drawing, based on Boeing study, of space vehicle designed for launching from orbiting platform for reconnaissance flight to Mars and return. Lunar, orbital and interplanetary system studies, and expanding programs such as the advanced Minuteman solid-propellant ICBM, are typical of challenging, long-range assignments Boeing offers electronic-electrical engineers.

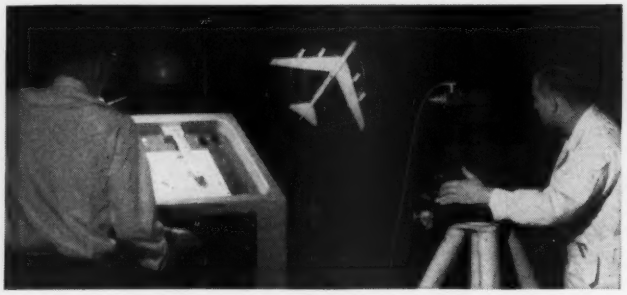

DARK TUNNEL. View in 100-foot dark tunnel, part of extensive Boeing infrared research and development facilities. Boeing investigations include use of infrared, visible and ultra-violet techniques for use in communication, navigation, detection and guidance at altitudes above tropopause. IR systems, inertial navigation, electrical power systems for satellites, shockwave radiation and refraction and irdome heating are other areas of assignments open at Boeing.

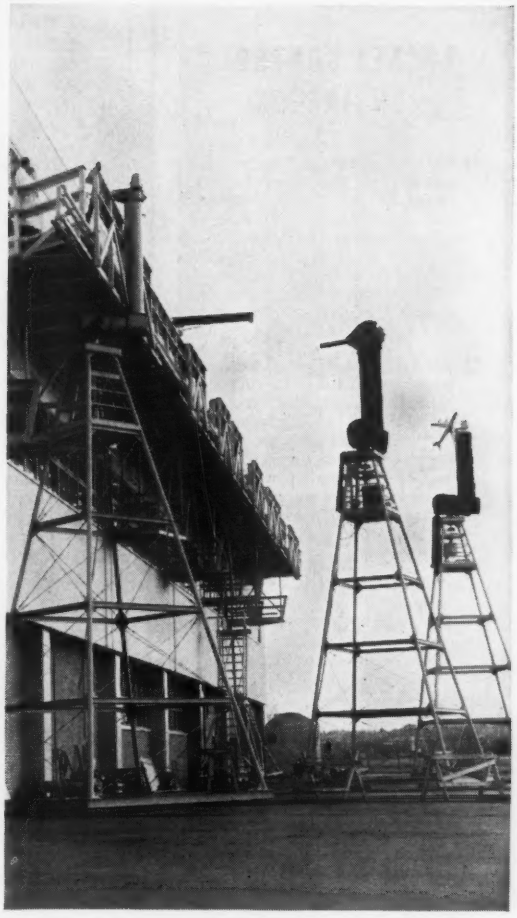

ANTENNA PATTERN RANGE, with movable towers capable of handling models up to 1000 pounds. Boeing has openings in ECM antenna development, and in gas, solid and liquid dielectric research, as well as large-aperture antennas for ASMs, orbital vehicles and airborne warning systems. Other openings are available in instrumentation, missile guidance and control.

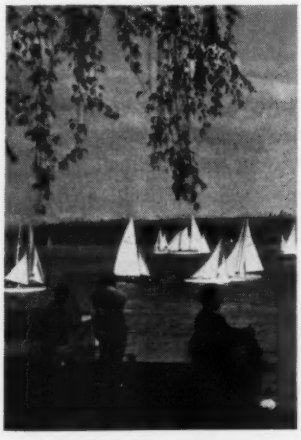

SEATTLE area, boating capital of U.S., offers world-famous recreational facilities. Fresh and salt water boating and fishing are only one hour from dramatic snow-capped mountains renowned for six-months-a-year skiing. Mild year-round climate. Excellent schools and universities, cultural activities, modern housing and shopping centers. Wonderful Western living for the whole family!

ELECTRONIC-ELECTRICAL ENGINEERS

Write today for details of challenging, long-range positions available to you right now at Boeing. You'll find at Boeing a dynamic professional environment that's conducive to rapid advancement and deeply rewarding achievement.

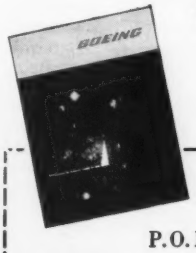

Mr. Stanley M. Little,
Boeing Airplane Company,
P. O. Box 3822 - JPC, Seattle 24, Wash.

Send me details of electronic-electrical positions, and the booklet, "Environment for Dynamic Career Growth."

Name..... Degree(s).....

Address .....

City..... State.....

Field of interest.....

BOEING

Seattle • Wichita • Cape Canaveral

ROCKET CONTROLS ENGINEERS

1) For development and analytical design of valves and controls for rocket engine systems. Develop specification requirements for components covering design, test and development. Prepare data for proposals. BS in ME or AE and 3–7 years' experience with hydraulic pneumatic devices and systems.

2) For dynamic analysis of mechanical systems associated with rocket propulsion. Mathematical descriptions of controlled rocket components with regard to systems stability. Interpretation of designs for controlling rocket components. Analogue simulation of systems. Supervision of above areas. BS, ME or EE. Experience in servo systems analysis and techniques.

To arrange interview call collect, Niagara Falls BUtler 5-7851, or send resume to:

SUPERVISOR ENGINEERING EMPLOYMENT

BELL AIRCRAFT CORPORATION
BUFFALO 5, NEW YORK

METALLURGIST

Caterpillar Tractor Co. World's Leading Manufacturer of Diesel Engines Tractors–Motor Graders Earthmoving Equipment

offers

Exceptional opportunity for experienced Metallurgist to assume responsibility of programs related to application and development of high temperature materials for gas turbine engines.

Production metallurgical or quality control experience desirable.

Salary commensurate with qualifications.

Send Resumé To:

John C. Myers ARS–129
Technical and Professional Employment

CATERPILLAR TRACTOR CO.
Peoria, Illinois

Calvin Stainback, *NASA Memo* 2-7-59L April 1959, 18 pp.

Mallier Enthalpy-entropy Charts for High Temperature Plasmas, by F. Bosnjakovic, W. Springe, K. F. Knache and P. Burgholte, *Rand Corp., Translation,* T-96, Aug. 1958, 26 pp.

Unified Dynamics and Thermodynamics of a Thermal Plasma, by H. Maecker and Th. Peters, *Rand Corp., Translation,* T-90 (translated from *Zeitschrift für Physik,* BD 144, 1956, pp. 586–611), June 1958, 38 pp.

Equilibria in a Thermal Plasma Composed of C + H_2 and C + $2H_2$ in a Temperature Range From 5000°K to 50,000° K at a Total Pressure of 1 Bar, by K. Kroepelin and K. K. Neumann, *Rand Corp.* T-99, Oct. 1958, 34 pp.

Equilibria in C + H_2 and C + 2H Systems at Temperatures between 1000°K and 6000°K, by H. Kroepelin and E. Winter, *Rand Corp.,* T-100, Oct. 1958, 29 pp.

Radiation of Plasma in a Magnetic Field, by B. A. Trubnikov, *Rand Corp.* T-101 (translated from *USSR Academy of Sciences,* Reps., vol. 118, no. 5, 1958), Oct. 1958, 10 pp.

The Electric Spark Method for Quantitative Measurements in Flowing Gases, by H. J. Bomelburg, J. Herzog and J. R. Weske, *Maryland Univer. Inst. for Fluid Rynam. & Appl. Math., TN* BN-157 (*AFOSR TN* 59–273; *ASTIA AD,* 212700, Jan. 1959, 20 pp.

Transport and Thermodynamic Properties in a Hypersonic Laminar Boundary Layer, Part I: Properties of the Pure Species, by Sinclaire M. Scala and Charles W. Baulknight, ARS JOURNAL, vol. 29, Jan. 1959, pp. 39–45.

Solution to the Linearized Quasi-Stationary External Diffuser Equations, by R. H. Edwards, ARS JOURNAL, vol. 29, Jan. 1959, p. 54.

A Note on Turbulent Boundary Layer Growth in Nozzles, by M. Sibulkin, ARS JOURNAL, vol. 29, Jan. 1959, pp. 61–63.

Frictional Electricity in Missile Systems, by P. Molmud, ARS JOURNAL, vol. 29, Jan. 1959, pp. 73–75.

Magnetohydrodynamics and Aerodynamic Heating, by Rudolf X. Meyer, ARS JOURNAL, vol. 29, March 1959, pp. 187–192.

Thrust of a Conical Nozzle, by Ellis M. Landsbaum, ARS JOURNAL, vol. 29, March 1959, pp. 212–213.

Determination of Transient Pressure Flow Relationship by Momentum Measurements, by Edward J. Croke and Jerry Grey, ARS JOURNAL, vol. 29, March 1959, pp. 213–214.

Similitude Treatment of Hypersonic Stagnation Heat Transfer, by Daniel E. Rosner, ARS JOURNAL, vol. 29, March 1959, pp. 215–216.

Arc-heated Plasma for Laboratory Hypersonics, by T. R. Hogness, ASTRONAUTICS, vol. 4, March 1959, pp. 40–42, 47.

Some Basic Aspects of Magnetohydrodynamic Boundary-layer Flows, by Robert V. Hess, *NASA Memo* 4-9-59L, April 1959, 42 pp.

Compressible Non-isoenergetic Two-dimensional Turbulent (Pr = 1) Jet Mixing at Constant Pressure; Auxiliary Integrals, Heat Transfer and Friction Coefficients for Fully Developed Mixing Profiles, by H. H. Korst and W. D. Chow, *Illinois Univ. Engng. Expt. Sta., Mech. Engng. Dep., ME Tech. Note* 392–4, Jan. 1959, 35 pp.

An Unusual Aerodynamic Stagnation Temperature Effect, by I. Glassman and James E. A. John, *Project Squid, Tech. Rep.* PR-88-P (*ASTIA AD* 207534), Dec. 1958, 8 pp.

Effect of Jet Mixing on the Annular Jet, by Harvey R. Chaplin, *David Taylor Model Basin, Aerodynam. Lab., Aero Rep.* 953, Feb. 1959, 28 pp.

Interaction Experiments of Lateral Jets With Supersonic Streams, by James L. Amick, Gerard F. Carvalho and Hans P. Liepman, *Univ. Michigan* (*Bumblebee Aerodynam. Panel meeting,* Texas, University, Sept. 30–Oct. 1, 1958), 17 pp.

Discontinuity Surfaces in Magneto Fluidynamics, by Luigi G. Napolitano, *Brooklyn Polytech. Inst., Dept. Aeron., Rep.* 503 (*AFOSR TN*-59-67; *ASTIA AD* 209842), Dec. 1958, 38 pp.

Simple Vorticity Laws in Magnetohydrodynamics, by Ching-Sheng Wu, *Princeton Univ., Dep. Aeron. Engng., Rep.* 445 (*AFOSR TN* 58-1044; *ASTIA AD* 206756), Nov. 1958, 15 pp.

A Class of Exact Solutions of the Magnetohydrodynamic Navier-Stokes Equations, by Ching-Sheng Wu, *Princeton Univ., Dep. Aeron. Engng., Rep.* 436 (*AFOSR TN* 58-895; *ASTIA AD* 204 134), Sept. 1958, 11 figs., 39 pp.

The Transmission of Electromagnetic Waves in the Presence of a Conducting Layer of Gas, by G. S. S. Ludford, *Univ. Maryland, Inst. Fluid Dynam. and Appl. Math., TN* BN-160 (*AFOSR TN* 59-1 159; *ASTIA AD* 211 118), Feb. 1959, 22 pp.

The Thermal Conductivity of Carbon Dioxide in the Region of the Critical Point, by Leslie A. Guildner, *Project Squid, Tech. Rep.* MIT-19-P (*ASTIA AD* 205694), Sept. 1958. (Available only on microcards.)

Measurements of the Thermal Conductivities of Gas at High Temperatures, by Robert G. Vines, *Project Squid Tech. Rep.* MIT 20-P (*ASTIA AD* 205694), Sept. 1958, 16 pp. (Available only on microcards.)

The Ablation of Melting Bodies With Heat Penetration Into the Solid, by Theodore R. Goodman, *Allied Res. Assoc., Inc.* (*AFOSR TN* 58-789; *ASTIA AD* 202115), Aug. 1958, 20 pp.

A Shock Tube Technique to Determine Steady Flow Losses of Orifices and Other Duct Elements, by George Rudinger, *Project Squid, Tech. Rep.* CAL-77-P (*ASTIA AD* 207034), Nov. 1958, 27 pp. (Available only on microcards.)

Studies of a Prctotype Wave Superheater Facility for Hypersonic Research, by William Smith and Roger G. Weatherston, *Cornell Aeron. Lab., Inc., Rep.* HF-1056-A (*AFOSR-TR*-58-158; *ASTIA AD* 207-244), Dec. 1958, 115 pp.

Radiation from Hot Air, by J. Keck, J. Camm, B. Kivel and T. Wentink Jr., *Avco Mfg. Corp., Avco Res. Lab., Res. Rep.* 42, Feb. 1959, 50 pp.

Review of the Published Literature Pertaining to the Annular Two Phase Flow of Liquid and Gaseous Media in a Pipe, by D. A. Charvonia, *Project Squid, Tech. Rep.* PUR-32-P (ASTIA AD 208040), Dec. 1958, 42 pp.

Viscosity of Fluids at High Pressures, A Rotating Cylinder Viscometer and the Viscosity of n-Pentane, by H. H. Reamer, G. Cokelet and B. H. Sage, *Project Squid, Tech. Rep.* CIT-4-P (*ASTIA AD* 208670), Jan. 1959, 33 pp. (Available only on microcards.)

Attenuation of Radio Waves as a Result of Boundary Layer Heating in Missiles Traveling at Supersonic Speeds, by Kil-

The Checkout that says "GO" or "NO GO"

APCHE

(Pronounced "AP-SHE")

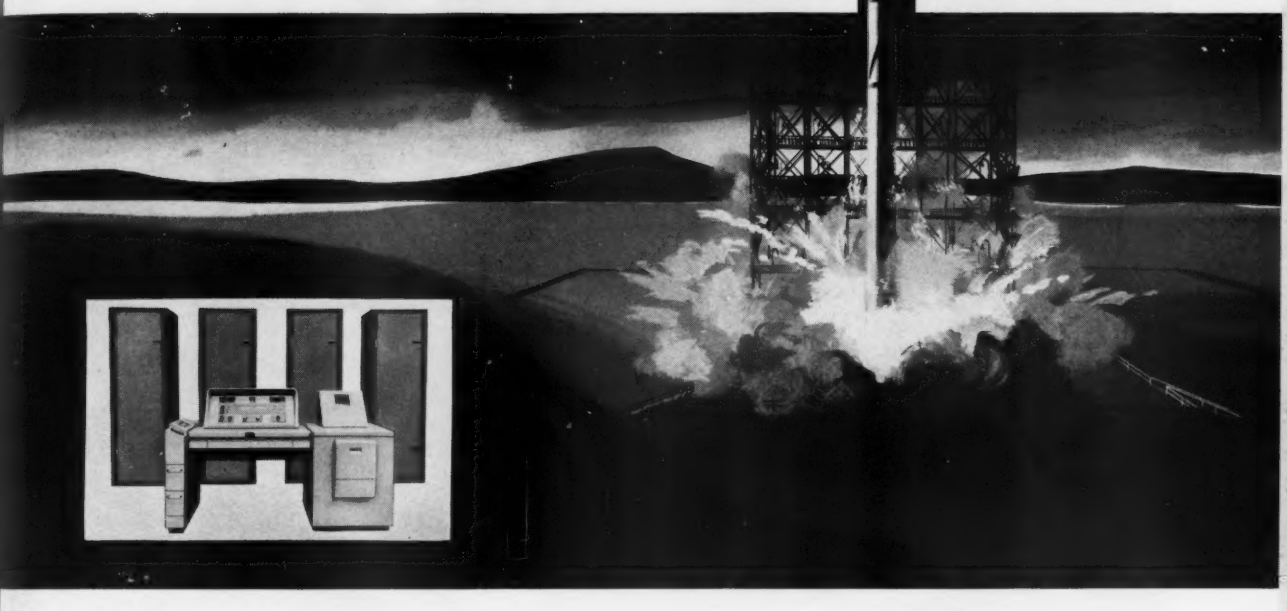

APCHE (Automatic Programmed Checkout Equipment) is a solid-state, universal, high-speed, highly reliable, compact general-purpose tester designed especially for automatic checkout of aircraft, missile and space systems and their supporting systems. In its various versions (differing in input media, size and weight) APCHE installations may be fixed, mobile, airborne or submarineborne. APCHE was designed and is being produced as a part of RCA's ground support electronics subcontract from the Convair (Astronautics) Division of General Dynamics Corporation, prime contractor for the ATLAS Intercontinental Ballistic Missile.

The system being supplied to Convair for the ATLAS Program includes a console and four rack cabinets providing both analog and discrete test functions with a resulting printed and GO-NO GO indication. As a product of RCA's Missile Electronics and Controls Department, Burlington, Massachusetts, APCHE is one of the latest RCA developments in the field of military weapon readiness equipments.

RCA Tmk(s) ®

RADIO CORPORATION of AMERICA

DEFENSE ELECTRONIC PRODUCTS • CAMDEN, NEW JERSEY

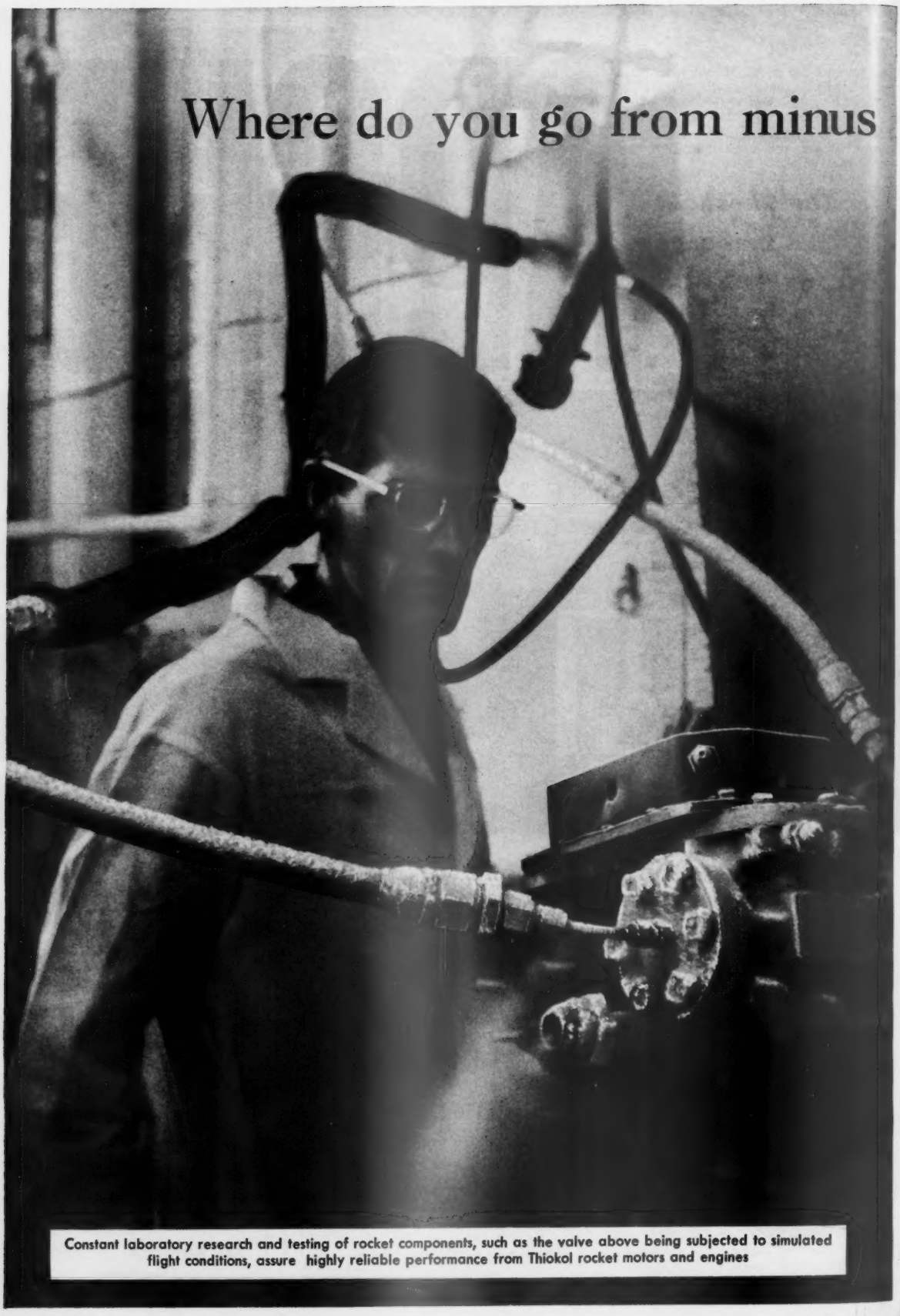

Constant laboratory research and testing of rocket components, such as the valve above being subjected to simulated flight conditions, assure highly reliable performance from Thiokol rocket motors and engines

320°F?

"Malfunction" is the most feared word a rocket scientist can hear. One of its most critical sources is *temperature.* Ranging from hundreds below zero to thousands above, temperature extremes can play havoc with milli-second performance specifications of complex valves and pumping systems.

In picture left, liquid nitrogen flowing through a turbo pump valve of a type used on the powerplant for the Air Force's X-15 drops the temperature within the valve to minus 320°F. This is slightly cooler than in actual operation, when the valve will pump highly combustible liquid oxygen (minus 297°F) and ammonia.

Laboratory tests are an essential part of the continuing research program in new materials, new design and new fuels, carried on by THIOKOL's rocket builders. In close support are the scientists of THIOKOL's Chemical Division, who continually seek new properties for their liquid polymers to meet increasing performance demands.

It is through such scientific team effort that THIOKOL has been able to design and build liquid and solid rocket propulsion systems having a remarkable record for flawless functioning.

To become a THIOKOL scientist is to enter today's most fascinating industrial arena. Challenging assignments exist for research chemists in:

Propellant Analysis; Propellant Formulation; Organic and Inorganic Polymers; Fluorine and Metal Hydrides Synthesis; High Vacuum Techniques; Fast Reaction Kinetics; Shock Wave Phenomena; Combustion Processes.

For engineers, there are scores of exciting career opportunities in the areas of servo system and electro mechanical design, in instrumentation and many other phases of advanced propulsion research.

THIOKOL plants are located in areas that are good places to live—Bristol, Pennsylvania; Elkton, Maryland; Huntsville, Alabama; Marshall, Texas; Denville, New Jersey; Trenton, New Jersey; Brigham City, Utah; Moss Point, Miss. For further information contact: Personnel Director at any plant address above.

Thiokol®

is Research to the Core

THIOKOL CHEMICAL CORPORATION

Bristol, Pennsylvania

®Registered trademark of the Thiokol Chemical Corp. for its rocket propellants, liquid polymers, plasticizers and other chemical products.

burn MacMurraugh, *NAVORD Rep.* 5816, revision I (*NOTS TP* 2163), Jan. 1959, 18 pp.

Viscous Aerodynamic Characteristics in Hypersonic Rarefied Gas Flow, by Ronald F. Probstein and Nelson H. Kemp, *Avco Mfg. Corp., Avco Res. Labs., Res. Rep.* 48, March 1959, 64 pp.

The Flow of Chemically Reacting Gas Mixtures, by J. F. Clarke, *Cranfield Coll. Aeron., Rep.* 117, Nov. 1958, 27 pp.

Superposability in Magnetohydrodynamics, by J. N. Kapur, *Appl. Sci. Res.*, Sect. A, vol. 8, no. 2–3, pp. 198–208.

Thermal Conductivity of Water at High Pressures, by A. W. Lawson, R. Lowell and A. L. Jain, *J. Chem. Phys.*, vol. 30, March 1959, pp. 643–647.

High Temperature Gas Dynamics Phenomena in Hypersonic Flight, by W. H. Wurster and C. E. Treanor, *Symposium on High-Speed Aerodynamics and Structures, 3rd, San Diego, March 25–27, 1958 (unclassified papers)*, vol. 1, pp. 89–107.

The Approach to Thermal Equilibrium in a Hypersonic Laminar Boundary Layer, by D. E. Knapp, *Symposium on High-Speed Aerodynamics and Structures, 3rd, San Diego, March 25–27, 1958 (unclassified papers)*, vol. 1, pp. 279–294.

General Characteristics of Binary Boundary Layers with Applications to Sublimation Cooling, by C. Gazley, J. Gross and D. J. Masson, *Symposium on High-Speed Aerodynamics and Structures, 3rd, San Diego, March 25–27, 1958 (unclassified papers)*, vol. 1, pp. 295–347.

A Technique for Experimental Investigation of Heat Transfer From a Surface in Supersonic Flow at Large Surface-to-Free Stream Temperature Ratios, by W. S. Bradfield, A. R. Hansom, J. J. Sheppard and R. E. Larson, *Symposium on High-Speed Aerodynamics and Structures, 3rd, San Diego, March 25–27, 1958 (unclassified papers)*, vol. 1, pp. 349–379.

Spaceflight

Low-thrust Transfer between Circular Orbits, by E. Levin, *Rand Corp.*, P-1536, Oct. 1958, 29 pp.

Problems of Range Measurement with Special Application to the Establishment of an Orbit of an Artificial Asteroid, by C. M. Crain, *Rand Corp.*, P-1518, Oct. 1958, 2 pp.

The Propagation of Errors in Keplerian Orbits, by R. T. Gabler and H. R. O'Mara, *Rand Corp.*, P-1481, Aug. 1958, 43 pp.

Some Information-theory Considerations in Space Communications, by P. Swerling, *Rand Corp.*, P-1393, Feb. 1958, 16 pp.

Communications in Space Operations, by C. M. Crain and R. T. Gabler, *Rand Corp.*, P-1394, Feb. 1958, 16 pp.

Space Communications, by Peter Swerling, *Rand Corp.*, P-1443, Dec. 1958, 5 pp.

Preliminary Analysis of a Satellite Recovery System, by Richard H. Frick, *Rand Corp.*, RM-2264 (*ASTIA AD* 209777), Sept. 1958, 47 pp.

On-off Control System for Attitude Stabilization of a Space Vehicle, by Josef S. Pistiner, ARS JOURNAL, vol. 29, April 1959, pp. 283–289.

Circular Orbit Stability in the Oblate Earth's Equatorial Plane, by Marvin H. Hewitt, ARS JOURNAL, vol. 29, April 1959, pp. 295–296.

Orientation of Research Needs Associated with Environment of Closed Spaces, by William T. Ingram, *J. Astron. Sci.*, vol. 5, Autumn-Winter 1958, pp. 51–57.

Temperature Equilibria in Space Vehicles, by R. A. Cornog, *J. Astron. Sci.*, vol. 5, Autumn-Winter 1958, pp. 64–67.

On the Motions of Rotating Satellites and Double Stars According to the Einstein Gravitation Theory, by N. St. Kalitzin, *Nuovo Cimento*, vol. 11, no. 2, Jan. 16, 1959, pp. 178–185. (In German.)

Minimal Impulse Requirements for Disorbiting Satellites, by I. S. Blumenthal, *Rand Corp.*, RM-2276 (*ASTIA AD* 209442), Oct. 1958, 25 pp.

Earth-period (24-hour) Satellites, by J. H. Hutchinson, *Rand Corp.*, P-1460, Aug. 1958, 18 pp.

Atmospheric Perturbations of Artificial Satellites, by E. Leeper, *Rand Corp.*, P-1496, Sept. 1958, 9 pp.

Physics of Solar-terrestrial Space: Lunar Flight, by E. H. Vestine, *Rand Corp.*, P-1344, Feb. 1958, 18 pp.

A Possible Transponding System for an Artificial Asteroid, by P. Swerling and C. M. Crain, *Rand Corp.*, RM-2172 (*ASTIA AD* 156036), 35 pp.

Prologue to a Syntax of Space Exploration, by A. G. Wilson, *Rand Corp.*, P-1425, July 1958, 11 pp.

The Space Environment, by A. G. Wilson, *Rand Corp.*, P-1427, Feb. 1958, 19 pp.

Types of Space Flights, by R. W. Buchheim, *Rand Corp.*, P-1428, Feb. 1958, 28 pp.

Some Aspects of Astronautics, by R. W. Buchheim, S. Herrick, E. H. Vestine and A. G. Wilson, *Rand Corp.*, P-1442, Dec. 1958, 12 pp.

Interplanetary Exploration, by A. G. Wilson, *Rand Corp.*, P-1432, Feb. 1958, 11 pp.

Cosmic Terrestrial Relations, by H. Korf Kallmann, *Rand Corp.*, P-1553, Nov. 1958, 6 pp.

The Space Environment, by S. H. Dole, *Rand Corp.*, P-1499, Sept., 1958, 18 pp.

Interplanetary Trajectories Under Low Thrust Radial Acceleration, by Jack Copeland, ARS JOURNAL, vol. 29, April 1959, pp. 267–271.

Reduction of Flight Time and Propellant Requirements of Satellites with Electric Propulsion by the Use of Stored Electrical Energy, by Morton Camac, *Avco Mfg. Corp., Avco Res. Lab. Div., Res. Rep.* 36 (*AFOSR-TN* 58-1013; *ASTIA AD* 206-156), Oct. 1958, 26 pp.

Orbital Storage of Cryogenic Fluids, by Kenneth R. Cramer, *Wright Air Dev. Center, TN* 58-282 (*ASTIA AD* 203527), Oct. 1958, 7 pp.

Space Trajectories and Flight Test Objectives, by J. W. Luecht, *SAE Preprint* 58, Jan. 1959, 6 pp.

Photochemistry of the Upper Atmosphere as a Source of Propulsive Power, by A. F. Charwat, ARS JOURNAL, vol. 29, Feb. 1959, pp. 108–114.

Two Simple Equations for Orbital Mechanics, by W. H. T. Loh, ARS JOURNAL, vol. 29, Feb. 1959, pp. 146–147.

Terminal Phase of Satellite Entry into the Earth's Atmosphere, by Elliott D. Katzen, ARS JOURNAL, vol. 29, Feb. 1959, pp. 147–148.

Determination of Elements of an Elliptic Orbit from the Orbital Velocity Vector, by H. Munick, ARS JOURNAL, vol. 29, Feb. 1959, p. 150.

Optimum Thrust Programming along Arbitrarily Inclined Rectilinear Paths, by A. Miele and C. R. Cavoti, *Astronautica Acta*, vol. 4, no. 3, 1959, pp. 167–181.

Heating of a Rocket Body in the Atmosphere, by W. Strubell, *Astronautica Acta*,

EXPLORE NEW AREAS AT IBM IN COMPUTER SYSTEMS

Now under development at IBM are new and unusual electronic computing systems that will greatly strengthen man's control of his environment. In one project, for example, advances in acoustics, oceanography, and information theory are being coordinated to yield a data system that will sentinel the ocean's depths. Another group is applying a computer's logic and computational capabilities to analyze, correlate, and identify input signals to data acquisition systems. In the late development stage is an extremely high-speed, large-capacity computing system which will automatically handle the large volume of detailed records and communications required by a nationwide sales operation. To staff such efforts, scientists, mathematicians, and engineers of vision are needed.

IBM's rapid expansion provides many opportunities for you to advance—either through technical achievement or engineering administration. You may work independently or with a small team, and you can choose your assignments from a broad range of research and development areas. Specialists of many different backgrounds are available to assist you in your work. This is an excellent opportunity for a scientific or engineering career that combines maximum growth potential with job stability.

QUALIFICATIONS: B.S. or advanced degree in Electrical or Mechanical Engineering, Physics or Mathematics—and proven ability to assume a high degree of technical responsibility in your assignments.

TYPICAL ASSIGNMENTS

Planning and logical design of solid state computers, input-output systems, and peripheral equipment. Knowledge of digital systems required with experience in transistor circuitry and switching techniques.

Analysis of ferrite "memory" and buffer systems and design of new high-speed configurations, including drive and addressing circuitry, for advanced solid state data processing systems. Familiarity with digital computer systems and magnetic core "memory" design.

Solutions of real-time control problems with digital techniques; mathematical analysis of navigation and fire control systems, ray tracings, and signal cross-correlations.

Application of information theory to signal processing. Familiarity with signal cross-correlation techniques, statistical data processing, sampled-data control theory, analog-digital data processing techniques, signal propagation, and beam formation. Naval experience required in at least one of these specialties: sonar, fire control, ASW, navigational systems, signal processing.

Investigation of new computer applications and techniques, based on observation and analysis of customer needs; establishment of broad systems concepts, assisting in both logic and machine design. Experience required in digital computer applications, technical organization of a medium or large machine installation.

Circuit design of advanced data processing systems and input-output equipment, working closely with logic designers. Experience required in design of arithmetical control and switching circuitry to reduce logic diagrams to component counts for cost-estimating development.

Application of transistor-diode logic to develop advanced circuitry; review of new circuits for possible use in digital control systems, defining basic techniques for improving performance characteristics.

Laboratory facilities are located in Endicott, Poughkeepsie, Kingston, Owego, and Yorktown Heights, N. Y.; Lexington, Ky.; and San Jose, California.

CAREERS ALSO AVAILABLE IN THESE AREAS . . .

Acoustics
Applied mathematics & statistics
Applied physics
Circuit design & development
Component engineering
Computer analysis
Cryogenics
Flight test analysis
Human factors
Inertial guidance
Information retrieval
Logical design
Magnetics
Microwaves
Operations research
Programming
Radar circuitry
Transistor circuit design

For details, write, outlining background and interests, to:

Mr. R. E. Rodgers, Dept. 572L
IBM Corporation
590 Madison Avenue
New York 22, N. Y.

IBM®

INTERNATIONAL BUSINESS MACHINES CORPORATION

vol. 4, no. 3, 1958, pp. 182–187. (In German.)

Observation of a Satellite near Its Culmination, by A. Boni, *Astronautica Acta*, vol. 4, no. 3, 1958, pp. 188–217.

Optimal Escape from a Circular Orbit, by D. F. Lawden, *Astronautica Acta*, vol. 4, no. 3, 1958, pp. 218–233.

Russian Technical Articles

Determination of Thermal Conductivity Coefficients of Gases with a Universal Plane Bicalorimeter, by G. M. Levin, *Instruments and Experimental Techniques (Translation of Pribory i Tekhnika Eksperimenta)*, no. 1, Jan.-Feb. 1958, p. 112.

Calculation and Design of Precision Thermostats, by V. V. Grigor'iants and M. E. Zhabotinskii, *Instruments and Experimental Techniques (Translation of Pribory i Tekhnika Eksperimenta)*, no. 1, Jan.-Feb. 1958, p. 117.

The Lighting of Gas Discharge Devices, by T. A. Sanina, A. A. Saninand and N. R. Fedorenkova, *Instruments and Experimental Techniques (Translation of Pribory i Tekhnika Eksperimenta)*, no. 1, Jan.-Feb. 1958, p. 129.

A Quick-Acting Resistance Thermometer, by V. A. Zamkov, *Instruments and Experimental Techniques (Translation of Pribory i Tekhnika Eksperimenta)*, no. 1, Jan.-Feb. 1958, p. 150.

Hydraulic Frictional Resistance to Flow of a Steam/Water Mixture in a Straight Horizontal Tube, by S. I. Kosterin and B. I. Sheynin, *Teploenergetika*, no. 6 (USSR), 1958, pp. 71–76. (In Russian.)

Heat Transfer During the Surface-Boiling of Water, by P. G. Poletavkin and N. A. Shapkin, *Teploenergetika*, no. 5 (USSR), 1958, pp. 49–54. (In Russian.)

On the Resistance and Heat Exchange in a Pulsating Flow, by K. P. Vishnevskiy, *Sb. nauchn. tr. Kuybyshevsk. industr. im-t*, no. 6, Book 1, 1956, pp. 207–212. (In Russian.)

Heat Transfer of a Round Cylinder in a Cross-Flow of a Pourable Substance (Sand), by S. V. Donskov, *Teploenergetika*, no. 10 (USSR), 1958, pp. 65–71. (In Russian.)

Heat Transfer of Tube Bundles in a Transverse-Flow of Pourable Substance (Sand), by S. V. Donskov, *Teploenergetika*, no. 11 (USSR), 1958, pp. 76–80. (In Russian.)

Heat Transfer to Liquid Metals, by S. S. Kutateladze, V. M. Borishansky and I. I. Novikov, *Atomnaya Energiya*, vol. 4, no. 5 (USSR), 1958, p. 422. (In Russian.)

Determination of the Degree of Blackness of Metals at High Temperatures by the Method of Regular Conditions, by V. A. Osipova, *Teploenergetika*, no. 4 (USSR), 1958, pp. 59–63. (In Russian.)

On the Heat Exchange in a Field Affected by Centrifugal Forces, by A. E. Kovalevskaya and R. G. Perel'man, *Akad. Nauk SSSR, Izvestiia, Otdelenie Tekh. Nauk*, no. 11 (USSR), 1958, pp. 92–94. (In Russian.)

The Formation of Turbulent Flow in the Presence of Free Convection, by D. F. Pavlov, Tr., *Sredneaz, un-ta*, no. 91, 1957, pp. 67–87. (In Russian.)

The Thermal Conductivity of Liquid Fuels, by V. N. Popov and N. V. Tsederberg, *Teploenergetika*, no. 11 (USSR), 1958, pp. 72–76. (In Russian.)

The Oscillations of a Degenerate Electron Fluid, by V. P. Silin, *Soviet Phys. JETP*, vol. 35 (8), May 1959, pp. 870–874.

Hydrodynamic Analysis of the Compression of a Rarefied Plasma in an Axially-Symmetric Field, by Iu. N. Barabanenkov, *Soviet Phys. JETP*, vol. 35 (8), May 1959, p. 893.

Diffraction Breakup of Light Nuclei, by A. G. Sitenko and Iu. A. Berezhnoi, *Soviet Phys. JETP*, vol. 35 (8), May 1959, pp. 899–900.

On Traveling Waves of Gas Dynamic Equations, by Iu. Ia. Pogodin, V. R. Suchov and N. N. Ianenko, *J. Appl. Math. Mech.* (*Translation of Prikladnaya Matematika i Mekhanika*), vol. 22, no. 2, 1958, pp. 256–267.

On the Propagation of Strong Discontinuities in a Multi-Component Medium, by Ia. Z. Klieman, *J. Appl. Math. Mech.* (*Translation of Prikladnaya Matematika i Mekhanika*), vol. 22, no. 2, 1958, pp. 268–278.

Flow with Detached Shock Wave about a Symmetrical Profile, by O. M. Belotserkovskii, *J. Appl. Math. Mech.* (*Translation of Prikladnaya Matematika i Mekhanika*), vol. 22, no. 2, 1958, pp. 279–296.

On the Stability of Some Particular Cases of Motion of a Symmetrical Gyroscope Containing Liquid Mass, by S. V. Zhak, *J. Appl. Math. Mech.* (*Translation of Prikladnaya Matematika i Mekhanika*), vol. 22, no. 2, 1958, pp. 330–337.

Index of Papers Published in ARS JOURNAL

Volume 29—January through December 1959

Issue	Pages
January	1–88
February	89–168
March	169–240
April	241–320
May	321–392
June	393–476
July	477–548
August	549–620
September	621–692
October	693–812
November	813–892
December	893–1008

TN, TC, and SA indicate Technical Note, Technical Comment, and Survey Article, respectively. RS indicates supplement of translated Russian articles, October issue.

AUTHORS

ADAMS, MAC C.
Recent Advances in Ablation (SA).... 625

AMSTER, ADOLPH B. and LEVY, JOSEPH B.
Solubility of Air, N_2 and O_2 in n-Propyl Nitrate (TN)..... 870

ANDERSEN, W. H. and CHAIKEN, R. F.
Application of Surface Decomposition Kinetics to Detonation of Ammonium Nitrate (TN)..... 49

ANTHONY, G. W., *see* WANG, C. J.

AROESTY, J., *see* SCHAAF, S. A.

BADE, W. L.
Simple Analytical Approximation to the Equation of State of Dissociated Air (TN)..... 298
See also JOHN, R. R..

BAKER, ROBERT M. L., JR.
Application of Astronomical Perturbation Techniques to the Return of Space Vehicles..... 207

BANTA, H. E., *see* MOAK, C. D.

BASEVICH, V. YA. and KOGARKO, S. M.
Structure of Turbulent Flame of Homogeneous and Heterogeneous Mixtures (RS)..... 756

BAUER, ERNEST and ZLOTNICK, MARTIN
Transport Coefficients of Air to 8000 K 721

BAULKNIGHT, CHARLES W., *see* SCALA, SINCLAIRE M.

BENEDIKT, E. T.
Scale of Separation Phenomena in Liquids Under Conditions of Nearly Free Fall (TN)..... 150

BENEZRA, JOSEPH N.
A Short Form Method for Determining Near-Circular Orbit Quantities (TN) 216

BERGER, W. J. and RICUPITO, J. R.
Prediction Theory of Missile and Satellite Orbits..... 428

BOCK, CHARLES D. and MUNDO, CHARLES, J.
Guidance Techniques for Interplanetary Travel..... 931

BOGGESS, R. L., *see* SPENCER, N. W.

BOHL, RICHARD J., *see* FELIX, BERNARD R.

BOISON, J. CHRISTOPHER and CURTISS, HOWARD A.
An Experimental Investigation of Blunt Body Stagnation Point Velocity Gradient..... 130

BOYARS, CARL
Surveillance of Solid Propellant Rockets (TN)..... 148

BOYD, BEMROSE
Motion Units to Simplify Space Travel Computations (TN)..... 216

BRAGG, S. L.
Changes in the Density and Temperature of Liquid Propellants in Rocket Engine Supply Systems (TN)..... 672
Comments on "Recent Advances in Cryogenic Engineering" (TC)..... 875

BRICE, DONAT B. and FISHMAN, NORMAN
Some Physical Properties for the System Nitrogen Tetroxide-Nitric Oxide.... 354

BROGAN, THOMAS R.
The Electric Arc Wind Tunnel—A Tool for Atmospheric Re-Entry Research. 648
Preliminary Evaluation of Helium as an Electric Arc Heated Propellant (TN) 662

BUILDER, CARL H.
General Solution for Optimization of Staging of Multistaged Boost Vehicles 497

BUTLER, JAMES N., *see* POTTER, A. E., JR.

CAMBEL, ALI BULENT, *see* LIU, CHING-SHI

CAMPBELL, GEORGE S.
Long Period Oscillations During Atmospheric Entry (TN)..... 525

CAPLAN, M. L., *see* MCJONES, R. W.

CARPENTER, RICHARD A.
Recent Advances in Boron Technology (SA)..... 8

CARTER, JAMES M., *see* GREEN, LEON, JR.

CHAIKEN, R. F., *see* ANDERSEN, W. H.

CHAO, GEORGE T. Y.
Isothermal Compressibility of Liquid Oxygen and RP-1..... 199

CHARWAT, A. F.
Photochemistry of the Upper Atmosphere as a Source of Propulsive Power 108

CHENG, SIN-I
Meteoric Ablation Through Interfacial Instability..... 579

CHERNOV, V. N. and YAKOVLEV, V. I.
Research on the Flight of a Living Creature in an Artificial Earth Satellite (RS)..... 736

CHINITZ, W., EISEN, C. L. and GROSS, R. A.
Aerothermodynamic and Electrical Properties of Some Gas Mixtures to Mach 20..... 573

COHEN, CLARENCE B., *see* LEES, LESTER
See also PHILLIPS, RICHARD L.

COLE, DANDRIDGE M. and MARRESE, MICHAEL A.
Optimization of Rockets for Maximum Payload Energy (TN)..... 71

COLICHMAN, E. L., *see* LOGAN, J. G.

COPELAND, JACK
Interplanetary Trajectories Under Low Thrust Radial Acceleration..... 267

CORNOG, ROBERT
Some Economic Aspects of Hypersonic Flight..... 706

CROKE, EDWARD J. and GREY, JERRY
Determination of Transient Pressure Flow Relationship by Momentum Measurements (TN)..... 213

CURTISS, HOWARD A., *see* BOISON, J. CHRISTOPHER

DEMETRIADES, ANTHONY
Heat Conduction in a Circular Cylinder Rotating With Its Axis Normal to the Direction of Flight..... 653

DEMETRIADES, S. T. and FARBER, M.
Theoretical Study of Recombination Kinetics of Atomic Oxygen (TN)... 528

DEMETRIADES, STERGE T.
Comments on "Photochemistry of the Upper Atmosphere as a Source of Propulsive Power" (TC)..... 375

DENHARD, WILLIAM G., *see* HOVORKA, JOHN

DICKEY, F. L. and KNIPP, G. H.
Sealed Cabin Reliability as Related to Structure and Internal Atmosphere.. 656

DUGGER, GORDON L.
Recent Advances in Ramjet Combustion (SA)..... 819

DWORETZKY, L. H. and EDWARDS, A.
Principles of Doppler-Inertial Guidance 967

EDELBAUM, T. N.
Some Extensions of the Hohmann Transfer Maneuver (TN)..... 864

EDELBAUM, THEODORE N.
Further Comments on the Powered Flight Trajectory of a Satellite (TC) 374

EDWARDS, A., *see* DWORETZKY, L. H.

EDWARDS, R. H.
Solution to the Linearized Quasi-Stationary External Diffuser Equations (TN)..... 54

EISEN, C. L., *see* CHINITZ, W.

ELLIS, JAMES W. and MCARTHUR, CHARLES W.
Applicability of Euler's Dynamical Equations to Rocket Motion (TN).. 863

ESSES, HARRY
Maximum Ejection Velocity for Return From Satellite Orbits (TN)..... 592

EVANS, MARTHA W. and HARLOW, FRANCIS H.
Calculation of Unsteady Supersonic Flow Past a Circular Cylinder (TN) 46

FAIN, W. W. and GREER, B. J.
Electrically Charged Bodies Moving in the Earth's Magnetic Field (TN)... 451

LIQUID NITROGEN

...AT THE TOUCH OF A BUTTON

Supplies laboratory or plant needs swiftly and economically

Convenience is unmatched. A ready supply of liquid nitrogen always available —literally at the touch of a button. Supply is obtainable days, nights, weekends or holidays – it is not subject to outside influences over which you have no control such as routing or delivery schedules.

The Norelco Liquid Nitrogen Generator consists of a single atmosphere separation column that employs a Norelco Gas Liquefier as the nitrogen condenser. Operating as a completely integrated and self-contained system, the generator produces pure liquid nitrogen from air. *An oil-free product is assured since neither nitrogen nor air ever comes in contact with oily surfaces of working parts.* There are no moving parts in nitrogen separation column. The Norelco Nitrogen Generator does not require expert supervision for operation. Automatic controls provide continuous reliable service.

Startling economies are available with the Norelco Liquid Nitrogen Generator. The unit produces an average of six liters of pure, (99.5%) liquid nitrogen per hour over an uninterrupted period of up to 200 hours. (Production figures are based on average locations and operating conditions. Output will vary according to altitude, humidity, temperature, etc.) On a regular production basis, cost per liter is but a small fraction of most existing commercial rates.

Vaporization losses are reduced to an absolute minimum. Users of moderate quantities of liquid nitrogen order in excess of actual requirements in order to insure adequate supply of this vital product. Losses are considerable, particularly if the commercial source is some distance away.

The Norelco Liquid Nitrogen Generator is supplied as a packaged unit ready for immediate installation. Present users of the Norelco Gas Liquefier may add the nitrogen separation column and convert their unit to liquid nitrogen production. *Send for details today!*

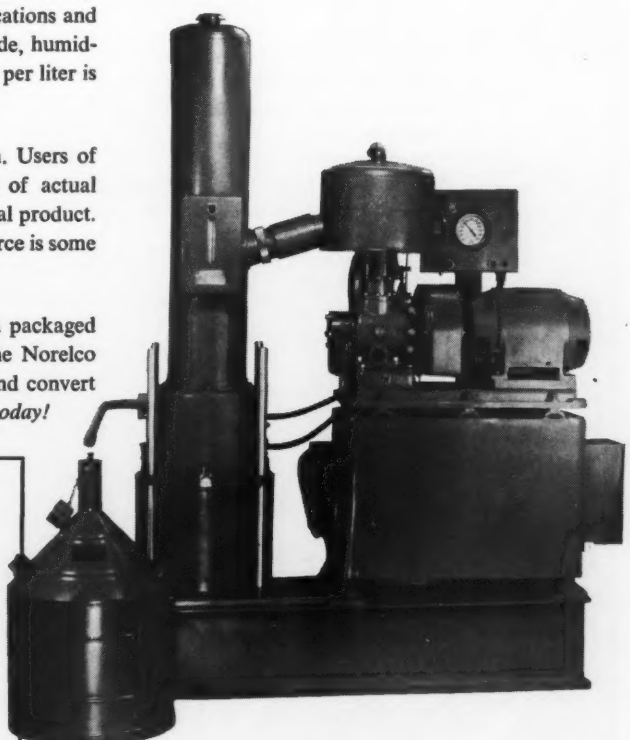

FEATURES

1. Low Cost
2. Fresh supply always available
3. Clean, *oil-free* product
4. High purity product
5. No evaporation or storage problems
6. No compressed air necessary
7. No expert supervision required
8. High production yield
9. Automatic controls for continuous reliable service

NORTH AMERICAN PHILIPS COMPANY, Inc.

Cryogenics Division 100 STEVENS AVENUE, MOUNT VERNON, N. Y.

A Professional Future

for

Physicists

and

Electronics Engineers

The Laboratory, with its staff of 900 employees, is primarily engaged in the conception and perfection of completely automatic control systems necessary for the flight and guidance of aircraft, missiles and space vehicles.

R and D opportunities exist in:

- System Design & Theoretical Analysis
- Astronautics
- High Performance Servomechanisms
- Power Supplies
- Magnetic Amplifiers
- Analog and Digital Computers
- Electro-mechanical Components
- Transistor Circuitry
- Printed Circuitry
- Environmental Instrumentation & Evaluation
- Research, Design & Evaluation of Gyroscopic Instruments
- Computer Programming
- Simulator Studies
- Classical Mechanics
- Optical Instrumentation
- Pulse Circuitry
- and in many other areas.

Call or write:

DR. C. S. DRAPER
Director

INSTRUMENTATION LABORATORY

MASSACHUSETTS INSTITUTE OF TECHNOLOGY

68 Albany Street
Cambridge 39, Massachusetts
UNiversity 4-6900, Ext. 3544

*Graduate courses may be taken for credit while earning full pay. • U. S. Citizenship Required

FALES, E. N., *see* GROVER, J. H.
FANSELAU, R. W.
Comments on "Exhaust Nozzle Contour for Maximum Thrust" (TC) 456
FARBER, M., *see* DEMETRIADES, S. T.
FEILER, CHARLES E.
Reflection of Weak Shock Waves From Nozzles With No Flow and Critical Flow 272
FELIX, BERNARD R. and BOHL, RICHARD J.
Dynamic Analysis of a Nuclear Rocket Engine 853
FISHMAN, NORMAN, *see* BRICE, DONAT B.
FLETCHER, EDWARD A., *see* SCHALLA, ROSE L.
FORDYCE, SAMUEL W.
Simple Method of Estimating the Variation of Impact Points for Ballistic Missiles (TC) 876
FREE, B. A. and SARNER, S. F.
A Rapid Method for Estimation of Specific Impulse (TN) 64
FREY, E. J., *see* HOVORKA, JOHN
FRIED, WALTER R.
Doppler Radars for Guidance—Design Techniques and Performance 957
FRIEDLANDER, S. K.
Particle Impaction on Spheres at High Mach Numbers (TN) 296
FRIEDMAN, HERBERT
IGY Solar Flare Program and Ionizing Radiation in the Night Sky 103
FRYE, WILLIAM E. and STEARNS, EDWARD V. B.
Stabilization and Attitude Control of Satellite Vehicles 927
GALL, JOHN F.
Recent Advances in Fluorine Chemistry and Technology (SA) 95
GEIGER, R. E., *see* NAGAMATSU, H. T.
GERSTEIN, MELVIN
Correlation and Prediction of Flame Properties With Special Reference to Liquid Hydrazine 514
GILINSON, P. J., JR., *see* HOVORKA, JOHN
GOL'DENBERG, S. A. and PELEVIN, V. S.
Effect of Pressure on the Speed of Flame Propagation in a Turbulent Stream (RS) 765
GOLDSMITH, MARTIN
Augmentation of Nuclear Rocket Specific Impulse Through Mechanical-Electrical Means (TN) 600
GORDON, JOHN S.
Comment on "Performance Calculations for Hybrid Nuclear-Chemical Rocket Propulsion Systems" (TC) 455
Estimation of Performance of Fuels With Hydrogen Peroxide Oxidizer (TN) 530
Remark on Thermodynamics of Al_2O_3 (TC) 455
GOULARD, ROBERT
Optimum Magnetic Field for Stagnation Heat Transfer Reduction at Hypersonic Velocities (TN) 604
GREEN, LEON, JR. and CARTER, JAMES M.
Performance Calculations for Hybrid Nuclear-Chemical Rocket Propulsion Systems 180
GREER, B. J., *see* FAIN, W. W.
GRETZ, RICHARD, *see* STAROS, BASIL
GREY, JERRY, *see* CROKE, EDWARD J.
GRIFFIN, DONALD N., TURNER, CHARLES F. and ANGELOFF, GEORGE T.
A Ballistic Bomb Method for Determining the Experimental Performance of Rocket Propellants 15
GROHE, LESTER R., *see* HOVORKA, JOHN
GROSS, R. A. and OPPENHEIM, A. K.
Recent Advances in Gaseous Detonation (SA) 173
See also CHINITZ, W.
GROSS, ROBERT A.
Research on Supersonic Combustion (TN) 63
GROVER, J. H., FALES, E. N. and SCURLOCK, A. C.
Turbulent Flame Studies in a Two-Dimensional Open Burner 275
GUMAN, WILLIAM J.
Comment on "Frictional Electricity in Missile Systems" (TC) 374
GUSTAFSON, W. A.
Aerodynamic Moment on Bodies Moving at High Speed in the Upper Atmosphere (TN) 301
HAEUSSERMANN, WALTER
An Attitude Control System for Space Vehicles 203

Spatial Attitude Control of a Spinning Rocket Cluster (TN)..... 56
HANEL, R. A.
Thermostatic Temperature Control of Satellites and Space Vehicles (TN). 358
HARLOW, FRANCIS H., *see* EVANS, MARTHA W.
HARTWIG, FREDERIC W., *see* LEES, LESTER
HEIDMANN, MARCUS F., *see* PRIEM, RICHARD J.
HEWITT, MARVIN H.
Circular Orbit Stability in the Oblate Earth's Equatorial Plane (TN)..... 295
Stability of a Globular Cluster in the Oblate Earth's Equatorial Plane (TN) 595
HOENIG, STUART A
Use of a Catalytic Probe for Detection of Dissociated Nonequilibrium States in Hypersonic Flow (TN)..... 361
HOROWITZ, R., *see* SPENCER, N. W.
HORSFALL, R. B.
Celestial Guidance..... 981
HOVORKA, JOHN, HURSH, JOHN W., FREY, E. J., DENHARD, WILLIAM G., GROHE, LESTER R., GILINSON, P. J., JR. and VANDER VELDE, W. E.
Recent Progress in Inertial Guidance... 946
HUPPERT, PAUL A.
New Aspects in Ceramic Coatings..... 19
HURLBUT, F. C., *see* SCHAAF, S. A.
HURSH, JOHN W., *see* HOVORKA, JOHN
HUTCHESON, J. H.
Earth-Period (24-Hr) Satellites..... 849
JACOBS, ROBERT B.
Recent Advances in Cryogenic Engineering (SA)..... 245
JASPER, NIELS *and* TEUBER, DIETER
The Cluster Spin Control System for Jupiter C Missiles (TN)..... 58
JOHN, R. R. and RECESSO, J.
Ablation Characteristics of a Subliming Material Using Arc Heated Air (TN) 663
JOHN, R. R. and BADE, W. L.
Stagnation Point Heat Transfer in a Subsonic Jet of Arc-Heated Air (TN) 523
JOHNSON, J. W., *see* MOAK, C. D.
KATZEN, ELLIOTT D.
Terminal Phase of Satellite Entry Into the Earth's Atmosphere (TN)..... 147
KELLY, ARNOLD J.
Effect of Thrust Termination Process Upon Range Dispersion of a Ballistic Missile 432
KING, R. F., *see* MOAK, C. D.
KNIGHT, W. P., *see* LAWRENCE, R. W.
KNIPP, G. H., *see* DICKEY, F. L.
KOGARKO, S. M., *see* BASEVICH, V. YA.
KOMISSAROV, O. D., NAZAROVA, T. N., NEUGODOV, L. N., POLOSKOV, S. M. and RUSAKOV, L. Z.
Investigation of Micrometeorites With the Aid of Rockets and Satellites (RS) 742
KOZACHENKO, L. S.
Effect of Flow Pulsations on the Turbulent Speed of Flame Propagation (RS) 761
KRAMER, SAUNDERS B.
Velocity of Tank Fragments (TN).... 363
KVASNIKOV, A. V.
Estimate of Internal Losses in a Liquid Fuel Jet Engine Chamber (RS)..... 745
LAGOW, H. E., *see* SPENCER, N. W.
LAITONE, E. V.
Effect of Acceleration on the Longitudinal Dynamic Stability of a Missile... 137
LANDSBAUM, ELLIS M.
Thrust of a Conical Nozzle (TN)..... 212
LAWRENCE, H. R., *see* WANG, C. J.
LAWRENCE, R. W. and KNIGHT, W. P.
Improvements in the Operating Characteristics of n-Propyl Nitrate..... 29
LEES, LESTER
Similarity Parameters for Surface Melting of a Blunt Nosed Body in a High Velocity Gas Stream..... 345
LEES, LESTER, HARTWIG, FREDERIC W. and COHEN, CLARENCE B.
Use of Aerodynamic Lift During Entry Into the Earth's Atmosphere..... 633
LEVY, JOSEPH B., *see* AMSTER, ADOLPH B.
LIEPMAN, H. P.
On the Use of Side-Jets as Control Devices (TN)..... 453
LIU, CHING-SHI and CAMBEL, ALI BULENT
Magnetogasdynamic Flow Regimes (TN) 871
LOGAN, J. G. and COLICHMAN, E. L.
Effect of Dissociation on the Performance of Working Fluids for Nuclear Propulsion 409

MISSILE HARDWARE
by NEWBROOK

- MOTOR CASES
  Solid and Liquid Propellants
- PLENUM CHAMBERS
- JATO CASES
- BLAST TUBES
- NOZZLES
- FUEL INJECTORS

The newest addition to the Quality Control facilities at Newbrook is the Hydrostatic Test Cell illustrated below. All controls are on the outside. A T.V. Camera inside the cell enables the engineers to watch the test on a T.V. screen. This is only one of many projects at this modern plant manned and equipped to produce the finest in missile components.

Hydrostatic Test Cell

Finest Welding Facilities
Certified Welders

X-Ray Inspection

Below: Machining Motor Cases

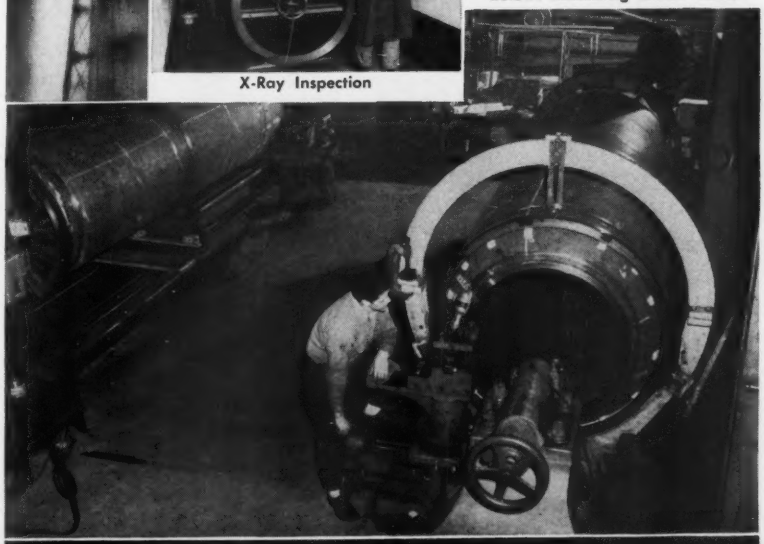

Newbrook
MACHINE CORPORATION

45 MECHANIC ST. Phone: Yellowstone 4-2644 SILVER CREEK, N. Y.

LOH, W. H. T.
Hypervelocity Vehicles at Large Angles of Inclination (TN) 522
Minor Circle Flight for Boost-Guide Vehicles (TN) 300
Minor Circle Flight for Orbital Launched or Boost-Glide Vehicles (TN) 789
Two Simple Equations for Orbital Mechanics (TN) 146
LOVE, E. S.
Prediction of Inviscid Induced Pressures From Round Leading Edge Blunting at Hypersonic Speeds (TN) 792
LUDLOFF, H. F.
Magnetic Boundary Layers (TN) 590
MCARTHUR, CHARLES W., *see* ELLIS, JAMES W.
MCJONES, R. W. and CAPLAN, M. L.
Generalized Solution for the Problem of Pipe Flow With Friction and Heat Addition (TN) 366
MCMANUS, H. N., JR.
Effect of Unequal Wall Roughness on Flow Between Flat Plates (TN) 144
MANDELL, MERVIN, *see* STAROS, BASIL
MARKSTEIN, GEORGE H.
Graphical Computation of Shock and Detonation Waves in Real Gases (TN) 588
MARRESE, MICHAEL A., *see* COLE, DANDRIDGE M.
MARTELLUCCI, ANTHONY, *see* VISICH, MARIAN, JR.
MAYER, E.
Vaporization Rate Limited Combustion in Bipropellant Rocket Chambers ... 505
MEAD, G. A.
Compression Sensitivity of Monopropellants 192
Relation of Droplet Consumption Rates to Liquid Strand Consumption Rate (TN) 440
MEYER, RUDOLPH X.
Magnetohydrodynamics and Aerodynamic Heating 187
MICKELWAIT, AUBREY B.
Lunar Trajectories 905
MIELE, ANGELO
Interrelationship of Calculus of Variations and Ordinary Theory of Maxima and Minima for Flight Mechanics Applications (TN) 75
MOAK, C. D., BANTA, H. E., JOHNSON, J. W. and KING, R. F.
New Ion Source for Propulsion of Space Vehicles (TN) 868
MOLMUD, P.
Frictional Electricity in Missile Systems (TN) 73
MUNDO, CHARLES J., *see* BOCK, CHARLES D.
MUNICK, H.
Determination of Elements of an Elliptic Orbit From the Orbital Velocity Vector (TN) 150
An Optimum Transfer Path From an Elliptical Orbit to a Higher Energy Circular Orbit (TN) 449
NAGAMATSU, H. T., GEIGER, R. E. and SHEER, R. E., JR.
Hypersonic Shock Tunnel 332
NAZAROVA, T. N., *see* KOMISSAROV, O. D.
NEUGODOV, L. N., *see* KOMISSAROV, O. D.
NEWBAUER, JOHN A.
Soviet Technical Literature in Translation (RS) 730
NEWGARD, JOHN J.
Utilization of Stored Energy in Solid Material as an Added Energy Source (TN) 603
NEWTON, ROBERT R.
Method of Stabilizing an Astronomical Satellite (TN) 665
NICHOLLS, J. A.
Stabilized Gaseous Detonation Waves (TC) 607
O'KEEFE, JOHN A.
IGY Results on the Shape of the Earth. 902
OLDS, R. H.
Optimum Proportioning of Two Propellants to Obtain Maximum Burnt Velocity (TN) 598
OPPENHEIM, A. K., *see* GROSS, R. A.
OSBORN, J. R., *see* ZUCROW, M. J.
PAGE, R. H.
On Turbulent Supersonic Diabatic Wakes (TN) 443
PALMER, HOWARD B.
Burning Rate of an H-Atom Propellant (TN) 365
PAULSON, WERNER M., *see* WEBER, RICHARD J.
PELEVIN, V. S., *see* GOL'DENBERG, S. A.
PHILLIPS, RICHARD L. and COHEN, CLARENCE B.
Use of Drag Modulations to Reduce Deceleration Loads During Atmospheric Entry 414
PISTINER, JOSEF S.
On-Off Control System for Attitude Stabilization of a Space Vehicle 283
PITKIN, EDWARD T.
Optimum Radiator Temperature for Space Power Systems (TN) 596
POLOSKOV, S. M., *see* KOMISSAROV, O. D.
POTTER, A. E., JR. and BUTLER, JAMES N.
A Novel Combustion Measurement Based on the Extinguishment of Diffusion Flames (TN) 54
POWELL, R. W.
Infrared Tracking 973
PRIEM, RICHARD J. and HEIDMANN, MARCUS F.
Vaporization of Propellants in Rocket Engines 836
RAO, G. V. R.
Evaluation of Conical Nozzle Thrust Coefficients (TC) 606
RECESSO, J., *see* JOHN, R. R.
RIBAUD, G.
Comments on "Recent Advances in Gaseous Detonation" (TC) 876
RICUPITO, W. J., *see* BERGER, W. J.
RIDER, LEONARD
Characteristic Velocity for Changing the Inclination of a Circular Orbit to the Equator (TN) 48
ROBERTSON, ROBERT E.
Time for Escape Using a Succession of Small Impulses (TN) 370
ROBILLARD, G.
Explorer Rocket Research Program 492

ENGINEERS:

INERTIAL GUIDANCE & NAVIGATION SYSTEMS

To perform analysis and synthesis of major space defense systems, including:

1. Interpretation and reduction of customer requirements to engineering terms
2. Determination of system and sub-system requirements
3. Coordination of sub-system work being performed by contributing units to assure overall compatibility with the complete system
4. Participation in proposal and technical presentations
5. Provision of creative ideas and advanced systems techniques and concepts

To qualify, you should hold a BS or advanced degree in Engineering. Must have eight years' experience in engineering with at least four years spent in complex systems synthesis and analysis in one or more of the following: missile and space guidance and navigation; satellite defensive and offensive systems; space defense.

Please send your resume in confidence to Mr. E. A. Smith, Dept. 12-M

DSD DEFENSE SYSTEMS DEPARTMENT
A Department of the Defense Electronics Division

GENERAL ELECTRIC

300 South Geddes Street, Syracuse, N. Y.

TOP SPOTS FOR A TECHNICAL SPECIALIST AND TECHNICAL LEADER ON A NEW SPACE TEAM

Two excellent openings in Chance Vought's newly formed Astronautics Division.

Senior Specialist in Heat Transfer and Fluid Mechanics.

Advanced A.E., Ph.D. preferred. To supervise group in fields of heat transfer, pressure distribution analysis, ablation theory and general fluid mechanics. Requires knowledge of real gas effects, capability for training people, supervising company R & D, keeping abreast of technology.

Physics M.S. with Minor in Meteorology (and meteorological experience.)

To study physics of upper atmosphere, including compilation of data. Interpret data on atmospheric density, pressure, temperature and composition. Keep abreast of space probe and satellite data. Plan test programs. Recommend experimental work and conduct feasibility studies for weather satellite programs.

Write to:
Professional Placement Office
Dept. JP-9

CHANCE VOUGHT
DALLAS, TEXAS

RODRIGUEZ, EDWARD
Method for Determining Steering Programs for Low Thrust Interplanetary Vehicles 783
RODEAN, HOWARD C.
Rocket Thrust Termination Transients. 406
ROSNER, DANIEL E.
Similitude Treatment of Hypersonic Stagnation Heat Transfer (TN).... 215
RUBIN, SYLVAN
General Equation for Rocket Velocity (TN) 219
RUSAKOV, L. Z., *see* KOMISSAROV, O. D.
SABERSKY, ROLF H.
Recent Developments in Convective Heat Transfer (SA)..... 325
SARNER, S. F., *see* FREE, B. A.
SCALA, SINCLAIRE M.
Hypersonic Viscous Shock Layer (TN) 520
Thermal Protection of a Re-Entry Satellite (TN)..... 670
SCALA, SINCLAIRE M. and BAULKNIGHT, CHARLES W.
Transport and Thermodynamic Properties in a Hypersonic Laminar Boundary Layer, Part I. Properties of the Pure Species..... 39
SCALA, SINCLAIRE M. and SUTTON, GEORGE W.
Energy Transfer at a Chemically Reacting or Slip Interface (TN)..... 141
SCHAAF, S. A., HURLBUT, F. C., TALBOT, L. and AROESTY, J.
Viscous Interaction Experiments at Low Reynolds Numbers (TN)..... 527
SCHALLA, ROSE L. and FLETCHER, EDWARD A.
The Ignition Behavior of Various Amines With White Fuming Nitric Acid.... 33
SCHINDLER, G. M.
On Satellite Librations (TN)..... 368
SCURLOCK, A. C., *see* GROVER, J. H.
SEARS, W. R.
Magnetohydrodynamic Effects in Aerodynamic Flows (SA)..... 397
SHEER, R. E., JR., *see* NAGAMATSU, H. T.
SHIEBER, HERBERT
Suppression of Combustion Instability in the Plungerjet Rocket Engine (TN) 446
SHVIDKOVSKII, E. G.
Measurements of Thermodynamic Parameters of the Stratosphere With Aid of Meteorological Rockets (RS). 733
SIBULKIN, M.
A Note on Turbulent Boundary Layer Growth in Nozzles (TN)..... 61
SMELT, RONALD
Lockheed X-17 Rocket Test Vehicle and Its Applications..... 565
SOHN, ROBERT L.
Attitude Stabilization by Means of Solar Radiation Pressure (TN)..... 371
A Proposed Kepler Diagram (TN).... 51
Rapid Method for Computing High Altitude Gravity Turns (TN)..... 139
SPALDING, D. B.
Adiabatic Wall Temperature Due to Mass Transfer Cooling With a Combustible Gas (TN)..... 666
Theory of Particle Combustion at High Pressures 828
SPENCER, N. W., BOGGESS, R. L., LAGOW, H. E. and HOROWITZ, R.
On the Use of Ionization Gage Devices at Very High Altitudes..... 290
SPENCER, N. W. and BOGGESS, R. L.
A Radioactive Ionization Gage Pressure Measurement System (TN)..... 68
STAROS, BASIL, GRETZ, RICHARD and MANDEL, MERVEN
Selection of an Aerodynamic Configuration for Improved Beam Rider Guidance 115
STEARNS, EDWARD V. B., *see* FRYE, WILLIAM E.
STERNE, THEODORE E.
Effect of the Rotation of a Planetary Atmosphere Upon the Orbit of a Close Satellite..... 777
STEWART, R. M.
Some Effects of Vibration and Rotation on the Drift of Gyroscopic Instruments 22
STODOLA, E. KING
Radio Guidance..... 940
SUMMERFIELD, MARTIN
Control of Solid Propellant Burning Rates by Acoustic Energy (TN).... 791
SUTHERLAND, GEORGE S.
Recent Advances in Space Propulsion (SA) 698

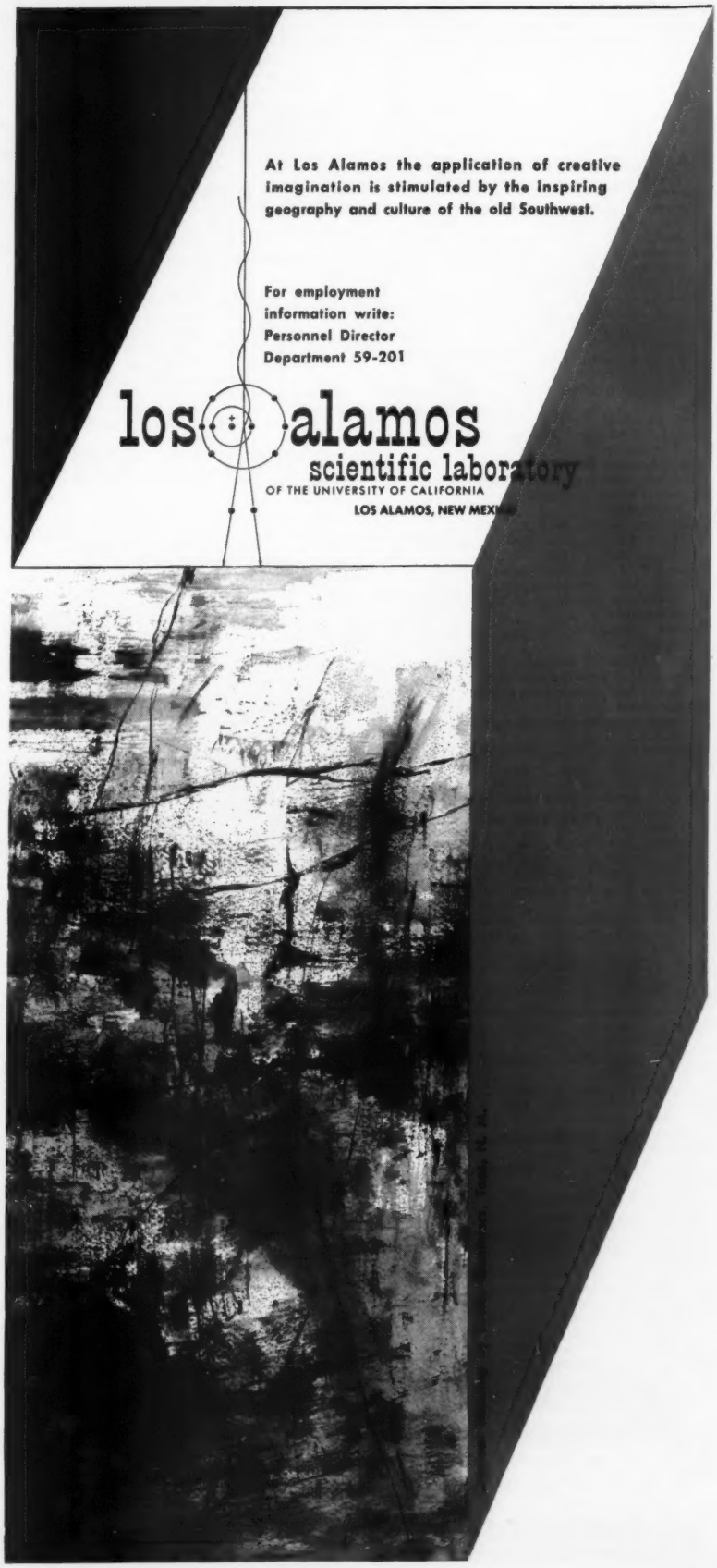
At Los Alamos the application of creative imagination is stimulated by the inspiring geography and culture of the old Southwest.
For employment information write:
Personnel Director
Department 59-201
los alamos
scientific laboratory
OF THE UNIVERSITY OF CALIFORNIA
LOS ALAMOS, NEW MEXICO

SUTTON, GEORGE W.
Adiabatic Wall Temperature Due to Mass Transfer Cooling With a Combustible Gas (TN) 136
See also SCALA, SINCLAIRE M.
TALANTOV, A. V.
Estimate of Operation of Simplest Ramjet Combustion Chamber (RS) 769
TALBOT, L., *see* SCHAAF, S. A.
TALLMAN, CHARLES R.
Transducer Frequency Response Evaluation for Rocket Instability Research. 119
TEISSEYRE, JERZY H.
Comment on "Generalized Trajectories for Free-Falling Bodies of High Drag" and "Vertical Re-Entry Into Earth's Atmosphere for Both Light and Heavy Bodies" (TC) 874
TEMPELMAN, WAYNE
Comparison of Minimum Energy Paths and Apogee Designation Paths (TN) 865
TEUBER, DIETER, *see* JASPER, NIELS
TROSHIN, YA. K.
Points on Lower Hugoniot Curve Describing Combustion Modes in Jet Engine Chambers (RS) 750
TSU, T. C.
Interplanetary Travel by Solar Sail 422
TURNER, CHARLES F., *see* GRIFFIN, DONALD N.
VAGLIO-LAURIN, ROBERTO
Laminar Heat Transfer on Three-Dimensional Blunt Nosed Bodies in Hypersonic Flow 123
VANDENKERCKHOVE, JEAN A.
Recent Advances in Solid Propellant Grain Design (SA) 483
VAN DER WAL, F. L. and YOUNG, W. D.
Project MIA (Mouse-in-Able), Experiments on Physiological Response to Spaceflight 716
VANDER VELDE, W. E., *see* HOVORKA, JOHN
VANPEE, M. and WOLFHARD, H. G.
Comparison Between Hot Gas Ignition and Limit Flame Temperatures 517
VARGO, LOUIS G.
Identification of Inert Objects in Space (TC) 608
VITCH, MARIAN, JR. and MARTELLUCCI, ANTHONY
Theoretical and Experimental Analysis of a Cowling as a Means of a Drag Reduction for an Axisymmetric Center Body (TN) 447
VISNOV, M.
The Useful Life of Solid Propellants at Very High Temperatures—Part I 500
WAESCHE, R. H. WOODWARD
Comments on "A Ballistic Bomb Method for Determining the Experimental Performance of Rocket Propellants" (TC) 375
WANG, C. J., ANTHONY, G. W. and LAWRENCE, H. R.
Thrust Optimization of a Nuclear Rocket of Variable Specific Impulse 341
WEBER, RICHARD J. and PAULSON, WERNER M.
Achieving Satellite Rendezvous (TN). 592
WEISBORD, LEON
Optimum Staging Techniques (TN) ... 445
WEISS, MALCOLM A. and WORSHAM, CHARLES H.
Atomization in High Velocity Airstreams 252
WHEELON, ALBERT D.
Free Flight of a Ballistic Missile 915
WILLIAMS, F. A.
Chemical Reactions in Supersonic Flow (TN) 442
WILLIAMS, HARRY
Hypersonic Conical Flow (TN) 668
WILLIAMS, M. L.
Some Thermal Stress Design Data for Rocket Grains 260
WILLINSKI, MARTIN I.
Beamed Electromagnetic Power as a Propulsion Energy Source (TN) 601
WOLFHARD, H. G., *see* VANPEE, M.
WORSHAM, CHARLES H., *see* WEISS, MALCOLM A.
WRIGHT, F. H.
Multiple Flameholder Arrays: Flame Interactions (TN) 143
YAKOVLEV, V. I., *see* CHERNOV, V. N.
YOUNG, W. D., *see* VAN DER WAL, F. L.
ZARUBIN, V. S.
One Problem in Nonstationary Heat Conduction (RS) 773
ZIEMER, RICHARD W.
Experimental Investigation in Magneto-Acrodynamics 642
ZIMMERMAN, ROBERT L., *see* ZWICK, EUGENE B.
ZLOTNICK, MARTIN, *see* BAUER,, ERNEST
ZUCROW, M. J. and OSBORN, J. R.
Reply to Crocco's Criticism of the Zucrow-Osborn Paper (TC) 221
ZWICK, EUGENE B. and ZIMMERMAN, ROBERT L.
Space Vehicle Power Systems (SA) ... 553

SUBJECTS

PROPULSION AND POWER (Combustion Systems)

RECENT ADVANCES IN RAMJET COMBUSTION, Gordon L. Dugger (SA) 819
ROCKET THRUST TERMINATION TRANSIENTS, Howard C. Rodean 406
VAPORIZATION RATE LIMITED COMBUSTION IN BIPROPELLANT ROCKET CHAMBERS, E. Mayer 505
ESTIMATE OF INTERNAL LOSSES IN A LIQUID FUEL JET ENGINE CHAMBER, A. V. Kvasnikov (RS) 745
ESTIMATE OF OPERATION OF SIMPLEST RAMJET COMBUSTION CHAMBER, A. V. Talantov (RS) 769
VAPORIZATION OF PROPELLANTS IN ROCKET ENGINES, Richard J. Priem and Marcus F. Heidmann 836
SURVEILLANCE OF SOLID PROPELLANT ROCKETS, Carl Boyars (TN) 148
THRUST OF A CONICAL NOZZLE, Ellis M. Landsbaum (TN) 212
GENERAL EQUATION FOR ROCKET VELOCITY, Sylvan Rubin (TN) 219
SUPPRESSION OF COMBUSTION INSTABILITY IN THE PLUNGERJET ROCKET ENGINE, Herbert Shieber (TN) 446
CHANGES IN THE DENSITY AND TEMPERATURE OF LIQUID PROPELLANTS IN ROCKET ENGINE SUPPLY SYSTEMS, S. L. Bragg (TN) 672
REPLY TO CROCCO'S CRITICISM OF THE ZUCROW-OSBORN PAPER, M. J. Zucrow and J. R. Osborn (TC) 221
COMMENTS ON "EXHAUST NOZZLE CONTOUR FOR MAXIMUM THRUST," R. W. Fanselau (TC) 456
EVALUATION OF CONICAL NOZZLE THRUST COEFFICIENT, G. V. R. Rao (TC) 606

PROPULSION AND POWER (Non-Combustion)

SPACE VEHICLE POWER SYSTEMS, Eugene B. Zwick and Robert L. Zimmerman (SA) 553
RECENT ADVANCES IN SPACE PROPULSION, George S. Sutherland (SA) 698
PHOTOCHEMISTRY OF THE UPPER ATMOSPHERE AS A SOURCE OF PROPULSIVE POWER, A. F. Charwat 108
COMMENTS ON "PHOTOCHEMISTRY OF THE UPPER ATMOSPHERE AS A SOURCE OF PROPULSIVE POWER," Sterge T. Demetriades (TC) 375
PERFORMANCE CALCULATIONS FOR HYBRID NUCLEAR-CHEMICAL ROCKET PROPULSION SYSTEMS, Leon Green Jr. and James M. Carter 180
COMMENT ON "PERFORMANCE CALCULATIONS FOR HYBRID NUCLEAR-CHEMICAL ROCKET PROPULSION SYSTEMS, John S. Gordon (TC) 455
THRUST OPTIMIZATION OF A NUCLEAR ROCKET OF VARIABLE SPECIFIC IMPULSE, C. J. Wang, G. W. Anthony and H. R. Lawrence 341
EFFECT OF DISSOCIATION ON THE PERFORMANCE OF WORKING FLUIDS FOR NUCLEAR PROPULSION, J. G. Logan and E. L. Colichman 409
INTERPLANETARY TRAVEL BY SOLAR SAIL, T. C. Tsu 422
DYNAMIC ANALYSIS OF A NUCLEAR ROCKET ENGINE, Bernard R. Felix and Richard J. Bohl 853
THEORETICAL STUDY OF RECOMBINATION KINETICS OF ATOMIC OXYGEN, S. T. Demetriades and M. Farber (TN) 528
OPTIMUM RADIATOR TEMPERATURE FOR SPACE POWER SYSTEMS, Edward T. Pitkin (TN) 596
AUGMENTATION OF NUCLEAR ROCKET SPECIFIC IMPULSE THROUGH MECHANICAL-ELECTRICAL MEANS, Martin Goldsmith (TN) 600
BEAMED ELECTROMAGNETIC POWER AS A PROPULSION ENERGY SOURCE, Martin J. Willinski (TN) 601
UTILIZATION OF STORED ENERGY IN SOLID MATERIAL AS AN ADDED ENERGY SOURCE, John J. Newgard (TN) 603
PRELIMINARY EVALUATION OF HELIUM AS AN ELECTRIC ARC HEATED PROPELLANT, Thomas R. Brogan (TN) 662
NEW ION SOURCE FOR PROPULSION OF SPACE VEHICLES, C. D. Moak, H. E. Banta, J. E. Johnson and R. F. King (TN) 868

COMBUSTION AND PROPELLANTS (Combustion)

RECENT ADVANCES IN GASEOUS DETONATION, R. A. Gross and A. K. Oppenheim (SA) 173
COMMENTS ON "RECENT ADVANCES IN GASEOUS DETONATION," G. Ribaud (TC) 876
TURBULENT FLAME STUDIES IN A TWO-DIMENSIONAL OPEN BURNER, J. H. Grover, E. N. Fales and A. C. Scurlock. 275
COMPARISON BETWEEN HOT GAS IGNITION AND LIMIT FLAME TEMPERATURES, M. Vanpée and H. G. Wolfhard 517
POINTS ON LOWER HUGONIOT CURVE DESCRIBING COMBUSTION MODES IN JET ENGINE CHAMBERS, Ya. K. Troshin (RS) 750
STRUCTURE OF TURBULENT FLAME OF HOMOGENEOUS AND HETEROGENEOUS MIXTURES, V. Ya. Basevich and S. M. Kogarko (RS) 756
EFFECT OF FLOW PULSATIONS ON THE TURBULENT SPEED OF FLAME PROPAGATION, L. S. Kozachenko (RS) 761
EFFECT OF PRESSURE ON THE SPEED OF FLAME PROPAGATION IN A TURBULENT STREAM, S. A. Gol'denberg and V. S. Pelevin (RS) 765
A NOVEL COMBUSTION MEASUREMENT BASED ON THE EXTINGUISHMENT OF DIFFUSION FLAMES, A. E. Potter Jr. and James N. Butler (TN) 54
RESEARCH ON SUPERSONIC COMBUSTION, Robert A. Gross (TN) 63
MULTIPLE FLAMEHOLDER ARRAYS: FLAME INTERACTIONS, F. H. Wright (TN) 143
VELOCITY OF TANK FRAGMENTS, Saunders B. Kramer (TN) 363
STABILIZED GASEOUS DETONATION WAVES, J. A. Nicholls (TC) 607

COMBUSTION AND PROPELLANTS (Liquid Propellants)

RECENT ADVANCES IN BORON TECHNOLOGY, Richard A. Carpenter (SA) ... 8
RECENT ADVANCES IN FLUORINE CHEMISTRY AND TECHNOLOGY, John F. Gall (SA) 95
RECENT ADVANCES IN CRYOGENIC ENGINEERING, Robert B. Jacobs 245
COMMENTS ON "RECENT ADVANCES IN CRYOGENIC ENGINEERING," S. L. Bragg (TC) 875
A BALLISTIC BOMB METHOD FOR DETERMINING THE EXPERIMENTAL PERFORMANCE OF ROCKET PROPELLANTS, Donald N. Griffin, Charles F. Turner and George T. Campbell 15
COMMENTS ON "A BALLISTIC BOMB METHOD FOR DETERMINING THE EXPERIMENTAL PERFORMANCE OF ROCKET PROPELLANTS," R. H. Woodward Waesche (TC) 375
IMPROVEMENTS IN THE OPERATING CHARACTERISTICS OF n-PROPYL NITRATE, R. W. Lawrence and W. P. Knight 29
THE IGNITION BEHAVIOR OF VARIOUS AMINES WITH WHITE FUMING NITRIC ACID, Rose L. Schalla and Edward A. Fletcher 33
COMPRESSION SENSITIVITY OF MONOPROPELLANTS, G. A. Mead 192

Isothermal Compressibility of Liquid Oxygen and RP-1, George T. Y. Chao. 199
Some Physical Properties for the System Nitrogen Tetroxide–Nitric Oxide, Donat B. Brice and Norman Fishman 354
Correlation and Prediction of Flame Properties With Special Reference to Liquid Hydrazine, Melvin Gerstein 514
A Rapid Method for Estimation of Specific Impulse, B. A. Free and S. F. Sarner (TN)..... 64
Burning Rate of an H-Atom Propellant, Howard B. Palmer (TN)..... 365
Relation of Droplet Consumption Rates to Liquid Strand Consumption Rates, G. A. Mead (TN)..... 440
Estimation of Performance of Fuels With Hydrogen Peroxide Oxidizer, John S. Gordon (TN)..... 530
Solubility of Air, N_2 and O_2 in n-Propyl Nitrate, Adolph B. Amster and Joseph B. Levy (TN)..... 870

COMBUSTION AND PROPELLANTS
(Solid Propellants)

Recent Advances in Solid Propellant Grain Design, Jean A. Vandenkerckhove (SA)..... 483
Some Thermal Stress Design Data for Rocket Grains, M. L. Williams.. 260
The Useful Life of Solid Propellants At Very High Temperatures—Part I, M. Visnov..... 500
Theory of Particle Combustion at High Pressures, D. B. Spalding..... 828
Application of Surface Decomposition Kinetics to Detonation of Ammonium Nitrate, W. H. Andersen and R. F. Chaiken (TN)..... 49
Optimum Proportioning of Two Propellants to Obtain Maximum Burnt Velocity, R. H. Olds (TN)..... 598
Control of Solid Propellant Burning Rates by Acoustic Energy, Martin Summerfield (TN)..... 791
Remark on Thermodynamics of Al_2O_3, John S. Gordon (TC)..... 455

MATERIALS

New Aspects in Ceramic Coatings, Paul A. Huppert..... 19

FLUID DYNAMICS, HEAT TRANSFER AND MHD

Atomization in High Velocity Airstreams, Malcolm A. Weiss and Charles H. Worsham..... 252
Reflection of Weak Shock Waves From Nozzles With No Flow and Critical Flow, Charles E. Feiler..... 272
Calculation of Unsteady Supersonic Flow Past a Circular Cylinder, Martha W. Evans and Francis H. Harlow (TN)..... 46
Solution to the Linearized Quasi-Stationary External Diffuser Equations, R. H. Edwards (TN)..... 54
A Note on Turbulent Boundary Layer Growth in Nozzles, M. Sibulkin (TN) 61
Frictional Electricity in Missile Systems, P. Molmud (TN)..... 73
Comment on "Frictional Electricity in Missile Systems," William J. Guman (TC)..... 374
Effect of Unequal Wall Roughness on Flow Between Flat Plates, H. N. McManus Jr. (TN)..... 144
Scale of Separation Phenomena in Liquids Under Conditions of Nearly Free Fall, E. T. Benedikt (TN)..... 150
Particle Impaction on Spheres at High Mach Numbers, S. K. Friedlander (TN) 296
Aerodynamic Moment on Bodies Moving at High Speeds in the Upper Atmosphere, W. B. Gustafson (TN).. 301
On Turbulent Supersonic Diabatic Wakes, R. H. Page (TN)..... 443
Theoretical and Experimental Analysis of a Cowling as a Means of

SINCE 1954---
PROVED IN USE
---CAE TC-106
(USAF TYPE MA-1A)
PORTABLE
STARTING UNIT
FOR
LARGE JET AIRCRAFT

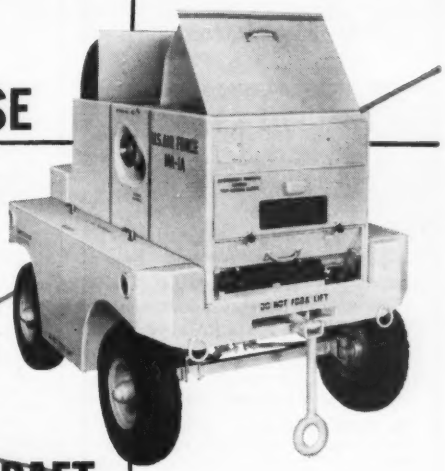

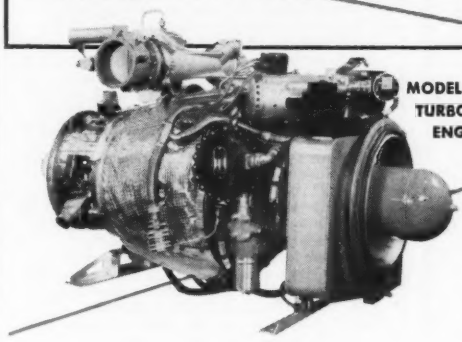

MODEL 141
TURBO-COMPRESSOR
ENGINE

• This fine product of Continental development and manufacture, with the CAE Model 141 turbo-compressor as its heart, has a five-year record of exceptional performance to its credit.

. . . More than 1,000 MA-1A's and their predecessor MA-1's have been delivered to the Air Force since 1954. There, actual experience has led to upward revision of hours-between-overhaul schedules, with an eventual period well in excess of 2,200 starts indicated as likely. USAF-type units in use by certain aircraft manufacturers, and not subject to Air Force requirements as to return to overhaul, have exceeded 3,400 starts and are still in excellent operable condition, no change of major parts having been made . . . Official Air Force records show low overhaul cost, in combination with 99.5 per cent service availability, and almost complete freedom from field down time for maintenance or modification—all in addition to the important factor of low initial price . . . When it comes to USE-PROVED ground support equipment, CAE is first choice.

☆ ☆ ☆

CAE gas turbine models—the famous J69's—are in Cessna's T-37A twin jet trainer, Ryan's Q2 Firebee target missile, Temco's TT-1 Navy jet trainer, and other aircraft. From the J69 have evolved the highly versatile new Series 356 turbines, including jet power for manned and unmanned aircraft up to 2,400 lbs. thrust, a boundary layer control air pump, and an aft-fan version turbojet, as well as a free shaft turbine of 3,500 hp.

CONTINENTAL AVIATION & ENGINEERING CORPORATION

GENERAL OFFICES AND RESEARCH AND DEVELOPMENT DEPARTMENTS AT 12700 KERCHEVAL AVENUE, DETROIT 15, MICHIGAN . . . PRODUCTION DIVISION AND FIELD SUPPORT, 1330 LASKEY ROAD, TOLEDO, OHIO.

SUBSIDIARY OF CONTINENTAL MOTORS CORPORATION

Just Published

PLASMA DYNAMICS

Edited by Francis H. Clauser

The Johns Hopkins University

A broad, unified treatment of plasma dynamics, carefully edited and coordinated from material presented by 50 distinguished participants in the 1958 international symposium at Woods Hole. An authoritative, timely reference book.

Chapter titles and Editors

Experimental research on high temperature plasmas by **Richard F. Post.** The problems of thermonuclear fusion and high temperature plasmas by **Marshall Rosenbluth.** Gaseous electronic phenomena by **Marvin H. Mittleman.** Dynamics of electron beams by **Roy W. Gould.** Statistical plasma mechanics by **Johannes M. Burgers.** Continuum plasma dynamics by **Hans W. Liepmann and Julian D. Cole.** Flight magnetohydrodynamics by **Arthur Kantrowitz.** Solar, planetary, and interplanetary magnetohydrodynamics by **Eugene N. Parker.** Cosmical magnetohydrodynamics by **Geoffrey Burbidge.**

368 pp, 98 illus, 1959—$12.50

QUANTITATIVE MOLECULAR SPECTROSCOPY AND GAS EMISSIVITIES

By S. S. Penner, Calif. Inst. of Tech.

Treats basic problems in quantitative molecular spectroscopy and gas emissivities, utilizing the classical results of radiation theory. Problems are representative of the types encountered in development of modern propulsion devices.

587 pp, 212 illus, 1959—$15.00

PROJECT SHERWOOD

The U. S. Program in Controlled Fusion

By Amasa S. Bishop, U.S.A.E.C.

"A clear description . . . of the U.S. effort to achieve the thermonuclear reaction. The well-written text and remarkable drawings make the reading of this book a pleasure." *Science*

216 pp, 50 illus, 1958—$6.50

ADDISON-WESLEY PUBLISHING COMPANY, INC.

Reading, Massachusetts, U. S. A.

DRAG REDUCTION FOR AN AXISYMMETRIC CENTER BODY, Marian Visich Jr. and Anthony Martellucci (TN).... 447

VISCOUS INTERACTION EXPERIMENTS AT LOW REYNOLDS NUMBERS, S. A. Schaaf, F. C. Hurlbut, L. Talbot and J. Aroesty (TN)..... 527

GRAPHICAL COMPUTATION OF SHOCK AND DETONATION WAVES IN REAL GASES, George H. Markstein (TN)..... 588

PREDICTION OF INVISCID INDUCED PRESSURES FROM ROUND LEADING EDGE BLUNTING AT HYPERSONIC SPEEDS, E. S. Love (TN)..... 792

FLUID DYNAMICS, HEAT TRANSFER AND MHD (Heat Transfer)

RECENT DEVELOPMENTS IN CONVECTIVE HEAT TRANSFER, Rolf H. Sabersky (SA)..... 325

RECENT ADVANCES IN ABLATION, Mac C. Adams (SA)..... 625

TRANSPORT AND THERMODYNAMIC PROPERTIES IN A HYPERSONIC LAMINAR BOUNDARY LAYER. PART I. PROPERTIES OF THE PURE SPECIES, Sinclaire M. Scala and Charles W. Baulknight..... 39

LAMINAR HEAT TRANSFER ON THREE-DIMENSIONAL BLUNT NOSED BODIES IN HYPERSONIC FLOW, Roberto Vaglio-Laurin..... 123

SIMILARITY PARAMETERS FOR SURFACE MELTING OF A BLUNT NOSED BODY IN A HIGH VELOCITY GAS STREAM, Lester Lees..... 345

METEORIC ABLATION THROUGH INTERFACIAL INSTABILITY, Sin-I Cheng..... 579

THE ELECTRIC ARC WIND TUNNEL—A TOOL FOR ATMOSPHERIC RE-ENTRY RESEARCH, Thomas R. Brogagn..... 648

HEAT CONDUCTION IN A CIRCULAR CYLINDER ROTATING WITH ITS AXIS NORMAL TO THE DIRECTION OF FLIGHT, Anthony Demetriades..... 653

TRANSPORT COEFFICIENTS OF AIR TO 8000 K, Ernest Bauer and Martin Zlotnick.. 721

ONE PROBLEM IN NONSTATIONARY HEAT CONDUCTION, V. S. Zarubin (RS)..... 773

ADIABATIC WALL TEMPERATURE DUE TO MASS TRANSFER COOLING WITH A COMBUSTIBLE GAS, George W. Sutton (TN)..... 136

ENERGY TRANSFER AT A CHEMICALLY REACTING OR SLIP INTERFACE, Sinclaire M. Scala and George W. Sutton (TN). 141

SIMILITUDE TREATMENT OF HYPERSONIC STAGNATION HEAT TRANSFER, Daniel E. Rosner (TN)..... 215

GENERALIZED SOLUTION FOR THE PROBLEM OF PIPE FLOW WITH FRICTION AND HEAT ADDITION, R. W. McJones and M. L. Caplan (TN)..... 366

STAGNATION POINT HEAT TRANSFER IN A SUBSONIC JET OF ARC-HEATED AIR, R. R. John and W. L. Bade (TN)..... 523

ABLATION CHARACTERISTICS OF A SUBLIMING MATERIAL USING ARC HEATED AIR, R. R. John and J. Recesso (TN)... 663

ADIABATIC WALL TEMPERATURE DUE TO MASS TRANSFER COOLING WITH A COMBUSTIBLE GAS, D. B. Spalding (TN).. 666

THERMAL PROTECTION OF A RE-ENTRY SATELLITE, Sinclaire M. Scala..... 670

FLUID DYNAMICS, HEAT TRANSFER AND MHD (Hypersonics)

AN EXPERIMENTAL INVESTIGATION OF BLUNT BODY STAGNATION POINT VELOCITY GRADIENT, J. Christopher Boison and Howard A. Curtiss..... 130

HYPERSONIC SHOCK TUNNEL, H. T. Nagamatsu, R. E. Geiger and R. E. Sheer Jr. 332

SIMPLE ANALYTICAL APPROXIMATION TO THE EQUATION OF STATE OF DISSOCIATED AIR, W. L. Bade (TN)..... 298

CHEMICAL REACTIONS IN SUPERSONIC FLOW, F. A. Williams (TN)..... 442

HYPERSONIC VISCOUS SHOCK LAYER, Sinclaire M. Scala (TN)..... 520

HYPERSONIC CONICAL FLOW, Harry Williams (TN)..... 668

FLUID DYNAMICS, HEAT TRANSFER AND MHD (MHD)

MAGNETOHYDRODYNAMIC EFFECTS IN AERODYNAMIC FLOWS, W. R. Sears (SA)..... 397

MAGNETOHYDRODYNAMICS AND AERODYNAMIC HEATING, Rudolph X. Meyer... 187

AEROTHERMODYNAMIC AND ELECTRICAL PROPERTIES OF SOME GAS MIXTURES TO MACH 20, W. Chinitz, C. L. Eisen and R. A. Gross..... 573

EXPERIMENTAL INVESTIGATION IN MAGNETO-AERODYNAMICS, Richard W. Ziemer..... 642

MAGNETIC BOUNDARY LAYERS, H. F. Ludloff (TN)..... 590

OPTIMUM MAGNETIC FIELD FOR STAGNATION HEAT TRANSFER REDUCTION AT HYPERSONIC VELOCITIES, Robert Goulard (TN)..... 604

MAGNETOGASDYNAMIC FLOW REGIMES, Ching-Shi Liu and Ali Bulent Cambel (TN)..... 871

FLIGHT MECHANICS (Terrestrial)

EFFECT OF THRUST TERMINATION PROCESS UPON RANGE DISPERSION OF A BALLISTIC MISSILE, Arnold J. Kelly.... 432

SOME ECONOMIC ASPECTS OF HYPERSONIC FLIGHT, Robert Cornog..... 706

INTERRELATIONSHIP OF CALCULUS OF VARIATIONS AND ORDINARY THEORY OF MAXIMA AND MINIMA FOR FLIGHT MECHANICS APPLICATIONS, Angelo Miele (TN)..... 75

EFFECT OF ACCELERATION ON THE LONGITUDINAL DYNAMIC STABILITY OF A MISSILE, E. V. Laitone (TN)..... 137

RAPID METHOD FOR COMPUTING HIGH ALTITUDE GRAVITY TURNS, Robert L. Sohn (TN)..... 139

MINOR CIRCLE FLIGHT FOR BOOST-GLIDE VEHICLES, W. H. T. Loh (TN)..... 300

HYPERVELOCITY VEHICLES AT LARGE ANGLES OF INCLINATION, W. H. T. Loh (TN)..... 522

MINOR CIRCLE FLIGHT FOR ORBITAL LAUNCHED OR BOOST-GLIDE VEHICLES, W. H. T. Loh (TN)..... 789

APPLICABILITY OF EULER'S DYNAMICAL EQUATIONS TO ROCKET MOTION, James W. Ellis and Charles W. McArthur (TN)..... 863

SIMPLE METHODS OF ESTIMATING THE VARIATION OF IMPACT POINTS FOR BALLISTIC MISSILES, Samuel W. Fordyce (TC)..... 876

FLIGHT MECHANICS (Extraterrestrial)

APPLICATION OF ASTRONOMICAL PERTURBATION TECHNIQUES TO THE RETURN OF SPACE VEHICLES, Robert M. L. Baker Jr. 207

INTERPLANETARY TRAJECTORIES UNDER LOW THRUST RADIAL ACCELERATION, Jack Copeland..... 267

USE OF DRAG MODULATION TO REDUCE DECELERATION LOADS DURING ATMOSPHERIC ENTRY, Richard L. Phillips and Clarence B. Cohen..... 414

PREDICTION THEORY OF MISSILE AND SATELLITE ORBITS, W. J. Berger and J. R. Ricupito..... 428

GENERAL SOLUTION FOR OPTIMIZATION OF STAGING OF MULTISTAGED BOOST VEHICLES, Carl H. Builder..... 497

USE OF AERODYNAMIC LIFT DURING ENTRY INTO THE EARTH'S ATMOSPHERE, Lester Lees, Frederic W. Hartwig and Clarence B. Cohen..... 633

EFFECT OF THE ROTATION OF A PLANETARY ATMOSPHERE UPON THE ORBIT OF A CLOSE SATELLITE, Theodore E. Sterne..... 777

COMPOSITE TRAJECTORIES YIELDING MAXIMUM COASTING APOGEE VELOCITY, Stanley Ross..... 843

EARTH-PERIOD (24-HR) SATELLITES, J. H. Hutcheson 849
CHARACTERISTIC VELOCITY FOR CHANGING THE INCLINATION OF A CIRCULAR ORBIT TO THE EQUATOR, Leonard Rider (TN) 48
A PROPOSED KEPLER DIAGRAM, Robert L. Sohn (TN) 51
OPTIMIZATION OF ROCKETS FOR MAXIMUM PAYLOAD ENERGY, Dandridge M. Cole and Michael A. Marrese (TN) ... 71
TWO SIMPLE EQUATIONS FOR ORBITAL MECHANICS, W. H. T. Loh (TN) 146
TERMINAL PHASE OF SATELLITE ENTRY INTO THE EARTH'S ATMOSPHERE, Elliott D. Katzen (TN) 147
DETERMINATION OF ELEMENTS OF AN ELLIPTIC ORBIT FROM THE ORBITAL VELOCITY VECTOR, H. Munick (TN) .. 150
MOTION UNITS TO SIMPLIFY SPACE TRAVEL COMPUTATIONS, Bemrose Boyd (TN) 216
A SHORT FORM METHOD FOR DETERMINING NEAR-CIRCULAR ORBIT QUANTITIES, Joseph N. Benezra (TN) 216
CIRCULAR ORBIT STABILITY IN THE OBLATE EARTH'S EQUATORIAL PLANE, Marvin H. Hewitt (TN) 295
ON SATELLITE LIBRATIONS, G. M. Schindler (TN) 368
TIME FOR ESCAPE USING A SUCCESSION OF SMALL IMPULSES, Robert E. Roberson (TN) 370
OPTIMUM STAGING TECHNIQUES, Leon Weisbord (TN) 445
AN OPTIMUM TRANSFER PATH FROM AN ELLIPTICAL ORBIT TO A HIGHER ENERGY CIRCULAR ORBIT, H. Munick .. 449
LONG PERIOD OSCILLATIONS DURING ATMOSPHERIC ENTRY, George S. Campbell (TN) 523
STABILITY OF A GLOBULAR CLUSTER IN THE OBLATE EARTH'S EQUATORIAL PLANE, Marvin H. Hewitt (TN) 595
ACHIEVING SATELLITE RENDEZVOUS, Richard J. Weber and Werner M. Paulson (TN) 592
MAXIMUM EJECTION VELOCITY FOR RETURN FROM SATELLITE ORBITS, Harry Esses (TN) 592
SOME EXTENSIONS OF THE HOHMANN TRANSFER MANEUVER, T. N. Edelbaum (TN) 864
COMPARISON OF MINIMUM ENERGY PATHS AND APOGEE DESIGNATION PATHS, Wayne Tempelman (TN) 865
FURTHER COMMENTS ON THE POWERED FLIGHT TRAJECTORY OF A SATELLITE, Theodore N. Edelbaum (TC) 374
COMMENT ON "GENERALIZED TRAJECTORIES FOR FREE-FALLING BODIES OF HIGH DRAG" AND "VERTICAL RE-ENTRY INTO EARTH'S ATMOSPHERE FOR BOTH LIGHT AND HEAVY BODIES," Jerzy H. Teisseyre (TC) 874

VEHICLE DESIGN, TESTING AND PERFORMANCE

EXPLORER ROCKET RESEARCH PROGRAM, G. Robillard 492
LOCKHEED X-17 ROCKET TEST VEHICLE AND ITS APPLICATIONS, Ronald Smelt .. 565
SEALED CABIN RELIABILITY AS RELATED TO STRUCTURE AND INTERNAL ATMOSPHERE, F. L. Dickey and G. H. Knipp. 656
THERMOSTATIC TEMPERATURE CONTROL OF SATELLITES AND SPACE VEHICLES, R. A. Hanel (TN) 358

GUIDANCE AND CONTROL

SOME EFFECTS OF VIBRATION AND ROTATION ON THE DRIFT OF GYROSCOPIC INSTRUMENTS, R. M. Stewart 22
SELECTION OF AN AERODYNAMIC CONFIGURATION FOR IMPROVED BEAM RIDER GUIDANCE, Basil Staros, Richard Gretz and Mervin Mandel 115
AN ATTITUDE CONTROL SYSTEM FOR SPACE VEHICLES, Walter Haeussermann 203
ON-OFF CONTROL SYSTEM FOR ATTITUDE STABILIZATION OF A SPACE VEHICLE, Josef S. Pistiner 283
METHOD FOR DETERMINING STEERING PROGRAMS FOR LOW THRUST INTERPLANETARY VEHICLES, Edward Rodriguez 783
SPATIAL ATTITUDE CONTROL OF A SPINNING ROCKET CLUSTER, Walter Haeussermann (TN) 56
THE CLUSTER SPIN CONTROL SYSTEM FOR JUPITER C MISSILES, Niels Jasper and Dieter Teuber (TN) 58
ATTITUDE STABILIZATION BY MEANS OF SOLAR RADIATION PRESSURE, Robert L. Sohn (TN) 371
ELECTRICALLY CHARGED BODIES MOVING IN THE EARTH'S MAGNETIC FIELD, W. W. Fain and B. J. Greer (TN) 451
ON THE USE OF SIDE-JETS AS CONTROL DEVICES, H. P. Liepman (TN) 453
METHOD OF STABILIZING AN ASTRONOMICAL SATELLITE, Robert R. Newton (TN) 665
IGY RESULTS ON THE SHAPE OF THE EARTH, John A. O'Keefe 902
LUNAR TRAJECTORIES, Aubrey B. Mickelwait 905
FREE FLIGHT OF A BALLISTIC MISSILE, Albert D. Wheelon 915
STABILIZATION AND ATTITUDE CONTROL OF SATELLITE VEHICLES, William E. Frye and Edward V. B. Stearns 927
GUIDANCE TECHNIQUES FOR INTERPLANETARY TRAVEL, Charles D. Bock and Charles J. Mundo 931
RADIO GUIDANCE, E. King Stodola 940
RECENT PROGRESS IN INERTIAL GUIDANCE, John Hovorka, John W. Hursh, E. J. Frey, William G. Denhard, Lester R. Grohe, P. J. Gilinson Jr. and W. E. Vander Velde 946
DOPPLER RADARS FOR GUIDANCE—DESIGN TECHNIQUES AND PERFORMANCE, Walter R. Fried 957
PRINCIPLES OF DOPPLER-INERTIAL GUIDANCE, L. H. Dworetzky and A. Edwards 967
INFRARED TRACKING, R. W. Powell 973
CELESTIAL GUIDANCE, R. B. Horsfall 981

INSTRUMENTATION AND COMMUNICATIONS

TRANSDUCER FREQUENCY RESPONSE EVALUATION FOR ROCKET INSTABILITY RESEARCH, Charles R. Tallman 119
ON THE USE OF IONIZATION GAGE DEVICES AT VERY HIGH ALTITUDES, N. W. Spencer, R. L. Boggess, H. E. LaGow and R. Horowitz 290
A RADIOACTIVE IONIZATION GAGE PRESSURE MEASUREMENT SYSTEM, N. W. Spencer and R. L. Boggess (TN) 68
DETERMINATION OF TRANSIENT PRESSURE FLOW RELATIONSHIP BY MOMENTUM MEASUREMENTS, Edward J. Croke and Jerry Grey (TN) 213
USE OF A CATALYTIC PROBE FOR DETECTION OF DISSOCIATED NONEQUILIBRIUM STATES IN HYPERSONIC FLOW, Stuart A. Hoenig (TN) 361

ATMOSPHERIC AND SPACE PHYSICS

IGY SOLAR FLARE PROGRAM AND IONIZING RADIATION IN THE NIGHT SKY, Herbert Friedman 103
MEASUREMENTS OF THERMODYNAMIC PARAMETERS OF THE STRATOSPHERE WITH AID OF METEOROLOGICAL ROCKETS, E. G. Shvidkovskii (RS) 733
INVESTIGATION OF MICROMETEORITES WITH THE AID OF ROCKETS AND SATELLITES, O. D. Komissarov, T. N. Nazarova, L. N. Neugodov, S. M. Poloskov and L. Z. Rusakov (RS) 742
IDENTIFICATION OF INERT OBJECTS IN SPACE, Louis G. Vargo (TC) 608

HUMAN FACTORS AND BIO-ASTRONAUTICS

PROJECT MIA (MOUSE-IN-ABLE), EXPERIMENTS ON PHYSIOLOGICAL RESPONSE TO SPACEFLIGHT, F. L. van der Wal and W. D. Young 716
RESEARCH ON THE FLIGHT OF A LIVING CREATURE IN AN ARTIFICIAL EARTH SATELLITE, V. N. Chernov and V. I. Yakovlev (RS) 736

Now available . . . the first complete report on the technical papers reflecting the results of the Soviet Union's first three satellites.

ARTIFICIAL EARTH SATELLITES
Volumes 1 and 2 Edited by
L. V. KURNOSOVA
TRANSLATED FROM RUSSIAN

This comprehensive work reports the results of the investigation carried out according to the IGY Program with the help of the Soviet Union's first three artificial earth satellites. The articles contained in this book are the revised texts of the reports that were presented at the Fifth Assembly of the Special IGY Committee, which took place at Moscow in August, 1958.

CONTENTS: **Volume 1**—Preface. Cosmic-Ray Measurements with Artificial Earth Satellites. Determination of Atmospheric Density from the Observed Deceleration of the First Artificial Earth Satellites. Determination of Density in the Upper Atmosphere from Secular Variations of Orbital Elements of the First Two Artificial Earth Satellites. Motion of an Artificial Earth Satellite about its Center of Mass. Optical Methods for the Observation of Artificial Earth Satellites. Use of the Doppler Effect for Determining Orbit Parameters of an Artificial Earth Satellite. Rocket Measurements of Electron Concentration in the Ionosphere by Means of an Ultrashortwave Dispersion Interferometer. Distribution of Electron Density as a Function of Height from Data of Experts with Rockets and Artificial Earth Satellite's Effect on Propagation of Radio Waves. Research on Animal Flight in an Artificial Earth Satellite. **Volume 2**—Dynamical Effects in the Motion of Artificial Earth Satellites. Some Results of Measurements of the Stratosphere Thermodynamic Parameters Carried Out by Means of Meteorological Rockets. The Perturbation of a Gaseous Medium by the Flight of an Artificial Earth Satellite. Preliminary Results of Density Determinations above 100 km. The Investigation of the Ionic Composition of the Terrestrial Atmosphere by Means of Rockets and Artificial Earth Satellites. Soviet Investigations of the Ionosphere by Means of Rockets and Artificial Earth Satellites. Preliminary Report on the Geomagnetic Measurements Carried Out on the Third Soviet Artificial Earth Satellite. Micrometeorite Research with Rockets and Artificial Earth Satellites. The Search for Corpuscles with the Help of the Third Artificial Earth Satellite. The Study of the Soft Component of Cosmic Rays Outside the Earth's Atmosphere. The Heavy Nuclei of the Primary Cosmic Radiation. Solar Batteries. An Accoustical Method for the Measurement of the Mechanical Parameters of Meteorites.

240 pages cloth illus. $9.50

PLENUM PRESS
227 W. 17TH ST. • NEW YORK 11, N.Y.

SOUTHWEST
"Monoball" ®
SELF-ALIGNING BEARINGS

CHARACTERISTICS

	ANALYSIS	RECOMMENDED USE
1	Stainless Steel Ball and Race	For types operating under high temperature (800-1200 degrees F.).
2	Chrome Alloy Steel Ball and Race	For types operating under high radial ultimate loads (3000-893,000 lbs.).
3	Bronze Race and Chrome Steel Ball	For types operating under normal loads with minimum friction requirements.

Thousands in use. Backed by years of service life. Wide variety of Plain Types in bore sizes 3/16" to 6" Dia. Rod end types in similar size range with externally or internally threaded shanks. Our Engineers welcome an opportunity of studying individual requirements and prescribing a type or types which will serve under your demanding conditions. Southwest can design special types to fit individual specifications. As a result of thorough study of different operating conditions, various steel alloys have been used to meet specific needs. Write for Engineering Manual No. 551. Address Dept. ARS-59.

SOUTHWEST PRODUCTS CO.
1705 SO. MOUNTAIN AVE., MONROVIA, CALIFORNIA

RESEARCH ENGINEERS

IF YOU—

1. are experienced and interested in dynamic analysis and vibration engineering,
2. have M.S. or Ph.D. degree or equivalent in specific experience, and have United States citizenship,
3. desire to apply your knowledge to a wide variety of technically significant industrial and government problems,
4. would enjoy a permanent staff position ensured by multiple sponsorship,
5. would appreciate the opportunity to proceed with your graduate studies on a convenient basis while functioning as a full-time staff member,
6. enjoy working in communications and close professional contact with men from other scientific and engineering fields,
7. would like to join the staff of one of the largest independent research organizations in the world,

please contact:

E. P. Bloch

ARMOUR RESEARCH FOUNDATION
of Illinois Institute of Technology
10 West 35th Street
Chicago 16, Illinois

Index to Advertisers

ADDISON-WESLEY PUBLISHING CO., INC. 1006

AEROJET GENERAL CORP. ..... 898, Back cover
D'Arcy Advertising Co., Los Angeles, Calif.

ARMOUR RESEARCH FOUNDATION OF ILLINOIS INSTITUTE OF TECHNOLOGY 1008

AVCO CORP., EVERETT RESEARCH LABORATORY ... 2nd cover
Allied Advertising Agency, Inc., Boston, Mass.

BELL AIRCRAFT CORP. 992
The Rumrill Co., Inc., Buffalo, N. Y.

BOEING AIRPLANE CO. 991
Fletcher Richards, Calkins & Holden, Inc., Seattle, Wash.

BULOVA WATCH CO. 893
Duncan-Brooks, Inc., Garden City, N. Y.

CATERPILLAR TRACTOR CO. 992
Thomson Advertising, Inc., Peoria, Ill.

CHANCE VOUGHT AIRCRAFT, INC. 1002
Tracy-Locke Co., Inc., Dallas, Texas

CONTINENTAL AVIATION & ENGINEERING CORP. 1005
The Hopkins Agency, Detroit, Mich.

CONVAIR, A DIV. OF GENERAL DYNAMICS CORP. ... 3rd cover
Lennen & Newell, Inc., Los Angeles, Calif.

GENERAL ELECTRIC CO., DEFENSE SYSTEMS DEPT. ... 1002
Deutsch & Shea, Inc., New York, N. Y.

INTERNATIONAL BUSINESS MACHINES CORP. 996, 997
Benton & Bowles, Inc., New York, N. Y.

LOCKHEED AIRCRAFT CORP. 896, 897
Foote, Cone & Belding, Los Angeles, Calif.

LOS ALAMOS SCIENTIFIC LABORATORY 1003
Ward Hicks Advertising, Albuquerque, N. Mex.

THE MARTIN CO., ACTIVATION DIV. 895
E. M. Holworson Co., Denver, Colo.

MASSACHUSETTS INSTITUTE OF TECHNOLOGY 1000
Allied Advertising Agency, Inc., Boston, Mass.

NEWBROOK MACHINE CORP. 1001
Melvin F. Hall Advertising Agency, Inc., Buffalo, N. Y.

NORTH AMERICAN PHILIPS CO., INC. 999
Anders Associates, New York, N. Y.

PLENUM PRESS, INC. 1007
H. J. Gold Co., New York, N. Y.

RADIO CORP. OF AMERICA 993
Al Paul Lefton Co., Inc., Philadelphia, Pa.

REPUBLIC AVIATION CORP. 989
Deutsch & Shea, Inc., New York, N. Y.

SOUTHWEST PRODUCTS CO. 1008
O. K. Fagan Advertising Agency, Los Angeles, Calif.

THIOKOL CHEMICAL CORP. 994, 995
Brown & Butcher, Inc., New York, N. Y.

PUBLIC LIBRARY

CONVAIR'S TARTAR AND ADVANCED TERRIER
STRONG RIGHT ARMS FOR YOUR DEFENSE
Convair's Tartar and Advanced Terrier are supersonic all-weather surface-to-air missiles which significantly increase the effectiveness of the U. S. Navy's defense against air attack. The Tartar will be used on destroyers and cruisers, and the Advanced Terrier will stand aerial "guard duty" aboard carriers, cruisers and missile frigates. The U. S. Marine Corps will also use Advanced Terriers from mobile ground launchers. Produced in Pomona, California, by Convair, a Division of General Dynamics Corporation, in cooperation with the U. S. Navy Bureau of Ordnance, the Tartar and Advanced Terrier are strong right arms for your defense!
GENERAL DYNAMICS CORPORATION

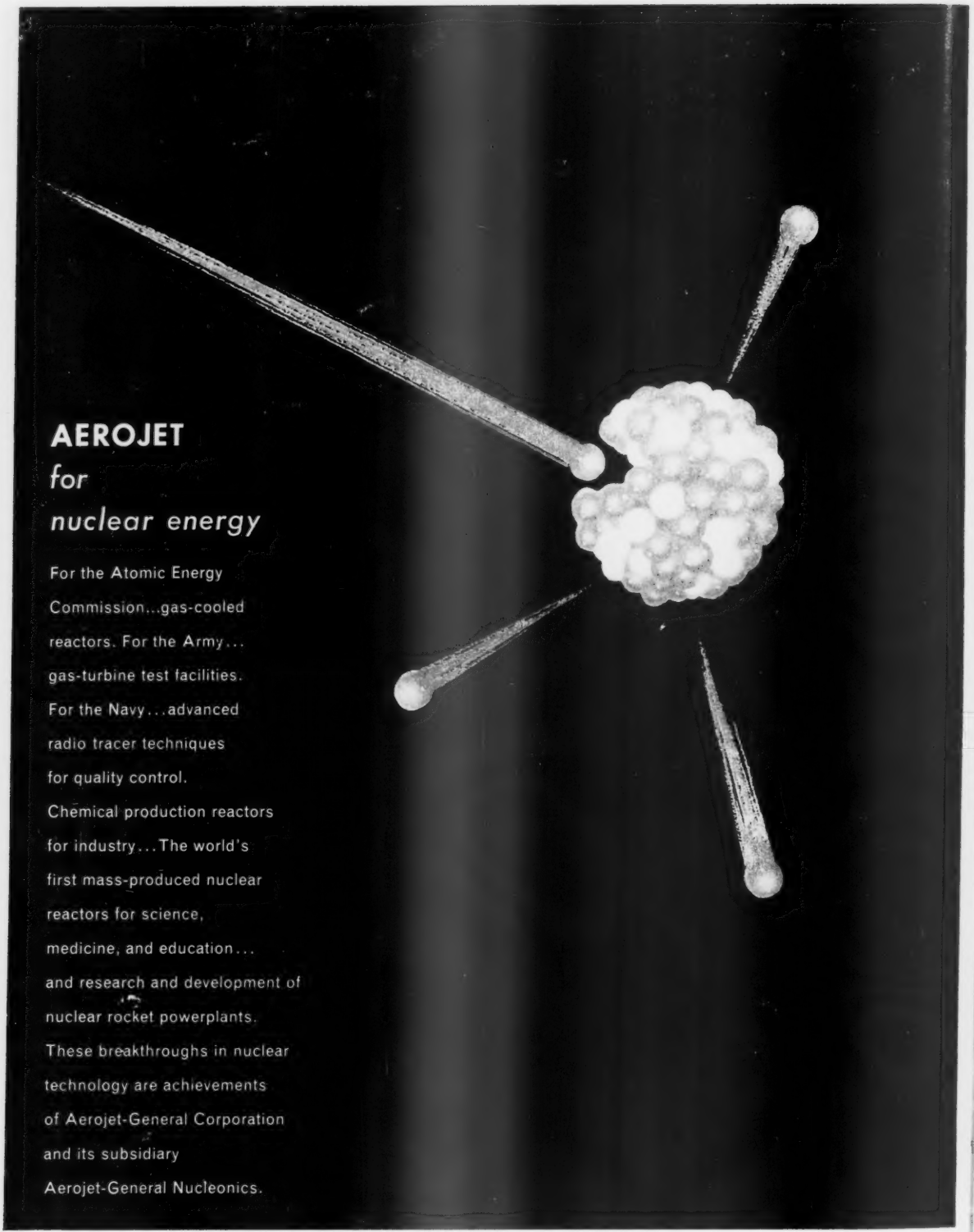

AEROJET
for nuclear energy

For the Atomic Energy Commission...gas-cooled reactors. For the Army... gas-turbine test facilities. For the Navy...advanced radio tracer techniques for quality control. Chemical production reactors for industry...The world's first mass-produced nuclear reactors for science, medicine, and education... and research and development of nuclear rocket powerplants. These breakthroughs in nuclear technology are achievements of Aerojet-General Corporation and its subsidiary Aerojet-General Nucleonics.

AEROJET-GENERAL CORP.

THE GENERAL TIRE

A SUBSIDIARY OF THE GENERAL TIRE & RUBBER COMPANY
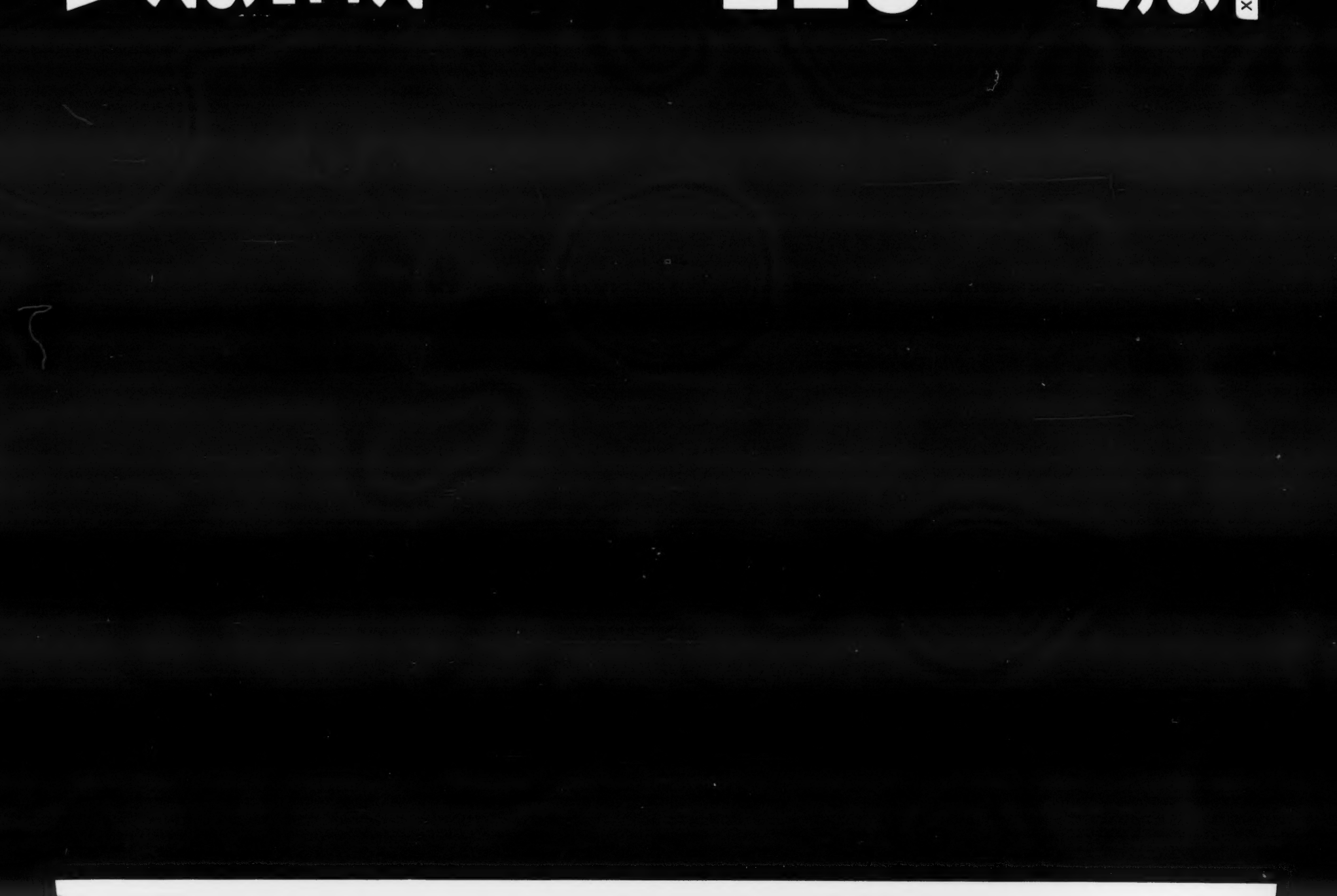
Engineers, scientists—investigate outstanding opportunities at Aerojet. (Plants at Azusa, San Ramon and near Sacramento, Calif.)